

Hybrid thermochemical-biological processes to enhance the energy recovery from waste

Zur Erlangung des akademischen Grades eines

DOKTORS DER INGENIEURWISSENSCHAFTEN

von der KIT-Fakultät für Chemieingenieurwesen und Verfahrenstechnik des

Karlsruher Instituts für Technologie (KIT)

genehmigte

DISSERTATION

von

M.Sc. Alberto Robazza

aus Padova, Italien

Tag der mündlichen Prüfung: 08 Juli 2024

Erstgutachter: Prof. Dr. rer. nat. Christoph Syldatk

Zweitgutachter: Prof. Dr. rer. nat. Nicolaus Dahmen

Zweitgutachterin: Dr. rer. nat. Anke Neumann

Acknowledgments

I am deeply grateful to Dr. Anke Neumann for her belief in me, her guidance and support throughout my PhD journey. Anke provided the perfect balance of freedom and guidance, allowing me to pursue my research interests and structure my work in the way I felt would be most effective. She was always there, available to offer advice and support during challenging times. Thank you for being an exceptional mentor.

I thank Prof. Christoph Syldatk for being my supervisor, for supporting my work and for all the valuable feedback at the Monday meetings after presenting my work. I must also thank Prof. Dirk Holtmann for his support, availability, networking and kindness in extending my contract and allowing me to stay at the institute.

I especially thank Flávio for his availability to collaborate and support in this work. Flávio's contribution together with Dr. Sabine Kleinsteuber and Ute Schwotzer with all the microbial community and statistical analyses significantly ($p < 0.05$) improved the quality of this work.

I am also grateful to Dr Habibu Aliyu for his mentorship, many hours of discussions and guidance on how to be a good scientist.

My heartfelt appreciation goes also to all my colleagues Aline, Andre, Anna-Lena, Arabi, Christin, Emily, Jakub, Kevin, Lea, Lisa, Lukas, Magda, Markus, Nebyat and Nicklas. You are all incredible people and great scientists. I am very lucky to have been your colleague. I learned so much from you all.

I thank Daniela, Delphine, Marvin, Michaela, Laura and Pascal for the technical assistance you provided me throughout all these years.

I thank Ada, Claudia and Elena for their efforts during their Bachelor and Master theses. Your hard work, commitment and feedback greatly contributed to this thesis and to my own development as scientist and mentor.

I am grateful to Egidio, Anna Maria, Paolo and Guido for being the immovable references that constantly guide me. I always wonder about what you would do and how you would approach challenging situations.

I am deeply in love with Carlo Jona and Ella Aurora. You are light that shines and illuminates everything with beauty. Spending time with you, playing with you and learning from your joyful lightness of being fills my heart with immense happiness.

Lastly, but most importantly, I must express my profound love and gratitude to Maja for her dedication, love and unwavering support. She is the cornerstone of my life and I cannot imagine it without her.

Preamble

This thesis aims to explore the feasibility of integrating syngas and pyrolysis aqueous condensate (PAC) as substrates for anaerobic mixed cultures to produce CH₄, H₂ or carboxylates, while evaluating potential, limitations, inhibitory PAC concentrations, process parameter effects and energy recovery. Additionally, it proposes a two-stage process where the carboxylates products of syngas and PAC co-fermentation are converted into high-value platform chemicals to enhance process selectivity. The work combines four research articles, each contributing to advancing knowledge in this field. Conceptualization, investigation and drafting of the manuscripts were done during the doctoral period. Minor changes in the text, format and figures were done to adapt the manuscripts into chapters.

Chapter 1 provides the theoretical background for the thesis, emphasizing the potential of combining fast pyrolysis with anaerobic digestion for converting fast pyrolysis by-products like syngas and pyrolysis aqueous condensate into biofuels or platform chemicals. It sets the context that led to identifying knowledge gaps and concludes with defining research questions and proposing the two-stage process.

Chapter 2 reports the potential of acetate-rich wastewaters as co-substrates during the fermentation of syngas via mixed cultures at different temperatures and pH. Particular attention was given to electron balance based on electron equivalents and microbial community composition. This chapter is based on the publication:

Enhancing CO uptake rates of anaerobic microbiomes via acetate shock loading. Alberto Robazza, Ada Raya i Garcia, Flávio C. F. Baleeiro, Sabine Kleinstauber and Anke Neumann

Manuscript submitted for publication

Chapter 3 demonstrates the viability of the two-stage process through batch bottle experiments. It examines syngas and PAC co-fermentation at various temperatures, identifying inhibitory concentrations for carboxydrotrophic and methanogenic reactions, as well as assessing the degradation of selected PAC components and energy recovery. The extent of PAC detoxification is evaluated by inoculating the carboxylates-rich effluent from stage-one with *Aspergillus oryzae* in a secondary fermentation. This chapter is based on the publication:

Co-Fermenting pyrolysis aqueous condensate and pyrolysis syngas with anaerobic microbial communities enables L-malate production in a secondary fermentative stage. Alberto Robazza, Claudia Welter, Christin Kubisch, Flávio César Freire Baleeiro, Katrin Ochsenreither and Anke Neumann

Fermentation (2022), 8, 512.

<https://doi.org/10.3390/fermentation8100512>

Chapter 4 elucidates the potential of other PACs from the pyrolysis of sewage sludge and polyethylene plastics as co-substrates during syngas fermentation via anaerobic mixed cultures. It identifies inhibitory concentrations for carboxyd-trophic and methanogenic reactions, examining the degradation of selected PAC components and assessing energy recovery. This chapter is based on the publica-tion:

Energy recovery from syngas and pyrolysis wastewaters with anaerobic mixed cultures. Alberto Robazza and Anke Neumann

Bioresources and Bioprocessing (2024), 11, 75.

<https://doi.org/10.1186/s40643-024-00791-3>

Chapter 5 further develops the two-stage process by presenting the results of mesophilic and thermophilic continuous syngas and lignocellulose-PAC co-fermen-tations in 2.5 L stirred tank reactors. It evaluates the feasibility of long-term culti-vation, microbial community composition and energy recovery. Additionally, the carboxylates-rich effluent from stage one is subjected to secondary fermentation with *Aspergillus oryzae* to assess the extent of PAC detoxification and further con-version of carboxylates into L-malate. This chapter is based on the publication:

Two-stage conversion of syngas and pyrolysis aqueous condensate into L-malate. Alberto Robazza, Flávio C. F. Baleeiro, Sabine Kleinsteuber and Anke Neumann

Biotechnology for Biofuels and Bioproducts (2024), 17, 85.

<https://doi.org/10.1186/s13068-024-02532-2>

List of publications and conferences participation

Peer-reviewed original publications on which this thesis is based

Co-Fermenting pyrolysis aqueous condensate and pyrolysis syngas with anaerobic microbial communities enables L-malate production in a secondary fermentative stage. Alberto Robazza, Claudia Welter, Christin Kubisch, Flávio César Freire Baleeiro, Katrin Ochsenreither and Anke Neumann

Fermentation (2022), 8, 512.

<https://doi.org/10.3390/fermentation8100512>

Energy recovery from syngas and pyrolysis wastewaters with anaerobic mixed cultures. Alberto Robazza and Anke Neumann

Bioresources and Bioprocessing (2024), 11, 75.

<https://doi.org/10.1186/s40643-024-00791-3>

Two-stage conversion of syngas and pyrolysis aqueous condensate into L-malate. Alberto Robazza, Flávio C. F. Baleeiro, Sabine Kleinsteuber and Anke Neumann

Biotechnology for Biofuels and Bioproducts (2024), 17, 85.

<https://doi.org/10.1186/s13068-024-02532-2>

Original manuscripts submitted to peer-reviewed journals on which this thesis is based

Enhancing CO uptake rates of anaerobic microbiomes via acetate shock loading. Alberto Robazza, Ada Raya i Garcia, Flávio C. F. Baleeiro, Sabine Kleinsteuber and Anke Neumann

Manuscript submitted for publication

Poster presentations in conferences

Rejoining two separated wastes: co-fermentation of syngas and pyrolysis aqueous condensate. Alberto Robazza, Claudia Welter, Christin Kubisch and Anke Neumann
VAAM – Jahrestagung (2022), Online

Co-Fermenting pyrolysis aqueous condensate and pyrolysis syngas with anaerobic microbial communities enables L-malate production in a secondary fermentative stage. Alberto Robazza, Claudia Welter, Christin Kubisch, Flávio César Freire Baleeiro, Katrin Ochsenreither and Anke Neumann
International Chain Elongation Conference (2022), Online

Co-Fermenting pyrolysis aqueous condensate and pyrolysis syngas with anaerobic microbial communities enables L-malate production in a secondary fermentative stage. Alberto Robazza, Claudia Welter, Christin Kubisch, Flávio César Freire Baleeiro, Katrin Ochsenreither and Anke Neumann
Carbon recycling Network (2022), Nottingham, UK

Two-stage conversion of pyrolysis syngas and pyrolysis aqueous condensate into L-malate with carboxylates as intermediate substrates. Alberto Robazza, Flávio C. F. Baleeiro, Sabine Kleinstauber and Anke Neumann
DECHEMA Himmelfahrtstagung (2023), Weimar, Germany

From pyrolysis by-products to short-chain carboxylic acids: the metabolic versatility of anaerobic mixed cultures enables carbon and energy recovery during the co-fermentation of syngas and different pyrolysis wastewaters. Alberto Robazza and Anke Neumann
VAAM – Jahrestagung (2023), Göttingen, Germany

Oral presentations in conferences

Hybrid Thermochemical-biological Processes for Enhanced Energy Recovery from Waste. Alberto Robazza and Anke Neumann
Carbon recycling Network (2024), Manchester, UK

Abstract

Pyrolytic conversion of anthropogenic waste holds promise for fuel and chemical production but technological advancements are necessary for optimal efficiency. Although highly toxic, the pyrolysis aqueous condensate (PAC), a pyrolysis by-product, can be valorised and detoxified via anaerobic digestion for biogas production. Syngas, another product of pyrolysis, can be fermented by anaerobic mixed cultures for methane or carboxylates production. Integrating syngas into anaerobic fermentation of PAC shows potential to enhance overall efficiency, yet knowledge gaps exist regarding co-fermentation effects and substrate toxicity.

This thesis aims to explore the feasibility of syngas and PAC integration as substrates for CH₄, H₂ or carboxylates production via anaerobic mixed culture fermentation, assessing potential and limitations, inhibitory PAC concentrations, process parameter effects and energy recovery. Additionally, a two-stage process is proposed where the carboxylates products of syngas and PAC co-fermentation are converted into to high-value platform chemicals to enhance process selectivity. The work combines four research articles, each contributing to advancing knowledge in this field. Below, you'll find a concise overview of the results drawn from the abstract of each article.

Acetate-rich wastewater as co-substrate in mixed culture syngas fermentation

Acetate is a common compound found in the wastewater generated during physiochemical or thermochemical conversion of lignocellulose biomass. Here, the impact of increasing shock loads of acetate during syngas co-fermentation with anaerobic mixed cultures was evaluated across different pH levels (6.7 and 5.5) and temperatures (37°C and 55°C), assessing microbial kinetics, metabolite production, and microbial community composition. The study reports that acetate supplementation consistently boosted carboxydrotrophic rates. Mixed cultures can tolerate up to 64 g/L at pH 5.5. High acetate loads inhibited methanogenic pathways, favouring hydrogenogenesis and carboxylate production. While species belonging to *Methanobacterium*, *Methanosarcina* and *Methanothermobacter* may have been involved into CO biomethanation, the bacterial species responsible for CO conversion in non-methanogenic experiments remain unclear. *Oscillibacter* is suggested as a potential *n*-valerate producer.

Proof of concept of the two stage process

This study investigates the potential of a two-stage process to convert the carbon and energy in syngas and lignocellulose PAC into L-malate. PAC and syngas were co-fermented by two mixed cultures at 37 and 55°C. The media from selected mixed culture fermentations were then inoculated with *Aspergillus oryzae* for L-malate production. The results show that mixed cultures can perform simultaneous

syngas fermentation and PAC detoxification for the production of volatile fatty acids or acetate/H₂ production, depending on the incubation temperature. Carboxydrotrophic activity showed higher resilience to PAC toxicity than methanogenesis. Substantial detoxification of PAC was observed under PAC concentrations up to 10% independently of the rates of syngas metabolism. PAC detoxification enabled the further valorisation of the acetate produced via syngas and PAC fermentations into L-malate.

Energy recovery potential from other pyrolysis aqueous condensates

In this study, the impact of two PACs from sewage sludge and polyethylene plastics pyrolysis on energy recovery potential through syngas co-fermentation with mixed cultures was examined. Results showed successful co-fermentation of syngas and certain PAC components into CH₄ and short-chain carboxylates. However, origin of the PAC and its composition influenced toxicity and energy recovery. Sewage sludge PAC inhibited carboxydrotrophic and methanogenic activity primarily likely as consequence of the high ammonium concentrations in the sewage sludge PAC. Polyethylene plastics PAC severely inhibited microbial activity as result of the synergistic toxic effect of the components of the aqueous condensate. Energy recovery from sewage sludge PAC was limited by its recalcitrant nature, while polyethylene plastics PAC showed great bioconversion potential and allowed for high energy recovery.

Upscaling the two-stage process and evaluation of reactors' microbiota

To assess the continuous co-fermentation of syngas and lignocellulose PAC, two reactors were operated at mesophilic (37°C) and thermophilic (55°C) conditions with increasing PAC loading rates. Both processes sequestered syngas and detoxified lignocellulose PAC, recovering over 50% of energy into short-chain carboxylates. In the mesophilic process, methanogenesis was inhibited, with primary metabolites being acetate, ethanol and butyrate and the reactor microbiota was dominated by *Clostridium sensu stricto* 12. In the thermophilic process, *Symbiobacteriales*, *Syntrophaceticus*, *Thermoanaerobacterium*, *Methanothermobacter* and *Methanosarcina* played crucial roles, with *Moorella thermoacetica* and *Methanothermobacter marburgensis* as predominant carboxydrotrophs. High biomass concentrations stabilized operations at high PAC loads. *Aspergillus oryzae* converted first-stage metabolites into L-malate in a second-stage reactor, confirming PAC detoxification.

This study confirms the potential of hybrid thermochemical-biological processes in enhancing resource circularity and reducing environmental impacts. It identifies crucial operational parameters for syngas and PAC co-fermentation, demonstrates long-term cultivation feasibility and highlights the resilience of mixed cultures to extreme conditions. Wastewater detoxification enables the valorization

Abstract

of carboxylates into platform chemicals via secondary fermentative processes. These insights are vital for developing biotechnologies maximizing carbon and energy recovery from waste streams, but further optimization and implementation in real pyrolysis processes are needed.

Zusammenfassung

Die pyrolytische Umwandlung von anthropogenen Abfällen ist vielversprechend für die Herstellung von Kraftstoffen und Chemikalien, doch für eine optimale Effizienz sind technologische Fortschritte erforderlich. Das wässrige Pyrolysekondensat (PAC), ein Nebenprodukt der Pyrolyse, ist zwar hochgiftig, kann aber durch anaerobe Vergärung zur Biogaserzeugung genutzt und dabei entgiftet werden. Synthesegas, ein weiteres Produkt der Pyrolyse, kann durch anaerobe Mischkulturen zur Methan- oder Carboxylatproduktion vergoren werden. Die Integration von Synthesegas in die anaerobe Vergärung von PAC hat das Potenzial, die Gesamteffizienz zu steigern, doch bestehen Wissenslücken hinsichtlich der Auswirkungen der Co-fermentation und der Toxizität des Substrats.

Ziel dieser Arbeit ist es, die Durchführbarkeit der Integration von Synthesegas und PAC als Substrate für die Produktion von CH_4 , H_2 oder Carboxylaten durch anaerobe Mischkulturfermentation zu untersuchen, wobei das Potenzial und die Grenzen, der hemmenden PAC-Konzentrationen, der Auswirkungen der Prozessparameter und der Energierückgewinnung bewertet werden. Darüber hinaus wird ein zweistufiges Verfahren vorgeschlagen, bei dem die Carboxylate aus der Co-fermentation von Synthesegas und PAC in hochwertige Plattformchemikalien umgewandelt werden, um die Prozessselektivität zu erhöhen. Die Arbeit fasst vier Forschungsartikel zusammen, von denen jeder zum Wissenszuwachs in diesem Bereich beiträgt. Nachfolgend finden Sie einen kurzen Überblick über die Ergebnisse, die sich aus den Zusammenfassungen der einzelnen Artikel ergeben.

Acetatreiche Abwässer als Co-Substrat in der Mischkultur-Synthesegasfermentation

Acetat ist eine häufig vorkommende Verbindung in Abwässern, die bei der physiochemischen oder thermochemischen Umwandlung von Lignozellulose-Biomasse entstehen. Hier wurde die Auswirkung steigender Acetat-Stoßbelastungen während der Syngas-Co-Fermentation mit anaeroben Mischkulturen bei verschiedenen pH-Werten (6,7 und 5,5) und Temperaturen (37°C und 55°C) untersucht, wobei die mikrobielle Kinetik, die Metabolitenproduktion und die Zusammensetzung der mikrobiellen Gemeinschaft bewertet wurden. Die Studie zeigt, dass die Zugabe von Acetat die carboxydotrophen Raten durchweg erhöhte. Mischkulturen können bis zu 64 g/L und pH 5,5 tolerieren. Hohe Acetatbelastungen hemmten die methanogenen Stoffwechselwege und begünstigten die Hydrogenogenese und die Carboxylatproduktion. Während Arten, die zu *Methanobacterium*, *Methanosarcina* und *Methanothermobacter* gehören, an der CO-Biomethanisierung beteiligt gewesen sein könnten, bleibt unklar, welche Bakterienarten für die CO-Umwandlung in nicht-methanogenen Experimenten verantwortlich sind. *Oscillibacter* wird als potenzieller *n*-Valerat-Produzent vorgeschlagen.

Konzeptnachweis für den zweistufigen Prozess

In dieser Studie wird das Potenzial eines zweistufigen Prozesses zur Umwandlung des Kohlenstoffs und der Energie in Synthesegas und Lignozellulose- PAC in L-Malat untersucht. PAC und Synthesegas wurden von zwei Mischkulturen bei 37 und 55°C Co-fermentiert. Die Medien ausgewählter Mischkulturfermentationen wurden dann mit *Aspergillus oryzae* zur L-Malat-Produktion beimpft. Die Ergebnisse zeigen, dass Mischkulturen in Abhängigkeit von der Inkubationstemperatur gleichzeitig eine Syngasfermentation und eine PAC-Entgiftung zur Produktion von flüchtigen Fettsäuren oder Acetat/H₂-Produktion durchführen können. Die carboxydotrophe Aktivität zeigte eine höhere Widerstandsfähigkeit gegenüber der PAC-Toxizität als die Methanogenese. Eine erhebliche Entgiftung von PAC wurde bei PAC-Konzentrationen von bis zu 10 % unabhängig von den Raten des Syngas-Stoffwechsels beobachtet. Die PAC -Entgiftung ermöglichte die weitere Valorisierung des durch Syngas- und PAC -Fermentationen erzeugten Acetats zu L-Malat.

Potenzial der Energierückgewinnung aus anderen wässrigen Pyrolysekondensaten

In dieser Studie wurde die Auswirkungen von zwei PACs aus der Klärschlamm- und Polyethylen-Kunststoff-Pyrolyse auf das Energiegewinnungspotenzial durch Syngas-Co-Fermentation mit Mischkulturen untersucht. Die Ergebnisse zeigten eine erfolgreiche Co-Fermentation von Synthesegas und bestimmten PAC-Komponenten zu CH₄ und kurzkettigen Carboxylaten. Die Herkunft der PAC und ihre Zusammensetzung beeinflussten jedoch die Toxizität und die Energierückgewinnung. Klärschlamm-PAC hemmte die carboxydotrophe und methanogene Aktivität, was in erster Linie auf die hohen Ammoniumkonzentrationen in der Klärschlamm- PAC zurückzuführen ist. Polyethylen-Kunststoff-Klärschlamm hemmte die mikrobielle Aktivität stark, was auf die synergistische toxische Wirkung der Bestandteile des wässrigen Kondensats zurückzuführen ist. Die Energierückgewinnung aus Klärschlamm-PAC war durch ihre widerspenstige Natur begrenzt, während Polyethylen-Kunststoff- PAC ein großes Biokonversionspotenzial aufwies und eine hohe Energierückgewinnung ermöglichte.

Hochskalierung des zweistufigen Prozesses und Bewertung der Mikrobiota der Reaktoren

Zur Bewertung der kontinuierlichen Co-Fermentation von Synthesegas und Lignocellulose-PAC wurden zwei Reaktoren unter mesophilen (37°C) und thermophilen (55 °C) Bedingungen mit steigenden PAC-Beladungsraten betrieben. In beiden Prozessen wurde das Synthesegas sequestriert und die Lignocellulose-PAC entgiftet, wobei über 50 % der Energie in kurzkettigen Carboxylaten zurückgewonnen wurden. Im mesophilen Prozess war die Methanogenese gehemmt, wobei die primären Metaboliten Acetat, Ethanol und Butyrat waren und die Mikrobiota des Reaktors von *Clostridium sensu stricto* 12 dominiert wurde. Im thermophilen Prozess

spielten *Symbiobacteriales*, *Syntrophaceticus*, *Thermoanaerobacterium*, *Methanothermobacter* und *Methanosarcina* eine entscheidende Rolle, wobei *Moorella thermoacetica* und *Methanothermobacter marburgensis* die vorherrschenden Carboxidotrophen waren. Hohe Biomassekonzentrationen stabilisierten den Betrieb bei hoher PAC-Belastung. *Aspergillus oryzae* wandelte die Metaboliten der ersten Stufe in einem zweitstufigen Reaktor in L-Malat um und bestätigte damit die Entgiftung von PAC.

Diese Studie bestätigt das Potenzial hybrider thermochemisch-biologischer Prozesse zur Verbesserung der Kreislauffähigkeit von Ressourcen und zur Verringerung der Umweltauswirkungen. Sie identifiziert entscheidende Betriebsparameter für die Co-Fermentation von Synthesegas und PAC, zeigt die langfristige Machbarkeit der Kultivierung und unterstreicht die Widerstandsfähigkeit von Mischkulturen unter extremen Bedingungen. Die Entgiftung von Abwässern ermöglicht die Valorisierung von Carboxylaten zu Plattformchemikalien durch sekundäre Fermentationsprozesse. Diese Erkenntnisse sind für die Entwicklung von Biotechnologien zur Maximierung der Kohlenstoff- und Energierückgewinnung aus Abfallströmen von entscheidender Bedeutung, müssen jedoch weiter optimiert und in realen Pyrolyseprozessen umgesetzt werden.

Table of Contents

Acknowledgments.....	i
Preamble	ii
List of publications and conferences participation.....	iv
Peer-reviewed original publications on which this thesis is based	iv
Poster presentations in conferences	v
Oral presentations in conferences	v
Abstract.....	vi
Zusammenfassung.....	ix
1. Theoretical background and research proposal	1
1.1 Waste as source of carbon and energy in a bio-based and circular economy ..	2
1.2 Fast pyrolysis of waste	3
1.2.1 Pyrolysis aqueous condensate valorisation	5
1.3 Anaerobic fermentation with mixed cultures	6
1.3.1 PAC as substrate of anaerobic mixed cultures	7
1.3.2 Syngas as substrate for anaerobic mixed cultures	11
1.4 Carboxylic acids as substrates for biological processes	16
1.4.1 L-malate production from carboxylic acids with <i>Aspergillus oryzae</i>	17
1.5 Integrating thermochemical and biological processes for waste valorisation	18
1.6 Open questions and research proposal	20
2. Acetate-rich wastewater as co-substrate in mixed culture syngas fermentation	23
2.1 Introduction.....	24
2.2 Materials and methods.....	25
2.2.1 Experimental setup, fermentation conditions and community analysis ..	25
2.2.2 Analytical methods and statistical analysis	27
2.3 Results and discussion	28
2.3.1 Syngas and acetate metabolism of anaerobic mixed cultures	28
2.3.2 Effects of acetate supplementation on carboxydrotrophic rates	35
2.3.3 Inhibition of methanogenic activity	38

2.3 Conclusions	39
3. Proof of concept of the two stage process	42
3.1 Introduction	43
3.2 Materials and Methods	45
3.2.1 Growth medium	45
3.2.2 Inocula and PAC	46
3.2.3 Bottle preparation and fermentation	47
3.2.4 Analytical methods and data processing.....	49
3.3 Results and discussion.....	50
3.3.1 Mesophilic and thermophilic anaerobic mixed microbial cultures grown on pyrolysis synthetic syngas	50
3.3.2 Co-fermentation of syngas and PAC	53
3.3.3 A. oryzae cultivation on acetate derived from syngas fermentation and PAC detoxification	58
3.4 Conclusions.....	61
4. Energy recovery potential from other pyrolysis aqueous condensates.....	63
4.1 Introduction	65
4.2 Materials and Methods	67
4.2.1 Inoculum and PACs	67
4.2.2 Fermentation	68
4.2.3 Analytical Methods.....	69
4.3 Results.....	71
4.3.1 Syngas and Sewage Sludge PAC co-fermentation	71
4.3.2 Syngas and Polyethylene Plastics PAC co-fermentation	74
4.4 Discussion	77
4.4.1 PACs inhibition on anaerobic mixed culture metabolism	77
4.4.2 PAC components degradation and energy recovery.....	79
4.5 Conclusions	82
5. Upscaling the two-stage process and evaluation of reactors' microbiota.....	84
5.1 Introduction.....	85

Table of content

5.2 Materials and Methods	87
5.2.1 Inocula and PAC	87
5.2.2 Mixed Culture Enrichments.....	87
5.2.3 Bioreactor Sampling and Analytical Methods.....	88
5.2.4 Microbial Community Analysis and Statistical Evaluation.....	89
5.2.5 <i>Aspergillus oryzae</i> Batch Fermentations	89
5.3 Results	90
5.3.1 Mesophilic co-fermentation of Syngas and PAC.....	90
5.3.2 Thermophilic co-fermentation of Syngas and PAC	94
5.3.3 L-malate production from SCCs with <i>Aspergillus oryzae</i>	98
5.4 Discussion.....	99
5.4.1 Reactor microbiomes and performances of the mesophilic and the thermophilic process.....	99
5.4.2 Process stability and re-inoculations.....	103
5.4.3 L-malate production	104
5.5 Conclusions.....	105
6. Final conclusions and outlook.....	108
Bibliography.....	i
List of figures	xxxii
List of tables.....	xxxiv
Supplementary information	xxxv
Additional file 1	xxxv
Additional file 2	xliii
Additional file 3	l
Additional file 4	lv

1. Theoretical background and research proposal

1.1 Waste as source of carbon and energy in a bio-based and circular economy

Growing concerns for the impact of anthropogenic activities on the environment are shifting the socio-economic interests from a linear fossil-based economy towards a more sustainable and circular one [1]. Among anthropogenic activities, waste production and its improper management can have detrimental consequences, not only leading to public and environmental health crises but also resulting in economic losses due to loss of valuable resources. Hence, it is crucial to implement proper waste management practices to mitigate the associated environmental issues and to ensure sustainable waste disposal, recycling and recovery of resources.

Biomass, sewage sludge and plastic waste collectively represent a significant portion of the waste generated by human activity. When not managed properly, agricultural waste can contribute to environmental issues polluting water, land and air. Common disposal methods of municipal sewage sludge and post-consumer plastics, such as landfilling and incineration have disadvantages and may present hazards to human health and the environment. Landfilling of sewage sludge can lead to leachate groundwater contamination and greenhouse gas emissions, whereas agricultural applications may elevate soil heavy metal concentrations. Incineration requires costly technologies to control pollutant emissions [2]. While only a small fraction of post-consumer plastic is recycled. This process is not entirely closed-loop and most plastic waste ends being landfilled, incinerated or persisting as micro plastics. Like other waste, plastic landfilling contributes leachate contamination while incineration produces noxious volatile compounds [3]. In view of the escalating volume of waste generated, the development of new technologies is imperative to reduce environmental impacts while maximising the energy recovery from wastes and residues of human activities is considered a key step towards carbon-neutrality [4], [5].

Lignocellulose biomass, for instance, is one of the primary renewable source of carbon and energy available, offering a sustainable alternative to fossil-derived materials [6]. Considering that the Earth's net biomass production amounts approximately to 2000 EJ/y, the energy potential of biomass is enormous [7]. However, the source of all the biomass required to meet the need of an increased bio industry is still an open debate [8]. On one hand, diverting part of the energetic reservoir built up by plants towards uses defined by anthropocentric needs could cause undesirable impacts on the environment and on its natural distribution of resources [7]. On the other hand, the production of biofuel crops competes with food and the increasing demands for biofuel could exceed agricultural capacity [8]. Utilizing lignocellulose biomass, a by-product of agricultural and municipal activities, could alleviate this competition and improve economic circularity. Nevertheless, the intri-

cate polymeric structure and recalcitrant nature of lignocellulose biomass pose significant challenges to its biological valorisation, particularly through biological processes like anaerobic digestion [9]. Enhancing biomass pre-treatment and conversion processes is therefore essential. Various pre-treatment methods have been developed to enhance the accessibility of biomass components for further conversion and thermochemical approaches are being explored to enhance the sustainability of biorefineries [10]. Compared to other pre-treatment technologies, thermochemical processes offer rapid conversion times ranging from seconds to hours, representing a viable alternative pre-treatment to maximize biodegradability of waste and energy recovery [11]. Another key advantage of thermochemical processes is their adaptability to handle various types of waste materials, including plastics, rubber and sewage sludge, among others. Thermochemical processes combine efficient management of diverse waste streams and facilitates the production of a wide array of valuable products. The thermochemical conversion of sewage sludge and post-consumer plastics, for instance, presents numerous advantages over alternative disposal methods. By addressing waste management challenges, it reduces reliance on landfilling, minimizes solid residue volumes and mitigates greenhouse gas emissions and other harmful pollutants [12], [13]. Among other thermochemical technologies, pyrolysis, for instance, can convert waste into energy carriers such as bio-char, syngas and bio-oil, which can be further processed into biofuels or other value-added chemicals contributing to the development of a circular and sustainable bio-economy [11].

1.2 Fast pyrolysis of waste

During pyrolysis, the waste is thermochemically deconstructed at high temperatures in the absence of oxygen. Depending on heating rate and residence time, pyrolysis can be divided into three main types including slow pyrolysis, fast pyrolysis and flash pyrolysis. The long residence times of slow pyrolysis maximises solids yields while flash pyrolysis results in primarily biooil (up to 80 wt %). Fast pyrolysis, positioned between slow and flash pyrolysis with intermediate heating rates and residence times [14]. Fast pyrolysis generally occurs at 450 to 550°C with heating rates of 100–200°C/s. A diagram of the fast pyrolysis reactor is depicted in Figure 1. The pyrolysis reactions occur within the pyrolysis reactor. Primary reactions pathways occurring during fast pyrolysis are char formation, depolymerisation and fragmentation while other secondary reactions are cracking or recombination [10]. Products of fast pyrolysis are an organic liquid, commonly known as bio-oil (20-30 wt %), an aqueous condensate (PAC) (20-30 wt %), bio-char (10–30 wt %) and syngas (15–20 wt %), a mixture of primarily CO₂, CO, CH₄, H₂ [15]–[18]. Biochar is collected via cyclone and separated by the pyrolysis vapours. Then the pyrolysis vapours undergo

fractional condensation through a series of condensation units with progressively decreasing temperatures to separate the bio-oil and the PAC from syngas [19].

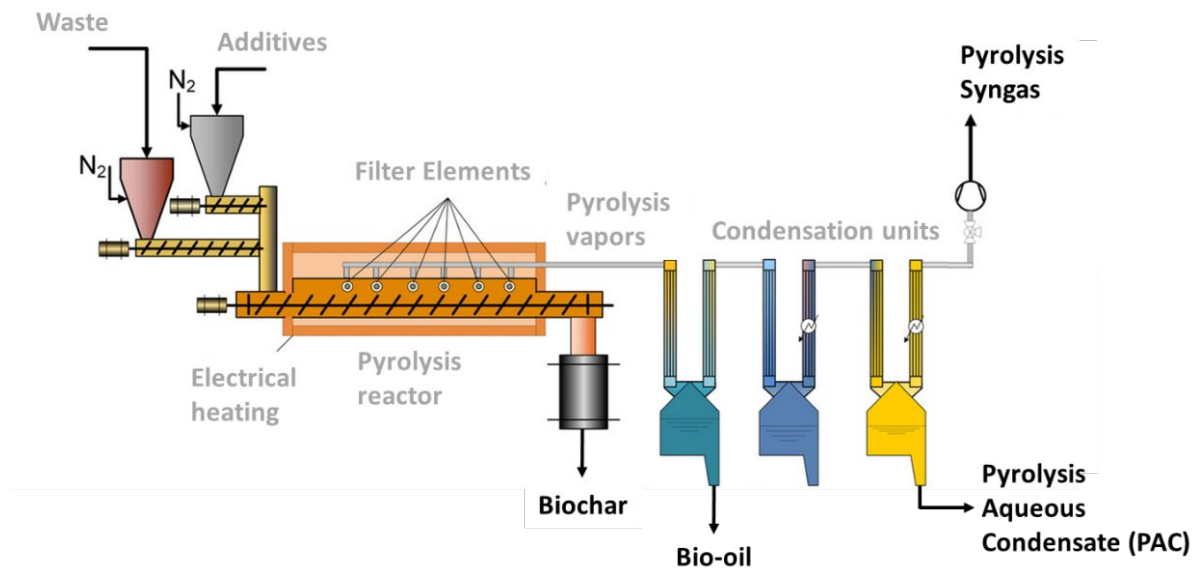


Figure 1. Schematic diagram of a pyrolysis process. Adapted from <https://www.itc.kit.edu/>

Process parameters heavily influence the composition and ratio of the products of fast pyrolysis and can be manipulated to redirect the carbon and energy flow of the process [20]. Critical factors include reactor design, residence time, heating rate, and catalyst, with temperature standing out as a major determinant [21]. For instance, when considering lignocellulose biomass, bio-oil yields peak between 400 and 550 °C. At temperatures beyond this range, bio-oils and char undergo secondary cracking reactions, leading to an increase in syngas formation [14]. The distribution of products in fast pyrolysis is also influenced by the composition of lignocellulosic biomass and the decomposition temperatures of its constituents (Figure 2). The first component to decompose is hemicellulose, starting at about 220°C up to around 400°C. Cellulose decomposes into non-condensable gases and condensable organic vapours within the temperature range of 320 to 420°C. Conversely, lignin decomposition is a slow and steady process starting already at 160°C and progresses up to 900°C [11]. Biochar and bio-oil stand as the primary targets of fast pyrolysis due to their comparable heating values to traditional fuels. They can be either reincorporated into the pyrolysis reactor for recycling or employed as energy carriers in alternative processes. Conversely, PAC typically exhibits a high water content, which constrains its utility as fuel. Given that PAC and syngas can collectively constitute about 45 wt% of the total waste fed into the pyrolysis reactor [16] and contribute up to 41% of the carbon balance [15], their production hinder the carbon and energy recovery from waste [22].

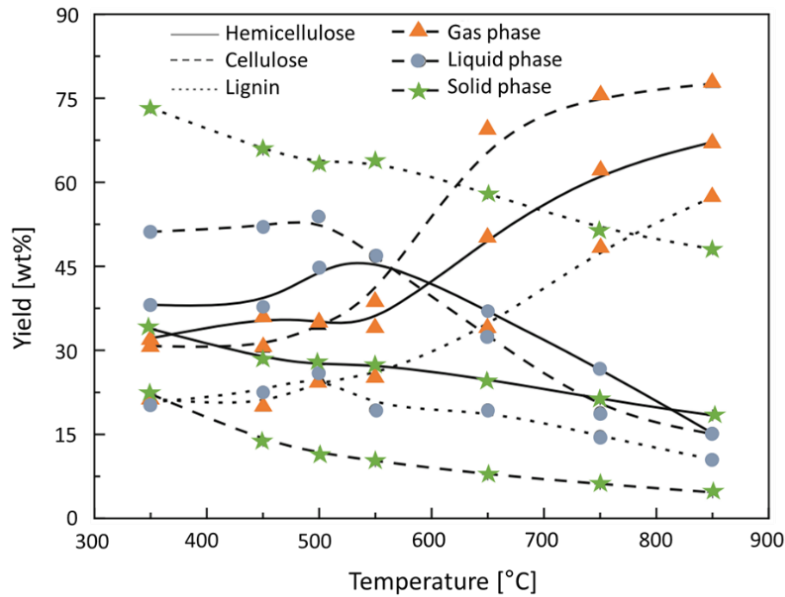


Figure 2. Effect of temperature on the product distribution during the pyrolysis of lignocellulose biomass. Adapted from [23].

1.2.1 Pyrolysis aqueous condensate valorisation

The PAC is a complex solution comprising a variety of compounds, including organic acids, anhydrous sugars, phenolics, amines, amides, guaiacols, furans, hydrocarbons, and nitrogen heterocycles, among others. Some of these constituents exhibit toxicity even at low concentrations [24]–[29]. Additionally, PAC may contain traces of bio-oil, further contributing to its complexity [30].

In the case of the PAC generated from the pyrolysis of lignocellulose biomass (LB-PAC), phenolic compounds such as phenol and cresol primarily originate from the decomposition of lignin at high temperatures. Furans derive from the decarboxylation and depolymerisation reactions of cellulose and hemicellulose [23]. Acetic acid, on the other hand, can originate from depolymerisation and deacetylation of cellulose and hemicellulose or alternatively from secondary cracking reactions such as ring scission and deacetylation or levoglucosan. Furthermore, acetic acid can originate as a by-product of lignin depolymerization and cracking reactions of lignin [31]. In the case of the PAC from sewage sludge (SS-PAC), for instance, the concentration of different compounds depends upon the levels proteins, lipids and lignin of the original waste [32]. Phenolic compounds can arise from the volatilization of polysaccharides and proteins, aromatic hydrocarbons stem from the decarboxylation of fatty acids within the lipid fraction, while ammonium and N-heterocycles are some products of protein decomposition [33]. Carbocyclic acids, phenolics can be found also in the PAC resulting from the pyrolysis of mixed plastics (PE-PAC) and originate from the organic impurities of the waste [34]–[36]. The type and concentration of PAC components determine the chemical properties and the toxicity of the

solution [24]. The PAC generated from pyrolysis of sewage sludge, for instance, exhibits basic pH, whereas LB-PAC and PE-PAC are acidic. Despite PACs may contain similar concentrations of carboxylic acids, the pH disparity can depend upon the presence of high concentration of ammonium and nitrogen aromatics in SS-PAC [15], [37].

The toxicity and complexity of PAC components severely hampers its possible applications and requires expensive treatments prior to disposal [20], [30]. Technical process optimization at the pyrolysis stage can reduce PAC toxicity. For instance, temperature combination of 120°C and 50°C on the first and second condensation units of the pyrolysis vapours during fast pyrolysis at 500°C resulted in an optimized PAC composition for further biological valorisation, increasing the yield of possible fermentable substrates at the expense of inhibitors [19]. It might be also worth investing into bioprocessing technologies able to convert PAC and syngas into industrially relevant biochemicals. Several works have already focused on the development of biological processes to valorise the constituents of the PAC and anaerobic mixed cultures, as we'll see in the next chapters, have emerged as promising technology for this task.

1.3 Anaerobic fermentation with mixed cultures

During anaerobic digestion, the degradation of the organic matter into biogas (a gaseous mixture primarily composed of CO₂ and CH₄) is carried out by anaerobic mixed cultures. Anaerobic digestion follows four primarily metabolic steps (hydrolysis, acidogenesis, acetogenesis and methanogenesis) and depends upon interactions between various microbial trophic groups, each performing a specific role within the process [38], [39]. Microbial interaction can be mutual, syntrophic or competitive depending on microbiota composition, process conditions and substrate availability. For instance, syntrophic interactions such those between syntrophic acetate oxidizers and hydrogenotrophic methanogens allow anaerobic digestion process to recover after acidification of ammonium inhibition [40], [41]. Alternatively, competition for resources such as acetate or H₂ between different microbial groups can negatively influence the metabolic pathways and biogas production rates [42]–[45].

The diverse microbiota, wide genetic spectrum and redundant metabolic pathways in anaerobic digesters offer advantages that pure cultures currently cannot replicate. Mixed cultures exhibit inherent resilience to environmental stresses and toxicity. Multiple parallel biochemical routes provide greater stability because of the potential distribution of toxic substrates to several populations [46], thereby increasing community resilience to disturbances [47]. Evolving environmental conditions provide competitive advantage to specific microbial groups favoured by the different thermodynamics, facilitating process recovery.

Critical factors affecting anaerobic digestion processes are pH, temperature, substrate loading rate and presence of toxic components. These factors play a vital role in determining the efficiency and effectiveness of anaerobic digestion. pH is a crucial factor, as it affects the activity of the microbial communities responsible for biogas production. The optimal pH range for anaerobic digestion generally ranges between 6.8 and 7.5 while pH fluctuations can disrupt the microbial balance in the digester, leading to process instability and lower biogas production rates [48], [49]. Temperature is another key factor that influences anaerobic digestion. The process can be carried out primarily under mesophilic (around 35-40°C) or thermophilic (around 50-60°C) conditions, favouring different microbial populations. Mesophilic microbial consortia show high tolerance to environmental changes resulting in high process stability. High temperatures, on the other hand, generally lead to faster digestion rates and increased biogas production. However, thermophilic processes are more susceptible to toxins and environmental changes [48]. High organic loading rates can lead to the accumulation of volatile fatty acids and process imbalances, while low loading rates may underutilize the digester capacity. Compounds such as heavy metals, phenols and certain organic pollutants can inhibit microbial activity and reduce biogas production efficiency. Toxic compounds can disrupt the microbial community structure, leading to process failures and reduced biogas yields [50], [51].

Nonetheless, numerous studies have confirmed the efficacy of anaerobic digestion in treating complex and toxic municipal and industrial wastewaters. By converting organic compounds into biogas and ensuring the stabilization of wastewater for safe disposal, anaerobic digestion has emerged as a cornerstone technology in wastewater treatment and energy recovery. Its capacity to effectively remove organic pollutants, coupled with its adaptability, has established it as a widely employed solution that can be customized to address various types of wastewater and contaminants [52]. Wastewaters from diverse industries, including swine farming, coal gasification plants, wineries, distilleries and food processing facilities have all been effectively treated using anaerobic digestion, significantly mitigating the environmental impact of organic pollutants [53]–[55]. Moreover, anaerobic digestion has been successfully integrated into decentralized sanitation systems, enhancing resource conservation and reuse while contributing to the advancement of sustainable wastewater management practices [56].

As we'll see in the next chapter, anaerobic digestion has emerged as viable technology for the valorisation of various PACs as substrate for biogas production, improving the carbon and energy recovery of pyrolysis process.

1.3.1 PAC as substrate of anaerobic mixed cultures

Several efforts have been made to develop bioprocessing technologies based on single-culture fermentations to valorise PAC. However, PAC was severely toxic,

albeit not all microorganisms exhibit the same tolerance to PAC toxicity. The ability of microorganisms to thrive on PAC is species-specific due to their varying resistance to toxins within PAC [22]. In a study assessing the toxicity of PAC from fir wood across a wide range of microbial groups, it was found that out of 42 tested strains, only 4 fungal strains exhibited tolerance to pure PAC, while many bacterial and yeast isolates required several PAC dilutions [57]. To enable PAC valorisation in pure culture fermentations, it appears that PAC must undergo one or more pre-treatment steps to reduce the toxicity, before enabling its bioconversion [58]–[65]. Alternatively to single culture processes, other studies successfully established anaerobic digestion with PACs as substrate for biogas production, proving how anaerobic mixed culture fermentation is a viable alternative to intricate physiochemical pre-treatments for PAC detoxification and valorisation. Low PAC concentrations can provide nutrients to microbial activity where many toxic components can act as substrates [50], [51]. PAC components such as carboxylic acids, anhydrous sugars and aromatic compounds, among others, can be easily fermented achieving high energy recovery into to biogas. For example, energy and carbon recoveries as high as 79 % were obtained in the production of biohythane (*i.e.*, a mixture of H₂ gas and CH₄) during the anaerobic degradation of the post hydrothermal liquefaction wastewater of corn stalk [66].

However, various influencing factors such as source of inoculum (*i.e.*, microbial composition of the inoculum), concentration of refractory and toxic compounds, the molecular weight of PAC components, PAC loading rate and process operating conditions affect PAC components degradation and recovery into CH₄, [67]–[70]. The concentration of refractory and toxic compounds is considered the primary factor affecting the energy recovery potential [20], [24], [70], [71]. Compounds in PAC, such as phenols, furans and N-heterocyclic compounds, have been reported to exhibit toxicity towards microorganisms, impacting their growth and metabolic activities [72]. The PAC loading rate is another critical factor that determines the success of PAC valorisation. For instance, studies on the tolerance of anaerobic digestion towards increasing concentrations of PAC as substrate reported that loadings of 3 % were inhibiting methanogenesis [73]. Similarly, a study examining methane production during the anaerobic digestion of PAC derived from non-catalyzed pyrolysis of sewage sludge reported severe methanogenesis inhibition at PAC loads of 2.3 g_{COD}/L. A 6 % load of a wastewater generated from the hydrothermal liquefaction of cyanobacteria inhibited of 50 % the methanogenic activity of an anaerobic sludge [50]. During the anaerobic digestion of a post-hydrothermal liquefaction wastewater, increasing toxicity as result of increasing loads from 10 % to 50 % resulted in decreased chemical oxygen demand (COD) removal rates from 76.8 % to 36.8 % [74].

The complexity of PAC is compounded by the presence of hundreds of compounds, some of which remain poorly characterized and lack model parameters in databases, posing challenges in assessing their specific inhibitory effects on microbial activity [19], [29]. Many studies have highlighted how the concentrations of individual compounds do not exceed previously reported inhibitory thresholds, concluding that the inhibitory effects of PAC result from the synergistic action of multiple toxicants [73]–[78]. Nevertheless, there are numerous documented instances of PAC component degradation during anaerobic digestion, albeit with varying removal rates and COD removal efficiencies. These differences can be attributed to the composition of PAC since the degradation of specific PAC components can be significantly influenced by the presence of other toxic compounds. For instance, in an anaerobic UASB fed with a wastewater containing 900 mg/l of phenol and 320 mg/l of *m*-cresol, removal efficiencies as high as 98 % and 20 % were recorded for phenol and *m*-cresol, respectively, but phenol availability was considered limiting *m*-cresol removal [79]. Vice versa, *m*-cresol highly affected phenol biodegradation in another work [80]. Another work reports of pyridine degradation inhibition at phenol concentrations exceeding 400 mg/L [81]. Contrarily, in a methanogenic anaerobic continuous reactor fed with 150 mg/L phenol and with 35 mg/L of *o*- and *p*-cresol (0.25 days hydraulic retention time and a loading rate of 880 mg/L/day), a 98 % removal rate was recorded for all substrates [82]. Figure 3 reports the putative degradation pathways of some selected PAC components. In methanogenic environments, anaerobic cultures have been reported to be degrading phenol into short-chain carboxylates and methane. Benzoyl-CoA is the central intermediate during anaerobic degradation of phenol via 4-hydroxybenzoate. Benzoyl-CoA is later converted via β -oxidation ring opening into three molecules of acetyl-CoA and further converted to acetate [76], [83].

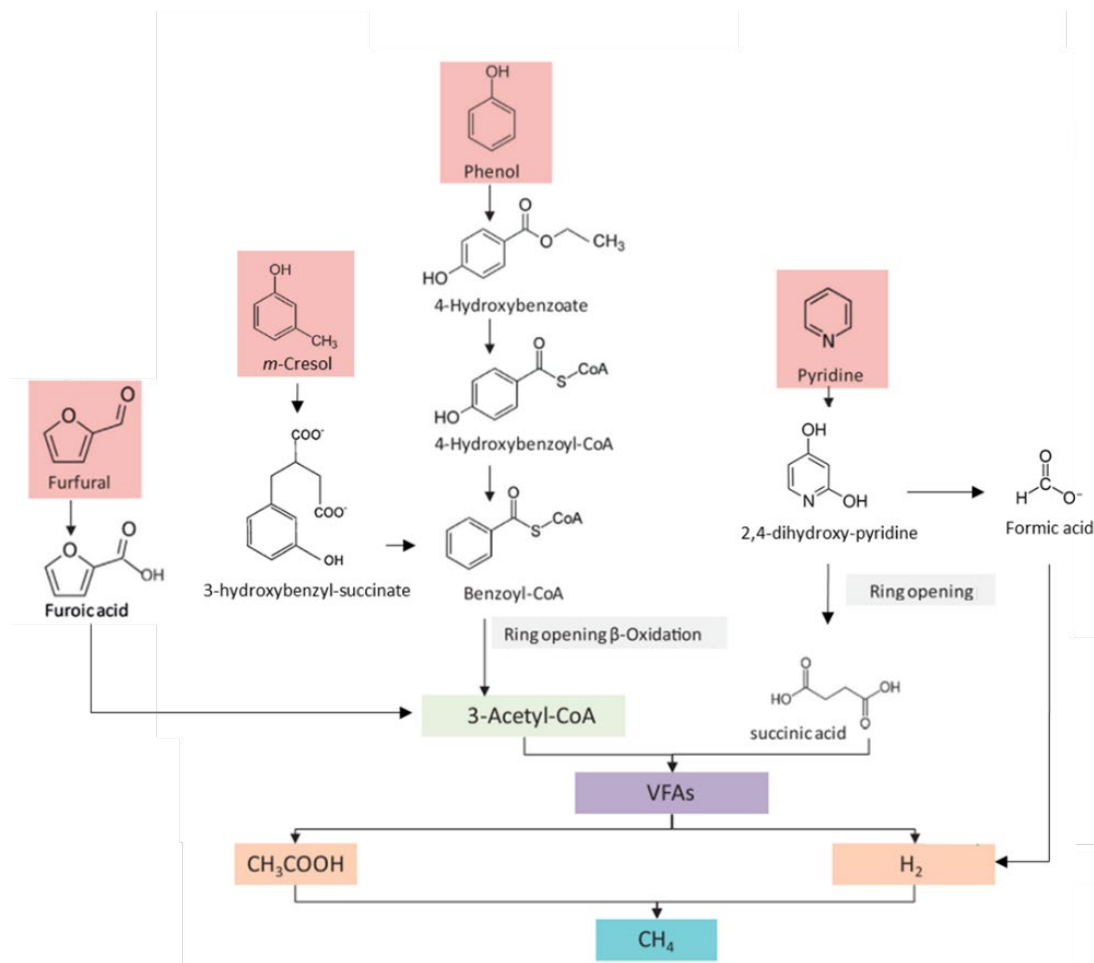


Figure 3. Putative anaerobic degradation pathways of some selected PAC components. Adapted from [76].

Anaerobic cresols degradation depends on the position of the hydroxyl group affecting also the anaerobic degradability. *m*-cresol, for instance, is generally accounted as the most recalcitrant to anaerobic degradation [84]. Nonetheless, during *m*-cresol degradation, fumarate is added to the methyl group of *m*-cresol to form 3-hydroxybenzyl succinate. Activation and β -oxidation lead to succinyl-CoA and 3-hydroxybenzoyl-CoA [80]. Furfural was reported to be firstly converted to furfuryl alcohol due to its weaker toxicity than furfural and further transformed into furoic acid. Finally, acetate can be produced from furoic acid [76]. N-heterocyclic components such as pyridine, although recalcitrant, have been reported to be converted into carboxylates and methane [69], [76], [85], [86]. Pyridine can undergo hydroxylation, ring cleavage between C1-C3, opening of the nitrogen ring and release of ammonium with formic and succinic acid as intermediate metabolites of its degradation. Increasing TAN concentrations are considered reflection of the degree of degradation of N-heterocyclic compounds. Methane was then produced directly from formic acid or from the acetate produced via succinic acid [76], [86]–[88]. The degradation of PAC components requires the synergistic activity of different microbial groups, including acidogens and methanogens, hence the presence of methanogens is crucial for the continuous anaerobic degradation of organic compounds in

anoxic environments, ensuring a balance between H₂ production and consumption [68].

Strategies such as sludge acclimation or the addition of suitable amendments such as biochar effectively mitigated toxic compounds inhibition, resulting in improved process performances and methane production [20], [24], [72], [73], [84], [85], [89]–[99]. Continuous processes allow for the acclimation of the inoculum and the enrichment of specific trophic groups, leading to improved chemical oxygen demand (COD) recoveries at higher PAC loads. The taxonomic profiling of the anaerobic communities acclimatized to different PACs showed abundance of anaerobic bacteria belonging to the genera *Longilinea*, *Acidobacterium*, and *Sedimentibacter* [73], or *Streptococcus*, *Acetobacterium*, *Bifidobacterium*, and *Megapshera* in another work [100]. *Alcaligenes*, *Petrimonas*, *Desulfobulbus* and *Sedimentibacter* were other genera enriched during the continuous anaerobic digestion of the wastewater from the hydrothermal liquefaction of rice straw [101][102]. Microorganisms belonging to the families of *Anaerolineaceae*, *Burkholderiaceae*, *Peptostreptococcaceae* and various acetogenic syntrophic bacteria were linked to the shortening of the lag-phase and to increasing rates of hydrothermal liquefaction wastewater detoxification [99]. Bacteria belonging to genera such as *Desulfovibrio*, *Geobacter*, *Bacillus*, *Parageobacillus*, and *Syntrophorhabdus*, among others, have been found able to degrade many components present in PAC to produce acetate and other carboxylic acids [76], [103]. In some other cases, methanogenic syntrophic associations of strictly anaerobic bacteria *Syntrophorhabdus* sp. and hydrogenotrophic methanogens such as *Methanobacterium* or *Methanoculleus* were reported during the anaerobic digestion of phenolic compounds [68], [83], [104], [105].

Fermentative and acidogenic microorganisms are pivotal in the degradation of PAC components and their enrichment or bio-augmentation could serve as a viable strategy to enhance PAC degradation and overall process performance [106]. Other studies have documented the accumulation of carboxylates alongside concurrent methanogenesis inhibition during the anaerobic digestion of PAC derived from corn stalk pellets [97], [100], highlighting the higher tolerance fermentative and acidogenic microorganisms to PAC components toxicity compared to methanogens. Such findings suggest the potential to develop processes aimed at producing carboxylates rather than biogas from PAC degradation.

1.3.2 Syngas as substrate for anaerobic mixed cultures

Syngas fermentation is a biotechnological process that is gaining attention due to its promising potential to transform gaseous waste such as CO and H₂/CO₂ into

valuable products contributing to a future zero-waste economy. Syngas fermentation has been explored for the production of biopolymers, single cell proteins, medium-chain fatty acids and other valuable compounds, showcasing its potential and versatility [107]. Carbon monoxide and/or CO₂ fermentation can be performed by aerobic and anaerobic microorganisms. Aerobic knallgas bacteria such as *Cupriavidus necator*, for instance, are currently employed for the production of single cell proteins as additives for animal feed from H₂/CO₂. Anaerobic gas fermentation, on the other hand, is performed by a specific group of anaerobic bacteria called acetogens. Acetogens such as *Clostridium ljungdahlii*, *Clostridium autoethanogenum*, *Acetobacterium woodii* and *Moorella thermoacetica* employ the Wood-Ljungdahl pathway to fix CO and H₂/CO₂, producing acetyl-CoA as the central intermediate [108]. The Wood-Ljungdahl (Figure 4) pathway consists of two parallel pathways, the methyl branch and the carbonyl branch. In the methyl branch, CO₂ is reduced to formate via formate dehydrogenase. Formate is then attached to tetrahydrofolate to form formyl-tetrahydrofolate at the expenses of one ATP. Formyl-tetrahydrofolate undergoes several reductive steps catalysed by enzymes including methylene-THF cyclohydrolase, methylene-THF dehydrogenase and methylene-THF reductase. Methyltransferase transfers the methyl group from methyl-THF to a corrinoid-FeS protein later used as the methyl group for the synthesis of Acetyl-CoA. In the carbonyl branch, CO can be either used directly or generated from CO₂ via a CO dehydrogenase providing the carbonyl group for acetyl-CoA synthesis. Acetyl-CoA is then converted into acetate via phosphotransacetylase and acetate kinase generating one ATP [109], [110]. During autotrophic growth, homoacetogens gain ATP thanks to the ion-motive force maintained generated via a transmembrane chemiosmotic potential generated by ion export complexes such as the Rnf or Ech complex and exploited by transmembrane ATP synthases for ATP synthesis. While the methyl branch is found from bacteria to humans, the carbonyl branch is unique to acetogens, methanogens and sulfate reducers. However, in methanogens the methyl branch involves different C₁-carriers, cofactors, electron transporters and enzymes [111]. The product pool of acetogens in single culture fermentation ranges from carboxylates such as formate, lactate, acetate, butyrate, caproate to solvents like ethanol, butanol, 2,3-butanediol and hexanol [107].

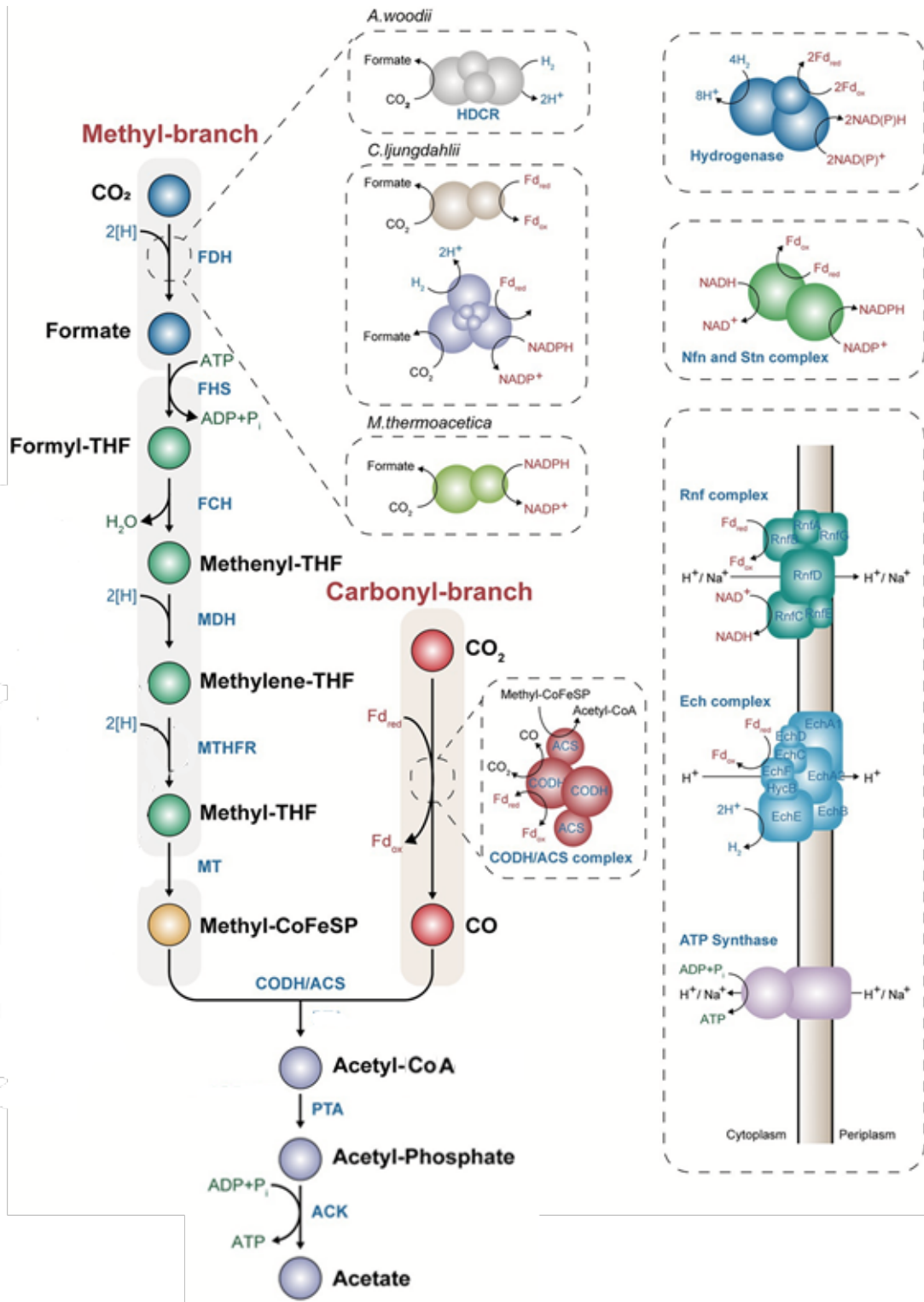


Figure 4. Scheme of the Wood–Ljungdahl pathway and energy conservation. The Wood–Ljungdahl pathway and energy conservation system in acetogens. CO, carbon monoxide; CO₂, carbon dioxide; THF, tetrahydrofolate; FDH, formate dehydrogenase; FHS, formyl-tetrahydrofolate synthase; FCH, formyl-cyclohydrofolate; MDH, methylene-tetrahydrofolate dehydrogenase; MTHFR, methylene-tetrahydrofolate reductase; MT, methyltransferase; CoFeSP, corrinoid iron–sulfur protein; CODH, CO dehydrogenase; ACS, acetyl-CoA synthase; PTA, phosphotransacetylase; ACK, acetate kinase; HDCR, hydrogen-dependent CO₂ reductase; Fdox, oxidized ferredoxin; Fdred, reduced ferredoxin. Adapted from [112].

Mixing two species together for synthetic cultures can improve the product spectrum for the production of octanol, for instance [113]. Similarly, mixed anaerobic cultures can be used for syngas fermentation offering some advantages compared to axenic processes such as lower capital costs (due to reduced requirements of equipment for sterilization, for instance) and higher process resilience to process perturbations.

Table 1. Most significant reactions in syngas fermentation with anaerobic mixed cultures. Adapted from [114], [115]. ΔG_r° is the Gibbs free energy of reaction for biochemical standard conditions (T= 298.15 K, activities equal to 1 and pH=7).

Reaction	$\Delta G_r^{\circ}/\text{reaction}$
Syngas fermentation	
Hydrogenotrophic acetogenesis $4\text{H}_2 + 2\text{CO}_2 \rightarrow \text{CH}_3\text{COO}^- + \text{H}^+ + 2\text{H}_2\text{O}$	- 95.1
Carboxydrotrophic acetogenesis $4\text{CO} + 2\text{H}_2\text{O} \rightarrow \text{CH}_3\text{COO}^- + \text{H}^+ + 2\text{CO}_2$	- 175
Hydrogenotrophic solventogenesis $6\text{H}_2 + 2\text{CO}_2 \rightarrow \text{CH}_3\text{CH}_2\text{OH} + 3\text{H}_2\text{O}$	- 105
Carboxydrotrophic solventogenesis $6\text{CO} + 3\text{H}_2\text{O} \rightarrow \text{CH}_3\text{CH}_2\text{OH} + 4\text{CO}_2$	- 224
Acetate reduction to ethanol with H_2 $\text{CH}_3\text{COO}^- + \text{H}^+ + 2\text{H}_2 \rightarrow \text{CH}_3\text{CH}_2\text{OH} + \text{H}_2\text{O}$	- 9.64
Acetate reduction to ethanol with CO $\text{CH}_3\text{COO}^- + \text{H}^+ + 2\text{CO} + \text{H}_2\text{O} \rightarrow \text{CH}_3\text{CH}_2\text{OH} + 2\text{CO}_2$	- 49.6
Carboxydrotrophic hydrogenogenesis (Water gas shift reaction) $\text{CO} + \text{H}_2\text{O} \rightarrow \text{H}_2 + \text{CO}_2$	- 20.0
Chain elongation	
Ethanol-acetate elongation to <i>n</i> -butyrate $\text{C}_2\text{H}_5\text{OH} + \text{CH}_3\text{COO}^- \rightarrow \text{CH}_3(\text{CH}_2)_2\text{COO}^- + \text{H}_2\text{O}$	- 38.6
Ethanol-butyrate elongation to <i>n</i> -caproate $\text{C}_2\text{H}_5\text{OH} + \text{CH}_3(\text{CH}_2)_2\text{COO}^- \rightarrow \text{CH}_3(\text{CH}_2)_4\text{COO}^- + \text{H}_2\text{O}$	- 38.8
Ethanol-propionate elongation to <i>n</i> -valerate $\text{C}_2\text{H}_5\text{OH} + \text{CH}_3\text{CH}_2\text{COO}^- \rightarrow \text{CH}_3(\text{CH}_2)_3\text{COO}^- + \text{H}_2\text{O}$	- 57.7
Pathways involved in methanogenesis	
Hydrogenotrophic methanogenesis $4\text{H}_2 + \text{CO}_2 \rightarrow \text{CH}_4 + 2\text{H}_2\text{O}$	- 131
Acetoclastic methanogenesis $\text{CH}_3\text{COO}^- + \text{H}^+ \rightarrow \text{CH}_4 + \text{CO}_2$	- 35.7
Carboxydrotrophic methanogenesis $4\text{CO} + 2\text{H}_2\text{O} \rightarrow \text{CH}_4 + 3\text{CO}_2$	- 210.9
Syntrophic acetate oxidation $\text{CH}_3\text{COO}^- + \text{H}^+ + 2\text{H}_2\text{O} \rightarrow 4\text{H}_2 + 2\text{CO}_2$	+ 104.6

In anaerobic communities, syngas can be metabolized by methanogenic archaea, hydrogenogenic bacteria, acetogenic bacteria and sulfate-reducing bacteria [116]. Table 1 and Figure 5 report the most significant reactions in syngas fermentation with anaerobic mixed cultures. By manipulating the fermentation environmental conditions such as temperature, pH, organic loading rate and hydraulic retention

time, it is possible to control the syngas conversion towards different catabolic routes [114], [117]–[119].

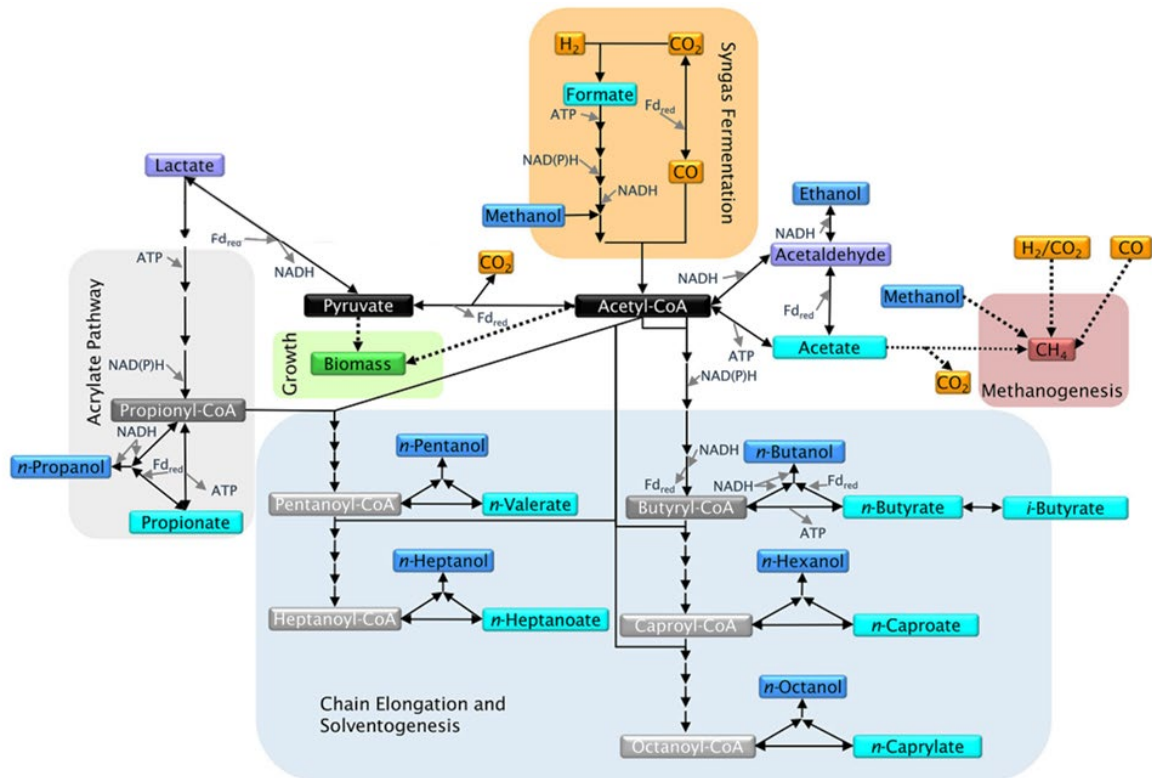


Figure 5. Overview of the general metabolism of anaerobic mixed cultures fed with syngas. Adapted from [114].

Methane is often the primary metabolite having the lowest free energy content per electron, regardless of the temperature range [119]–[121]. Acetate, formate and H_2/CO_2 are central metabolites and interspecies electron donors in methanogenic environments [122]–[125]. Acetoclastic methanogenesis is generally the preferential methanogenic pathway at mesophilic conditions and neutral pH [126]. Hydrogenotrophic methanogenesis via syntrophic acetate oxidation, on the other hand, is the preferable route to methane production in mixed cultures at low pH and high acetate concentrations. Additionally, thermophilic conditions provide advantage to the syntrophic acetate oxidizers and hydrogenotrophic methanogens as dominant acetate consumers at the expense of acetoclastic methanogens [115]. Syntrophic acetate oxidation is favorable at low H_2 partial pressures, hence it can occur only in association with H_2 -consuming reactions such as hydrogenotrophic methanogenesis [40], [126].

On the other hand, when methanogenesis is inhibited and in mesophilic environments with electron donors such as ethanol, H_2 and/or lactate, the mixed culture can elongate C1 compounds from syngas into short- (SCCs) and medium-chain carboxylates (MMCs). Such wide array of metabolic products at mesophilic temperatures is the result of an intricate metabolic network ultimately limited by thermodynamics [127]. Thermophilic temperatures, on the other hand, promote higher water-

gas shift reaction kinetics at the expenses of a smaller product pool, with H₂ and short-chain carboxylates being the primary products [128].

The production of MCCs via mixed culture anaerobic fermentation is gaining more scientific and industrial interest for their use as specialty chemicals, food additives and fuel precursors [129], [130]. This process is generally referred to as chain elongation and involves a pathway known as reverse β -oxidation. The reverse β -oxidation pathway is a cyclic process that adds an acetyl-CoA derived from ethanol to a carboxylate, elongating its carbon chain length two carbons at a time. Other electron donors for chain elongation could be CO and H₂ from syngas [119]. Integration of syngas fermentation and chain elongation has already been tested [131], [132]. In syngas chain-elongating processes, the acetate and ethanol required for MMCs production is generated via syngas fermentation from homoacetogenic reactions from CO and/or H₂/CO₂.

Nevertheless, the success of technologies for the production of H₂, SCCs or MCCs is only achievable by inhibiting competing pathways such as methanogenesis. Other works achieved this by using specific methanogenesis inhibitors [133]–[136] or by a specific process design [137]. For instance, researchers have been using CO at high partial pressures [49], [116], [138] to inhibit methanogens or low pH to increase the concentrations of undissociated carboxylic acids [139], [140].

In an alternative approach to waste methanation, acetate and the other carboxylic acids could subsequently be utilized as feedstock in secondary bioprocesses.

1.4 Carboxylic acids as substrates for biological processes

Nowadays, nearly 90 % of the total market demand for carboxylic acids is satisfied via the petroleum-based thermochemical production route. However, the depletion of fossil fuels and the environmental impact of conventional processes are pushing the development of technological advancements towards more sustainable bio-based methods. Syngas fermentation and methane-arrested anaerobic fermentation of waste streams are among the technologies that can contribute to the development of a bioeconomy and biorefinery concept [141], [142].

The acetic acid production via syngas fermentation is a promising alternative to other industrial large-scale production platforms. Acetogenic microorganisms that produce solely acetate from C₁ compounds are *Acetobacterium backii*, *A. woodii*, *Clostridium aceticum*, *M. thermoacetica* and *Thermoanaerobacter kivui* among others [112]. Albeit much lower compared to other established processes, the titers of acetate currently achieved in a lab scale process are as high as 59 g/L recorded during the continuous fermentation of H₂/CO₂ with *A. woodii* [143], [144]. The acetate generated via homoacetogenesis can be further upgraded via secondary fermentative stages into bioproducts with higher market value [144]. Some works

have already investigated the two-stage concept for single cell protein, malic acid, lipids and polyhydroxyalkanoates [145]–[150]. Several industrially relevant biocatalysis such as *Escherichia coli*, *Corynebacterium glutamicum*, *Pseudomonas putida*, *Cupriavidus necator*, *Cryptococcus curvatus*, *Yarrowia lipolitica*, *Rhodotorula glutinis* and *Aspergillus oryzae* are some microorganisms naturally capable of growing on acetate. Products of acetate fermentation can be very wide ranging from platform chemicals, to bioplastics or biofuels, depending on the microbial chassis of choice [144]. Similarly to acetic acid-rich effluents, also mixed SCCs solutions produced by anaerobic mixed culture fermentation can have multiple applications as substrate for further bioprocessing technologies for the production of bioplastics, biofuels, microbial oils/lipids, chemicals such as esters, ketones, aldehydes, alcohols and alkanes and as carbon source in nitrogen and phosphorus removal from wastewaters [151]–[155].

Utilizing carboxylic acids as substrates could provide also some process advantages. At the secondary stage, the microbial acetate metabolization and conversion into products would be associated with an increase of the pH. The acetate-rich medium from stage one could be used as both titrating agent and feed in the second stage in a pH coupled feeding strategy, reducing the need of salts and consequently costs of titration. This strategy has been already proven successful during malic acid production from acetate with *A. oryzae* in a lab scale setup [156].

1.4.1 L-malate production from carboxylic acids with *Aspergillus oryzae*

Aspergillus oryzae belongs to the Ascomycetes group and its industrial application spans from food processing to commodity chemicals production [157], [158]. Several studies have evaluated the potential of producing biochemicals, biofuels or cell biomass (single cell proteins) with *A. oryzae* from carboxylates-rich waste streams or from acetate [159]–[161]. One product of the glyoxylate pathway from the acetate metabolism of *A. oryzae* is L-malate [162]. L-malate has a wide array of applications, ranging from taste-enhancer in the food industry to biopolymer production [162]. In 2004, L-malate was regarded as one of the 12 most important biomass-derived biochemicals [163]. In 2020, the annual global L-malate production was estimated to be around 80 000 to 100 000 tons, whilst the market demands up to 200 000 tons per year, a value expected to increase in the following years [162]. L-malate production from non-food feedstock could be an economical and efficient way to meet market needs [164].

Several works have focussed on L-malate production from acetate with *A. oryzae*. L-malate production was reported to be highly dependent on acetate concentration with the highest yield 0.20 grams of malic acid per gram of acetate for concentrations of 40 g/L. Higher concentrations of acetate did not affect the yield [161]. Other researchers presented a process concept, in which malate was produced from

acetate generated from syngas fermentation by *C. ljungdahlii* [148]. L-malate production by *A. oryzae* in the medium from the syngas fermentations with acetate as sole carbon source reached yields of 0.33 grams of malate per gram of acetate [148]. The overall conversion of CO and H₂ into malate was calculated to be 0.22 g malate per gram of syngas [148]. Similarly, *A. oryzae* can utilize SCCs from the anaerobic digestion of food waste, with concentrations of acetate of about 9 g/L, to yield 0.29 g_{CDW}/g_{SCCs} [165].

Moreover, the fungus was reported to tolerate small concentrations of pyrolysis oils and various PAC components. Previous works have evaluated the inhibitory effects on *A. oryzae*'s growth of some components generally found in the PAC generated from the fast pyrolysis of lignocellulose biomass. Phenolic compounds such as phenol, *o*-, *m*-, *p*-cresol and guaiacol resulted in a strong inhibition of growth even at low concentrations [166]. Although *A. oryzae* possesses genes encoding for enzymes enabling the degradation of cresols, it only tolerates cresol in very low concentrations. Among the compounds tested, 2-cyclopenten-1-one was reported to be the most toxic compound among the tested ones. *A. oryzae* proved to be able to produce L-malate growing on the acetate contained in pre-treated PAC from wheat straw [63], positioning it as an ideal candidate for the conversion of pre-treated PAC [63], [167].

1.5 Integrating thermochemical and biological processes for waste valorisation

Currently, coal gasification and steam reforming of natural gas stand as the primary methods for syngas production, albeit generating substantial greenhouse gas emissions. Conversely, the steel-manufacturing industry and thermochemical conversion of waste offer alternative sources of syngas characterized by lower greenhouse gas emissions [168]. However, with ongoing technological advancements in electrolysis for hydrogen production, there is potential for steel-manufacturing industries to achieve full decarbonization of their processes [169], leaving thermochemical conversion of waste as one of the remaining sources of syngas.

As previously emphasized, waste pyrolysis presents significant technological potential due to its versatility in treating various waste streams, ranging from agricultural residues and sewage sludge to mixed plastics, thereby contributing to the needs of an evolving bio-based economy [170]. Moreover, technologies like gasification and pyrolysis can serve as preliminary treatments [171], circumventing challenges associated with low hydrolysis rates by converting biomass into syngas, improving conversion rates.

Several investigations have already explored the complete integration of pyrolysis and anaerobic digestion for methane production. In a recent study, the utilization of a real syngas generated from a two stage pyrolysis process treating food waste, resulted in significantly improved methanation rates, yielding nearly 100 % more CH₄ compared to fermentations using synthetic syngas as control [172]. Other works have evaluated the effects of adding all pyrolysis by-products, including biochar, PAC and syngas, into an anaerobic digester. While the biochar produced during the thermochemical treatment of the biomass can act as support for biofilm formation or absorption matrix for the removal of some PAC toxicants improving methanation rates, incorporating syngas as a substrate has the potential to enhance energy recovery while minimizing gaseous emissions [92], [97], [173]. During the continuous fermentation of syngas and increasing loadings of PAC derived from the pyrolysis of fir sawdust in a mesophilic biochar-packed bioreactor, the acclimatized microbiota recovered an average of 82 % COD, yielding 45 % of the COD input into carboxylates. Approximately 46 % of the CO fed was consumed, but syngas accounted for only 5 % of the total COD input. While the unreacted/recalcitrant COD fraction from PAC in the effluent was estimated between 25 % to 52 % [100].

Techno-economical assessments have also highlighted the potential of integrating thermochemical and biological processes to improve carbon and energy recovery and to minimize the environmental impact of waste. The economic feasibility of the process is subject to several factors and depends primarily upon location and overall process design. For instance, initial assessments of integrating anaerobic digestion, hydrothermal liquefaction, and biomethanation systems appeared economically feasible only with subsidies. However, further studies demonstrated that this integrated approach not only maximizes resource recovery but also mitigates environmental impacts associated with dairy farming [174]. Recovering internal heat and power emerged as a critical factor in achieving significant reductions in external energy demands, thereby lowering environmental risks and costs [175]. In another case study, the enhanced energy recovery from the integrated process resulted in increased annual revenues [176]. Nevertheless beyond specific cases, there is a widespread acknowledgment of the potential of integrated systems for improving energy and resource recovery, reducing environmental impacts and greenhouse gas emissions, and producing carbon-negative fuels [20], [173]–[175], [177]–[180]. Furthermore, integrated systems offer additional advantages such as reduced digestate and PAC management costs, with potential economic benefits in terms of waste disposal cost reduction and reduced reliance on external energy procurement [181].

While the energy and economic advantages of integrated processes could alone bolster the economic sustainability of large-scale industrial operations [60], [63],

[106], all the positive environmental implications should promote the further development of integrated technologies that aim to enhance resource circularity, mitigate environmental impacts and decrease the dependence on fossil fuels.

1.6 Open questions and research proposal

The potential of thermochemical and biological processes in waste management has been thoroughly discussed and it has emerged as viable technology to maximise energy recovery and minimize environmental impacts via reducing greenhouse gases emissions and detoxifying pyrolysis wastewater.

The anaerobic digestion of PAC holds promise for substantial biodegradation of the organics present in PAC, thereby reducing its toxicity. By integrating pyrolysis and anaerobic digestion, it becomes feasible to produce biogas, a mixture of H₂ and CH₄, or SCCs. Microbial adaptation and the addition of amendments like biochar further enhance process efficiency. Overall, anaerobic digestion of the aqueous phase of pyrolysis offers a promising avenue for sustainable waste treatment and bioenergy generation.

Similarly, the syngas platform for CH₄ or carboxylates production is gaining importance for the production of carbon negative compounds. The integration of the anaerobic digestion of organic waste with syngas has been shown to significantly enhance CH₄ production. Alternatively, the integration of syngas into chain elongation processes has shown promise in enhancing process efficiency providing additional electron donors, crucial for the progressive reduction of SCCs into longer ones.

Despite syngas and PAC being generated from the pyrolysis process, knowledge about syngas and PAC co-fermentation is practically non-existent, leaving numerous questions unanswered:

- Can we establish a multifunctional process performing simultaneously carbon capture and wastewater detoxification?
- Can mixed cultures co-ferment syngas and PAC?
- Do mixed cultures degrade PAC components? Is PAC detoxified below inhibitory levels?
- How do different pyrolysis feedstocks affect syngas and PAC co-fermentation and energy recovery?
- What microorganisms are involved in the co-fermentation?
- Is it possible to establish continuous fermentation of syngas and PAC? What are the critical parameters?
- Is it possible to develop a two stage process for the conversion of syngas and PAC into commodity chemicals with carboxylates as metabolic intermediates?

These questions served as the motivation for this work. It was initially assumed that anaerobic mixed cultures could perform mixotrophic fermentation of syngas and PAC and that it is possible to steer community metabolism towards carboxylic acids by manipulating process parameters such as temperature, pH and PAC load. Figure 6 illustrates a simplified diagram of the putative metabolic network of mixotrophic anaerobic cultures co-fermenting syngas and PAC.

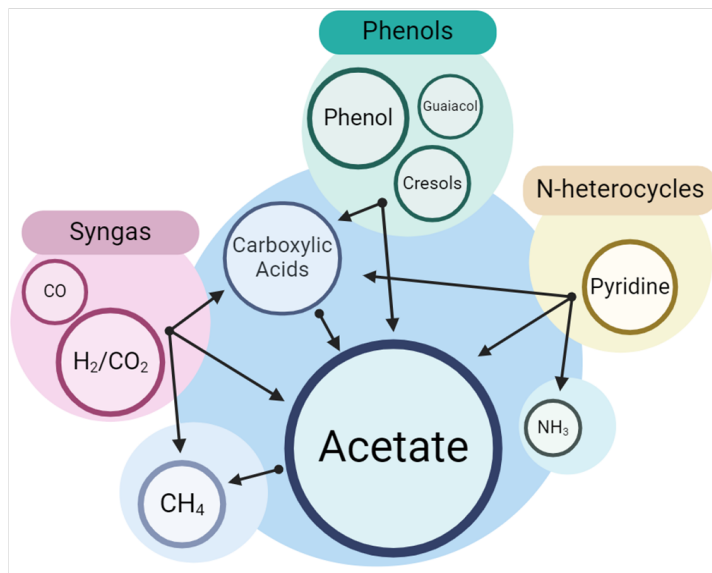


Figure 6. Schematic diagram of the putative metabolic network of mixotrophic anaerobic cultures co-fermenting syngas and PAC. Created with BioRender.com

At start, the potential of a synthetic acetate-rich wastewater as co-substrate during syngas fermentation with anaerobic mixed cultures was evaluated across different pH levels (6.7 and 5.5) and temperatures (37°C and 55°C) in 250 mL serum bottles, assessing microbial kinetics, metabolite production and microbial community composition.

Then the co-fermentation of syngas and a real PAC with mixed cultures was tested at pH 6.7, different temperatures (37°C and 55°C) and increasing PAC loads in 250 mL serum bottles, identifying products pool, PAC inhibitory concentrations and removal of PAC components. The carboxylates product of the mixed culture co-fermentations were then valorised with *Aspergillus oryzae* into L-malate as proof of concept of the two stage process.

Further research aimed to investigate how the composition of PAC derived from sewage sludge and polyethylene plastics pyrolysis affects the co-fermentation and energy recovery potential. Experiments were performed at mesophilic and thermophilic (37°C and 55°C) conditions and increasing loads of the different PACs in 250 mL serum bottles, identifying products pool, PACs inhibitory concentrations, removal of PAC components and energy recovery.

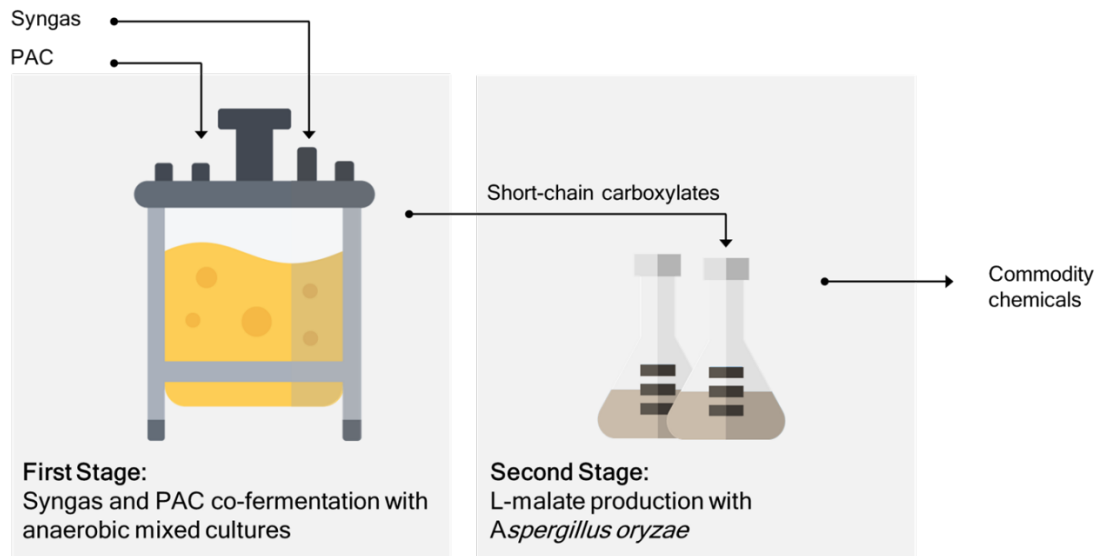


Figure 7. Scheme of the two-stage process developed in this work. In the first stage, syngas and PAC are co-fermented with anaerobic mixed cultures. Process parameters are adjusted in order to inhibit methanogenesis leading to the accumulation of carboxylates in the fermentation medium. After centrifugation/filtration the effluent from stage one is fed to a secondary fermentative stage for the production of commodity chemicals. In the case of this work, the carboxylates were converted into L-malate with *Aspergillus oryzae*.

At last, we tested the first-stage in a continuous setting in stirred tank reactors under mesophilic (37°C) and thermophilic (55°C) conditions at pH of 5.5 and increasing PAC loading rates, evaluating product pool of the co-fermentation with particular attention to electron balancing and composition of reactors' microbiota. The carboxylates-rich effluent from the mesophilic and thermophilic processes then valorised with *Aspergillus oryzae* into L-malate as proof of concept of the viability of the two-stage process in a continuous setting.

2. Acetate-rich wastewater as co-substrate in mixed culture syngas fermentation

This chapter is based on the publication:

Enhancing CO uptake rates of anaerobic microbiomes via acetate shock loading. Alberto Robazza, Ada Raya i Garcia, Flávio C. F. Baleeiro, Sabine Kleinsteuber and Anke Neumann

Manuscript submitted to publication

Author's contributions

Alberto Robazza	conceptualization, methodology, investigation, data curation and analysis, visualization, first draft and manuscript revision
Ada Raya i Garcia	conceptualization, methodology, investigation and data curation and analysis
Flávio C. F. Baleeiro	conceptualization, methodology, data analysis, visualization and manuscript revision
Sabine Kleinsteuber	conceptualization, methodology, data analysis support and manuscript revision
Anke Neumann	conceptualization, methodology, data analysis support, project supervision and manuscript revision,

2.1 Introduction

Lignocellulose biomass stands out as a primary renewable source of carbon and energy, offering a sustainable alternative to fossil-derived materials [6]. However, due to the intricate polymeric structure and recalcitrant nature of the lignin within biomass, pretreatment technologies are essential to enhance conversion and recovery efficiencies [9]. Physiochemical and thermochemical conversion processes are possible pathways for the valorization of lignocellulose biomass into substrates available to secondary processes. Acetate is a common compound present in both process waters generated during hydrolysis or pyrolysis of lignocellulose biomass [31], [182]. During the hydrolysis of biomass, acetate is formed as a major by-product from the enzymatic hydrolysis reaching up to 20 g/L [182], [183]. During pyrolysis the lignin, cellulose and hemicellulose fractions undergo depolymerisation and deacetylation/cracking reactions producing acetate as by-product [31]. The acetate contained in the pyrolysis vapors undergoes condensation through a series of units, ultimately concentrating in an aqueous condensate. This condensate stands as wastewater of pyrolysis and is produced alongside with other products such syngas (a mixture of gases including CO, CO₂ and H₂), biochar and biooil.

To fully optimize and utilize all components of lignocellulosic biomass, it is crucial to recover secondary products such as process water and syngas generated during its conversion and transform them into valuable products [184]. Biological processes offer a promising approach to valorize these residues thanks to their versatility and variety of products such as biofuels, biochemicals and bioplastics [6], [9], [185], [186]. However, both process waters can contain toxic compounds that inhibit microbial activity. Inhibitory compounds commonly found in both wastewaters are phenolics, furans, organic acids and heavy metals [76], [187]–[190]. Anaerobic digestion stands out as a promising technology for wastewater valorization into CH₄, owing also to its increased resilience to the toxicity compared to axenic processes [191], [192]. This process relies on the metabolic interplay of various microorganism groups to execute diverse parallel reactions with acetate as central metabolic intermediate [126], [193]. Anaerobic cultures are pivotal for organic waste and wastewater management, enabling nutrient and energy recovery into biogas. Moreover, anaerobic microbiomes can exhibit tolerance to carbon monoxide toxicity in syngas. The microorganisms able to convert CO are also called carboxydrotrophs. Within anaerobic microbiomes, the products of their metabolism such as H₂/CO₂ or acetate can be directly utilized by methanogens to generate methane [49], [194]. The integration of anaerobic digestion of organic waste with syngas has been shown to significantly enhance methane production through syngas biomethanation [195], [196]. Alternatively, in scenarios where methanogenesis is inhibited, anaerobic mixed cultures have demonstrated the capacity to accumulate

short- and medium-chain carboxylates through a process known as chain elongation. The integration of syngas into chain elongation processes has shown promise in enhancing process efficiency providing additional electron donors, crucial for the progressive reduction of short-chain carboxylates into longer ones [125], [197]. Moreover, the acetate produced from syngas fermentation by homoacetogens can undergo conversion in the presence of electron donors such as hydrogen, ethanol, or lactate, contributing to the production of longer-chain carboxylates [198], [199]. The production of these compounds from waste streams is gaining interest due to their high value and their potential to serve as biofuel precursors, thereby mitigating reliance on fossil fuels [114], [200].

Short-chain carboxylates, such as acetate, serve as both substrates for methanogenesis and chain elongation processes, yet they can also exert inhibitory effects on microbial activity. Consequently, the loading of acetate-rich wastewaters emerges as a crucial factor influencing microbial pathways and potential inhibition during syngas fermentation processes with anaerobic mixed cultures. Despite the significance of this factor, limited understanding exists regarding the co-fermentation dynamics of acetate-rich wastewater and syngas by anaerobic mixed cultures, particularly regarding how varying acetate loadings impact culture metabolism and product profiles. In this study, acetate was chosen as a model compound representing lignocellulose-derived wastewater due to its dual role as both a substrate and inhibitor in anaerobic digestion processes. The investigation focused on assessing the effects of increasing shock loads of acetate during syngas co-fermentation with unacclimated anaerobic mixed cultures. Batch bottle experiments were conducted at different pH levels (6.7 and 5.5) and temperatures (37°C and 55°C) to evaluate microbial kinetics, metabolite production and microbial community composition.

2.2 Materials and methods

2.2.1 Experimental setup, fermentation conditions and community analysis

Triplicates of each experimental condition (detailed in Table 2) were conducted in 250 mL serum bottles, each containing 50 mL of active volume, over a fermentation period of 16 days. The fermentation broth comprised 5 mL of sludge (10 v/v %), 5 mL of basal anaerobic (BA) medium (refer to Additional file 1, Table S1 for the composition), acetate (glacial acetic acid), 4M NaOH for pH adjustment and deionized water to reach a final volume of 50 mL. All chemicals were purchased from Sigma-Aldrich (Taufkirchen, Germany) or Carl-Roth (Karlsruhe, Germany). The sludge utilized in the experiments was obtained from an anaerobic digester treating cow manure, later sieved to 0.5 mm and stored under anaerobic conditions at 4°C. Total suspended solids and volatile suspended solids were quantified at 41.6 ± 0.2 g/L and 17.7 ± 0.1 g/L, respectively, employing previously established methodologies [201].

Table 2. Summary of the concentrations of acetate, acetic acid (HAc) and Na⁺ under the different experimental conditions.

Acetate [g/L]	pH 6.7			pH 5.5		
	Na ⁺ eq. [g/L]	HAc [g/L]		Na ⁺ eq. [g/L]	HAc [g/L]	
	37/55°C	37°C	55°C	37/55°C	37°C	55°C
0	0.85	0	0	0.22	0	0
1	1.21	0.01	0.01	0.51	0.16	0.17
2	1.58	0.02	0.02	0.85	0.31	0.33
4	2.5	0.05	0.05	1.49	0.63	0.67
6	3.6	0.07	0.07	2.13	0.94	1
8	3.97	0.09	0.1	2.87	1.25	1.33
12	7.1	0.14	0.15	3.79	1.88	2
16	7.83	0.19	0.2	4.89	2.51	2.67
24	11.69	0.28	0.3	7.28	3.76	4
32	15.37	0.37	0.4	9.67	5.02	5.34
40	18.5	0.46	0.5	11.73	6.27	6.67
48	22.17	0.56	0.6	14.62	7.53	8
56	24.38	0.65	0.7	16.75	8.78	9.34
64	29.16	0.74	0.8	20.33	10.04	10.67

Following the aliquoting of BA medium into each bottle, acetate was added and pH was adjusted to either 5.5 or 6.7. Deionized water was added to meet a volume of 44 mL. Subsequently, the serum bottles, deionized water and a 4M NaOH solution were transferred into an anaerobic tent containing 5% H₂ in N₂ to anaerobize overnight. The bottles were inoculated with the anaerobic sludge, the pH levels were readjusted to the desired values and any remaining volume was filled with anoxic deionized water. After sealing the bottles with rubber stopper and aluminium cap, the bottles underwent syngas flushing for 5 minutes, with a composition of 3 kPa H₂, 20 kPa CO, 25 kPa CO₂ and N₂ at a total flow rate of 1 L/min, followed by pressurization at room temperature up to a final absolute pressure of 210 kPa. The gas flow was controlled using high precision mass flow controllers from Vögtlin (Muttenz, Switzerland), while bottle's pressure was monitored utilizing a precision pressure indicator GMH 3100 Series (Greisinger, Mainz, Germany). Incubation was conducted at either 37° or 55°C and 210 rpm in two Thermotron shaker incubators (Infors, Bottmingen, Switzerland). Three millilitres of the gas phase were sampled daily or depending on the rates of CO consumption. When the partial pressure of the system was found to be below 180 kPa or when the CO concentration in the gas phase was below 1%, the bottles were first flushed and then repressurized according to the method described above. The molar concentrations of CO, CO₂, H₂, CH₄ and N₂ were

determined using an Inficon 3000 Micro GC System equipped with a Thermal Conductivity Detector (TCD), which employed a CP-Molsieve 5 Å column and a PoraPLOT Q column at 80°C, with argon and helium serving as carrier gases, respectively. One millilitre of the fermentation broth was sampled every second day and centrifuged. The supernatant was filtered and stored at -20° C for later analytics. The concentrations of formate, acetate, ethanol, propionate, *n*-butyrate and *n*-valerate in the initial and final sample of each fermentation were measured by high-performance liquid chromatography (HPLC) (Agilent 1100 Series, Agilent, Waldbronn, Germany). The HPLC was equipped with a Rezex ROA organic acid H+ (8%) column (300x7.8 mm, 8 µm; Phenomenex, Aschaffenburg, Germany) and a Rezex ROA organic acid H + (8%) guard column (50 by 7.8 mm) and run at 55°C with 5 mM H₂SO₄ at a flow of 0.6 mL/min. After the collection of the last sample, three 2 mL samples of the fermentation broth of each bottle were centrifuged for 15 min at 17,000 x g. The pellet was re-suspended in 1 mL of phosphate-buffered saline solution (pH 7.4) and underwent another round of centrifugation for 15 minutes at 17,000 x g. Upon removal of the supernatant, the pellets were stored at -20°C. Procedures for DNA extraction, sample purification, PCR and amplification were described previously [136]. Amplicon sequencing of the 16S rRNA (region V3-V4) and *mcrA* genes was conducted using the Illumina MiSeq platform. The library preparation for the visualization of the microbial community and elaboration of Spearman correlations was performed as described in another work [134].

2.2.2 Analytical methods and statistical analysis

The total amount produced or consumed of each gas specimen was calculated via the ideal gas law as described by Eq.1.

$$n_{\text{gas},i} = \sum_{t=0}^j \frac{p_j \cdot V_j}{R \cdot T} \text{ [mmol]} \quad \text{Eq.1}$$

Where $n_{\text{gas},i}$ is the cumulative consumption/production of a gas specimen *i*; p_j [Pa] is the pressure of the head space of the bottle at sampling time; V_j [m³] is the bottle's head space volume corrected for liquid sampling; R [J/mol/K] is the gas constant; T [K] is the incubation temperature; j is the number of samples.

Electron moles (e-mol) were used to quantify the consumption and production of chemical compounds within the cultures as described in previous works [30]. The determination of the e-moles space-time consumption/production rate for gases and metabolites was done following Eq.2.

$$q_{\text{e-mol},i} = \frac{n_i \cdot \text{eeq}_i}{V_{\text{start}} \cdot t} \text{ [e-mM/d]} \quad \text{Eq.2}$$

Where n_i [mmol] is absolute amount of each metabolite produced or consumed during the total fermentation time; eeq_i is the amount of the substance *i* which re-

leases 1 e-mol during complete oxidation (conversion tables are available in the Additional file 2, Table S2); V_{Start} [L] is the volume of the fermentation broth at the start of the fermentation; t [d] is the total fermentation time.

The e-mol recoveries were calculated as described in Eq. 3. Hydrogen gas and acetate are considered as substrates only when consumed, otherwise are products.

$$q_{\text{e-mol},i} = \frac{n_i \cdot e_{\text{eq}i}}{V_{\text{Start}} \cdot t} [\text{e-mM/d}] \quad \text{Eq.2}$$

Calculations were conducted individually for each bottle and the results were averaged across the replicates ($n=3$).

The library preparation for the visualization of the microbial community and elaboration of Spearman correlations was performed as described in another work [31].

The term acetic acid (HAc) used throughout this study refers only to the undissociated form of acetate. Acetate, on the other hand, refers to the sum of both the dissociated and undissociated form of acetate. The concentration of HAc was calculated using a derivation of the Henderson-Hasselbalch equation (Eq. 4), as described in another work [32].

$$\text{HAc} = \frac{C_{\text{Acetate}} \cdot C_{\text{H}^+}}{K_a + C_{\text{H}^+}} [\text{g/L}] \quad \text{Eq.4}$$

Where C_{Acetate} is the total concentration of acetate [mol/L], C_{H^+} is the proton concentration [mol/L], m is molecular mass of acetic acid [g/mol] and K_a is the dissociation constant [mol/L]. The K_a values for acetate were assumed to be $1.70 \cdot 10^{-5}$ [mol/L] and $1.58 \cdot 10^{-5}$ [mol/L] at 37°C and 55°C , respectively [202].

2.3 Results and discussion

The following sections discuss the effects of increasing acetate concentration at different pH (6.7 and 5.5) and temperature (37°C and 55°C) on the metabolism of anaerobic mixed cultures, on production yields, inhibitory effects and changes in community composition.

2.3.1 Syngas and acetate metabolism of anaerobic mixed cultures

Syngas constituents and acetate were converted into methane, SCCs and ethanol or H_2/CO_2 depending upon the environmental conditions and the thermodynamics of the various metabolic pathways involved. E-mol yields are reported in

Figure 8 (C-mol yields are available in the Additional file 1, Figure S1).

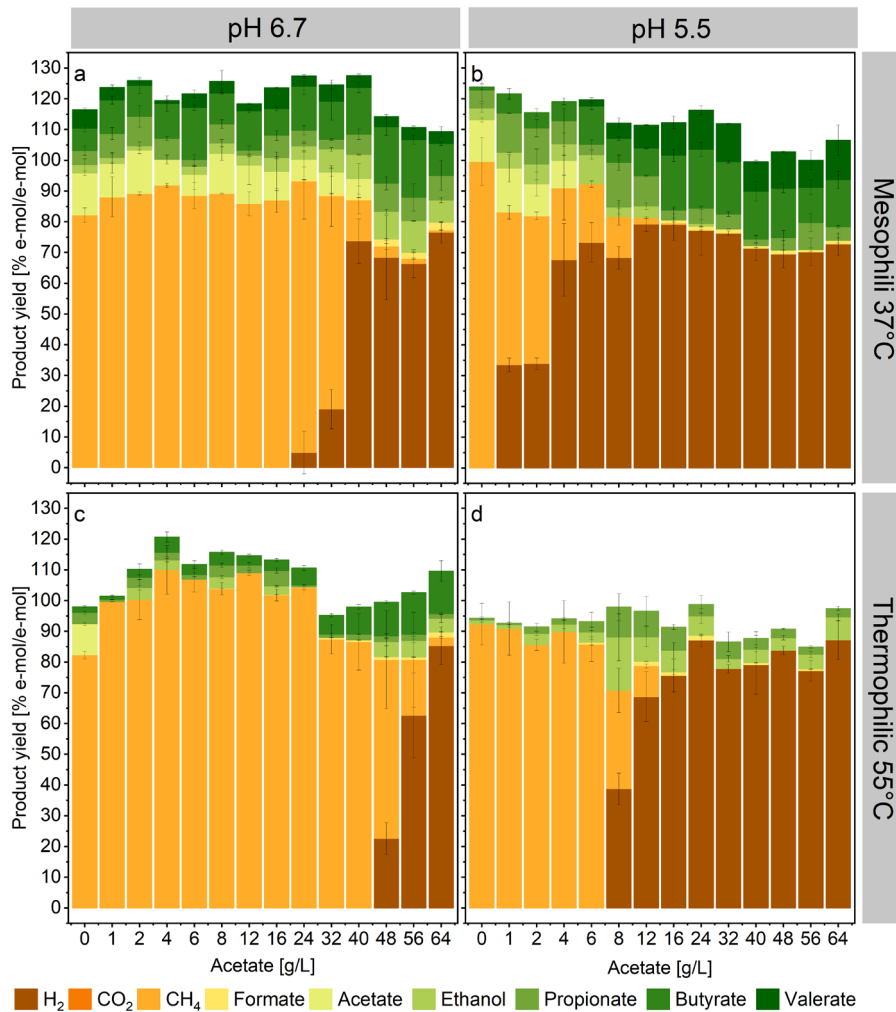


Figure 8. Electron mole balancing between substrates (CO and H₂, acetate if consumed) and products (CH₄, formate, ethanol, propionate, butyrate and valerate and H₂ and acetate if produced) at different process conditions and increasing acetate concentrations. Error bars represent standard deviation among replicates ($n=3$).

In general, mesophilic experiments resulted in high yields of methane, H₂, SCCs and ethanol. Thermophilic conditions, on the other hand, decreased the production of SCCs and enhanced methanogenesis and hydrogenogenesis when compared to mesophilic experiments. Generally, methane is the primary metabolite in mesophilic and thermophilic anaerobic environments [119] and here, under low acetate concentrations and regardless of pH or temperature, over 80% of the electron equivalents from syngas and acetate were converted to methane. Other products in methanogenic experiments were acetate, propionate and butyrate, especially at pH 37°C. The accumulation of SCCs during syngas methanation processes has been already reported and its extent depends also upon microbiota composition [127], [194].

Mesophilic and thermophilic non-methanogenic experiments predominantly yielded hydrogen with an increased production of formate, ethanol, propionate butyrate and valerate detected primarily at pH 6.7 or 37°C. The thermodynamics of

CO-consuming reactions at 55°C favor hydrogenogenesis over other carboxydrotrophic reactions [203], as detected here. At mesophilic conditions, on the other hand, homoacetogenesis should be the primary pathway of CO metabolism [204], [205]. The dominance of hydrogenogenic rates over homoacetogenic ones in this work likely results from the elevated concentration of acetate, which may have inhibited acetate-producing reactions, thereby prompting a shift in the community's metabolism towards other products [206]. A thermodynamic analysis determined at 310 K and pH 7, corroborates this hypothesis [114].

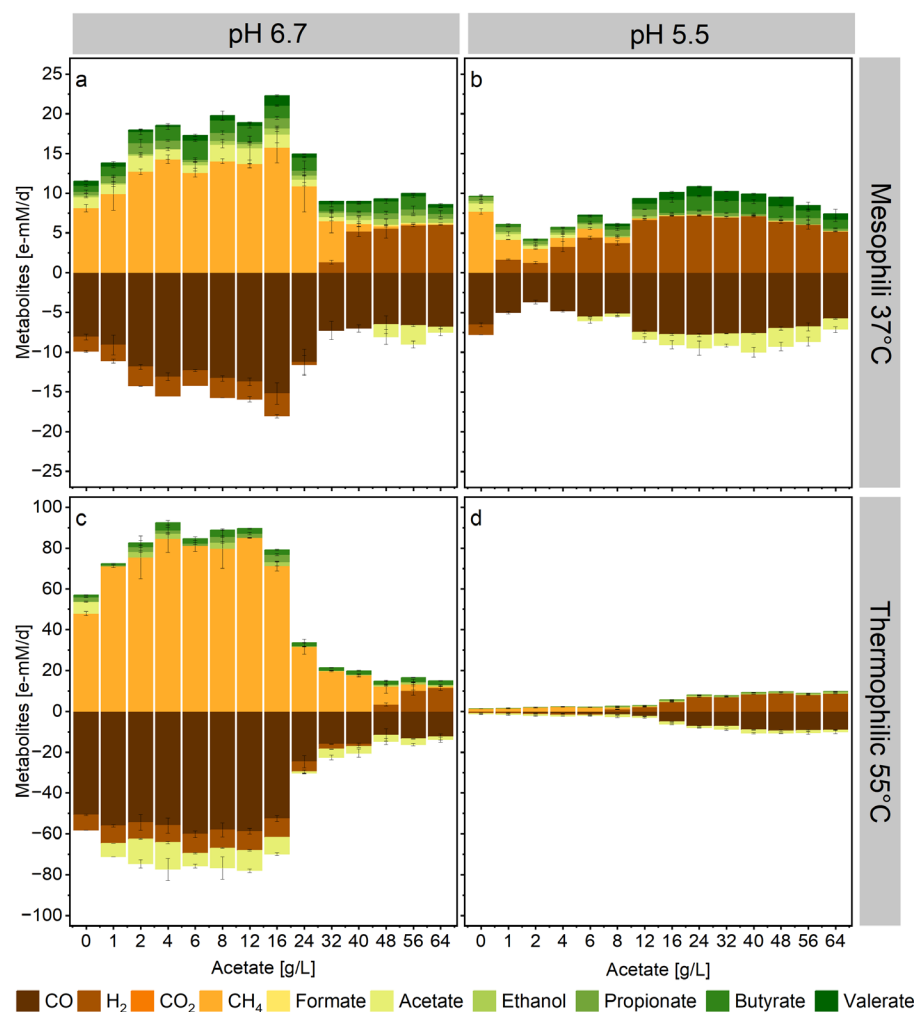


Figure 9. Consumption and formation rates of syngas components (CO, H₂ and CH₄) and of some short-chain carboxylates (formate, acetate, propionate, butyrate and valerate) and ethanol at different process conditions and increasing acetate concentrations. Negative values indicate consumption. Error bars represent standard deviation among replicates ($n=3$).

The Gibbs free energy of carboxydrotrophic and hydrogenotrophic acetogenic reactions increases from -88 KJ/mol to -66.4 KJ/mol and -172 KJ/mol to -162 KJ/mol, respectively, when lowering the pH from 7 to 5.5 and in the presence of 100 mM acetate. Conversely, the Gibbs free energy of carboxydrotrophic hydrogenogenesis, calculated under identical conditions, decreases from -20.9 KJ/mol to -24.1

KJ/mol. This may also explain the peaking acetate production rates detected at pH 6.7 and initial acetate concentrations up to 16 g/L (Figure 9 and Additional file 1, Figure S2), where the thermodynamic favorability of acetogenic reactions was possibly at its highest. Low pH or thermophilic conditions promoted acetate consumption. However, depending on the environmental conditions, two different pathways for acetate metabolism may have emerged. In methanogenic experiments with exogenous H₂ consumption, acetoclastic methanogenesis or syntrophic acetate oxidation likely served as the primary pathways for acetate consumption. Acetoclastic methanogenesis is usually the primary methanogenic pathway during anaerobic digestion, accounting for about 60-70% of the total methane produced [126]. Hydrogenotrophic methanogenesis via syntrophic acetate oxidation, on the other hand, is the preferable route to methane production in anaerobic digestion processes affected by acidosis. Syntrophic acetate oxidation occurs only at low H₂ partial pressures in association with H₂-consuming reactions such as hydrogenotrophic methanogenesis [40], [126]. At mesophilic conditions (37°C), the overall reaction (syntrophic acetate oxidation coupled to hydrogenotrophic methanogenesis) is exergonic only between 0.8 to 18 Pa H₂, while at 55°C, the window is higher, ranging from 1.5 Pa to 39 Pa H₂ [207], [208]. Experimental studies reported that the H₂ partial pressure during syntrophic acetate oxidation ranged from 1.6-6.8 Pa at mesophilic conditions [208], while 20 to 40 Pa H₂ at thermophilic ones [40], [207]. Here, in most methanogenic experiments with exogenous H₂ consumption, H₂ partial pressures at sampling time were 0. The average H₂ partial pressures are available in the Additional file 1, Figure S6. Additionally, *Syntrophaceticus*, *Tepidianaerobacter*, *Tepidimicrobium* and *Gelria* (

Figure 10), genera that harbour known syntrophic acetate oxidizers [209], [210], were enriched in the fermentation broths. Furthermore, members of *Limnochorda*, MBA03 and DTU014, genera already present in the inoculum, are considered to be syntrophic acetate oxidizers [115], [211]–[213]. The enrichment of a *Tepidianaerobacter* sp. (ASV 009) and *Tepidimicrobium* sp. (ASV 023), were likely promoted in experiments at 37°C (p<0.05) (Additional file 1, Figure S7). However, the low abundance of *Tepidianaerobacter* and *Tepidimicrobium* in those conditions may suggest a higher competitive advantage of acetotrophic microorganisms such as acetoclastic methanogenesis over syntrophic acetate oxidizers. At very high (40 g/L and more) acetate concentrations, there's little microbial growth (or DNA turnover) as the community looks very similar to inoculum. The high abundance of *Methanosarcina* detected at 37°C, pH 6.7 (

Figure 11) and low acetate concentrations supports the latter statement. Although *Methanosarcina* are versatile methanogens capable of acetoclastic, methylotrophic and hydrogenotrophic methanogenesis, they are often considered the primary acetoclastic methanogens during anaerobic digestion processes [214].

Some species of *Methanosarcina* such as *Ms. barkeri* and *Ms. acetivorans* have been reported to be able to consume CO for methanogenesis [215], [216]. Higher temperatures, on the other hand, may have promoted the development of syntrophic associations, thereby yielding the highest observed acetotrophic and methanogenic rates within this study.

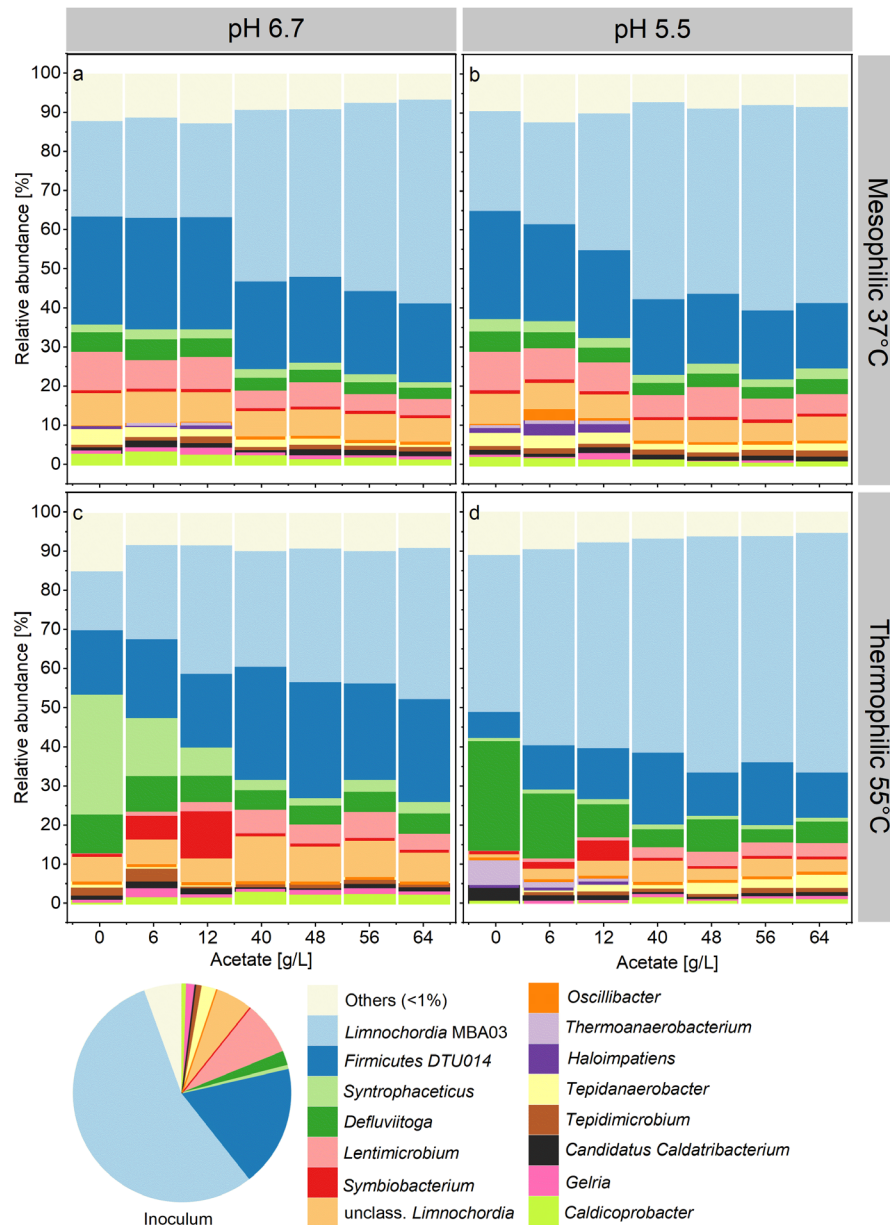


Figure 10. Average relative abundance of triplicate samples of the enriched microbial genera (based on 16S rRNA amplicon sequencing variants). Only the top 15 most abundant genera are shown. The rest is others.

Syntrophaceticus was primarily enriched at 55°C and the *Syntrophaceticus* sp. ASV 015 was significantly correlated to acetate consumption ($p < 0.05$), high temperatures ($p < 0.05$) and to the highest methanogenic rates of this work ($p < 0.05$) (Additional file 1, Figure S7). At 55°C and initial acetate concentrations lower than 16 g/L, concomitantly to the enrichment of *Syntrophaceticus*, also *Methanothermobacter*,

a hydrogenotrophic methanogen, was enriched up to 90% abundance. This highlights the importance of syntrophic acetate oxidation as a pathway to methanogenesis under thermophilic conditions. Thermophilic conditions were already proven to provide advantage to the syntrophic acetate oxidizers and hydrogenotrophic methanogens as dominant acetate consumers at the expense of acetoclastic methanogens [115]. Increasing acetate concentration and pH 6.7 may have also advantaged other hydrogenotrophic species such as *Methanosarcina thermophila* ASV 008 (Additional file 1, Figure S8) ($p < 0.05$). *Methanoculleus* and *Methanobacterium*, other hydrogenotrophic methanogens, did not show major changes in abundance compared to the inoculum.

Under non-methanogenic conditions, acetate may have undergone reduction reactions contributing together with CO to the formation of longer chain carboxylates, especially at 37°C. The interplay of high acetate concentrations and elevated H₂ partial pressures likely steered the metabolic pathways of the microbial communities towards the synthesis of more reduced compounds. Another work evaluated the effects of acetate loads comparable to this work (0-50 g/L acetate, pH 5.5) during the mesophilic H₂ production from sucrose with a non-methanogenic anaerobic microbiome. Increasing the acetate load reduced sucrose consumption and hydrogen production. However, similarly to the results obtained here acetate loads of 35 and 50 g/L promoted acetate uptake and the production of short- and medium-chain carboxylates such as butyrate, valerate and caproate and ethanol [217].

While the conversion of CO into even-number carboxylates like butyrate can happen either through direct pathways [218], [219] or via chain elongation processes [132], [220], the direct production of odd-number carboxylates such as propionate or valerate from CO hasn't been yet documented [221]. Other works report of propionate accumulating in the fermentation processes involving mixed cultures fed with CO [132], [220]–[222], but it is considered to originate from lactate through the acrylate pathway or from protein-rich waste via deamination and oxidation reactions [223]. The propionate detected in this work may have stem from cell lysate generated during the inoculation phase and it was subsequently converted to valerate through the reverse β -oxidation, as described to occur even within chain elongating reactors solely fed with CO [220], [224]. Albeit not abundant, *Oscillibacter* may have contributed to the chain elongation in this work. *Oscillibacter* was previously associated to the production of medium chain carboxylates in reactor microbiomes, some of which were fed with syngas [131], [199], [225].

The thermophilic genus *DeFluviitoga*, here enriched predominantly at 55°C, are hydrolytic bacteria that may have thrived on the solids from the inoculum or acted as dead cell scavengers as reported during syngas biomethanation in a trickle-bed reactor [226]. Similarly, *Symbiobacterium*, a thermophilic syntrophic genus that requires the assistance of other microbes to supplement growth factors [227]

may have benefited from cell lysate or from the cooperation with other community members.

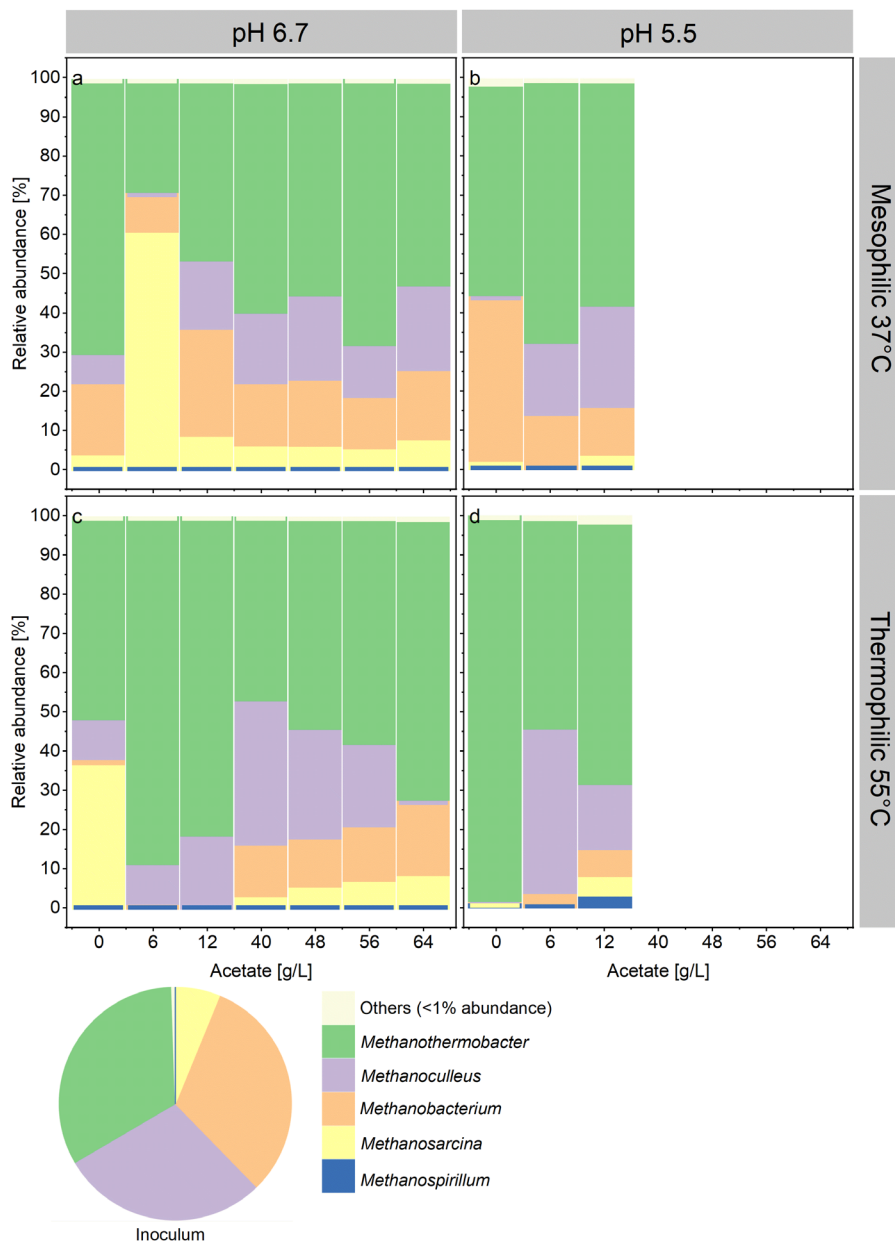


Figure 11. Relative abundance of the enriched methanogenic genera (based on mcrA gene amplicon sequencing variants). Only the top 5 most abundant genera are shown. The rest is others. Community analysis was performed only for methanogenic experiments.

Carbon dioxide was determined to be the critical factor for *Symbiobacterium thermophilum* to grow in single culture [228], [229] while other *Symbiobacterium* species can produce acetate, propionate, butyrate and valerate from tryptone and yeast extract [230]. Some other works report *Symbiobacterium* to be involved in syntrophic acetate oxidation [212], [231].

Thermophilic non-methanogenic processes fed with syngas typically generate primarily H₂/CO₂ and traces of carboxylates, with high selectivity above 90% towards acetate [232]. However, such a trend was not observed in this study. Although H₂ was indeed the major products, butanol and ethanol emerged as the primary metabolites in fermentation broths alongside with acetate consumption. Acetate impeded the acetate-producing reactions, leading to its conversion into more reduced compounds. The acetate produced (up to about 6 g/L) during the microbial electro-synthesis of CO₂ with anaerobic mixed cultures at pH 4 and 50°C was converted into ethanol and butyrate. While ethanol was likely produced via solventogenesis, butyrate was considered the result of the chain elongation of ethanol and acetate [233]. Similarly, 10 g/L acetate stimulated the ethanol production from thermophilic sugars fermentations by *Clostridium thermocellum* [234].

2.3.2 Effects of acetate supplementation on carboxydrotrophic rates

Few of the genera enriched in this work are reported to be carboxydrotrophs or to have been enriched in processes with syngas as substrate. Several archaeal ASVs belonging to *Methanothermobacter*, *Methanosacina* and *Methanobacterium*, genera that comprise carboxydrotrophic microorganisms [204], [235], [236], were significantly correlated to CO uptake ($p < 0.05$) (Additional file 1, Figure S8). These genera were abundant in the inoculum and the presence of carboxydrotrophic species and their potential involvement in CO uptake in methanogenic experiments cannot be excluded. *Thermoanaerobacterium*, here enriched up to about 5% at 55°C and pH 5.5, was considered to be responsible for CO consumption during syngas fermentations in hollow fiber bioreactors at thermophilic conditions [237], [238]. *Oscillibacter* was previously correlated to H₂/CO₂ metabolism [239]. It is plausible that the 16-day incubation period was insufficient for the carboxydrotrophic bacteria, assuming they contributed to CO consumption, to reach the top 15 most abundant genera. Multiple subculturing steps are typically necessary to enrich a defined and stable carboxydrotrophic community in batch bottle experiments, a task not within the scope of this study. Nevertheless, in some conditions, increasing exogenous acetate supplementation enhanced carboxydrotrophic rates, as depicted in Figure 12.

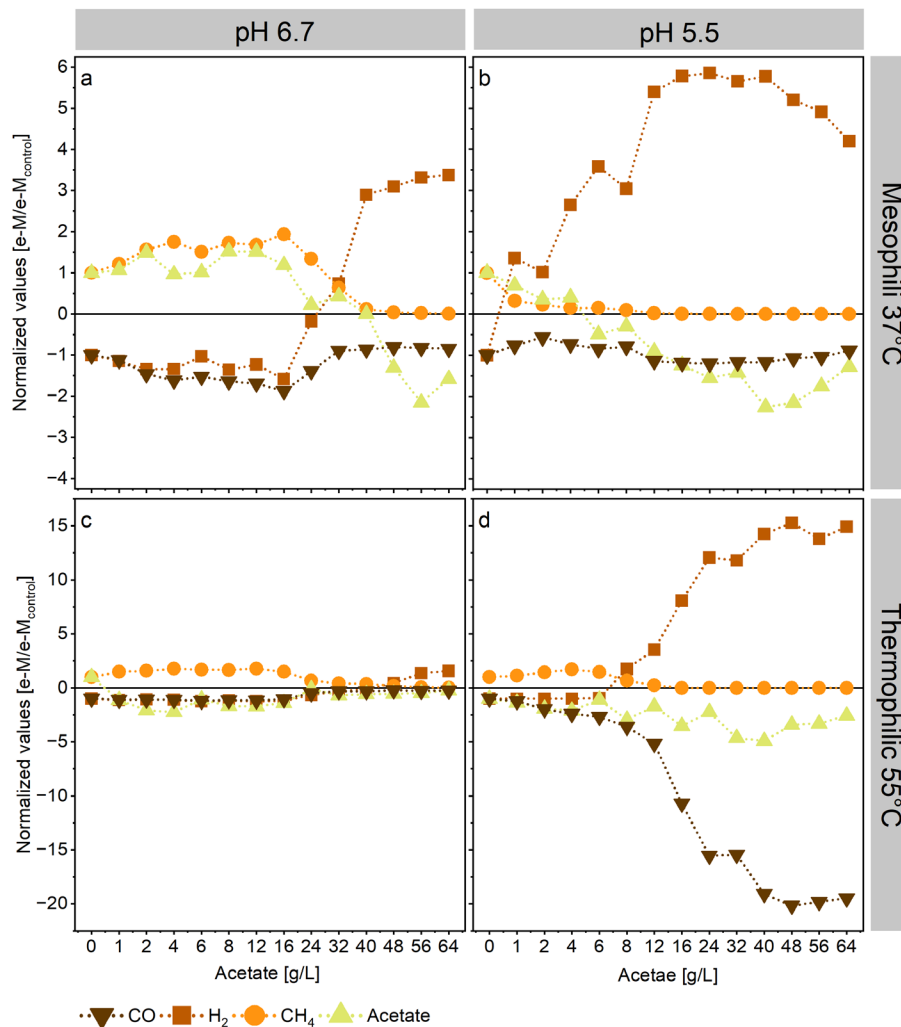


Figure 12. Normalized cumulative values for CO, H₂, CH₄ and acetate compared to control experiments in the absence of supplemented acetate. Negative values indicate consumption while positive values production. Changes in sign (positive to negative, for instance) for a compound mark the switch of the metabolism compared to the control experiments.

At 37°C and pH of 6.7, for instance, CO consumption peaked to 15.2 ± 1.3 e-mM/d at 16 g/L initial acetate, nearly double the rate compared to the absence of acetate (8.1 ± 0.4 e-mM/d at 0 g/L acetate). At 55°C and pH 6.7, experiments supplemented with acetate showed a reduced lag phase and enhanced CO conversion rates throughout the whole fermentation period (Additional file 1, Figure S2). An initial acetate concentration of 12 g/L resulted in a 16% increase in CO uptake rates. However, the kinetics of these experiments were constrained by experimental design, as syngas feeding was limited to once a day. At 37°C and pH 5.5, carboxydrotrophic rates rose by 20% with initial acetate concentrations ranging from 16 to 24 g/L (equivalent to 2.5 and 5 gHAc/L). Despite significant inhibition compared to experiments at pH 6.7, all acetate-supplemented bottles at pH 5.5 and 55°C exhibited at least a 24% increase in CO uptake rates compared to experiments without acetate supplementation. There, carboxydrotrophic rates peaked at 20.1 ± 1.3 e-

mM/d, marking a 20-fold increase compared to controls with 0 g/L acetate, when the initial acetate concentration reached 48 g/L (8 gHAc/L).

Literature evaluating syngas fermentation at acetate concentrations comparable to this study is scarce. The highest recorded acetate concentrations produced from syngas have been achieved with *Acetobacterium woodii* [143], [240], [241]. One work reports of 59.2 g/L of acetate accumulated in the broth after 3 days of batch fermentation at pH of 7. However, H₂/CO₂ uptake rates peaked at about 20 g/L. 40 g/L [143]. Such high concentrations were achievable only because of the high pH, reducing the presence of HAc in the medium [240]. Nevertheless, some studies have highlighted the beneficial impact of acetate supplementation on single-culture syngas fermentation. Although these studies used much lower acetate concentrations than this work, they reported shorter lag phases, increased CO conversion rates, higher cell densities and improved growth rates.

For instance, in batch fermentations with *Clostridium* sp. AWRP, 40 mM sodium acetate mitigated CO inhibition, eliminated the lag phase, and increased CO consumption and production of ethanol and 2,3-butanediol [242]. Similarly, adding 30 mM acetate to *Eubacterium limosum* fermentations improved cells growth rates, CO uptake and butyrate production. The reduced ferredoxin generated from CO oxidation was possibly used for ATP synthesis, which in turn drove acetate assimilation and butyrate production [243]. Carboxydrotrophic microorganisms utilize membrane-bound enzyme complexes such as Rnf or Ech to transfer electrons from reduced ferredoxin, produced during CO oxidation, to NAD⁺, while concurrently establishing an ion (H⁺ or Na⁺) potential across the cytoplasmic membrane [244], [245]. This electrochemical potential is then utilized by an ATP synthase to drive ATP synthesis [246]–[248]. An acetate-oxidizing, rod-shaped bacterium was reported to be able to perform homoacetogenesis from H₂/CO₂ or to oxidize acetate when co-cultured with *Methanobacterium* depending on the H₂ partial pressure [249], [250]. Additionally, in Clostridia such as *Clostridium ljungdahlii* or *Clostridium autoethanogenum*, the acetate in the fermentation broth determines the thermodynamic driving force of the aldehyde:ferredoxin oxidoreductase, enzyme that regulates the availability of reduced ferredoxin necessary for CO oxidation during the reduction of acetate to ethanol. An unfavourable acetate to ethanol ratio triggered oscillatory CO uptake rates of *Cl. autoethanogenum*, while external acetate supplementation improved the ethanol production from CO of *Cl. ljungdahlii* [251], [252].

Here, acetate indeed served as additional substrate in the systems, supporting different microbial trophic groups favoured by the varying environmental conditions. In general, acetate may have been directly assimilated by carboxydrotrophic microorganisms, akin to the mechanisms in single-culture studies mentioned above.

Alternatively, carboxydrotrophic microorganisms might have been indirectly advantaged by the availability of metabolic intermediates produced by the acetate metabolism of other trophic groups. Overall, two general trends can be observed. At pH 6.7 and initial acetate concentrations below 16 g/L, acetate or the H₂ generated from acetate oxidation may have promoted the activity of carboxydrotrophic microorganisms such as the methanogens *Methanothermobacter*, *Methanobacterium* or *Methanosacina* possibly contributing to the enhanced CO uptake rates. At initial acetate concentrations higher than 16 g/L, inhibition possibly inhibited the processes but this aspect will be discussed in the next section.

At pH 5.5, on the other hand, the inhibition of methanogenesis coincided with the increase of carboxydrotrophic, hydrogenogenic and carboxylates production rates. Another work focussing on continuous mixed culture syngas fermentation in psychrophilic conditions reported of a 4.7-fold increase of carboxydrotrophic rates as consequence of the inhibition of methanogenesis due to the lowering of the pH [253]. Hydrogenotrophic methanogens generally outcompete homoacetogens, especially at low H₂ partial pressures like in this study [44]. However, methanogenesis inhibition may have allowed for the accumulation of H₂ and formate, as mentioned before. Formate and H₂ are the primary interspecies electron donors in anaerobic environments and are key metabolites in the Wood-Ljungdahl pathway of acetogens [122]–[125], [254], [255]. A higher H₂ availability may have improved the redox state of the cells via the activity of hydrogenases or promoted acetate chain elongation into longer-chain carboxylates [112], [256]. Formate was reported to increase CO tolerance of *A. woodi* and of chain elongating microbiomes via the formate dehydrogenase [131], [257], [258].

2.3.3 Inhibition of methanogenic activity

The inhibition of methanogenic activity likely resulted from the presence of HAc and Na⁺ in the fermentation media. Under conditions of salt or acid stress, cells typically expel potassium ions to counteract the levels of intracellular Na⁺ ions or HAc. This process places an added energy burden on the cells, diverting ATP resources towards maintaining pH homeostasis rather than catabolic reactions, thus lowering microbial activity [259]. At a pH of 6.7, severe inhibition of methanogenesis was observed at approximately 18.4 gNa⁺/L (40 g/L acetate or 0.46 gHAc/L) at temperature of 37°C, while at thermophilic conditions, achieving similar inhibition levels required 24 g/L Na⁺ (56 g/L acetate or 0.7 gHAc/L). At a pH of 5.5, on the other hand, methanogenesis was completely inhibited by 2 gHAc/L (3.7 gNa⁺/L and 12 g/L initial acetate) for both mesophilic and thermophilic experiments. Experiments at pH 5.5 and 55°C showed very low chemical activity possibly as consequence of the pH and temperature shocks after inoculation, extending the lag phase. The IC₅₀ values (*i.e.* inhibitor concentrations causing a 50% decrease in microbial activity) of Na⁺ for the anaerobic digestion reported in the literature span from 3 to 53

gNa⁺/L [51], [260]. Sodium chloride concentrations higher than 9 g/L increased the lag phase and decreased both the growth rates and CO conversion of *Clostridium carboxidivorans*, while 18 g/L NaCl (about 6.8 gNa⁺/L) caused complete inhibition [261]. Six grams per liter of sodium ions inhibited the microbial electrosynthesis of acetate from bicarbonate via anaerobic mixed cultures [262]. Additionally, 8 gNa⁺/L inhibited of 50% hydrogen production during dark fermentation with anaerobic mixed cultures [263]. The high variability of sodium inhibition thresholds depend on several factors such as reactor microbiota, process design, substrate and presence of other cations [264]. Here, Na⁺ inhibitory concentrations fall within 18-24 gNa⁺/L range but the presence of HAc may have contributed in a synergistic effects to increasing process inhibition. HAc, on the other hand, was probably the primary inhibitor of methanogenesis at a pH of 5.5. Results consistent with findings from other studies where 2.3 gHAc/L resulted in at least 90% inhibition of methanogenesis [133], [139], [238].

When comparing methanogenesis with carboxydrotrophic activity, methanogenic reactions exhibited earlier signs of inhibition than carboxydrotrophic reactions in response to both HAc and Na⁺. The tolerance to high salt or other ions concentrations depends upon the amount of energy that can be generated during the catabolic reactions and on the coping mechanisms employed by the various microorganisms [259]. In this work, the lower inhibition of carboxydrotrophic reactions may suggest that they were among the most energetically favorable pathways. While some homoacetogens such *A. woodii* require external supplementation of Na⁺ (about 0.7 g/L) during growth on H₂/CO₂, others were reported to survive in acidic and alkaline environments or to have a upper salt limit than methanogens [259], [265]–[268]. *Clostridium ljungdahlii* was reported to form biofilm as stress response to 3.5 gNa⁺/L while growing on fructose at 200 mM [269]. Granules or biofilm formation improves resilience to stress and microbial interactions [270], but no evidence was found here. Nonetheless, signs of inhibition in mesophilic and thermophilic experiments are evident also for CO conversion at pH 6.7 and high acetate concentrations. Initial acetate concentrations of 40 g/L (about 18 gNa⁺/L) inhibited of about 20% and 70% mesophilic and thermophilic CO uptake rates, respectively.

2.3 Conclusions

Recovering energy from lignocellulose biomass is essential for reducing reliance on fossil fuels, enhancing resource circularity and mitigating environmental impacts. This study highlights the potential of utilizing acetate-rich wastewater as a co-substrate in batch syngas fermentation with mesophilic and thermophilic microbiomes under varying pH levels (6.7 and 5.5). Microbiomes proved to be able to undertake syngas fermentation even at high acetate concentrations and acidic pH levels. Secondly, the microbial diversity of mixed cultures allowed for a highly flexible

and resilient metabolism capable of adapting to changing environmental conditions. Manipulating process conditions and acetate loads allowed for steering the metabolism of the mixed culture, promoting favourable reactions while inhibiting others. Specifically, a pH of 6.7 promoted methanogenic reactions, whereas lowering the pH to 5.5 intensified the toxicity of undissociated acetic acid, thereby inhibiting methanogenesis at lower acetate loads. Under non-methanogenic conditions, acetate stimulated hydrogenogenesis and the production of various carboxylates, including valerate, contingent upon temperature. Acetate supplementation enhanced carboxydrotrophic rates providing extra carbon and energy sources to the process. The results obtained in this work may be relevant for technologies that aim to combine different waste streams. Future research should focus on assessing the feasibility of acetate and syngas co-fermentation in continuous cultivation setups to elucidate process performance nuances and identify key carboxydrotrophic microorganisms capable of thriving under high acetate loads.

Acknowledgments

The authors thank Ute Lohse for technical assistance in DNA extraction and library preparation for MiSeq amplicon sequencing and all the technical staff at EBT.

Supplementary information

Additional file 1: Table S1. Conversion factors for electron balances. Figure S1. Carbon balancing between substrates (CO and acetate if consumed) and products (CH₄, CO₂, formate, ethanol, propionate, butyrate and valerate and H₂, acetate if produced) at different process conditions and increasing acetate concentrations. Error bars represent standard deviation among replicates ($n=3$). Figure S2. Kinetics of consumption and formation of syngas components (CO, H₂, CO₂ and CH₄) and some short-chain carboxylates (formate, acetate, propionate, butyrate and valerate) and ethanol at different process conditions and increasing acetate concentrations. Negative values indicate consumption. Error bars represent standard deviation among replicates ($n=3$). Figure S3. Consumption of CO over time. Error bars represent standard deviation among replicates ($n=3$). Figure S4. Production of CH₄ over time. Error bars represent standard deviation among replicates ($n=3$). Figure S5. Production of H₂ over time. Negative values indicate consumption. Error bars represent standard deviation among replicates ($n=3$). Figure S6. Average H₂ partial pressure throughout the whole fermentation time. Values were determined from H₂ concentrations in the headspace of the bottles at sampling time. Figure S7. Spearman's rank correlations between relative abundance of dominant amplicon sequencing variants

(ASVs) based on 16s rRNA gene and process parameters. The strength of the correlation is represented by the size of the circle and intensity of the colour. Blue circles indicate positive correlations. Red circles indicate negative correlations. p values are shown for non-significant correlations ($p > 0.05$). Figure S8. Spearman's rank correlations between relative abundance of dominant amplicon sequencing variants (ASVs) based on *mcrA* gene and process parameters. The strength of the correlation is represented by the size of the circle and intensity of the colour. Blue circles indicate positive correlations. Red circles indicate negative correlations. p values are shown for non-significant correlations ($p > 0.05$).

3. Proof of concept of the two stage process

This chapter is based on the publication:

Co-fermenting pyrolysis aqueous condensate and py-rolysis syngas with anaerobic microbial communities enables L-malate production in a secondary fermentative stage. Alberto Robazza, Claudia Welter, Christin Kubisch, Flávio C. F. Baleeiro, Katrin Oschsenreither and Anke Neumann

Fermentation (2022), 8, 512.

<https://doi.org/10.3390/fermentation8100512>

Author's contributions

Alberto Robazza	conceptualization, methodology, investigation, data curation and analysis, visualization, first draft and manuscript revision
Claudia Welter	conceptualization, methodology, investigation and data analysis
Christin Kubisch	conceptualization, methodology, investigation and manuscript revision
Flávio C. F. Baleeiro	conceptualization, methodology and manuscript revision
Katrin Oschsenreither	conceptualization, methodology and manuscript revision
Anke Neumann	conceptualization, methodology, data analysis support, project supervision and manuscript revision

3.1 Introduction

Growing concerns for the impact of anthropogenic activities on the environment are shifting the socio-economic interests from a fossil-based economy towards a more sustainable and circular one. According to the Intergovernmental Panel on Climate Change and the International Energy Agency, it is estimated that the total share of biofuels will double in the next decades [1]. The source of all the biomass required to meet the need of an increased bio industry is still an open debate [8]. The energy potential of biomass is enormous considering that the Earth's net biomass production amounts approximately to 2000 EJ/y [7]. However, the diverting part of the energetic reservoir built up by plants towards uses defined by anthropocentric needs could cause undesirable impacts on the environment and on its natural distribution of resources [7]. Similarly, many biofuel crops are competing with food production, and the increasing demands for biofuel could exceed agricultural capacity [8]. The development of new technologies to maximize the energy recovery from wastes and residues of human activities is considered a key step towards carbon-neutrality [5].

The pyrolysis of lignocellulosic waste from municipal and agricultural activities could represent a great opportunity contributing to meet the needs of a developing bio-based economy [170]. During pyrolysis, the biomass is thermochemically deconstructed at temperatures ranging between 350 and 600 °C in the absence of oxygen [6]. The products of pyrolysis are pyrolysis syngas (PS) (15–20 wt %), a viscous energy-rich pyrolysis organic fraction (POF) (20–30 wt %), an aqueous condensate (PAC) (20–30 wt %) and bio-char (10–30 wt %) [15], [16]. Biochar and bio-oil can be either fed back into the pyrolysis reactor or used as fuels. On the other hand, the PAC's use is limited by the high concentrations of various toxic compounds and the high water content [22]. Similarly, the release of PS into the atmosphere should be avoided, due to its high concentrations of greenhouse gases (GHGs). In general, PAC and PS represent about 45 wt % of the total biomass fed into the pyrolysis reactor [16] and up to 41 % of the carbon balance [15]. Thus, it might be worth investing into bioprocessing technologies able to convert PAC and syngas into industrially relevant biochemicals.

Several works have already focused on the development of biological processes to valorize the constituents of the PAC. The ability of microorganisms in single culture fermentations to grow on PAC is species-specific due to their varying resistance to toxins contained in PAC [22]. Basaglia et al. [57] studied the toxicity of PAC from fir wood to a wide range of different microbial groups. Out of the 42 strains tested, only 4 fungal strains showed tolerance to pure PAC, whereas several PAC dilutions are required for many bacterial and yeast isolates [57]. However, it appears that PAC must undergo one or more pre-treatment steps to reduce the toxicity, before enabling its bioprocessing in pure culture fermentations [58]–[65].

Anaerobic digestion is an established technology for the treatment of agricultural residues and industrial wastewaters[52]. The degradation of the organic matter into CH₄ follows four primarily metabolic steps (hydrolysis, acidogenesis, acetogenesis, and methanogenesis) and depends upon mutual and syntrophic interactions between various microorganisms and trophic groups [38]. The wide and diverse genetic spectrum and functional redundancy of thousands of microbial species in anaerobic digesters offer what pure cultures currently cannot achieve: a higher tolerance to environmental stresses and toxicity. Multiple parallel biochemical routes provide greater functional stability because of the potential distribution of the substrate to several populations [46], resulting in a higher community resilience to perturbations [47].

Many studies successfully established anaerobic digestion with pre-treated and raw PACs for biomethane production [24], [73], [84], [96], [97], proving how anaerobic mixed culture fermentation is a viable alternative to intricate physicochemical pre-treatments for PAC detoxification and valorization. For example, Zhou et al. [73] studied the tolerance of anaerobic digestion towards increasing concentrations of raw and overlimed PAC as the sole carbon source for biomethane production in batch processes and direct evolution studies, respectively. The batch tests showed that loadings of 3 % raw PAC were inhibiting methanogenesis. Extensive studies have been conducted towards a complete integration of pyrolysis and anaerobic digestion for methane production where all the by-products of pyrolysis (PAC and PS included) are fed into an anaerobic digester [92], [97], [173]. During the anaerobic digestion of PAC derived from corn stalk pellets, volatile fatty acids (VFAs) production was observed even though PAC severely inhibited methanogenesis [97]. Giwa et al. [172] evaluated the effects of a real PS generated from a two stage pyrolysis process treating food waste on methanation rates. The process, designed to minimize POF and PAC, generated syngas with a high H₂-to-CO ratio (60:20 %). Methanation rates were enhanced, producing almost 100 % more CH₄ than the synthetic syngas control fermentations. The topic has been evaluated also from a techno-economical perspective [177], [178], [180]: pairing anaerobic digestion with pyrolysis allows relevant energy savings in handling pyrolysis by-products and strongly reduces GHGs emissions [177]. Salman et al. [176] estimated a higher annual revenue for the integrated process compared to the sole incineration of green waste.

In anaerobic communities, syngas is commonly metabolized by methanogenic archaea, hydrogenogenic bacteria, acetogenic bacteria, and sulfate-reducing bacteria [116]. By manipulating the fermentation environmental conditions, it is possible to control the syngas conversion towards different catabolic routes [114], [117]–[119]. Methane is often the primary metabolite having the lowest free energy content per electron, regardless of the temperature range [119]. On the other hand, when

methanogenesis is inhibited and in mesophilic environments with high concentrations of reduced compounds such as ethanol and/or lactate, the mixed culture can elongate C1 compounds from syngas into medium-chain carboxylates (MCCs). Such a wide array of metabolic products at mesophilic temperatures is the result of an intricate metabolic network ultimately limited by thermodynamics [127]. Syngas-converting microbial communities at thermophilic temperatures show higher water–gas shift reaction (WGSR) kinetics than mesophilic ones. The high diversity of carboxidotrophic hydrogenogenic bacteria and the thermodynamics of H₂-producing reactions in thermophilic environments favor higher CO conversion rates to produce primarily H₂ and short-chain carboxylates [128]. Hydrogen or MCC production via mixed culture anaerobic fermentation are gaining more scientific and industrial interest [129], [130]. However, the success of these technologies is linked to the identification of cheap and recoverable methane inhibitors [133], [134].

A. oryzae belongs to the Ascomycetes group and its industrial application spans from food processing to commodity chemicals production [157], [158]. Several studies have evaluated the potential of producing biochemicals, biofuels or cell biomass (single cell proteins) with *A. oryzae* from VFAs rich waste streams or from acetate [159]–[161]. Moreover, the fungus was reported to tolerate small concentrations of pyrolysis oils and various PAC components [166] and to be able to grow on the acetate contained in pre-treated PAC from wheat straw [63].

To extend the knowledge about the integration of thermochemical and biochemical processes treating lignocellulose waste, this work evaluates a two-stage process where the products from the co-fermentation of PAC and syngas by anaerobic mixed cultures are fed to an aerobic fermentation to produce L-malate by *A. oryzae*. Several anaerobic mixed culture bottle fermentations were performed at 37 and 55 °C at increasing PAC concentrations in order to understand the effects of PAC on the metabolism of gaseous and liquid compounds. After the syngas fermentation stage, the media from selected mixed culture fermentations were inoculated with *A. oryzae*, focusing on the conversion of acetate from syngas and PAC metabolism into L-malate. Fungal growth, together with the quantification of the removal of selected PAC components, was used to prove the occurrence and the extent of PAC detoxification.

3.2 Materials and Methods

3.2.1 Growth medium

All reagent grade chemicals were purchased from Sigma-Aldrich (Schnelldorf, Germany) or Carl-Roth (Karlsruhe, Germany). The fermentation medium used in all serum-bottle and flasks experiments was a modified basal anaerobic medium (BA) composed of the following stock solutions: mineral salts solution (NH₄Cl, 161.2

g/L; $\text{MgCl}_2 \times 6\text{H}_2\text{O}$, 5.4 g/L; $\text{CaCl}_2 \times 2\text{H}_2\text{O}$ 6.5 g/L); phosphate buffer solution (KH_2PO_4 , 136 g/L); vitamins solution (Biotin, 0.002 g/L; Folic Acid, 0.002 g/L; Pyridoxin, 0.01 g/L; Thiamin, 0.005 g/L; Riboflavin, 0.005 g/L; Nicotinic Acid, 0.005 g/L; Ca-Panthothenate, 0.005 g/L; Vitamin B12, 0.005 g/L; Aminobenzoic Acid, 0.005 g/L; Liponic Acid, 0.005 g/L); trace elements solution ($\text{FeCl}_2 \times 4\text{H}_2\text{O}$, 1.5 g/L; MnCl_2 , 0.1 g/L; $\text{CoCl}_2 \times 6\text{H}_2\text{O}$, 0.19 g/L; ZnCl_2 , 0.07 g/L; $\text{CuCl}_2 \times 2\text{H}_2\text{O}$, 0.002 g/L; $\text{NiCl}_2 \times 6\text{H}_2\text{O}$, 0.024 g/L; $\text{Na}_2\text{MoO}_4 \times 2\text{H}_2\text{O}$, 0.036 g/L; H_3BO_3 , 0.006 g/L; $\text{Na}_2\text{SeO}_3 \times 5\text{H}_2\text{O}$, 0.003 g/L; $\text{Na}_2\text{WO}_4 \times 2\text{H}_2\text{O}$, 0.02 g/L); reducing agent solution (L-Cysteine, 100 g/L); resazurin solution (Resazurin sodium salt, 1 g/L). For each liter of medium were added: 100 mL of mineral salt solution, 800 mL of phosphate buffer solution, 10 mL of vitamins solution, 10 mL of trace elements solution, 5 mL of resazurin solution and 3 mL of reducing agent solution. Once all the solutions were mixed, the pH was adjusted to 6 with 4M NaOH solution as pH adjusting agent and sodium source. The remaining volume was filled with deionized water to 1 L.

3.2.2 Inocula and PAC

The anaerobic sludge was collected from an anaerobic digester treating cow manure (Alois & Simon Frey Biogas GbR, Bräulingen, Germany). Due to the high content of straw residues, right after collection, the sludge was sieved down to 0.5 mm discarding the straw and the retained solids. The sludge was then poured into an anaerobic container and stored in a fridge at 4 °C until needed. The pH, the total suspended solids (TSS) and volatile suspended solids (VSS) concentration of the sieved sludge corresponded to 8.46, 41.36 ± 2.25 g/L and 12.27 ± 0.13 g/L, respectively. The TSS and VSS analytics were performed in triplicate and determined as described in [201].

Aspergillus oryzae DSM 1863 was obtained from the DSMZ strain collection (Deutsche Sammlung von Mikroorganismen und Zellkulturen GmbH, Braunschweig, Germany). The cryo-stock of fungal conidia was prepared and stored as described by [161].

The PAC used in this experiment was produced during the fast pyrolysis of miscanthus at BioLiq plant (Karlsruhe Institute of Technology, Karlsruhe, Germany). The chemical oxygen demand (COD) and total organic carbon (TOC) were 253.25 ± 10.25 g/L and 118.58 ± 0.11 g/L, respectively. The total nitrogen (TN) was 140.25 ± 4.24 mg/L. The pH of raw PAC was 2.8 while acetate, propionate and *n*-butyrate concentrations were about 34 g/L, 5.07 g/L and 0.5 g/L, respectively. The fast pyrolysis at the BioLiq plant is run as described in [7] and [41]: the flue gases (composed primarily of 20 % CO, 25 % CO₂, 1.5 % H₂, alkanes and N₂) coming from the combustion chamber pass through a hot cyclone to separate the biochar from the product gas stream. Then, the gaseous phase is sent through a series of two quench condensers at ~ 85–90 °C and at ~30 °C separated by an electrostatic precipitator. The PAC used in this study is the product of the second condensation step.

3.2.3 Bottle preparation and fermentation

Mesophilic and thermophilic experiments with (M-CTRL and T-CTRL) and without methanation (M-BES and T-BES) were run as controls to evaluate the metabolism and the performances of the inoculum grown on synthetic pyrolysis syngas. To inhibit methanogenesis, 50 mM of Sodium 2-bromoethanesulfonate (BES) were dissolved into the BA medium. All experiments not containing PAC were performed in triplicate. To test PAC inhibition, exponentially increasing concentrations ranging from 0.5 to 30 %v/v were added in the M-PAC and T-PAC fermentations. As control, abiotic experiments with equal concentrations of PAC (M-PAC-AB and T-PAC-AB) were also prepared and run simultaneously to the corresponding experiments. The mixed culture fermentations and abiotic PAC incubations were performed in 250 mL serum bottles with 50 mL of active volume. Figure 13 and Table 3. Overview of experiments. MC is mixed culture; AB is abiotic; Asp is *Aspergillus oryzae*. summarize the experimental design.

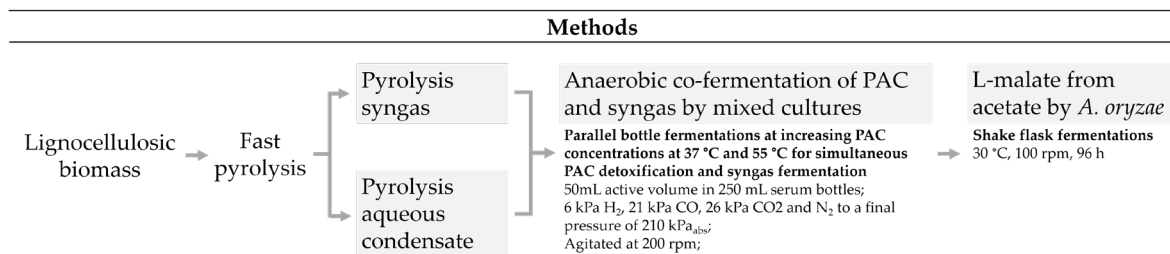


Figure 13. Schematic representation of the experimental design. Pyrolysis aqueous condensate and pyrolysis syngas were co-fermented by two mixed cultures at mesophilic and thermophilic temperatures. The media from selected mixed cultures fermentations were centrifuged and inoculated with *A. oryzae* to convert acetate into L-malate.

The liquid phase was composed of 5 mL of BA medium, increasing PAC concentrations depending on the experimental design and 4M NaOH as needed to re-adjust the pH of the medium back to 6 after PAC addition. The remaining volume was filled with deionized water up to 45 mL. The serum bottles were stored into an anaerobic tent (5 % H₂ in N₂) to anaerobise overnight at room temperature. The bottles were then inoculated with 10 %v/v anaerobic sludge and sealed with butyl rubber stoppers and aluminium rings. After sealing the flasks, the bottles were initially flushed and then pressurised with a synthetic pyrolysis gas mixture consisting of 6 kPa H₂, 21 kPa CO, 26 kPa CO₂ and N₂ to a final pressure of 210 kPa_{abs}. Bottle pressurization was performed using a precision pressure indicator GMH 3100 Series (Greisinger, Germany) at room temperature.

Table 3. Overview of experiments. MC is mixed culture; AB is abiotic; Asp is *Aspergillus oryzae*.

	T (°C)	Medium	BES (50 mM)	Raw PAC (0.5-30 %)	Inoculum	Syngas
Control Syngas Fermentations						
M-CTRL	37	BA	-	-	MC	+
M-BES	37	BA	+	-	MC	+
T-CTRL	55	BA	-	-	MC	+
T-BES	55	BA	+	-	MC	+
Mesophilic and Thermophilic PAC Fermentations						
M-PAC	37	BA	-	+	MC	+
T-PAC	55	BA	-	+	MC	+
Mesophilic and Thermophilic Abiotic Control						
M-PAC-AB	37	BA	-	+	-	+
T-PAC-AB	55	BA	-	+	-	+
Aspergillus oryzae Fermentations						
M-PAC-Asp	30	from M-PAC	-	detoxified PAC	<i>A.oryzae</i>	-
M-PAC-AB-Asp	30	from M-PAC-AB	-	-	<i>A.oryzae</i>	-
T-PAC-Asp	30	from T-PAC	-	detoxified PAC	<i>A.oryzae</i>	-
T-PAC-AB-Asp	30	from T-PAC-AB	-	-	<i>A.oryzae</i>	-

A total of 3 mL of gas phase were sampled daily or depending on the rates of CO or H₂ consumption. The ambient temperature and pressure and the gauge pressure of the bottles were recorded at each sampling, right after taking the bottle from the incubator. When the CO and/or H₂ molar concentrations or the absolute pressure of the serum bottles were about zero or below 190 kPa_{abs}, respectively, then the headspace of the bottle was re-pressurized with the synthetic pyrolysis gas mixture. The maximum possible theoretical uptake rate for CO was about 1.650 mmol/d, while for exogenous H₂ it was 0.570 mmol/d. 1 mL of liquid samples were withdrawn twice a week. The pH of the sample was measured, and the samples were then centrifuged at 17,000 x g and ambient temperature for 15 minutes. The resulting supernatant was filtered with 0.2 µm cellulose acetate syringe filters (Restek GmbH, Bad Homburg, Germany) and stored in a freezer at -20 °C for later analytics. All bottles were incubated in the dark in shaker incubators (multitron incubator shaker, Infors, Bottmingen, Switzerland) at temperatures of 37 °C or 55 °C. The agitation was set to 200 rpm. All mixed culture fermentations and abiotic controls lasted 39 days of elapsed fermentation time (EFT).

The medium from selected mesophilic and thermophilic fermentations M-PAC and T-PAC (2.5 %, 5 %, 7.5 %, 10 %, 20 %) and from the corresponding abiotic controls was centrifuged at 4700 x g for 8 hours. The supernatant was collected and 9 mL of which together with 1 mL fresh BA medium were then poured into 100 mL baffled Erlenmeyer shake flasks. The shake flasks were inoculated with 0.1 mL of the *A. oryzae* conidia cryo-stock, with spore concentration of 3x10⁷ spores/mL. The pH of the medium was not adjusted. All the shake flasks were incubated at 30 °C

and 100 rpm. 0.2 mL of liquid samples were taken every 24 h from inoculation for 5 consecutive days. The pH of the sample was measured, and the samples were then stored in a freezer at -20 °C for later analytics. All fermentations with *A. oryzae* were done in triplicate.

3.2.4 Analytical methods and data processing

The concentration in the fermentation medium of linear and branched monocarboxylates C1-C8 (lactate, acetate, propionate, iso- and *n*-butyrate, iso- and *n*-valerate, iso- and *n*-caproate), of the normal alcohols (ethanol, propanol, butanol and pentanol) and of some selected PAC compounds (2-cyclopenten-1-one, furfural, phenol, guaiacol and *o*-,*m*-,*p*-cresol) were measured by a high performance liquid chromatography (HPLC) device (Agilent 1100 Series, Agilent, Waldbronn, Germany) operated with an oven set at 55 °C equipped with a Rezex ROA organic acid H + (8 %) column (300 by 7.8 mm, 8 µm; Phenomenex, Aschaffenburg, Germany) and a Rezex ROA organic acid H + (8 %) guard column (50 by 7.8 mm). The mobile phase was 5 mM H₂SO₄ with a flow of 0.6 mL/min. Short- and medium-chain carboxylates and PAC compounds detection was performed with an UV detector at 220 nm at 55 °C while normal alcohols were detected with a RID detector at 50 °C.

The gas phase samples were analysed with an Inficon 3000 Micro GC System with a Thermal Conductivity Detector (TCD) equipped with a CP-Molsieve 5 Å column and a PoraPLOT Q column at 80 °C using argon and helium as carrier gases, respectively. The molar composition of the headspace gas of the bottles was computed assuming the ideal gas law after subtracting any air contamination caused by sampling. The accumulation or consumption of each gas was first corrected by a factor accounting for the pressure lost by sampling withdrawal and then cumulated.

The yields and recoveries (in terms of carbon (C-mol) and electron (e-mol) equivalents) for control experiments were calculated using only CO/CO₂ and CO/H₂ as substrates, respectively, as described by Grimalt-Alemany et al. [272]. For M-PAC and T-PAC experiments, CO was accounted as the sole carbon source while CO and H₂ were assumed as electron donors. The multitude of compounds present in PAC interfered with the identification of other metabolites beyond acetate, propionate, and *n*-butyrate. Therefore, only these three acids as well as CO₂, CH₄ and H₂ were accounted as products. The IC₅₀ value was adopted from Zhou et al. [73], indicating the toxicant concentration that causes 50 % reduction in cumulative CO consumption or CH₄ production over a fixed period of exposure time. Acetate selectivity is the ratio between acetate and metabolites with carbon atom number greater than two.

3.3 Results and discussion

3.3.1 Mesophilic and thermophilic anaerobic mixed microbial cultures grown on pyrolysis synthetic syngas

The first set of experiments aimed to understand whether the synthetic pyrolysis syngas used in this study is a suitable carbon and electron source for production of methane, short and medium chain carboxylates as well as solvents with mixed microbial cultures. M-CTRL and T-CTRL are bottle fermentations incubated at 37 °C and 55 °C, respectively, performing syngas methanation. M-BES and T-BES are bottle fermentations at 37 °C and 55 °C with addition of 50 mM BES as methanogenesis inhibitor. The metabolism of the communities under M-CTRL, T-CTRL, M-BES and T-BES conditions were characterized and later used as reference for comparison with the fermentations in presence of PAC. The initial pH of all control bottles after inoculation was 6.7 ± 0.2 . Figure 14 shows C-mol recovery and e-mol recovery from all control experiments.

C-mol (a) and e-mol (b) balances for experiments M-CTRL, T-CTRL, M-BES and T-BES. Conversion factors for electron balances are available in the Additional file 2 (Table S1). CO, CO₂ and H₂ were considered as the sole carbon and/or electron donors for all experiments but for T-BES, where CO was the only carbon and electron donor. Alcohols are ethanol, propanol and butanol. Short-chain carboxylates C₃- C₅ (SCCs) are lactate, iso- and n-butyrate, propionate and iso- and n-valerate. Medium chain carboxylates (MCCs) are iso- and n-caproate. The productivities of alcohols, some SCCs and MCCs are available in the Additional file 2, Table S2.

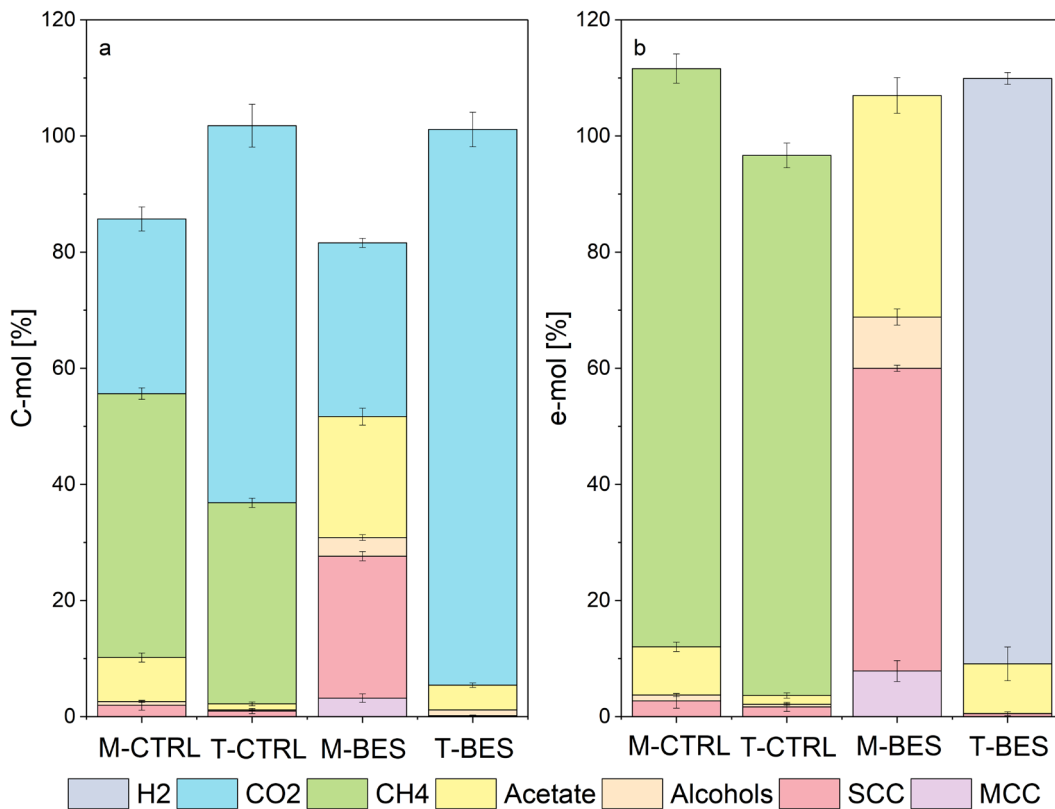


Figure 14. C-mol (a) and e-mol (b) balances for experiments M-CTRL, T-CTRL, M-BES and T-BES. Conversion factors for electron balances are available in the Additional file 2 (Table S1). CO, CO₂ and H₂ were considered as the sole carbon and/or electron donors for all experiments but for T-BES, where CO was the only carbon and electron donor. Alcohols are ethanol, propanol and butanol. Short-chain carboxylates C₃- C₅ (SCCs) are lactate, *iso*- and *n*-butyrate, propionate and *iso*- and *n*-valerate. Medium chain carboxylates (MCCs) are *iso*- and *n*-caproate. The productivities of alcohols, some SCCs and MCCs are available in the Additional file 2, Table S2.

During syngas methanation at mesophilic range (M-CTRL), the mixed culture produced primarily CH₄ (45.5 ± 1 %) and CO₂ (30.1 ± 2.1 %) while 7.6 ± 0.1 % of the total carbon metabolized was fixed into acetate. Acetate accounted for 83.7 ± 1.7 % of the total C₂-C₆ metabolites detected in the liquid phase. The carbon stored in carboxylates other than acetate was about 2.6 %. The average CO and H₂ uptake rates were 0.34 ± 0.02 mmol/d and 0.28 ± 0.02 mmol/d while CH₄ was produced at a rate of 0.15 ± 0.01 mmol/d.

From about 20 days EFT, methanogenic rates increased concomitantly to homoacetogenic/hydrogenotrophic activity from exogenous CO₂ and H₂ consumption (Additional file 2, Figure S1-S4). Simultaneously, decreasing acetate concentrations in the bottles might indicate acetoclastic methanation. However, acetoclastic methanogenesis appears to have barely contributed to the methanation yield. At 37 °C, pH 5.5, and 100 mM acetate hydrogenotrophic methanogenesis has more favourable thermodynamics than acetoclastic methanogenesis [114]. Considering that CO and H₂/CO₂ metabolisms have been reported to have similar kinetics [49], changes in the rates of gases uptake or production might be attributed to shifts

within the composition of the microbial population. With the progression of M-CTRL experiments, CO uptakes rates lowered the CO partial pressures favouring acetogenic/methanogenic hydrogenotrophism. High CO partial pressures are known to be inhibiting cellular hydrogenase and H₂ uptake [251], [273] and might have contributed to the delayed start of H₂/CO₂ metabolism. Liu et al. [274], detected a two-phased process characterized by an initial CO consumption followed by the onset of H₂/CO₂ metabolism to acetate attributed to homoacetogenic microorganisms while performing CO biomethanation with anaerobic granular sludge. In M-CTRL bottles, carboxidotrophic methanation, if any, had a limited contribution towards methane production. Carboxidotrophic methanogens are expected to be easily outcompeted by carboxidotrophic acetogens and hydrogenogens as the few species that are capable of directly converting CO into CH₄ do so at very low reaction rates [236], [275].

The thermophilic syngas methanation (T-CTRL) occurred at higher kinetics but lower yield when compared to M-CTRL. 34.6 ± 0.8 % of the carbon from CO was converted into CH₄ while CO₂ accounted for 65 ± 3.7 %. Acetate accounted for about 1 % for the total carbon from CO and the acetate selectivity was 63 ± 3.51 %. The average CO and H₂ uptake rates were 1.48 ± 0.05 mmol/d and 0.56 ± 0.01 mmol/d, respectively. CO₂ and CH₄ were produced at 0.98 ± 0.05 mmol/d and 0.515 ± 0.01 mmol/d, respectively. T-CTRL bottles have been performing primarily carboxidotrophic hydrogenogenesis via the WGSR followed by hydrogenotrophic methane generation, as also described by other studies [116], [118], [127].

Mesophilic and thermophilic metabolic rates calculated in this study correspond to those reported by Sipma et al. [276] who tested several mesophilic anaerobic sludges from wastewater treatment reactors to convert CO at 30 and 55 °C. The sludges were incubated at 30 °C in serum bottles with 50 mL initial active volume and produced primarily CH₄ and/or acetate. Incubation at 55 °C resulted in the formation of mainly CH₄ and/or H₂ [276]. Sipma et al. detected CO conversion rates ranging between 0.14 and 0.62 mmol/d for the cultures incubated at 30 °C while thermophilic CO depletion rates varied between 0.73 and 1.32 mmol/d.

The BES addition inhibited all methanogenic pathways in both control mesophilic syngas (M-BES) and control thermophilic syngas (T-BES) fermentations. M-BES fermentations consumed CO at a rate of 0.36 ± 0.03 mmol/d, a similar value to what calculated for M-CTRL. H₂ uptake rate was 0.03 ± 0.01 mmol/d and CO₂ production rate was 0.11 ± 0.01 mmol/d. HPLC analytics showed that M-BES cultures have been chain elongating CO to *n*-caproate with a net exogenous H₂ consumption to a final caproate concentration of 2.18 ± 0.47 mM. About 60 % of the e-mol recovery was accounted for metabolites with carbon atoms number higher than two. CO₂ (29.9 ± 0.8 %) and acetate (20.8 ± 1.5 %) were the two major carbon sinks.

T-BES experiments showed greater CO consumption kinetics than M-BES. The mixed culture performed almost solely WGSR, generating 1.04 ± 0.33 mmol/d of CO₂ and 1.05 ± 0.31 mmol/d H₂ while the average CO uptake rate was 1.18 ± 0.09 mmol/d. CO₂ accounted for more than 95 % of the total carbon fed while acetate was only about 5 %. Acetate was the primary metabolite produced by the consortium with selectivities higher than 80 %. More than 99 % of the e-mol recovery was molecular H₂. These results are corroborated by the work carried out by other research groups. Grimalt-Alemany et al. [127] characterized the conversion of CO by a thermophilic enriched consortium in presence of BES resulting in the production of H₂ and acetate as primary metabolites. Slepova et al. [277] traced ¹⁴CO to study the metabolism of mixed cultures collected from three pH-neutral hot springs of Uzon Caldera (Kamchatka) under temperatures from 60 °C to 90 °C. A major part of ¹⁴CO was oxidized to ¹⁴CO₂. Samples from the spring with a temperature of 60 °C converted less than 5 % of the CO into carboxylates and only 1 % in springs with higher temperatures [277]. High acetate selectivities were reported also by Wang et al. [238] showing a 99 % acetate selectivity at the end of their thermophilic (55 °C) enrichment process with H₂ and CO₂ as substrates. Shen et al. [237] achieved final acetate selectivity of 96.7 % and 96.3 % in two hollow fibre membrane bioreactors after 60 days EFT starting from an inoculum from an anaerobic digester. Alves et al. [117] tested different enrichment strategies in bottles experiments at 55 °C and obtained syngas-converting communities able to fix approximately 97 % of product recovery into acetate from CO₂ and H₂.

3.3.2 Co-fermentation of syngas and PAC

The effects of increasing PAC concentrations were evaluated on two mixed microbial cultures growing on pyrolysis gas at 37 and 55 °C. The aim was to identify kinetic inhibition and changes in metabolites production patterns of syngas metabolism caused by PAC. Additional interest was to test the PAC detoxification potential of the microbial cultures.

3.3.2.1 Impact of PAC on the syngas metabolism of the anaerobic mixed culture at 37 °C and 55 °C

Figure 15 reports the rates of syngas metabolism at increasing PAC concentration both at mesophilic (37 °C) and thermophilic (55 °C) temperatures. Similar to the control experiments, the initial pH of all M-PAC and T-PAC experiments was 6.7 ± 0.2 after inoculation.

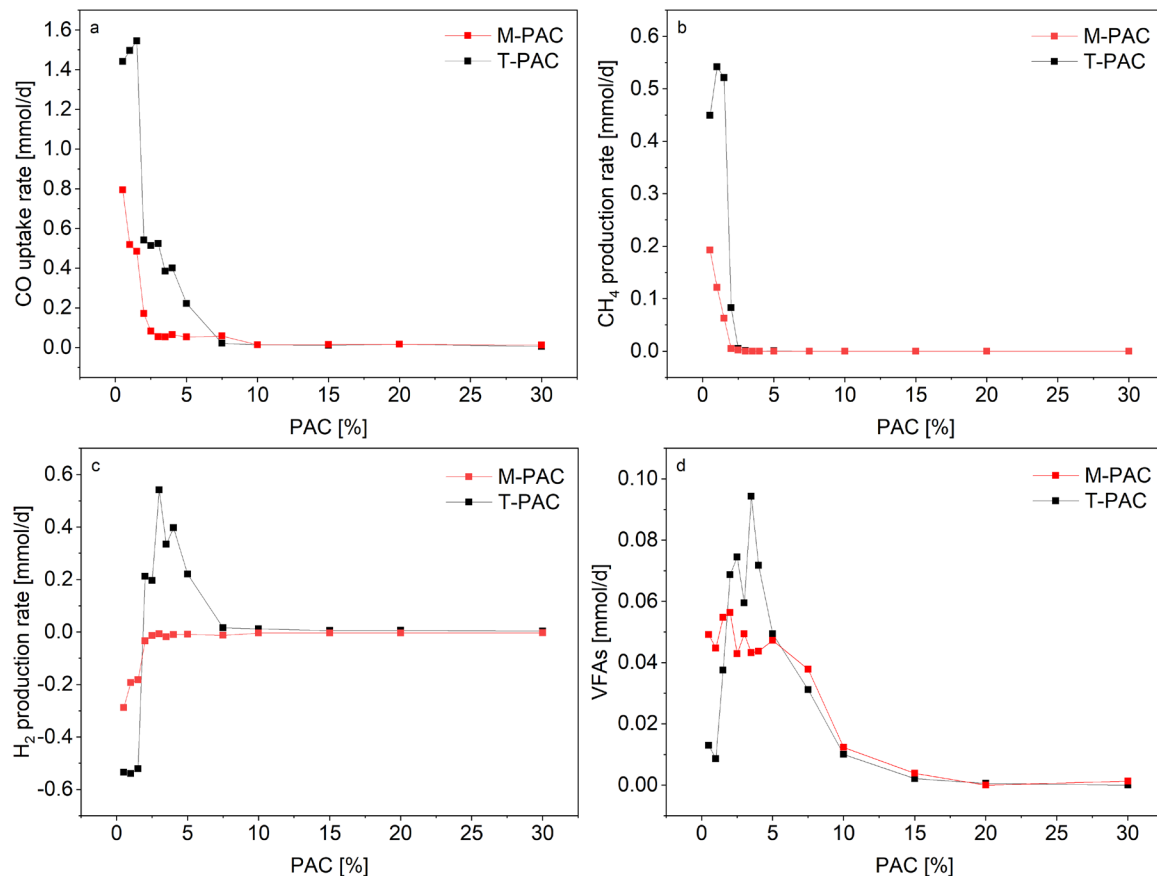


Figure 15. Rates of consumption and/or production of CO (a), CH₄ (b) and H₂ (c) at increasing PAC loadings at mesophilic (37 °C) and thermophilic (55 °C) temperatures. Negative production rates for H₂ indicate consumption. Volatile fatty acids (VFAs) (d) are acetate, propionate and *n*-butyrate. Productivities for all experiments are available in the Additional file 2 Table S3 and Table S4.

The CO consumption rates for mesophilic fermentations M-PAC at PAC concentrations of 0.5, 1 and 1.5 were all above 0.4 mmol/d. For PAC concentrations higher than 5 %, the rates of CO consumption rapidly decreased towards zero. Exogenous H₂ consumption was detected in all M-PAC bottles. Additionally, CO₂ production rates were 60 % lower than the stoichiometry of the WGSR, suggesting that the mesophilic mixed culture co-fermented CO and H₂/CO₂. While the methane production rates quickly dropped to zero for concentrations above 1.5 % PAC, the VFAs daily production decreased only from PAC concentrations above 7.5 %.

At thermophilic range, PAC concentrations below 1.5 % did not significantly affect CO consumption (Figure 15.a). The average CO consumption rates at 55 °C with PAC concentrations from 0.5 to 1.5 % were all above 1.4 mmol/d, similar to what was achieved in the control experiments T-CTRL. Above 5 % PAC, the kinetics of CO consumption rapidly decreased towards zero. At thermophilic range, methanogenesis was detected for PAC concentrations from 0.5 to 2.5 % PAC. The highest CH₄ production rate was 0.54 mmol/d for bottles containing 1 % PAC. In T-PAC fermentations with 1.5, 2, 2.5 % PAC, the methane production showed a delayed start of about 6 days when compared to T-CTRL (Additional file 2, Figures S5-S8).

In Figure 15.c, H₂ was consumed to generate methane via hydrogenotrophic methanogenesis under conditions with up to 1.5 % PAC. At higher PAC loadings, net H₂ production occurred concomitantly to the inhibition of the methanogenic activity. The highest H₂ production rate was detected at 3 % PAC with values of 0.54 mmol/d but it decreased at rates equivalent to CO consumption for higher PAC percentages. Similar to mesophilic bottles, the VFAs production rates were low under low PAC loadings and peaked at 3.5 % PAC when no methane production was detected.

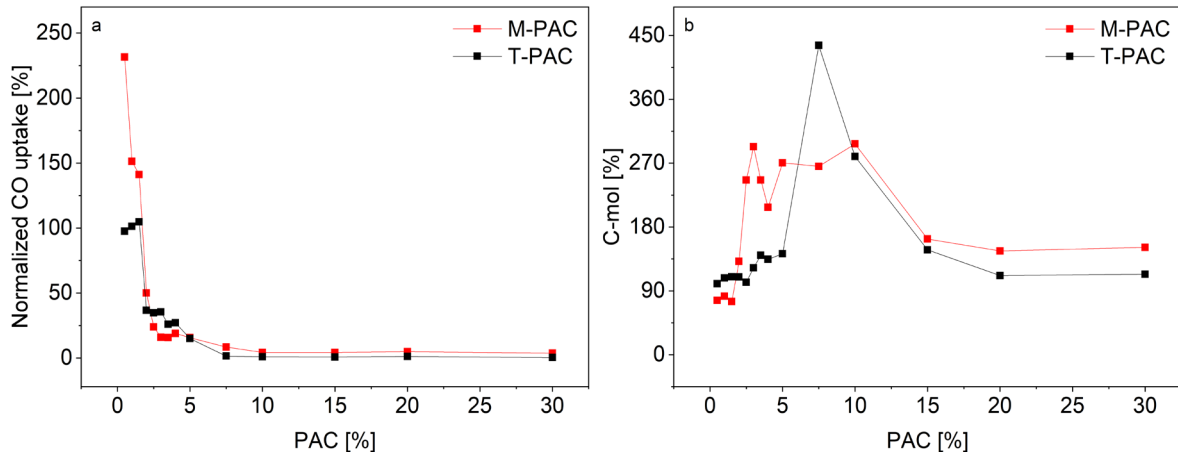


Figure 16. (a) M-PAC and T-PAC CO uptake rates normalized to control experiments M-CTRL and T-CTRL, respectively. (b) C-mol balances for M-PAC and T-PAC experiments.

The kinetics of syngas metabolism for thermophilic PAC fermentations were consistently higher than at mesophilic range, a result consistent to the kinetics of the control experiments. However, Figure 16.a shows that, when normalizing M-PAC and T-PAC CO uptake rates to the corresponding rates of M-CTRL and T-CTRL, the overall effects of PAC toxicity did not differ between mesophilic and thermophilic experiments. Thus, thermodynamic limitations and different gas solubilities at different temperatures were likely the dominant factors affecting the kinetics of syngas metabolism.

Additionally, Figure 16.a shows that M-PAC bottles with low PAC concentrations (0.5 to 1.5 % PAC) had at least 40 % higher CO consumption rates compared to the respective M-CTRL values, peaking at 231 % at 0.5 % PAC. For bottles with 0.5 to 1.5 % M-PAC, from about 20 days EFT, CO oxidation rates higher than 0.36 mmol/d (average CO uptake for M-BES) were detected, matching those of T-CTRL experiments rather than M-CTRL or M-BES (Additional file 2, Figures S1-S4). Factors such as CO and PAC toxicity probably contributed to hinder acetogenic and methanogenic activity at early fermentation stages and the high CO uptake rates might be the result of changes in microbial population consequently to PAC detoxification. However, contrarily to M-CTRL fermentations, the higher kinetics of the WGSR provided enough endogenous CO₂ to all metabolic routes resulting in a net CO₂ production (Additional file 2, Figure S1, S2 and S3).

3.3.2.2 Different PAC tolerance of different trophic groups

Methane production was inhibited by lower PAC concentrations than CO consumption in both M-PAC and T-PAC cultures. The IC₅₀ values for CO uptake rates at mesophilic range correspond to 2 % PAC. Methane production, on the other hand, is halved at PAC concentrations between 1 to 1.5 %. At thermophilic range, the IC₅₀ values for CO uptake rates fell within the 2 to 3 % PAC range. Regarding methane, the IC₅₀ was found to be between 1.5 to 2 % PAC. Zhou et al. [73] reported that the IC₅₀ of mesophilic biomethane potential tests of overlimed PAC was 4.8 % PAC. Even though Zhou et al. [73] did not report the IC₅₀ for raw PAC, it could be assumed that the higher tolerance of methanogens towards PAC achieved in their study was the result of the synchrony of the pre-treatment and a lower specific PAC availability, as both factors are known to affect methanation rates [135]. Here, raw PAC loading rates that severely inhibited methanogenesis were 3.4 g_{COB}/g_{VSS} (2 % PAC) at both mesophilic and thermophilic range, respectively (Additional file 2, Table S4).

When comparing methanogenic versus carboxydrotrophic/homoacetogenic activity under PAC influence, homoacetogenesis had a higher tolerance to PAC than methanogenesis. Compounds present in PAC such as furfural, phenol and phenolic compounds can be produced also from the hydrolysis of lignocellulosic matter [22], [278], [279]. Acetogens are involved in syntrophic interactions with other microorganisms during the anaerobic degradation of compounds deriving from the degradation of lignin. Synthetic co-cultures with *Pelobacter acidigallici*, *Acetobacterium woodii*, and *Methanosarcina barkeri* have been reported to convert phenylmethylethers to CH₄ and CO₂ [280]. *A. woodii* metabolizes phenylmethylethers to yield acetate and phenols [281]. Phenols can be degraded to acetate by *P. acidigallici* [282]. In another work studying the degradation of lignin-derived monoaromatic compounds, the initial step was catalysed by *Sporomusa* spp. to generate acetate via O-demethylation of the methoxylated aromatics. The demethoxylated aromatics were then metabolized into acetate, H₂ and CO₂ by *Firmicutes*. Finally, methane was generated from acetate and H₂/CO₂ by acetoclastic and hydrogenotrophic methanogens, respectively [283]. The latter examples represent interactions between microorganisms that might have occurred in the inoculum in the presence of PAC. Methanogens work at the end of the chain of syntrophic interactions resulting in the production of CH₄ as the primary end-product of the fermentative process. Thus, methanogenic activity is highly influenced by the degradation of those compounds that would otherwise be inhibitory. Low concentrations of lignin derivatives with aldehyde groups or apolar substituents are known to be highly toxic to methanogens [51]. Aromatic carboxylates, on the other hand, were reported to be only mildly toxic. Phenols and their derivatives are known for being methanogenic inhibitors

[69], [135], [284], however, phenolic compounds have been already proven to be degraded to CH₄ [285], [286].

Hübner et al. [84] reported longer lag phases at increasing initial PAC concentrations in anaerobic digestion experiments. PAC extended the lag phase of methanogenesis from a few days to some weeks, indicating temporary inhibition [84]. Inhibition of anaerobic digestion by PAC from corn stalk was also observed by Torri and Fabbri [92]. Longer lag-phases at increasing PAC loadings were also detected in this work at mesophilic and thermophilic range for both carboxydolithotrophism and methanogenesis (Additional file 2 Figures S4, S8). In general, an extended lag-phase could be related to a lack of acclimatization of the inoculum to an inhibiting organic compounds hard to degrade, therefore requiring enrichment of the microbial community [69]. Alternatively, the inoculation/bioaugmentation of fermentations with cultures collected from particular ecosystems could be a strategy to increase the performances of biological processes [287]–[290].

3.3.2.3 PAC detoxification

The C-mol and e-mol recoveries for bottles with 2.5 to 10 % PAC at both temperatures showed balances much higher than 100 % (Figure 16.b). Most of the VFAs (primarily acetate) produced in those bottles were not the result of syngas metabolism but from the degradation of aromatic compounds, as proven in other works [104], [280], [283]. This is also supported by the detoxification efficacy of selected PAC compounds (Figure 17) where high degradation efficacies were recorded at low PAC concentrations.

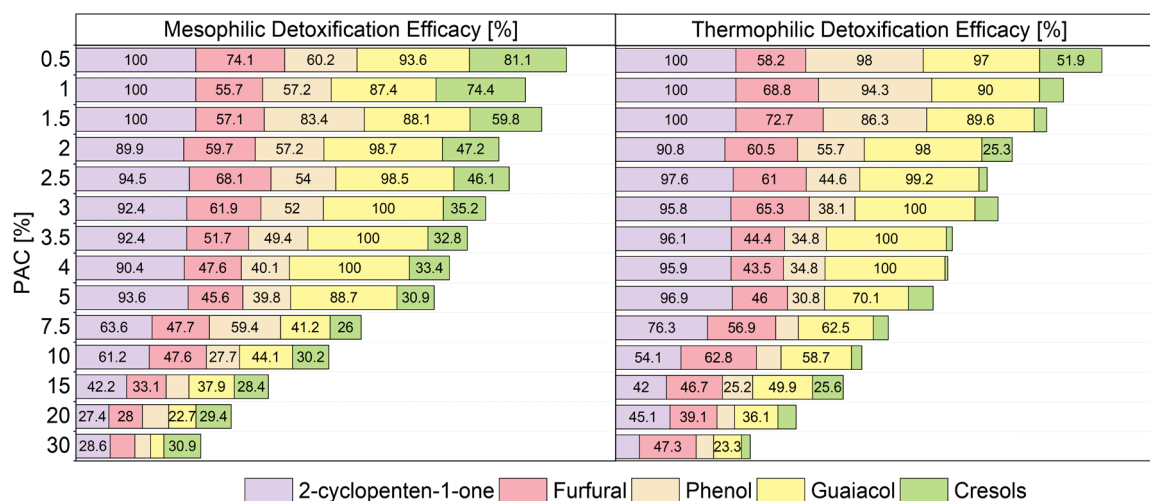


Figure 17. Removal efficacies for some selected PAC compounds after syngas mixed culture fermentations performed at 37 °C and 55 °C. Numeric values of the removal efficacies below 25 % are now shown.

For PAC concentrations above 5 %, the efficacy of degradation decreased both at thermophilic and mesophilic range. A work performed by Fedorak and Hrudehy [291] reporting high removal of phenol and *m*- and *p*-cresol from a wastewater of a

coal liquefaction plant during anaerobic batch culture experiments supports what was detected here. Hübner and Mumme [84] suggested that low cresols degradation efficacies might be accounting for cresols production via phenol degradation, as cresols and guaiacol are phenol derivatives.

Considering that bottles with low CO consumption rates showed high PAC detoxification efficacies, it can be assumed that PAC detoxification was independent from syngas metabolism and it occurred at concentrations inhibiting carboxyd-trophic reactions and homoacetogenesis. On the other hand, the longer lag phases at increasing PAC concentration might suggest that syngas metabolism was dependent on the detoxification of toxins in PAC and it recovered once the concentration of some PAC components fell below toxic levels.

3.3.3 A. oryzae cultivation on acetate derived from syngas fermentation and PAC detoxification

To further test the degree of PAC detoxification and to valorise the carboxylates from the M-PAC and T-PAC experiments, the media from some selected bottles were centrifuged and the resulting supernatant inoculated with *A. oryzae*. No fungal growth was detected in the media containing the broth from syngas abiotic control experiments with syngas, M-PAC-AB-Asp and T-PAC-AB-Asp (Figure 18). Thus, abiotic incubation over extensive amount of time did not lower toxicity levels of PAC towards *A. oryzae*. On the contrary, *A. oryzae* growth was detected in all fermentations up to M-PAC-Asp 10 % and T-PAC-Asp 10 %. Inhibitory effects of pyrolysis products of wheat straw on *A. oryzae* growth were previously elucidated by Dörsam et al. [166] who studied the toxicity of some selected PAC components. Phenolic compounds such as phenol, o-, m-, p-cresol and guaiacol resulted in a strong inhibition of *A. oryzae* growth even at low concentrations. Although it is known that *A. oryzae* has genes encoding for enzymes enabling the degradation of cresols, it only tolerates cresol in very low concentrations [292]. Additionally, 2-cyclopenten-1-one was reported to be the most toxic compounds among the tested ones [166].

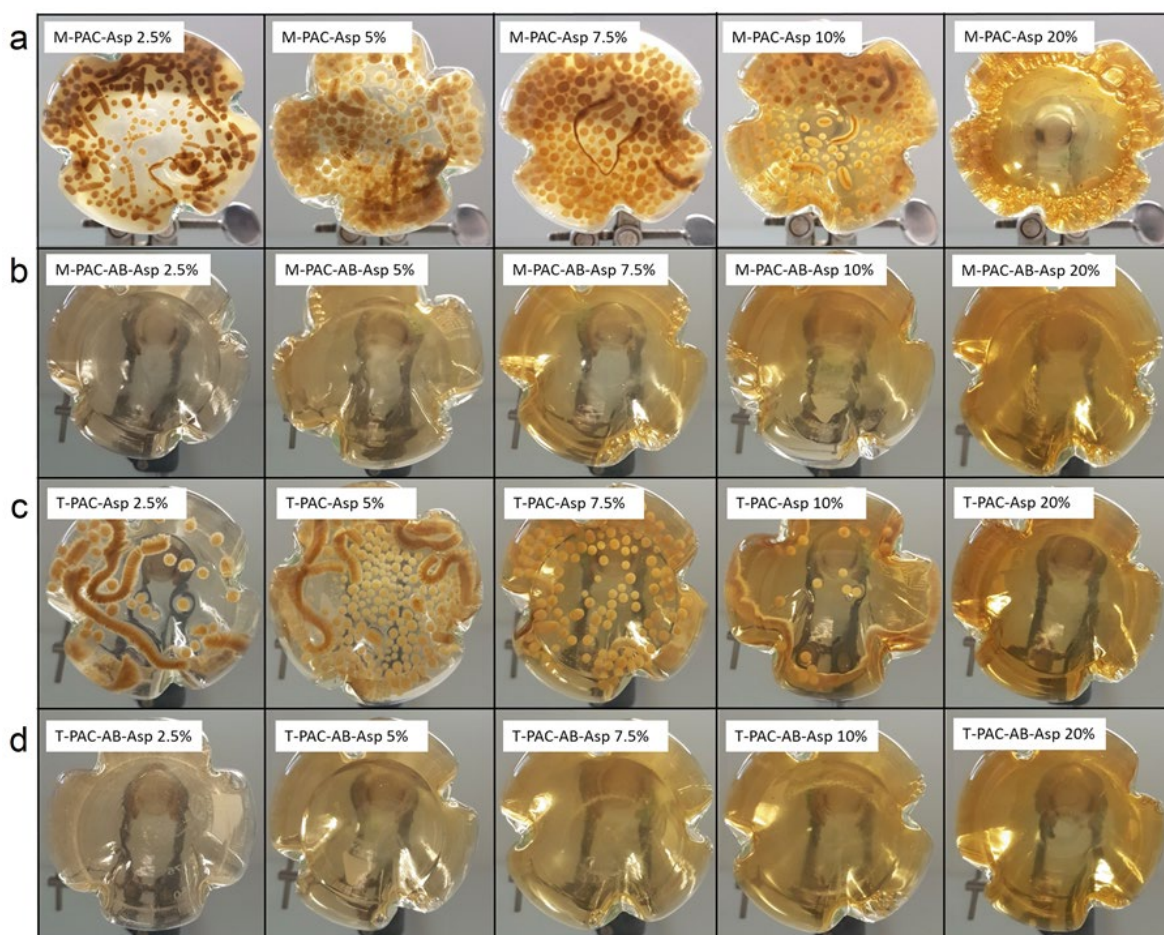


Figure 18. Growth of *A. oryzae* in aerobic flasks containing medium from syngas fermentations and abiotic controls. Rows (a) and (c) show fungal growth in medium from mesophilic and thermophilic syngas culture fermentations, respectively. Rows (b) and (d) show the results of fungal growth in medium from the abiotic incubation of PAC and BA medium.

3.3.3.1 L-malate production from acetate by *A. oryzae*

The ability of *A. oryzae* to convert glucose and VFAs from various sources into L-malate or biomass has been studied in previous works [148], [161], [165], [293], [294]. Here, the acetate detected at the start of the *A. oryzae* fermentations derived from different sources: syngas fermentation; acetate originally contained in the PAC; and PAC detoxification. Complete acetate consumption was recorded in all flasks containing medium from bottle fermentations with up to 10 % PAC (Figure 19.a and Figure 19.c). L-malate production was detected in all bottles alongside acetate consumption. For both A-M-PAC 20 % and A-T-PAC 20 %, no acetate consumption nor L-malate production were detected. For the medium from mesophilic syngas fermentations the highest amount and yield of malate from acetate of 8.47 ± 0.21 mM and 0.21 mM/mM, respectively, were obtained in M-PAC-Asp 2.5 %. Overall, L-malate yields decreased at increasing PAC concentrations for M-PAC-Asp fermentations. On the other hand, when considering the medium from thermophilic syngas fermentations, the highest amount of L-malate produced was detected for T-PAC-Asp 10 % at 11.46 ± 0.16 mM with the highest yield of 0.17 mM/mM. Contrarily

to M-PAC-Asp fermentations, L-malate yields increased at increasing PAC concentrations. Process optimization for L-malate production exceeded the scope of this work, however, the highest malate yields detected in this study are comparable to the 0.20 grams of malic acid per gram of acetate for concentrations of 40 g/L of acetate reported by Kövilein et al. [161].

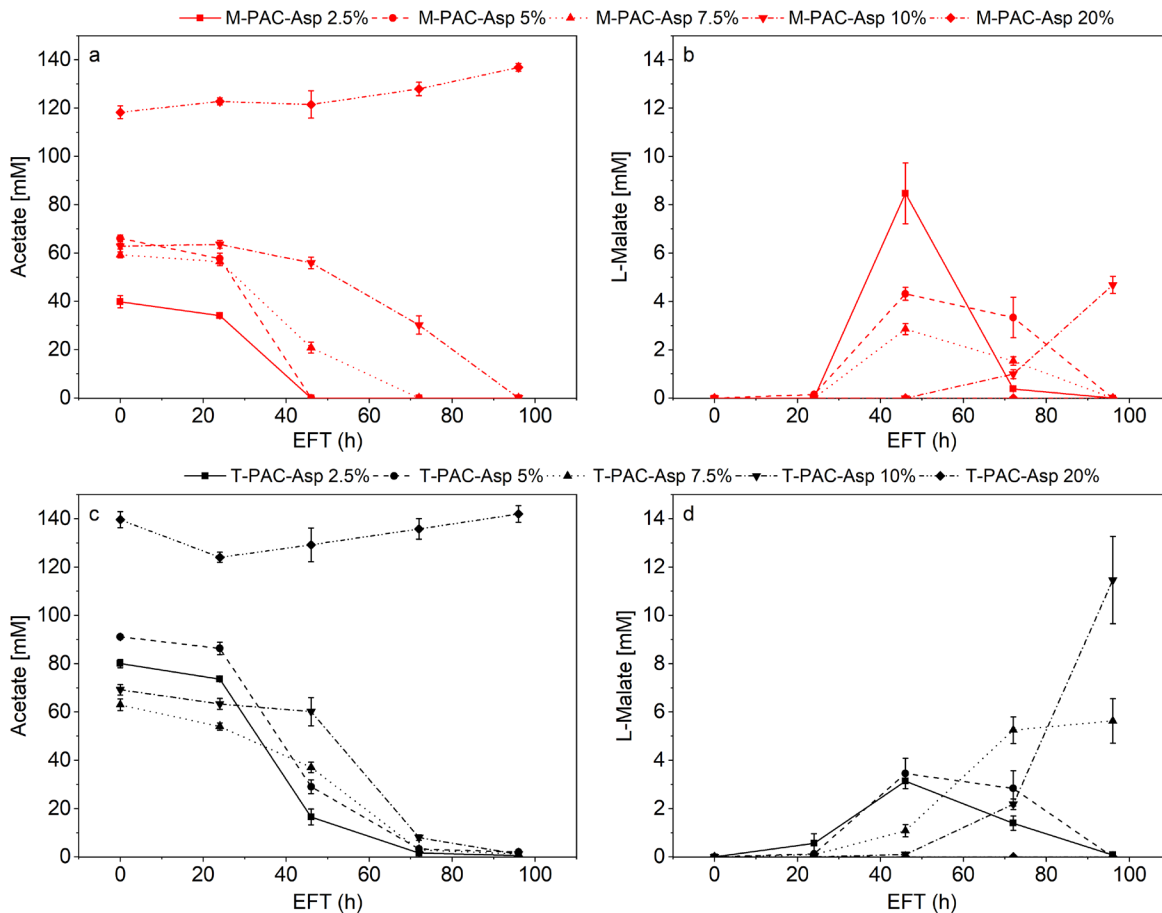


Figure 19. Acetate and L-malate from *A. oryzae* fermentations in the medium from meso-philic syngas fermentations (a), (b) and thermophilic syngas fermentations (c), (d),.

Kövilein et al. [161] tested acetate concentrations between 10 and 55 g/L for malate production in *A. oryzae* shake flasks cultures. Malate production was reported to be highly dependent on acetate concentration with the highest yield for concentrations of up to 40 g/L [161]. Similarly, Uwineza et al. [165] grew *A. oryzae* on VFAs from the anaerobic digestion of food waste with maximum concentrations of acetate of 9 g/L yielding 0.29 gCDW/gVFAs. Higher concentrations of acetate did not affect the yield. Oswald et al. [148] presented a process concept, in which malate was produced from acetate generated from syngas fermentation by *C. ljungdahlii*. Malate production by *A. oryzae* in the medium from the syngas fermentations with acetate as sole carbon source reached yields of 0.33 grams of malate per gram of acetate [148]. The overall conversion of CO and H₂ into malate was calculated to be 0.22 g malate per gram of syngas [148]. The high malate yields achieved in this work,

as already hypothesised by Oswald et al. [148], might be linked to the richness in micronutrients of the medium from the previous fermentations.

3.4 Conclusions

In this study, PAC and syngas were co-fermented by mesophilic and thermophilic mixed cultures and the effects of increasing concentrations of PAC were evaluated. PAC could be used effectively to inhibit methanogenesis and steer microbial metabolism towards other metabolites. Fermenting PAC and syngas in the mesophilic range led to acetate, propionate and *n*-butyrate accumulation in the fermentation broth with net H₂ consumption. Whereas fermentations at thermophilic range produced primarily acetate and H₂. These results show that the mixed cultures performed the dual task of fixing C₁ compounds from syngas and detoxifying PAC. Treating PAC together with syngas enabled carboxylates valorisation to platform chemicals such as L-malate by *A. oryzae* via a sequential secondary fermentation stage. Mesophilic carboxylates production or thermophilic biohydrogen production via mixed culture syngas fermentations are becoming the centre of extensive interest for biochemical or biofuels production. Thus, exploring alternative and effective methods for the inhibition of methanogenesis is still necessary, and inhibitors, such as PAC, are ideal candidates. This work contributes towards a better understanding of efficient integration of thermochemical processes and mixed culture anaerobic fermentations. Further studies should test the feasibility of this work in continuous bioreactors, aiming to a better understanding of the microbial interactions that are contributing to the PAC degradation and syngas metabolism.

Acknowledgments

The authors acknowledge Institute of Catalysis Research & Technology, Karlsruhe Institute of Technology, for providing the PAC, Habibu Aliyu for mentoring and the technical staff at Institute of Process Engineering in Life Sciences 2: Technical Biology, Karlsruhe Institute of Technology.

Supplementary information

Additional file 2. Table S1: Conversion factors for carbon and electron balances; Table S2: Productivities (mM/d) of selected metabolites calculated at 39 days EFT for bottles of the control experiments M-CTRL, T-CTRL, M-BES, T-BES; Table S3: Acetate, propionate and *n*-butyrate productivities for all bottles of M-PAC and T-PAC experiments; Table S4: Productivities of CO, CH₄, H₂, CO₂ and VFAs in mM/d at increasing PAC concentrations and different temperatures. Negative productivity indicates consumption; Figure S1: Cumulative CO uptake rate in mmol for experiments M-BES, M-CTRL and M-PAC; Figure S2: Cumulative H₂ uptake rate in mmol

for experiments M-BES, M-CTRL and M-PAC; Figure S3: Cumulative CO₂ uptake rate in mmol for experiments M-BES, M-CTRL and M-PAC. Negative values mean consumption; Figure S4: Cumulative CH₄ uptake rate in mmol for experiments M-BES, M-CTRL and M-PAC; Figure S5: Cumulative CO uptake rate in mmol for experiments T-BES, T-CTRL and T-PAC; Figure S6: Cumulative H₂ uptake rate in mmol for experiments T-BES, T-CTRL and T-PAC. A negative uptake means production; Figure S7: Cumulative CO₂ uptake rate in mmol for experiments T-BES, T-CTRL and T-PAC. A negative uptake means production; Figure S8: Cumulative CH₄ uptake rate in mmol for experiments T-BES, T-CTRL and T-PAC.

4. Energy recovery potential from other pyrolysis aqueous condensates

This chapter is based on the publication:

Energy recovery from syngas and pyrolysis wastewaters with anaerobic mixed cultures. Alberto Robazza and Anke Neumann

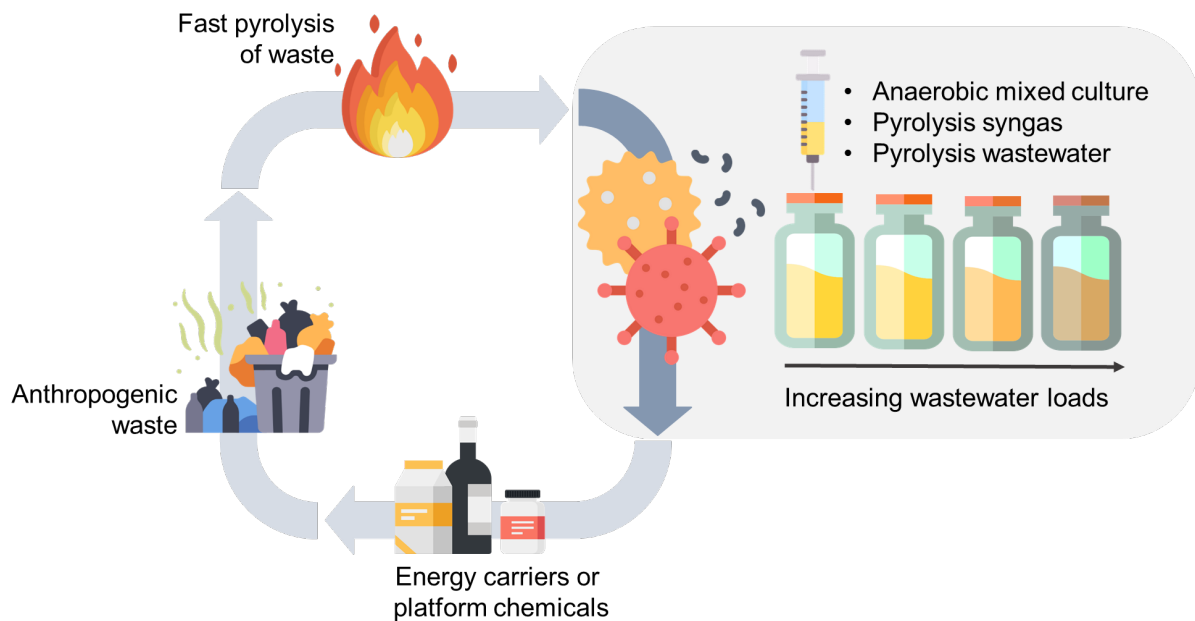
Bioresources and Bioprocessing (2024), 11, 75.

<https://doi.org/10.1186/s40643-024-00791-3>

Author's contributions

Alberto Robazza	conceptualization, methodology, investigation, data curation and analysis, visualization, first draft and manuscript revision
Anke Neumann	conceptualization, methodology, data analysis support, project supervision and manuscript revision

Graphical abstract



Abbreviations

PAC: pyrolysis aqueous condensate

SS: sewage sludge

PE: polyethylene

SS-PAC: pyrolysis aqueous condensate derived from the pyrolysis of sewage sludge

PE-PAC: pyrolysis aqueous condensate derived from the pyrolysis of polyethylene plastics

M-SS-PAC: experiments evaluating the mesophilic co-fermentation of syngas and SS-PAC

T-SS-PAC: experiments evaluating the thermophilic co-fermentation of syngas and SS-PAC

M-PE-PAC: experiments evaluating the mesophilic co-fermentation of syngas and PE-PAC

T-PE-PAC: experiments evaluating the thermophilic co-fermentation of syngas and PE-PAC

COD: chemical oxygen demand

SCCs: short-chain carboxylates

VSS: volatile suspended solids

TAN: total ammonia nitrogen

eeq: electron equivalents

e-mol: electron moles

IC₅₀: inhibitory concentration of a toxicant reducing of 50% microbial activity

4.1 Introduction

Improper management of municipal sewage sludge (SS) and post-consumer plastics such as polyethylene (PE) poses risks to both human health and the environment. Common disposal methods, including landfilling, agricultural use of SS and incineration have some drawbacks. For example, landfilling can cause leachate pollution and greenhouse gas emissions, while agricultural applications of SS may elevate the concentrations of heavy metals in the soil. Incineration, on the other hand, produces noxious volatile compounds, requiring costly technologies to control pollutant emissions [2]. Additionally, the recycling of post-consumer plastics is not entirely closed-loop, resulting in some waste persisting as micro plastics in the environment [3].

Considering the escalating volume of waste generated, a reassessment of available technologies is imperative to reduce environmental impacts whilst maximising energy and resources recovery from both wastes [4]. Thermochemical recycling technologies (such as hydrothermal conversion, gasification or pyrolysis) have the potential to address waste management challenges by reducing dependence on landfilling, minimizing solid residue volumes and mitigating greenhouse gas emissions and other harmful pollutants [37]. Pyrolysis, for instance, yields products such as biochar, bio-oil, syngas (a mixture of CO, H₂, CO₂, CH₄ and other alkanes and alkenes in smaller concentration) and a pyrolysis aqueous condensate (PAC) [20]. In general, biochar, bio-oil and syngas are the target products of thermochemical processes, exhibiting heating values comparable to other fuels. The PAC, on the other hand, although accounting for about 20-30% of the wet mass of the original feed, is considered a by-product due to high water content and low calorific value, thereby lowering pyrolysis efficiency [16]–[18].

The applications and handling of PAC are limited by its toxicity and complexity [20], [30]. PAC can contain hundreds of compounds including organic acids, phenolics, amines, amides, guaiacols, furans, hydrocarbons and nitrogen heterocycles [24]–[28]. Many more remain poorly characterized posing challenges in assessing their specific inhibitory effects on microbial activity [19], [29]. In addition, traces of bio-oil can be also contaminating the aqueous condensate [30]. In general, the composition of PAC is primarily determined by the type of feedstock. In the case of the PAC generated from the pyrolysis of sewage sludge (SS-PAC), for instance, the concentration of different constituents depends upon the levels proteins, lipids and lignin of the original waste [32]. Phenolic compounds can arise from the volatilization of polysaccharides and proteins, aromatic hydrocarbons stem from the decarboxylation of fatty acids within the lipid fraction, while ammonium and N-heterocycles are some products of protein decomposition [33]. Carbocyclic acids, phenolics and hydrocarbons can be found also in the PAC resulting from the pyrolysis of mixed polyethylene plastics (PE-PAC) and originate from organic impurities of the waste

[34]–[36]. The type and concentration of PAC components determine the chemical properties and the toxicity of the solution [24]. SS-PAC, for instance, exhibits basic pH, whereas PE-PAC is acidic. Despite both PACs may contain similar concentrations of carboxylic acids, the pH disparity may depend upon the presence of high concentration of ammonium and nitrogen aromatics in SS-PAC [15], [37]. The integration of thermochemical and biological processes into a unified platform represents a technology that could improve the energy and resource recovery from pyrolysis by-products and enhance the economic sustainability of the process on an industrial scale [60], [63], [106]. Previous attempts to valorise various PACs in single-culture fermentations encountered challenges that required extensive detoxification through physicochemical pre-treatments [58]. Anaerobic digestion, on the other hand, stands out as a viable technology for recovering energy from PAC components such as carboxylic acids, anhydrous sugars and aromatic compounds, among others, fermenting them into biogas. Various factors such as the microbial composition of the inoculum, concentration of refractory and toxic compounds, the molecular weight of PAC components, PAC loading rate and process operating conditions affect process performances [67]–[70]. The addition of suitable amendments such as biochar has been proven successful to mitigate the toxicity of PAC compounds on methanogenesis [84], [85], [89], [90], [97]–[99]. Alternatively, since syntrophic and acidogenic microorganisms play a crucial role in the degradation of PAC components, their enrichment or bio-augmentation could serve as a viable strategy to enhance PAC degradation and overall process performance [68], [73], [105], [106], [76], [83], [99]–[104].

Currently, coal gasification and steam reforming of natural gas stand as the primary methods for syngas production, albeit generating substantial green-house gas emissions. Conversely, the steel-manufacturing industry and thermochemical conversion of waste offer alternative sources of syngas characterized by lower green-house gas emissions [168]. However, with ongoing technological advancements in electrolysis for H₂ production, there is potential for steel-manufacturing industries to achieve full decarbonisation of their processes [169], leaving thermochemical conversion of waste as one of the remaining sources of syngas. The biological conversion of syngas into biofuels or other valuable commodity chemicals is emerging as a key biotechnological tool for establishing a circular bioeconomy [200]. Syngas fermentation has been explored for the production of biopolymers, single cell proteins, medium-chain carboxylates and other valuable compounds, showcasing its potential and versatility [107]. Research on anaerobic syngas fermentation centers predominantly on acetogens such as *Clostridium ljungdahlii*, *Clostridium autoethanogenum*, *Acetobacterium woodii* and *Moorella thermoacetica*, which employ the Wood-Ljungdahl pathway to fix CO and H₂/CO₂, producing acetyl-CoA as the central intermediate [108]. Alternatively, syngas fermentation with mixed anaerobic cultures has shown potential for CH₄ or carboxylates production. Beyond acetogens,

other microbes capable of metabolizing syngas within anaerobic cultures include certain hydrogenogenic bacteria, methanogenic archaea and sulfate-reducing bacteria [116]. While CH_4 is often the primary metabolite of mixed culture syngas fermentation [119]–[121], innovative research has developed processes for producing short and medium-chain carboxylates [114], [117]–[119], [132], [220]. Incorporating syngas as a substrate during the anaerobic fermentations of organic waste could provide extra electron donors to the process, enhancing energy recovery while minimizing gaseous emissions [119].

In this context, despite both syngas and PAC originating from the pyrolysis process, knowledge regarding their co-fermentation remains limited. Only few works have focussed on the co-fermentation of syngas and lignocellulose PAC, demonstrating the capability of anaerobic mixed cultures to concurrently perform syngas sequestration and degradation of pyrolysis-derived organic components for biogas and short-chain carboxylates (SCCs) production [100], [295]. One study explored the co-fermentation of syngas, PAC and glucose for carboxylates production in a continuous biochar-packed reactor [100], while another one demonstrated the potential of a two-stage process, aerobic to anaerobic, for converting the carboxylates produced from syngas and PAC co-fermentation in the initial stage into L-malate in the second stage [295]. However, additional research dedicated to syngas and PACs co-fermentation is necessary to broaden the understanding of this technology and its potential for integrating thermochemical waste conversion with biological processes to enhance energy recovery from waste.

The objective of this work is to investigate the effects of the PAC composition on the metabolism of mesophilic and thermophilic anaerobic mixed cultures during the co-fermentation of syngas and either SS-PAC or PE-PAC. By conducting tests at increasing PAC loadings in 250 mL bottles, the study elucidates kinetic inhibitions, metabolic shifts and the energetics of the process in correlation to the specific PAC cell load. The results of this work will contribute to a deeper understanding of anaerobic mixed cultures' potential to perform syngas sequestration and wastewater detoxification under diverse toxicants pressure. Bridging this knowledge gap is essential for unlocking the full potential of these waste streams in achieving a more sustainable and efficient waste conversion and energy recovery.

4.2 Materials and Methods

4.2.1 Inoculum and PACs

The inoculum was collected at an anaerobic digester treating cow-manure as described in another work [295]. The total suspended solids (TSS) and the volatile

suspended solids (VSS) of the inoculum were 41.1 ± 0.8 g/L and 18.9 ± 0.8 g/L, respectively, and were determined following the procedure described in the Method 1684 [201].

Both SS-PAC and PE-PAC were provided by the Institute of Technical Chemistry (ITC) at the Karlsruhe Institute of Technology, Campus Nord (Karlsruhe, Germany). The pyrolysis experiments were carried out using a pilot scale screw reactor system [17]. The SS-PAC used in this work was a 1:1 mixture of the PACs generated during the pyrolysis of a dried and non-dried sewage sludge. The pyrolysis process was non-catalyzed and performed at 500°C , with a residence time of 15 mins and a loading rate of 1.2 kg/h. SS-PAC had a pH of 9.6, a chemical oxygen demand (COD) of 185 g/L, a total organic carbon of 109 g/L, a total nitrogen concentration of 84.2 g/L and contained 92.6 ± 3.5 g/L of NH_4^+ , 9.9 ± 0.02 g/L acetate, 3.7 ± 0.05 g/L propionate and 1.8 ± 0.01 g/L butyrate. Similarly, the PE-PAC was a 1:1 mixture of two PACs produced during the pyrolysis of heavy weight and light weight mixed PE plastics. The pyrolysis was run at 450°C with a residence time of 30 min and a waste loading rate of 1 kg/h using zeolite as catalyst. PE-PAC had a pH of 1.8, a COD of 89.9 g/L, a total organic carbon of 30 g/L and contained 10.96 g/L of total nitrogen, 7.82 ± 0.01 g/L of NH_4^+ , 14.3 ± 0.3 g/L acetate, 2.7 ± 0.01 g/L propionate and 0.6 ± 0.1 g/L of butyrate. The mass balances of the pyrolysis processes and a more detailed composition of the PACs are available in the Supplementary Information (Additional file 3, Table S1, Table S2 and Table S3).

4.2.2 Fermentation

The bottle fermentations were conducted over a 10-day period, in triplicate, in 250 mL serum bottles with a 50 mL active volume. The fermentation medium comprised 5% v/v BA medium [295], a variable PAC amount based on the experimental design and deionized water as required to meet 45 mL. Either 4M NaOH or 4M H_3PO_4 was employed to adjust the pH post PACs addition. To account for the significant pH disparity between the two PACs and the necessity to minimize salts addition, the pH for SS-PAC bottles was set to 7.2, while PE-PAC bottles were set at 6.6. SS-PAC loading for mesophilic and thermophilic co-fermentations ranged from 2 to 24% v/v with 2% increments, while PE-PAC concentrations ranged from 0.5 to 6% v/v with 0.5% increments. The PACs loading during co-fermentation experiments were designed to achieve at least 90% methanation inhibition compared to controls under either mesophilic or thermophilic conditions.

After 24 hours of anaerobization in an anaerobic tent (5% H_2 in N_2), the bottles were inoculated with 10% v/v anaerobic sludge (resulting in 1.89 gvss/L at inoculation) and were then sealed with butyl rubber stoppers and aluminium rings. Subsequently, each triplicate underwent syngas flushing (6 kPa H_2 , 21 kPa CO, 26 kPa CO_2 , and N_2 at 1 L/min) and pressurization at room temperature to a final pressure of 210 kPa_{abs}. The gas flow was regulated by high precision mass flow controllers

(Vögtlin, Muttentz, Switzerland) and bottle pressure was monitored using a precision pressure indicator GMH 3100 Series (Greisinger, Mainz, Germany). Incubation occurred at 37° or 55°C and 210 rpm in two Thermotron shaker incubators (Infors, Bottmingen, Switzerland).

4.2.3 Analytical Methods

Daily pressure analysis and gas sampling were performed immediately after removal from the incubators. Three millilitres of the gas phase were sampled and analysed for the determination of the molar concentration of CO, CO₂, H₂, CH₄, H₂S and N₂ using an Inficon 3000 Micro GC System with a Thermal Conductivity Detector (TCD) equipped with a CP-Molsieve 5 Å column and a PoraPLOT Q column at 80° C using argon and helium as carrier gases, respectively. Every second day, 1 mL of the fermentation broth was sampled, centrifuged, filtered and stored at -20° C for later analytics. The concentrations of formate, acetate, propionate, *n*-butyrate and of some selected PAC compounds (phenol, guaiacol and *o*-,*m*-, *p*-cresol) were measured by a high-performance liquid chromatography (HPLC) (Agilent 1100 Series, Agilent, Waldbronn, Germany) at 55 °C with a Rezex ROA organic acid H⁺ (8%) column (300x7.8 mm, 8 µm; Phenomenex, Aschaffenburg, Germany) and a Rezex ROA organic acid H⁺ (8%) guard column (50 by 7.8 mm). The mobile phase was 5 mM H₂SO₄ at a flow of 0.6 mL/min. Benzene, triacetoneamine, benzonitrile and pyridine were quantified by means of high-performance liquid chromatography with an Agilent 1100 Series (Agilent, Waldbronn, Germany) at 40° C with a Kinetex 250x4.6 mm, 2.6 µm EVO C18 column (Phenomenex, Aschaffenburg, Germany) and a SecurityGuard 4x3.0 mm C18 guard column (Phenomenex, Aschaffenburg, Germany). The eluents were composed by a mixture of 0.1% v/v ethanolamine in H₂O and 0.1% v/v ethanolamine in acetonitrile flowing at 1.1 mL/min. The elution profile was: 0.5% at 0 min; 0.5% at 5 mins; 38.5% at 18 mins; 90% at 20 mins; 90% at 23 mins; 0.5% at 25 mins. Sulphate and nitrate concentrations were measured by ion chromatography with a Metrohm 930 Compact IC Flex (Metrohm, Filderstadt, Germany) equipped with a Metrosep A Supp 5-150/4.0. A solution of 1 mM of NaHCO₃ and 3.2 mM of Na₂CO₃ at 0.8 mL/min was used as eluent while 500 mM H₂SO₄ was used as suppressor. Photometrical quantification of the total ammonia nitrogen (TAN) concentrations were performed with a Spectroquant kit 114752 (Merck KGaA, Darmstadt, Germany). Free ammonia nitrogen (FAN) represents the un-ionized part of TAN and depends primarily upon pH and temperature (Eq. 5 and 6) [296].

$$C_{\text{FAN}} = \frac{C_{\text{TAN}}}{1+10^{(\text{pK}_a-\text{pH})}} \text{ [mM]} \quad \text{Eq.5}$$

$$\text{pK}_a = 0.09018 + \frac{2792.92}{T+273.15} \quad \text{Eq.6}$$

pK_a is the dissociation constant for ammonium ion, 8.892 at 37°C while 8.408 at 55°C. T is the temperature, °C. The molar amounts of each gas specimen (CO, H₂,

CO₂, CH₄) were determined at each sampling point using the ideal gas law, taking into account both pressure loss and air contamination during sampling. The differences in molar amounts between successive samplings were cumulated to yield the total quantity of gas produced or consumed (Eq.7).

$$n_{\text{gas},i} = \sum_{t=0}^j \frac{p_j \cdot V_j}{R \cdot T} [\text{mmol}] \quad \text{Eq.7}$$

Where $n_{\text{gas},i}$ is the cumulative absolute consumption/production of a gas specimen throughout the total fermentation time; p_j is the pressure of the bottle's head space at sampling time corrected to account for pressure loss by sampling; V_j is the bottle's head space volume; R is the gas constant; T is the incubation temperature; j is the number of samples.

The amount of gases and the difference in metabolites levels (Eq.8) (formate, acetate, propionate and butyrate) between initial and final samples were multiplied by the corresponding electron equivalents (eeq) and divided by the total fermentation time and initial broth volume to calculate space-time consumption/production rates of electron moles (e-mol).

$$q_{\text{e-mol},i} = \frac{n_i \cdot \text{eeq}_i}{V_{\text{Start}} \cdot t} [\text{e-mM/d}] \quad \text{Eq.8}$$

Where n_i is absolute amount of each metabolite produced or consumed during the total fermentation time; eeq_i is the amount of the substance i which releases 1 e-mol during complete oxidation; V_{Start} is the active volume at the start of the fermentation; t is the total fermentation time.

The e-mol recoveries were calculated as described in Eq. 9.

$$\text{e- mol recovery} = \frac{\sum n_i \cdot \text{eeq}_i}{n_{\text{Syngas, fed}} \cdot \text{eeq}_{\text{syngas}} + 8 \cdot \text{gCOD}_{\text{PAC, fed}}} * 100 [\%] \quad \text{Eq.9}$$

The e-mol_{PAC} were calculated assuming that 8 gCOD is equal to one e-mol. Considering that the COD is the oxygen required to completely oxidize the carbonaceous fraction of organic compounds and that 1 eeq. is released upon complete oxidation of carbonaceous compounds, then from the half reaction RS1, it can assumed that 1/4 mol of O₂ (8 g) would be consumed in accepting the 1 e-mol.



The e-mol balances and e-mol recoveries from PAC were calculated as outlined in the following equations.

$$\text{e- balance} = \frac{\sum n_i \cdot \text{eeq}_i}{n_{\text{CO}} \cdot \text{eeq}_{\text{CO}} + n_{\text{H}_2} \cdot \text{eeq}_{\text{H}_2}} * 100 [\%] \quad \text{Eq.10}$$

$$\text{e- mol recovery from PAC} = \frac{\sum n_i \cdot \text{eeq}_i - n_{\text{Syngas, fixed}} \cdot \text{eeq}_{\text{syngas}}}{8 \cdot \text{g}_{\text{PAC, fed}}} * 100 [\%] \quad \text{Eq.11}$$

Where n_i is absolute amount of each metabolite produced or consumed during the total fermentation time; eeq_i is the amount of the substance i which releases 1 e-mol during complete oxidation of any organic carbonaceous compound. Table S5

in the Additional file 3 reports the conversion factors used for electron balancing. All calculations were conducted individually for each bottle and the results were subsequently averaged across the replicates ($n=3$).

4.3 Results

This chapter illustrates the potential for carbon and e-mol recovery from syngas and two distinct PACs through anaerobic mixed culture fermentations. These waste streams result from the pyrolysis of sewage sludge and a combination of high and low density PE plastics. The analysis focuses on the space-time rates of syngas conversion into short-chain carboxylates at increasing PACs loading, evaluates the energy recoveries from both syngas and PACs and assesses the efficiency of removing some selected PAC components.

4.3.1 Syngas and Sewage Sludge PAC co-fermentation

The results from the mesophilic syngas and SS-PAC co-fermentation experiments (M-SS-PAC) will be presented first, followed by the thermophilic syngas and SS-PAC co-fermentation experiments (T-SS-PAC). In general, at both temperatures conditions, the cultures exhibited the ability to perform concurrent syngas sequestration and carbon-energy recovery from SS-PAC.

At 37° C, CO consumption rates showed no significant inhibition up to the SS-PAC loading of 9.8 g_{COD}/g_{VSS} but decreased linearly at greater loads (Figure 20a). At the SS-PAC load of 23.4 g_{COD}/g_{VSS}, carboxydrotrophic rates were 2.1±0.2 e-mM_{CO}/d, marking a four-fold decrease from control experiments. Methanation, on the other hand, was inhibited at lower specific SS-PAC loadings: a 1.9 g_{COD}/g_{VSS} SS-PAC loading caused a 12% inhibition of methanogenic rates compared to the control experiments, while at 11.7 g_{COD}/g_{VSS} the methanation was reduced by over 90%. Corresponding initial FAN and TAN concentrations were 13.36±0.3 mM (226.6 mg/L) and 629±6.7 mM (11,342 mg/L), respectively. Initial concentrations of FAN and TAN in the other broths of M-SS-PAC experiments are available in the Supplementary Information (Additional file 3, Figure S1a). The inhibitory concentration causing 50% inhibition (IC₅₀) of SS-PAC was determined to be 15.6 g_{COD}/g_{VSS} for carboxydrotrophic activity and around 7.8 g_{COD}/g_{VSS} for methanogenesis. Hydrogenotrophic activity was detected up to SS-PAC loadings of 9.8 g_{COD}/g_{VSS}, coincidentally to methane production. For higher SS-PAC loadings, the highest hydrogen production rate was 1.6±0.38 e-mM_{H₂}/d at 15.6 g_{COD}/g_{VSS}. Acetate constituted approximately 58% of the total e-mol sequestered from syngas during control experiments alongside traces of propanol and butyrate. Similarly, acetate, propionate and butyrate were the primary metabolites accumulating in the fermentation broth during syngas and SS-PAC degradation. The final pH for each condition are available in the Additional file 3 (Figure S4a). The e-mol recovery from syngas and SS-PAC (Figure

20e) peaked to $34.3 \pm 0.7\%$ at $1.9 \text{ g}_{\text{COD}}/\text{g}_{\text{VSS}}$. Similarly, the highest e-mol recovery from exclusively SS-PAC was $17.3 \pm 2.9\%$ at $1.9 \text{ g}_{\text{COD}}/\text{g}_{\text{VSS}}$ (Additional file 1, Figure S3a). Both recoveries decreased towards zero at increasing loadings of SS-PAC. The removal efficiency of selected SS-PAC components supports the degradation of phenolics, pyridine and possibly other SS-PAC constituents during the co-fermentation (Figure 20c). All SS-PAC components exhibited a positive removal efficacy, albeit with a diminishing trend as SS-PAC loadings increased.

During the thermophilic control experiments, CO oxidation occurred at a rate of $48.1 \pm 0.4 \text{ e-mM}_{\text{CO}}/\text{d}$, 6 times greater than the mesophilic control experiments (Figure 20b). However, it sharply declined concomitant with the incremental addition of SS-PAC. Methanogenic rates mirrored to those of syngas uptake. Traces of carboxydrotrophic activity ($2.4 \pm 0.2 \text{ e-mM}_{\text{CO}}/\text{d}$, 95% inhibition) were detectable up to $23.4 \text{ g}_{\text{COD}}/\text{g}_{\text{VSS}}$. Methanation was completely arrested at $11.7 \text{ g}_{\text{COD}}/\text{g}_{\text{VSS}}$. Corresponding initial FAN and TAN concentrations were $41.7 \pm 0.6 \text{ mM}$ (709.8 mg/L) and $674 \pm 10.3 \text{ mM}$ (12,169 mg/L), respectively. Initial concentrations of FAN and TAN in the other broths of T-SS-PAC experiments are available in the Supplementary Information (Additional file 3, Figure S1b). The influence of increasing SS-PAC loadings at 55°C had a more pronounced impact on carboxydrotrophic rates compared to mesophilic experiments. The IC_{50} was determined to fall between 3.9 and 6.8 $\text{g}_{\text{COD}}/\text{g}_{\text{VSS}}$ SS-PAC loadings for both carboxydrotrophic and methanogenic reactions. No significant hydrogen production was detected for SS-PAC loading higher than $17.6 \text{ g}_{\text{COD}}/\text{g}_{\text{VSS}}$. In control experiments, acetate and propionate constituted over 95% of the metabolites in the medium, with selectivities of approximately 85% and 10%, respectively.

Similarly, acetate and propionate were the primary metabolites in T-SS-PAC experiments. However, with higher SS-PAC amounts, increasing levels of butyrate were observed, reaching a peak productivity of $1.31 \pm 0.2 \text{ e-mM}_{\text{Butyrate}}/\text{d}$ at $11.7 \text{ g}_{\text{COD}}/\text{g}_{\text{VSS}}$. Methane inhibition coincided to formate accumulation in the medium at a maximum rate of $0.67 \pm 0.01 \text{ e-mM}_{\text{Formate}}/\text{d}$ at $15.6 \text{ g}_{\text{COD}}/\text{g}_{\text{VSS}}$. Thermophilic control experiments produced about 25% fewer e-mol_{SCCs} than mesophilic controls. Conversely, between loads of 1.9 and $15.6 \text{ g}_{\text{COD}}/\text{g}_{\text{VSS}}$, T-SS-PAC experiments produced 17% more e-mol_{SCCs} than M-SS-PAC experiments, peaking at approximately 60% at $11.7 \text{ g}_{\text{COD}}/\text{g}_{\text{VSS}}$. The average final pH for each SS-PAC loading is provided in the Supplementary information (Additional file 3, Figure S2b). Fermentations with low SS-PAC loadings (between 0 and $11.7 \text{ g}_{\text{COD}}/\text{g}_{\text{VSS}}$) resulted in a final pH lower than that recorded at the time of inoculation. Conversely, as SS-PAC loadings increased, the final pH exceeded the initial pH at inoculation.

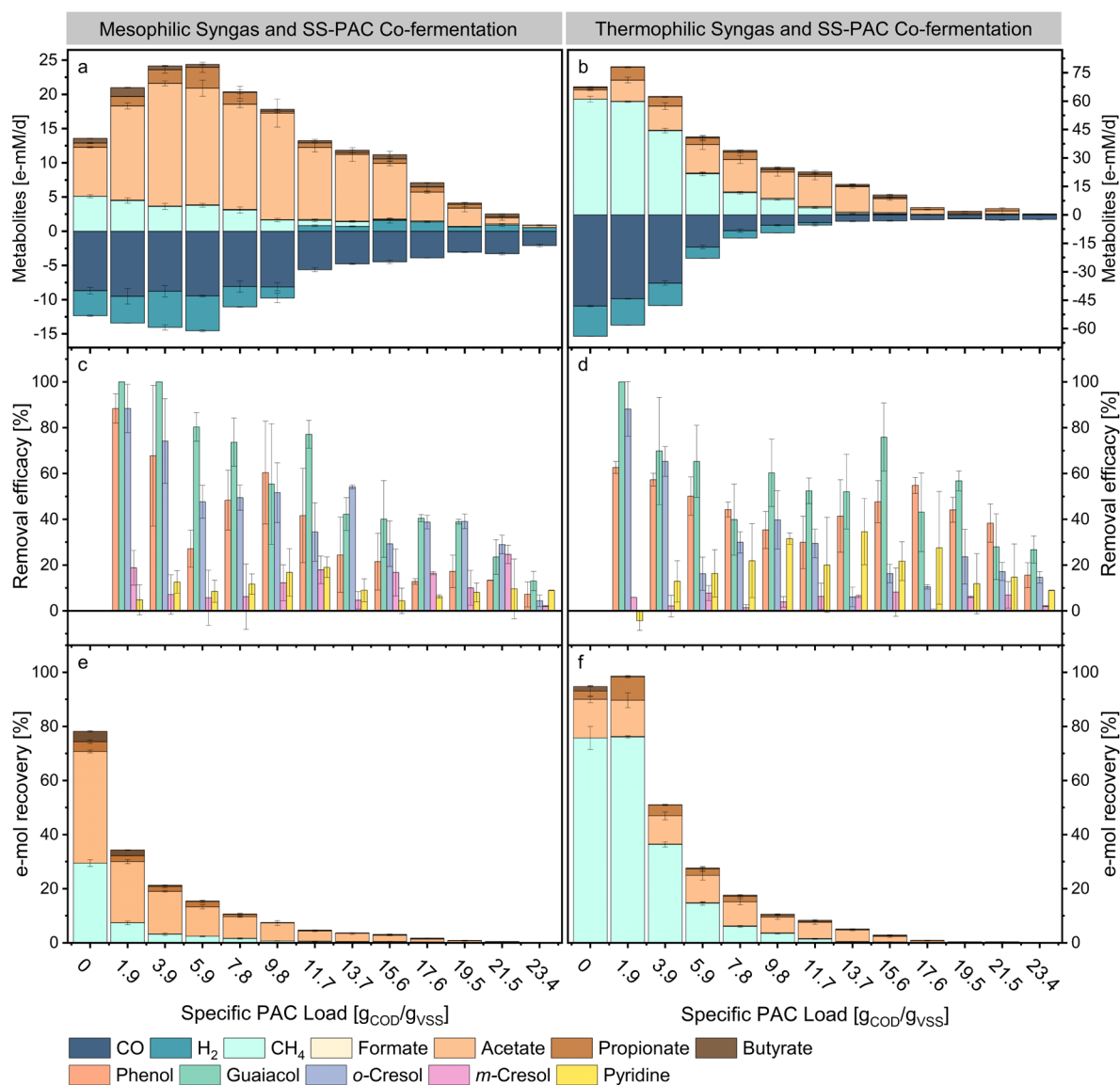


Figure 20. Effects of increasing SS-PAC loading on the metabolism of mesophilic (a, c, e) and thermophilic (b, d, f) mixed cultures. The graphs a and b show the kinetic rates of CO, H₂, CH₄, formate, acetate, propionate and *n*-butyrate for each load of SS-PAC. The colours highlight increasing e-equivalence of the metabolites detected. Negative values indicate consumption. The bar-graphs c and d show the removal efficacies of some SS-PAC compounds clustered for each load of SS-PAC. The bar-graphs e and f illustrate the e-mol recoveries from substrates (syngas fed and PAC) into products (methane, formate, acetate, propionate and butyrate). Error bars represent standard deviation among replicates ($n=3$).

During the thermophilic co-fermentation of syngas and SS-PAC, phenolics and pyridine were removed from the fermentation broths (Figure 20d). The removal of *m*-cresol was very low.

The higher syngas uptake rates at thermophilic temperatures than those observed in mesophilic experiments contributed to higher e-mol recoveries from both syngas and SS-PAC. For instance, the peak e-mol recovery of $98.6 \pm 6.2\%$ at a loading of $1.9 \text{ g}_{\text{COD}}/\text{g}_{\text{VSS}}$ was approximately three times higher than the corresponding mesophilic experiment. Averaging across all conditions, T-SS-PAC fermentations recovered 1.4-fold more e-mols than the M-SS-PAC experiments (Figure 20f). Similarly,

the thermophilic e-mol recovery from SS-PAC alone was, on average, about 50% higher than mesophilic e-mol recoveries (Additional file 3, Figure S3b).

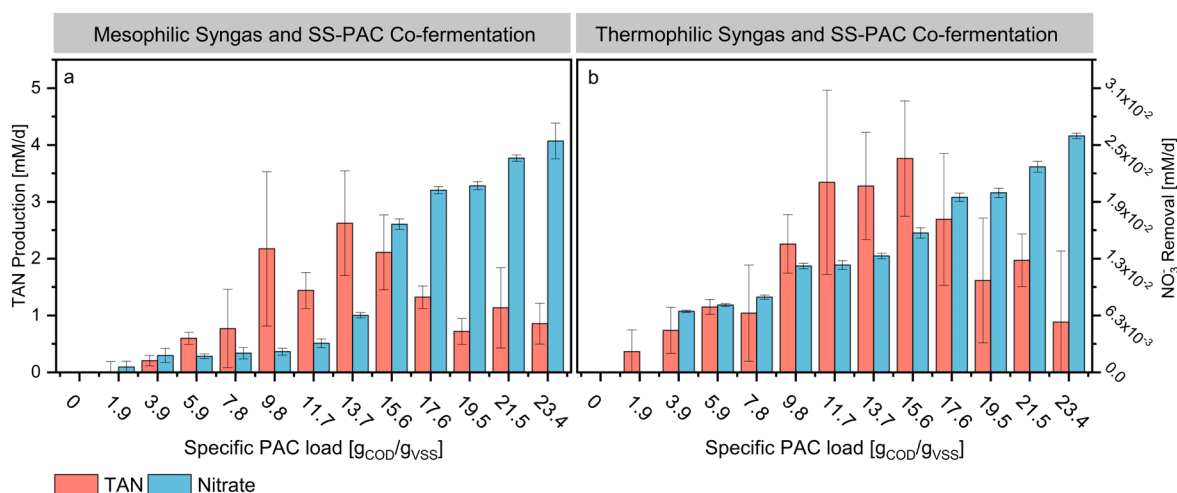


Figure 21. Total ammonium nitrogen (TAN) production rates and nitrate removal rates for mesophilic (a) and thermophilic (b) SS-PAC experiments. TAN production rates are red while nitrate removal rates are blue. The left Y-axis of graph a represents the scale for both M-SS-PAC and T-SS-PAC experiments. The right Y-axis of graph b represents the scale for both M-SS-PAC and T-SS-PAC experiments. Error bars represent standard deviation among replicates (n=3).

When evaluating the e-mol balance between products (SCCs, methane and hydrogen) in comparison to syngas (excluding PAC), recoveries higher than 100% were consistently observed between SS-PAC loadings of 1.9 and 19.5 g_{COD}/g_{VSS} (Additional file 3, Figure S4). This trend corroborates the fact that some products originate from the degradation of PAC components into SCCs. However, in both M-SS-PAC and T-SS-PAC and at specific SS-PAC loadings higher than 19.5 g_{COD}/g_{VSS}, the e-mol recoveries decreased below 100%. Mesophilic and thermophilic peak TAN production rates were 2.6 ± 0.9 mM/d and 3.8 ± 0.6 mM/d at 13.7 and 15.6 g_{COD}/g_{VSS}, respectively (Figure 21a and Figure 21b). At the same SS-PAC loadings, SCCs production rates were 10.5 ± 1.2 e-mM_{SCCs}/d and 10.1 ± 1.6 e-mM_{SCCs}/d. Nitrate was completely depleted in all of the fermentation media from both experimental sets. Sulphate, on the other hand, exhibited no significant changes between initial and final samples.

4.3.2 Syngas and Polyethylene Plastics PAC co-fermentation

The following results illustrate the biomethanation and e-mol recovery capabilities of syngas and PE-PAC via anaerobic fermentations. The results from the mesophilic syngas and PE-PAC co-fermentation experiments (M-PE-PAC) will be presented first, followed by the thermophilic syngas and PE-PAC co-fermentation experiments (T-PE-PAC). In general, PE-PAC showed significantly higher toxicity to syngas conversion rates for both mesophilic and thermophilic mixed cultures compared to SS-PAC.

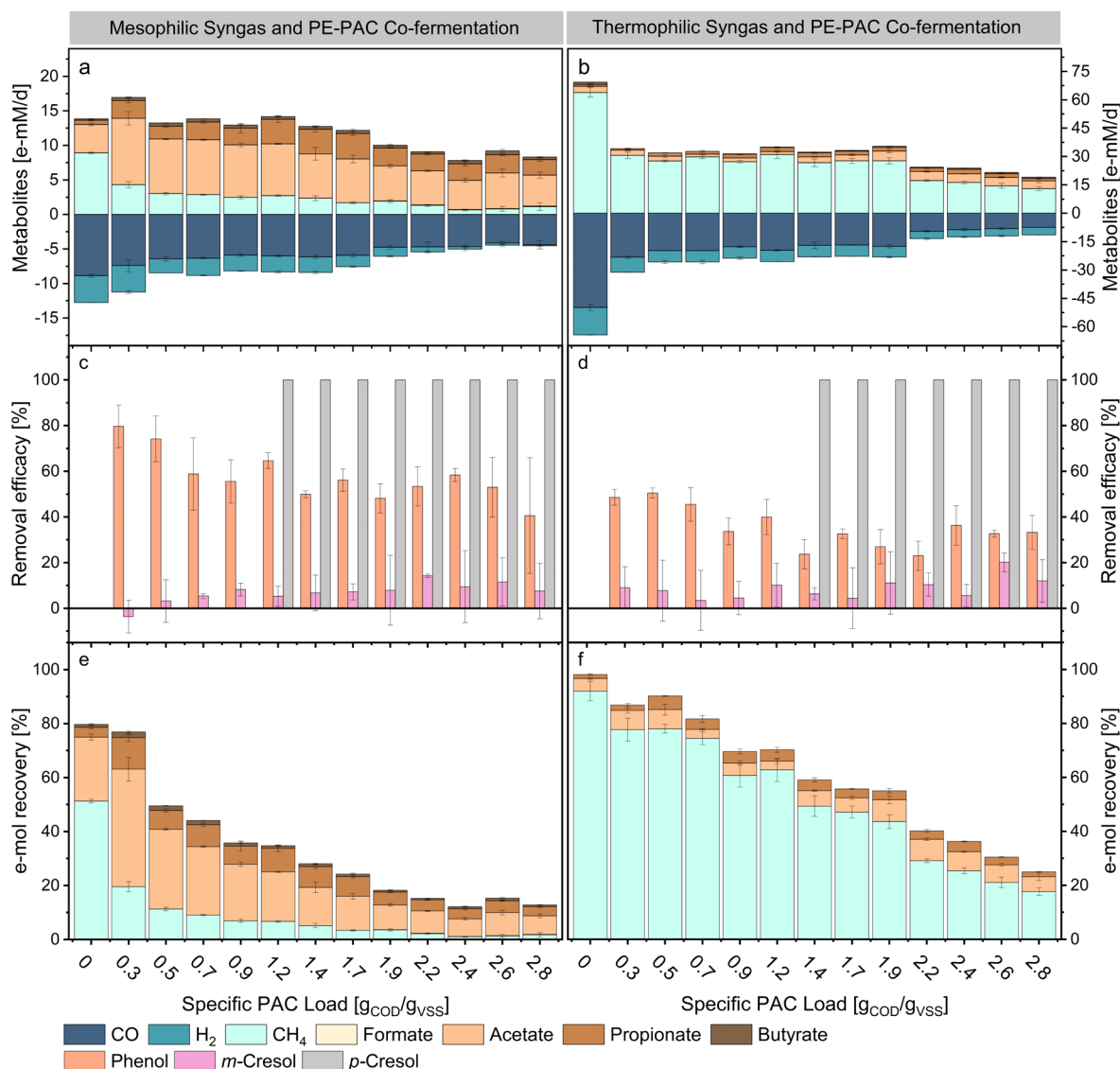


Figure 22. Effects of increasing PE-PAC loading on the metabolism of mesophilic (a, c, e) and thermophilic (b, d, f) mixed cultures. The graphs a and b show the kinetic rates of CO, H₂, CH₄, formate, acetate, propionate and butyrate for each load of PE-PAC. The colours highlight increasing e-equivalence of the metabolites detected. Negative values indicate consumption. The bar-graphs c and d show the removal efficacies of some PE-PAC compounds clustered for each load of PE-PAC. The bar-graphs e and f illustrate the e-mol recoveries from substrates (syngas fed and PAC) into products (methane, formate, acetate, propionate, butyrate). Error bars represent standard deviation among replicates (n=3).

At 37°C, CO uptake rates exhibited a linear decrease with increasing loadings of PE-PAC (Figure 22a). In control experiments, carboxydrotrophic activity measured 8.9 ± 0.2 e-mM_{CO}/d but decreased to 4.4 ± 0.6 e-mM_{CO}/d at a PE-PAC specific loading of 2.8 g_{COD}/g_{VSS}. Methanation rates, on the other hand, experienced a substantial reduction of approximately 90%, decreasing to 1.1 ± 0.6 e-mM_{CH₄}/d at 2.8 g_{COD}/g_{VSS} PE-PAC compared to the 8.9 ± 0.1 e-mM_{CH₄}/d observed in control experiments. The PE-PAC loading causing 50% reduction of carboxydrotrophic activity was 2.8 g_{COD}/g_{VSS}, whilst the IC₅₀ for methanogenesis was 0.3 g_{COD}/g_{VSS}. Hydrogen consumption was detected in all conditions, with hydrogenotrophic rates decreasing linearly, paralleling the decline in methanogenic rates.

In mesophilic control fermentations, acetate and propionate constituted approximately 100% of the SCCs, with production rates of 4.1 ± 0.2 e-mM_{Acetate}/d and 0.6 ± 0.1 e-mM_{Propionate}/d, respectively. Traces of butyrate were also detected. Co-fermentation of syngas and PE-PAC enhanced acetate, propionate and butyrate productivities, reaching a peak cumulative value of 11.4 ± 0.8 e-mM_{SCCs}/d at 1.2 g_{COD}/g_{VSS}. Acetate selectivity progressively decreased in favour of propionate but always remained above 60%. Propionate selectivity, on the other hand, increased from about 12% of the control experiments to about 35% at 1.7 g_{COD}/g_{VSS}. Formate production was detected concomitantly to reducing methanation rates. When considering PE-PAC components degradation, phenol was consistently removed from the fermentation media (Figure 22c). Between loadings of 0.3 to 0.9 g_{COD}/g_{VSS}, the initial concentrations of *p*-cresol were below detection limit. At higher PE-PAC concentrations, *p*-cresol was completely removed from the fermentation broths. Similar to the removals obtained for SS-PAC, *m*-cresol showed minimal removal during the M-PE-PAC tests.

The e-mol recovery for mesophilic control experiments was 79.2 ± 2.4 % (Figure 22e). During syngas and PE-PAC co-fermentation, the e-mol recovery decreased linearly at increasing PE-PAC loadings. At a loading of 0.3 g_{COD}/g_{VSS}, the e-mol recovery from syngas and PAC was at its highest (76.9 ± 2.4 %), while nearly 100% recovery was observed from PAC alone. Higher PE-PAC loadings hindered e-mol recovery, lowering it to 11.5 ± 0.2 % at 2.8 g_{COD}/g_{VSS}.

At 55°C , even the smallest PE-PAC loading of 0.3 g_{COD}/g_{VSS}, caused a 50% reduction in CO uptake rates. Carboxydrotrophic rates remained above 17 e-mM_{CO}/d (a 66% reduction compared to thermophilic controls) up to 1.9 g_{COD}/g_{VSS}. However, higher PE-PAC loadings led to a drop of CO uptake rates a drop to 7.5 ± 0.1 e-mM_{CO}/d at 2.8 g_{COD}/g_{VSS} (about 80% inhibition). Methane was the primary metabolite, regardless of the PE-PAC load (Additional file 3, Figure S5a). Similar to the T-SS-PAC tests, methanogenic rates were limited by CO oxidation kinetics and exogenous H₂ availability, resulting in an identical IC₅₀ of 0.3 g_{COD}/g_{VSS} for methanogenesis.

In the control experiments, acetate, propionate and butyrate selectivities were about 59, 19 and 21%, respectively. Low PE-PAC loading favoured higher propionate ratios at the expenses of acetate but increasing PE-PAC loadings led to higher acetate and butyrate ratios. Acetate production rates increased steadily from 3.2 ± 0.2 e-mM_{Acetate}/d of the control experiments to 5.1 ± 0.9 e-mM_{Acetate}/d at 1.9 g_{COD}/g_{VSS}. Higher PE-PAC loadings, on the other hand, progressively lowered the acetate productivity to 4.1 ± 0.5 e-mM_{Acetate}/d at 2.8 g_{COD}/g_{VSS}. Propionate productivity followed a trend similar to the one of acetate with decreasing rates after peaking to 2.45 ± 0.1 e-mM_{Propionate}/d at 2.4 g_{COD}/g_{VSS}. Traces of butyrate production were detected at high PE-PAC loadings with the highest rate of 0.7 ± 0.03 e-mM_{Butyrate}/d at 2.8 g_{COD}/g_{VSS}. Phenol showed stable removals, throughout all conditions (Figure

22d). Similarly to M-PE-PAC tests, between loadings of 0.3 to 1.2 g_{COD}/g_{VSS}, initial *p*-cresol concentrations were too low to be detected. At higher PE-PAC loadings, *p*-cresol was completely removed from the fermentation broths. No consistent removal of *m*-cresol was detected.

High PE-PAC loadings resulted in the accumulation of acetate, propionate and butyrate in the fermentation medium possibly resulting from the degradation of PE-PAC compounds (Additional file 1, Figure S5b). Thermophilic temperatures improved energy recovery from both syngas and PE-PAC exhibiting e-mol recoveries on average two times higher than the M-PE-PAC experiments. The highest e-mol recoveries from syngas and PE-PAC were 99.8%, 86.8% and 90.2%, recorded at low PE-PAC loadings ranging between 0 to 0.5 g_{COD}/g_{VSS}. Higher PE-PAC loadings progressively lowered the e-mol recovery to about 25% at the PE-PAC loading of 2.8 g_{COD}/g_{VSS}. Similarly, the thermophilic mixed cultures recovered 72.6% of the e-mol of PE-PAC at 0.3 g_{COD}/g_{VSS} but recoveries decreased to about 26% at PE-PAC loadings of 2.8 g_{COD}/g_{VSS} (Additional file 3, Figure S7b).

4.4 Discussion

4.4.1 PACs inhibition on anaerobic mixed culture metabolism

Total ammonium nitrogen, phenolics and N-heterocycles are among the components of SS-PAC that may have contributed in a synergic manner to the inhibition of methanogenic and carboxydrotrophic activity. A study examining the methane production during the anaerobic digestion of a PAC (with COD > 200 g/L and approximately 63 g_{TAN}/L), derived from a non-catalyzed pyrolysis of sewage sludge, reported severe methanogenesis inhibition at PAC loads of 2.3 g_{COD}/L. Although the specific PAC load was not mentioned, the mixture of compounds such as phenol, cresol, ethylbenzene and styrene, among others, was considered the primary cause of inhibition [24]. Similarly, a 6% load of a wastewater (89 g_{COD}/L and 10.1 g_{TAN}/L) from the hydrothermal liquefaction of cyanobacteria inhibited of 50% the methanogenic activity of an anaerobic sludge [50]. In this work, PAC loads completely inhibiting methanogenesis were 22.2 g_{COD}/L for both the mesophilic and thermophilic conditions. The lower toxicity of the SS-PAC used in this study may be the result of a different PAC composition resulting from pyrolysis process condition and waste type. Even though some phenolic compounds detected in this SS-PAC are toxic and inhibit microbial activity, their concentrations in the raw SS-PAC are below previously reported IC₅₀ values for methanogenesis [291], [297]. Similarly, some N-heterocycles, such as triacetoneamine and 2-pyrrolidinone can cause a synergistic cytotoxicity only when mixed [78]. Among the other toxic compounds present in this SS-PAC, TAN is the only one at concentrations that have been previously reported to inhibit methanogenesis. In this work, a reduction of at least 80% of methanogenic activity was detected at SS-PAC loadings of 9.8 g_{COD}/g_{VSS} with 575.6 ± 26.4 mM_{TAN}

(equivalent to 10.4 ± 0.5 g_{TAN}/L) under both mesophilic and thermophilic conditions. TAN and FAN are well known microbial inhibitors of anaerobic digestion processes [298], [299]. Consistent with the findings obtained here, studies examining the effects of increasing TAN concentrations on the anaerobic digestion of calcium acetate found that 9 g_{TAN}/L caused a 90% reduction of methane production rates compared to control experiments with no additional TAN [24]. Similarly, 10 g_{TAN}/L (with a pH ranging between 7.4 and 7.6) inhibited approximately 90% of the specific methanogenic activity of an anaerobic granular sludge [300]. Another study evaluating TAN inhibition of H₂/CO₂ methanation reported that 7 g_{TAN}/L (at a pH of about 8) inhibited methane yield by 41% and 22.3% in mesophilic and thermophilic conditions, respectively [301]. Here, a higher FAN to TAN ratio (approximately 3.2 times higher), as consequence of the higher temperatures of the thermophilic conditions, may have caused the stronger inhibition observed compared to mesophilic conditions. FAN is generally considered more toxic than the ammonium ion and FAN concentrations ranging from 0.15 up to 1.2 g_{FAN}/L were recorded to be severely toxic to anaerobic digestion [299]. FAN toxicity alters intracellular pH, increasing maintenance energy requirements to balance pH and depleting intracellular potassium reservoirs [302].

Numerous studies have documented an accumulation of SCCs during anaerobic digestion processes under TAN stress, suggesting for a potentially higher tolerance of fermentative bacteria compared to methanogens [301], [303]–[305]. Consistent with those findings, in this work carboxydrotrophic activity and carboxylates production persisted at higher SS-PAC loads than methanogenesis, especially at mesophilic conditions. This competitive advantage may be correlated to the Gibbs free energy of the involved metabolic reactions [306]. However, the resistance of homoacetogens to high TAN concentrations appears to be specie specific and may involve direct inhibition of specific enzymatic reactions such as hydrogenases. High TAN concentrations showed a non-competitive type of inhibition to the hydrogenase activity of *Clostridium ragsdalei* when grown on syngas [307]. Five grams per litre of TAN (at pH 6) inhibited the growth and CO uptake of *C. autoethanogenum*, *C. ljungdahlii* and *C. ragsdalei* in batch bioreactor fermentations fed with a synthetic syngas mixture [308]. On the contrary, 10 g_{TAN}/L did not affect the growth and CO consumption of *C. carboxidivorans* in batch fermentations while 5 g_{TAN}/L doubled CO oxidation rates compared to control results [309].

In general, high TAN concentrations in anaerobic digestion processes have been reported to favour syntrophic acetate oxidation and hydrogenotrophic methanogenesis over acetoclastic methanogenesis [296], [303], [310]–[312]. Therefore, process recovery and tolerance to TAN toxicity can be enhanced through bioaugmentation with syntrophic acetate-oxidizing bacteria and/or hydrogenotrophic methanogens [41], [312], [313], or by supplementing exogenous H₂ as a substrate

to methanogens [301]. However, it is not clear whether in this work exogenous H₂ supplementation from syngas (or endogenous H₂ production from the water gas shift reaction) contributed to alleviate ammonium toxicity.

Despite having a lower COD compared to SS-PAC, PE-PAC exhibited higher toxicity. This increased toxicity was likely a consequence of its composition and concentrations of compounds. Many of the components of PE-PAC are known to be toxic to microorganisms. For instance, phenol, *o*-cresol, *m*-cresol, benzene and benzonitrile exhibited IC₅₀ values for methanogenesis of 2.1, 0.9, 1.2 and 1.1 g/L, respectively [297]. Phenol alters membrane proteins and cell wall permeability and its toxic impacts to anaerobic digestion are well documented [314]. Cyclopentanone, at a concentration of 1 g/L, inhibited methane production from acetate by 21% [315]. Furthermore, 1,4-dioxane compromises cell membrane integrity. At 2 g/L, it reduced the specific activity of an anammox microbial consortium by 55% [316]. Like SS-PAC, none of the organic compounds in PE-PAC was present at concentrations high enough to be considered a primary inhibitor and, accordingly to other works, the overall toxic effects may have been enhanced the synergistic effect of the multiple toxicants present in PE-PAC [73]–[77].

4.4.2 PAC components degradation and energy recovery

In addition to defining the extent of inhibition, the composition and loading of PAC greatly influenced the energy (*i.e.*, electron equivalents) recovery potential. Sewage sludge-derived PAC exhibited lower toxicity to carboxydrotrophic rates than PE-PAC, however it was recalcitrant to bioconversion. Conversely, despite the strong inhibition caused to CO conversion rates, PE-PAC showed high e-mol recoveries. Furthermore, thermophilic conditions enhanced the e-mol recovery.

The degradation of PAC components in anaerobic cultures is subject to various influencing factors, including the source of inoculum (*i.e.*, microbial composition), the molecular weight of PAC components, process operating conditions and the presence of other compounds [67]–[70]. Low PAC concentrations can provide nutrients to microbial activity where many toxic components can act as substrates [50], [51]. Energy recovery from sewage SS-PAC into methane and SCCs likely resulted from the degradation of phenol, guaiacol and cresol, for instance. Conversely, nitrogen heterocyclic compounds and amides, despite being the most abundant components of SS-PAC, are considered recalcitrant to anaerobic degradation [24], [70], [71], thus diminishing overall energy recovery potential from this substrate [20]. However, there are documented instances of anaerobic degradation of certain N-heterocyclic components, such as pyridine, into carboxylates and methane [69], [76], [85], [86]. The efficacy of N-heterocycles removal is also affected by the presence of other compounds. For example, another work reports of pyridine degradation inhibition at phenol concentrations exceeding 400 mg/L [81]. Pyridine can undergo hydroxylation, ring cleavage between C₁-C₃, opening of the nitrogen ring and

release of ammonium with formic and succinic acid as intermediate metabolites of its degradation. Methane was then produced directly from formic acid or from the acetate produced via succinic acid [76], [86]–[88]. Increasing TAN concentrations are considered reflection of the degree of degradation of N-heterocyclic compounds. For instance, TAN concentrations in the effluent from the anaerobic digestion of hydrothermal liquefaction wastewater of algal biomass were approximately 6 times higher compared to the influent stream and were assumed to be the result of N-heterocycles degradation [77]. Similar results were obtained in this work, where the production of TAN in both mesophilic and thermophilic SS-PAC processes may corroborate the degradation of N-heterocycles such as pyridine. Alternatively, a part of the TAN generated here may also derive from the degradation of proteins released in the fermentation broth from cell lysis following inoculation. In previous attempts to improve the anaerobic degradability of N-heterocyclic compounds, nitrate supplementation was shown to enhance the anaerobic degradation of compounds such as pyridine while serving as electron acceptor [70], [317]. At high SS-PAC loads, concurrent nitrate removal, pyridine degradation and electron balances below 100% may suggest the occurrence of analogous mechanisms in this work, where the nitrate in SS-PAC acted as an electron acceptor and may have facilitated pyridine degradation.

In PE-PAC experiments, similarly to SS-PAC, phenol and cresol accounted for about 40% of the initial COD and their degradation possibly contributed to the higher energy recoveries. Knowledge about the anaerobic phenol and cresol degradation is already available and was reported to occur also in un-acclimatised anaerobic microbial consortia [50], [295]. For instance, removal efficiencies of cresol ranging from 10% to 60%, depending on pyrolysis temperature, were observed during biochemical methane potential studies of the aqueous phase from solid digestate at 40°C [84]. One hundred milligram per litre of phenol were completely removed in 10 days during specific methanogenic activity tests at thermophilic conditions [318]. In the same work, inoculum acclimation to phenol improved removal to 378 mg/L/d. The low *m*-cresol removal recorded in this work was possibly result of the complexity of the PAC and the presence of various compounds, impeding higher removal efficiencies. In an anaerobic UASB fed with a wastewater containing 900 mg/l of phenol and 320 mg/l of *m*-cresol, removal efficiencies as high as 98% and 20% were recorded for phenol and *m*-cresol, respectively, but phenol availability was considered limiting *m*-cresol removal [79]. Vice versa, *m*-cresol highly affected phenol biodegradation in another work [80]. On the other hand, in a methanogenic anaerobic continuous reactor fed with 150 mg/L phenol and with 35 mg/L of *o*- and *p*-cresol (0.25 days hydraulic retention time and a loading rate of 880 mg/L/day), a 98% removal rate was recorded for all substrates [82]. The likelihood of anaerobic degradation of other PE-PAC components such as benzene, cyclopentanone, benzonitrile, 2-chloroethanol and 1,4-dioxane seems improbable in this study. Although

reports of anaerobic degradation for some exist, it is very slow, requires long adaptation times or more selected microbial consortia [316], [319]–[321].

Reports of syngas co-fermentation with wastewaters from thermochemical processes are limited. For instance, during the continuous fermentation of syngas and increasing loadings of PAC derived from the pyrolysis of fir sawdust in a mesophilic biochar-packer bioreactor, the acclimatized microbiota recovered an average of 82% COD, yielding 45% of the COD input into carboxylates. Approximately 46% of the CO fed was consumed, but syngas accounted for only 5% of the total COD input. While the unreacted/recalcitrant COD fraction from PAC in the effluent was estimated between 25% to 52% [100]. Here, at low PACs loading, syngas was the substrate with the highest conversion rates. However, higher PAC loadings resulted in greater inhibition of syngas conversion rates compared to PAC conversion rates. The increased availability of PAC components may have favoured microorganisms capable of utilizing them as carbon and energy sources. Nevertheless, higher PAC loads inhibited degradation and energy recovery from PAC too. Similarly to the findings of this study, increasing loads (from 10% to 50%) of a post-hydrothermal liquefaction wastewater decreased the COD removal rates (from 76.8% to 36.8%) during their anaerobic digestion and were linked to the increasing toxicity and recalcitrant compounds such as N-heterocycles [74]. Continuous processes allow for the acclimation of the inoculum and the enrichment of specific trophic group, leading to higher COD recoveries at higher wastewater loads. For instance, energy and carbon recoveries as high as 79% were recovered into biohythane (*i.e.*, a mixture of hydrogen gas and methane) from the anaerobic degradation of furfural, phenolics and N-heterocycles present in the post hydrothermal liquefaction wastewater of corn stalk [66]. Compared to other studies [66], [74], [100], the e-mol recovery achieved at low PAC loads in this study was relatively high for an un-acclimated inoculum and such short fermentation time. Here, syngas co-fermentation may have contributed to improve energy recovery providing extra electron donors such as CO and H₂ to the degradation of PAC components into CH₄, H₂ or SCCs. Hydrogen partial pressure of 0.8 atm were reported to enhance phenol removal rates by 42% by promoting the syntrophic associations between *Syntrophorhabdus*, a phenol degrader, and methanogens during the anaerobic fermentation of phenol at high TAN concentrations (up to 8 grams) [322].

Furthermore, similar to the effects of amendments such as zeolite or biochar observed during the anaerobic digestion of other PACs [50], [95], [97], [100], [106], the clays and silts present in the non-volatile solid fraction of the inoculum used in this work may have enhanced process performances by improving the detoxification activity of microorganisms or even absorbed PAC compounds [323]–[325].

4.5 Conclusions

Recovering energy from anthropogenic and post-consumer wastes is essential to maximize resources circularity whilst minimizing environmental impacts. In this study, we proved the potential of mesophilic and thermophilic anaerobic mixed cultures to simultaneously ferment syngas and components of PACs derived from the pyrolysis of sewage sludge and mixed polyethylene plastics. However, origin and composition of the PAC influenced process performances and e-mol recovery. Comparatively, while sewage sludge-derived PAC showed lower toxicity towards carboxydrotrophic activity compared to its polyethylene plastic counterpart, its components were resistant to degradation, resulting in reduced e-mol recovery. Conversely, despite its high toxicity, anaerobic mixed cultures successfully degraded some components of polyethylene plastic-derived PAC, leading to high e-mol recoveries from PAC. Products of the co-fermentations such as methane or carboxylates could be used either as energy carrier or intermediate metabolites in secondary fermentative processes, respectively. Future research should focus on the evaluation of the feasibility of the co-fermentation in continuous cultivation and on the identification of technologies that will improve the energy recovery potential and reduce PAC toxicity.

Acknowledgments

The authors acknowledge Institute for Technical Chemistry, Karlsruhe Institute of Technology, for providing the PACs. We thank Grazyna Straczewski, Axel Heidt and Habibu Aliyu for assistance and mentoring.

Supplementary Information

Additional file 3: Table S1. Mass balances of the pyrolysis of sewage sludge and HDPE, LDPE plastics. Table S2. Anions and cations concentration for sewage sludge PAC and the mixed PE plastics PAC. Table S3. HPLC and GC-MS characterization of the raw aqueous condensate deriving from the fast pyrolysis of sewage sludge. The GC-MS characterization was performed by the Thünen Institute of Wood Research, (Hamburg, Germany). The total GC-MS chromatogram area: $1.06E+08$. Area of 12 identified peaks = $9.30E+07$ (88 %). Area of unknown peaks = $1.27E+07$ (12 %). Error bars represent standard deviation among replicates ($n=2$). Table S4. HPLC and GC-MS characterization of the raw aqueous condensate deriving from the fast pyrolysis of mixed PE plastics. The GC-MS characterization was performed by the Thünen Institute of Wood Research, (Hamburg, Germany). The total GC-MS chromatogram area: $2.89E+07$. Area of 11 identified peaks = $2.22E+07$ (76.8 %).

Area of unknown peaks = $6.70\text{E}+06$ (23.2 %). Error bars represent standard deviation among replicates ($n=2$). Table S5. Conversion factors for electron balances. Figure S1. Total ammonium nitrogen (TAN), free ammonia nitrogen (FAN), and nitrate concentrations [mM] at inoculation conditions for M-SS-PAC and T-SS-PAC experiments. Error bars represent standard deviation among replicates ($n=3$). Figure S2. Final average pH from fermentation at increasing sewage sludge PAC loadings. Error bars represent standard deviation among replicates ($n=3$). Figure S3. e-mol recoveries from SS-PAC calculated as described in Eq.2 for M-SS-PAC and T-SS-PAC experiments. Error bars represent standard deviation among replicates ($n=3$). Figure S4. The graphs a and b show the e-equivalents balance [$\text{e-mol}_{\text{products}}/\text{e-mol}_{\text{syngas, fixed}}$] for each load of SS-PAC. Values above 100 % indicate that the sum of the e-mol in the products is higher than the e-mol consumed from syngas. Error bars represent standard deviation among replicates ($n=3$). Figure S5. The graphs a and b show the e-equivalents balance [$\text{e-mol}_{\text{products}}/\text{e-mol}_{\text{syngas, fixed}}$] for each load of PE-PAC. Values above one indicate that the sum of the e-mol in the products is higher than the e-mol consumed from syngas. Error bars represent standard deviation among replicates ($n=3$). Figure S6. Final average pH from fermentation at increasing mixed PE plastics PAC loadings. Error bars represent standard deviation among replicates ($n=3$). Figure S7. e-mol recoveries from SS-PAC calculated as described in Eq.2 for M-SS-PAC and T-SS-PAC experiments. Error bars represent standard deviation among replicates ($n=3$).

5. Upscaling the two-stage process and evaluation of reactors' microbiota

This chapter is based on the publication:

Two-stage conversion of syngas and pyrolysis aqueous condensate into L-malate. Alberto Robazza, Flávio C. F. Baleeiro, Sabine Kleinsteuber and Anke Neumann

Biotechnology for Biofuels and Bioproducts (2024), 17, 85.

<https://doi.org/10.1186/s13068-024-02532-2>

Author's contributions

Alberto Robazza	conceptualization, methodology, investigation, data curation and analysis, visualization, first draft and manuscript revision
Flávio C. F. Baleeiro	conceptualization, methodology, data analysis, visualization and manuscript revision
Sabine Kleinsteuber	conceptualization, methodology, data analysis support and manuscript revision
Anke Neumann	conceptualization, methodology, data analysis support, project supervision and manuscript revision

5.1 Introduction

The fast pyrolysis of lignocellulosic biomass generates bio-char, bio-oil and two by-products: pyrolysis syngas and pyrolysis aqueous condensate (PAC). These by-products contain up to 60% of the carbon of the original biomass [22], [106]. Their composition varies depending on the source material and the pyrolysis process conditions, such as the residence time, pressure, temperature and heating rate [317]. Generally, pyrolysis syngas consists of CO, CO₂, CH₄, H₂, with low concentrations of alkanes and alkenes. Syngas fermentation by acetogenic microorganisms is an attractive technology because it has the potential to reduce carbon emissions from C₁-rich exhaust gases while simultaneously producing valuable platform chemicals or biofuels. Axenic processes (*i.e.*, fermentation processes using pure cultures) have been already established at the industrial level, and ongoing research is focused on process optimization and strain development to improve the potential of this technology [326]. On the other hand, PAC contains high concentrations of organic acids, phenolics, aldehydes, ketones, furans, N-heterocyclic and other hazardous compounds. Some PAC components are harmful even at low concentrations, making PAC a challenging substrate for biological conversion [20], [22], [72]. Nonetheless, new technological developments are necessary to improve the overall efficiency of the pyrolysis process, maximizing the recovery of carbon and energy stored in syngas and PAC.

Techno-economical assessments have highlighted the potential of integrating thermochemical and biological processes to improve carbon and energy recovery and to minimize the environmental impact of agricultural wastes [174], [177]–[180]. In recent studies focusing on the biochemical conversion of some PAC components, researchers combined physiochemical pre-treatments with axenic fermentations to produce a wide range of products [60], [64], [65], [327], [328]. Others have utilized the diversity and functional redundancy of the microbial network in the anaerobic digestion process to convert PAC components into biogas. However, methanogenesis was severely inhibited by the toxicity of PAC, leading to the accumulation of short-chain carboxylates in the medium [84], [100]. To improve methane production, recent efforts have successfully employed community enrichment or biochar amendments [20], [24], [95]–[97], [72], [73], [84], [89], [91]–[94]. The taxonomic profiling of the anaerobic communities acclimatized to different PACs highlighted the relevance of syntrophic and acidogenic microorganisms during PAC components degradation [68], [73], [105], [76], [83], [99]–[104] and their enrichment/bio-augmentation might be a possible strategy to improve PAC degradation and methane production [106].

In an alternative approach to waste methanation, acetate and other carboxylic acids are the primary products of anaerobic fermentation and could subsequently be utilized as feedstock in secondary bioprocesses. Methane is the most favored

product with the lowest free energy content per electron ensuring the highest carbon and energy recovery from organic wastes [120], [121]. Thus, methane-arrested anaerobic fermentation for carboxylate production is only achievable by using specific methanogenesis inhibitors [135], [136] or by a specific process design that suppresses the competitiveness of methanogenic pathways [137]. For instance, researchers have been using CO at high partial pressures [49], [116], [138] to inhibit methanogens or low pH to increase the concentrations of undissociated carboxylic acids [139], [140]. Some other studies successfully attempted to exploit the toxicity of PAC to inhibit or mitigate methanogenic microorganisms, allowing for carbon and energy recovery from PAC and syngas into carboxylates [100], [295]. Acetate and other carboxylic acids can be used as intermediate substrates in two-stage (anaerobic to aerobic) biological processes to produce high value chemicals from syngas and wastewaters. Combining two bioprocesses into sequential fermentations with carboxylates as intermediates is considered a promising approach for the production of high-energy-density and high-value chemicals from waste streams [144], [148], [329]–[333]. However, when dealing with biological processes to treat toxic wastewater, the success of the second fermentation stage depends on the detoxification achieved in the first stage. Besides improving toxicant removal rates in the first stage, the selection of appropriate microorganisms for the second stage might affect process performance and carboxylate conversion rates [295]. Fungi have been reported to be the microorganisms most tolerant to the oil fraction of the condensates from pyrolysis [57], and the tolerance of *Aspergillus oryzae* to PAC and some selected PAC components has been characterized before [63], [166], [295]. *A. oryzae* is known for its metabolic versatility to grow on sugars and carboxylic acids present in various waste streams for the production of single cell proteins [158], [159], [165], [334] or L-malate [156], [161], [293], among other chemicals. L-malate has a wide array of applications, ranging from taste-enhancer in the food industry to biopolymer production [162]. In 2004, L-malate was regarded as one of the 12 most important biomass-derived biochemical [163]. In 2020, the annual global L-malate production was estimated to be around 80,000 to 100,000 tons, whilst the market demands up to 200 000 tons per year, a value expected to increase in the following years [162]. L-malate production from non-food feedstock could be an economical and efficient way to meet market needs [164]. L-malate production from PAC was viable only after an extensive physiochemical detoxification process [63], [167]. Biological detoxification via anaerobic mixed cultures, on the other hand, has been proven to be a valid alternative to reduce PAC components' toxicity below inhibitory levels whilst producing carboxylic acids [295].

However, very limited knowledge is available about the continuous co-fermentation of syngas and PAC by anaerobic mixed cultures in stirred tank reactors (STRs) for short-chain carboxylates production. In this work, a two-stage sequential fermentation process was tested, where the products of the anaerobic fermentation of

syngas and PAC were valorized to produce L-malate with *A. oryzae*. Two mesophilic (37°C) and thermophilic (55°C) enrichment processes were run in identical semi-continuous STRs at slightly acidic pH and increasing PAC loading rates to evaluate the effects of temperature and PAC on the process performances and on the microbial community composition. In the second stage, the effluent from the first-stage fermentation was inoculated with *A. oryzae* to grow on the acetate, propionate and butyrate to produce L-malate.

5.2 Materials and Methods

5.2.1 Inocula and PAC

The anaerobic sludge was collected at a biogas reactor treating cow manure and handled as described in a previous work [295]. The total solids, total fixed solids and total volatile solids of the anaerobic sludge were 79.6 ± 0.5 g/L, 26.1 ± 1.1 g/L, and 53.5 ± 0.7 g/L, respectively, as determined following Method 1684 [201]. *A. oryzae* DSM 1863 was provided by the DSMZ strain collection (Deutsche Sammlung von Mikroorganismen und Zellkulturen GmbH, Braunschweig, Germany). The lignocellulose PAC was generated during the fast pyrolysis of miscanthus at the BioLiq plant (Karlsruhe Institute of Technology, Karlsruhe, Germany). The GC-MS analysis of the PAC performed by the Thünen Institute of Wood Research (Hamburg, Germany) is available in the Additional file 4 (Table S1).

5.2.2 Mixed Culture Enrichments

The enrichments were performed in two identical 2.5 L semi-continuous stirred tank reactors (Minifors, Infors HT, Bottmingen, Switzerland) with a working volume of 1.5 L. The bioreactor design was already optimized for gas fermentation [148]. The cultivations were carried out at 37°C or 55°C, 500 rpm, pH 5.5, and atmospheric pressure. The pH was monitored online with an EasyFerm Plus PHI K8 225 (Hamilton Bonaduz AG, Bonaduz, Switzerland) and controlled with 4 M NaOH or 4 M H₃PO₄ solutions. Changes in the oxidation-reduction potential of the broth were measured with the ORP sensor Polilyte Plus ORP Arc 225 (Hamilton Bonaduz AG, Bonaduz, Switzerland) and used as an indicator of metabolic activity and to control for air contamination. A synthetic syngas consisting of about 3 kPa H₂, 25 kPa CO₂, and 20 kPa CO in N₂ was fed at a gassing rate of 18 mL/min (0.012 vvm). The gases were controlled individually via mass flow controllers (red-y smart series, Vögtlin, Muttenz, Switzerland), and injected via a micro-sparger into the vessel. The fermentation broth and the feed were composed of a modified basal anaerobic (BA) medium and PAC. The composition of the modified BA medium is available in the Additional file 4. The BA medium for the feed bottles was poured into 2 L glass bottles (Schott AG, Mainz, Germany), autoclaved, flushed and pressurized with N₂ up to 0.5 bar to make it anoxic and prevent oxygen leaks. One milliliter per liter of a

100 g/L cysteine solution was added into the feed bottles as a reducing agent and sulfur source. After autoclaving, the feed bottles and the bioreactors were connected by platinum-cured silicone tubing of 1.6 mm wall thickness (Watson Marlow, Bergenfield, New Jersey, USA). The PAC was poured into a 2 L glass bottle, made anoxic, and stored at 4°C. During continuous operations, the BA medium and PAC were injected at the same time of the day to achieve a total average feed rate of 75 mL/d, resulting in a hydraulic retention time (HRT) of 20 days. Depending on the PAC loading, the required volume of PAC was withdrawn from the bottle with a syringe and then injected into the bioreactor via a silicon septum on the head plate of the bioreactor. The PAC loadings in the feed were 1 % (2.53 g_{COD}/L), 2 % (5.06 g_{COD}/L), 3 % (7.59 g_{COD}/L), 4 % (10.13 g_{COD}/L), 5 % (12.66 g_{COD}/L), 6 % (15.19 g_{COD}/L). Additional information about the feed composition and load (of syngas and PAC) are available in the Additional file 4 (Table S2). Except for PAC loadings of 1 % and 2 %, each loading of PAC was maintained constant for a period corresponding to at least 40 days (*i.e.*, twice the HRT).

Before the first inoculation, 15 mL PAC (1 % v/v) was injected into the bioreactors and the pH was adjusted to 5.5. Both bioreactors were inoculated with 400 mL inoculum (27 % v/v). Only after the first inoculation, due to the buffering capacity of the inoculum, the pH rose up to 6.7 but lowered naturally at 0.1 per day to the desired pH of 5.5.

If both the CO partial pressure at the gas outlet and the ORP value were increasing close to 20 kPa and above -100 mV, respectively, then the bioreactor was re-inoculated with the original inoculum to reach about 12 g/L of total suspended solids (TSS). If any of the bioreactors required several inoculation events, the TSS was controlled in the range of 8 to 12 g/L by weekly re-inoculations with on average of 75 mL of inoculum. The TSS and volatile suspended solids (VSS) were determined as explained in the Additional file 4.

5.2.3 Bioreactor Sampling and Analytical Methods

Five milliliters of the liquid phase of the bioreactors were sampled daily, collected in 15 mL pre-weighed Falcon tubes, and centrifuged at 14,000 x g for one hour.

The supernatant was collected, filtered, and stored at -20°C for later analyses. The pellet was dried for 24 hours at 80°C and used to determine the total suspended solids. The concentrations of formate, acetate, propionate, *n*-butyrate (from here onwards defined as short-chain carboxylates, SCCs), L-malate and ethanol together with the concentrations of few selected PAC components (furfural, phenol, guaiacol, and *o*-, *m*-, *p*-cresol) were determined by a high-performance liquid chromatography (HPLC) device run as described previously [295].

The online determination of the fractions of CO, H₂, CO₂, N₂, O₂, and CH₄ in the gas phase of the bioreactors was performed via gas chromatography (GC) using a GC-2010 Plus AT (Shimadzu, Japan) with a thermal conductivity detector equipped with a ShinCarbon ST 80/100 column (2 m × 0.53 mm ID, Restek, Germany) and an Rtx-1 capillary column (1 μm, 30 m × 0.25 mm ID, Restek, Germany) with helium as carrier gas. Assuming N₂ to be biologically inert and the inflowing gas composition constant throughout the whole fermentation period, it was possible to compute the molar consumption and production of gaseous substrates and products via the ideal gas law as explained in a previous work [148]. Electron mole (e-mol) recovery was used to calculate the chemical fluxes in the process. The e-mol recovery is the ratio between the daily cumulated e-mol production of H₂, CH₄, formate, acetate, propionate and butyrate and the daily e-mol fed into the bioreactors as syngas and PAC. Further details of the calculations are described in the Additional file 1. Table S3 in the Additional file 1 lists the metabolites and their conversion factors for the e-mol recoveries. All the other calculations are available in the Additional file 4.

5.2.4 Microbial Community Analysis and Statistical Evaluation

Every 20 days or before and after any inoculation event, technical duplicates of 2 mL of fermentation broth were sampled and centrifuged for 30 min at 17,000 x g. After discarding the supernatant, the pellet was re-suspended in 1 mL phosphate-buffered saline solution (pH 7.4). The pellets from both samples were combined and centrifuged for another 30 min at 17,000 x g. The pellets were stored at -20°C. Details on the procedures for DNA extraction, sample purification, PCR, and description of the amplification primers are described previously [136]. Amplicon sequencing of the 16S rRNA (region V3-V4) and mcrA genes was done using the Illumina MiSeq platform. Library preparation for the visualization of the microbial community and elaboration of Spearman correlations was performed as described in another work [125]. The raw sequence data without adapters used in this study has been deposited in the European Nucleotide Archive (ENA) under the study accession number PRJEB72504 (<http://www.ebi.ac.uk/ena/data/view/PRJEB72504>).

5.2.5 *Aspergillus oryzae* Batch Fermentations

At every increase in PAC loading, 50 mL broth were withdrawn from the bioreactors and centrifuged for 1 hour at 14,000 x g. The pH of the supernatant was corrected to 6.5 with 4 M NaOH solution. Nine milliliters of the supernatant together with 1 mL BA medium were poured into 100 mL baffled Erlenmeyer flasks and inoculated with 0.1 mL of *A. oryzae* conidia (spore concentration of 3 × 10⁷ spores/mL). The shaking flasks were incubated at 30°C and 100 rpm. The aqueous phase (0.2 mL) was sampled daily and controlled for pH; the concentrations of SCCs

and L-malate concentrations were determined with HPLC. All fermentations with *A. oryzae* were performed in triplicates.

5.3 Results

Initially, syngas and PAC were co-fermented by two mixed microbial cultures at 37°C and 55°C in semi-continuous STRs to test the carbon and energy recovery potential from the two pyrolysis process streams. Some samples of the supernatant of the fermentation broth from the bioreactors were inoculated with *A. oryzae* to produce L-malate from the carboxylates.

5.3.1 Mesophilic co-fermentation of Syngas and PAC

Overall, the mesophilic reactor showed stable performance throughout most of the fermentation period. Figure 1 reports the combined graphs of the relevant parameters for the mesophilic reactor treating syngas and PAC at increasing PAC loadings. CO consumption started ten days after the inoculation of the reactor. After peaking at 4.2 mM/h on day 15, CO consumption rates were about 3 mM/h until day 145 (Figure 23a). Concomitantly, exogenous H₂ consumption remained relatively stable at about 0.45 mM/h. No methane production was detected. The redox potential of the medium ranged between -360 to -380 mV (Additional file 4, Figure S1a). The partial pressures of CO and H₂, together with redox potential and the pH of the medium are shown in the Additional file 4 (Figure S1b). From day 20 to day 145, CO partial pressure averaged to about 10 kPa while the H₂ partial pressure did not exceed 3 kPa. Acetate and ethanol were the primary metabolites detected in the fermentation broth (Figure 23b), with selectivities ranging between 44-92% and 2-42%, respectively. From day 150 on, the acetate concentration increased to about 350 mM within less than ten days. Small amounts of butyrate (up to 30 mM) were detected between days 120 and 150. Small amounts of propionate were also found. The concentrations of undissociated acids are shown in the Additional file 4 (Figure S1c). Acetic acid concentration never exceeded 60 mM while butyric acid concentration was always below 10 mM. Phenol, furfural and guaiacol removal reached efficiencies higher than 80% within the first 40 days of fermentation and remained stable until the end of the fermentation (Figure 23d). The cumulative removal of *o*-, *m*-, *p*-cresols was negative. *m*- and *p*-cresols were produced, whereas *o*-cresol was the only cresol that showed consistent removal efficacy (Additional file 4, Figure S1c). Between day 10 and day 120, the mesophilic enrichment recovered on average about 50% into SCCs and ethanol of the total e-mol of syngas and PAC fed daily (Figure 23c). For the mesophilic process, the e-mol recovery accounts for SCCs only as products (H₂ is a substrate), not including longer-chain carboxylates (with high electron equivalents) and biomass production. From about day 120, the e-mol recovery decreased to values close to 0 on day 145. Then, the CO consumption rates decreased

sharply concomitant with an increase of the redox potential to about -150 mV. This result suggests that the carboxydrotrophic portion of the reactor microbiota (i.e., microbes contributing to CO consumption) underwent severe stress. Decreasing CO consumption rates were not accompanied by changes in the PAC components removal, which remained somewhat constant. To recover syngas metabolism, the fermenter was re-inoculated with about 350 mL of inoculum (sufficient to reach at least 12 g_{TSS}/L) to increase biomass concentration and microbial diversity within the bioreactor. About four days after the first re-inoculation event, CO consumption rates recovered. From day 150, the amount of VSS was maintained within 1 to 5.6 g/L by regular re-inoculations (Additional file 4, Figure S1d). After 195 days, CO and H₂ conversion rates dropped to zero and never recovered, suggesting that PAC loads of 15.19 g_{COD}/L/d are too high to maintain carboxydrotrophic activity.

From day 20 to day 150, the reactor microbiota (Figure 23e) was dominated by five amplicon sequencing variants (ASVs) (ASV 002, 005, 010, 012 and 023) belonging to *Clostridium sensu stricto* 12 (over 90% abundance), a genus that comprises acetogenic microorganisms such as *Cl. ljungdahlii* and *Cl. autoethanogenum*. Other microorganisms enriched during this period were belonging to the genera *Anaerococcus* (ASV 018) and *Caproiciproducens* (ASV 028). From about day 100, the cumulative relative abundance of *Anaerococcus* and *Caproiciproducens* spp. increased up to about 10% at the expense of *Clostridium sensu stricto* 12. At the same time, acetate and ethanol concentrations decreased whilst butyrate concentration increased.

Increasing abundance of *Anaerococcus* and *Caproiciproducens* coincided with the decrease in e-mol recovery. From day 150, the abundance of *Firmicutes* DTU014, *Limnochordia* MBA03, *Caldicoprobacter* (ASV 018) and two unclassified *Limnochordia* species (ASV 016 and 019) increased as results of the weekly re-inoculations. Similarly, *Clostridium sensu stricto* 12 and *Caproiciproducens* abundance recovered up to about 40% and about 5%, respectively.

Upscaling the two-stage process and evaluation of reactors' microbiota

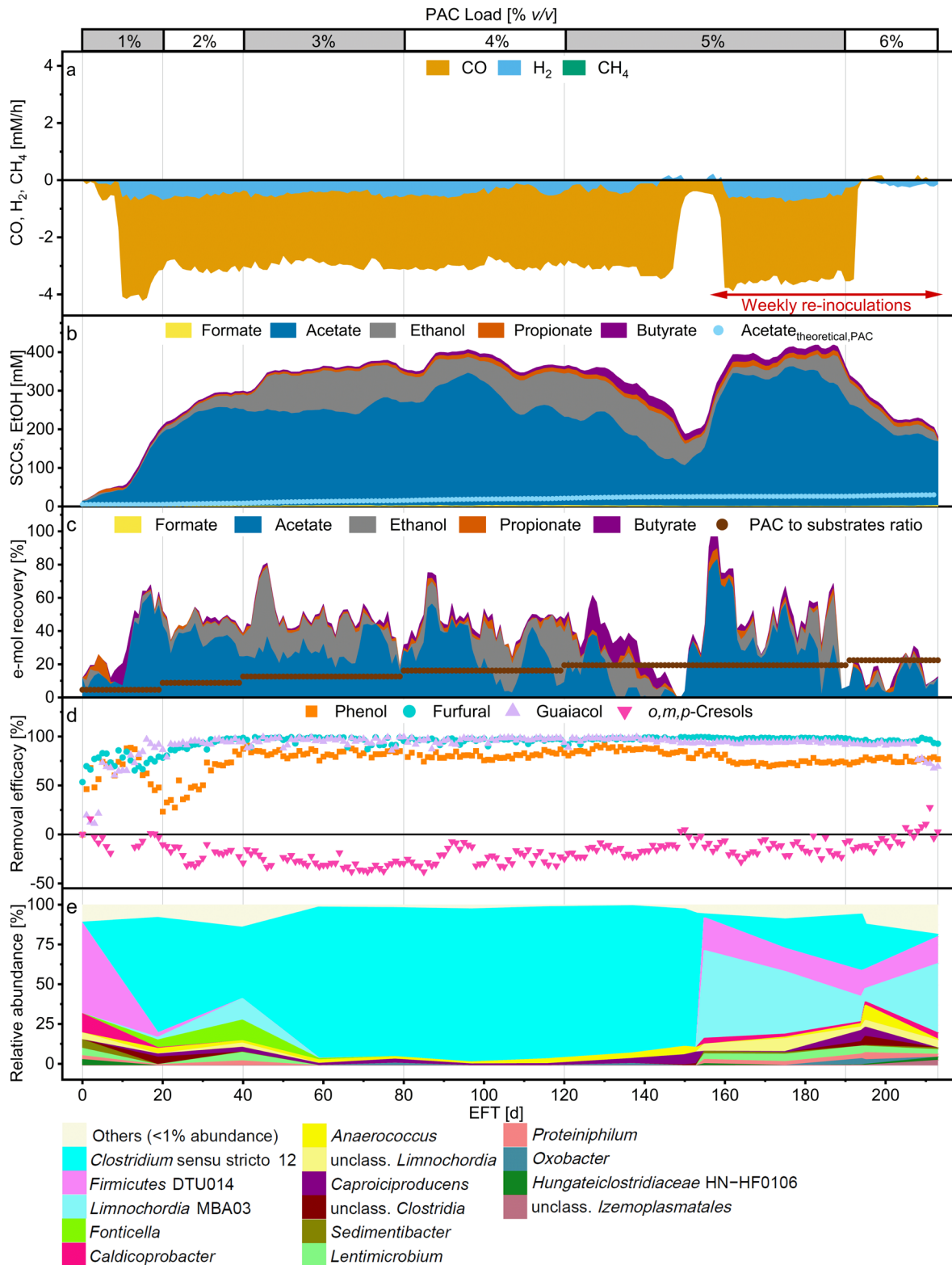


Figure 23. Fermentation profile of the mesophilic process. Top x-axis marks the PAC loading, bottom x-axis shows the elapsed fermentation time (EFT). The red bar indicates the period of weekly re-inoculations. (a) Consumption and production rates of gaseous compounds. Negative values indicate consumption. (b) Formate, acetate, propionate and butyrate (SCCs) and ethanol concentrations in the fermentation broth. Acetate_{theoretical,PAC} is the theoretical acetate concentration from PAC. (c) Daily e-mol recovery into products from syngas and PAC fed; daily ratio of e-mol of PAC in the feed to total e-mol of syngas and PAC fed (brown). (d) Removal efficacies of selected PAC components. Negative efficacy values indicate production. (e) Relative abundance of the enriched microbial genera (based on 16S rRNA amplicon sequencing variants).

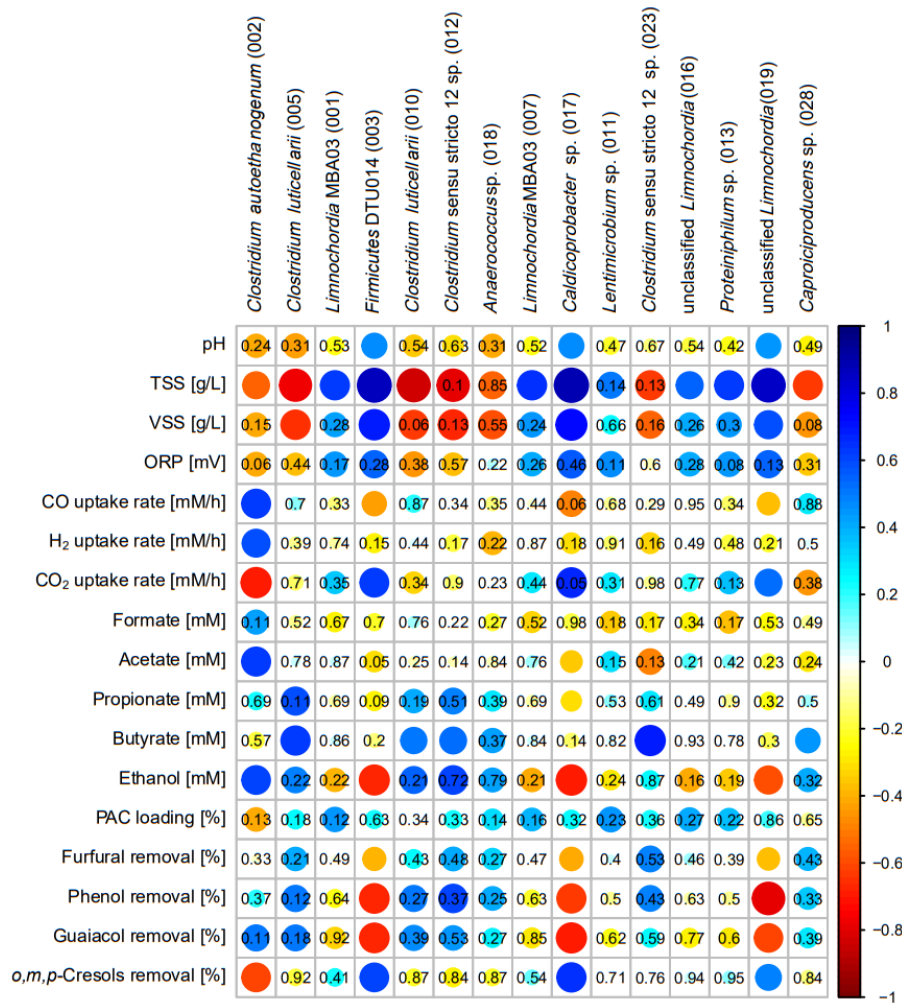


Figure 24. Spearman's rank correlations between relative abundance of dominant amplicon sequencing variants (ASVs) and process parameters for the mesophilic semi-continuous STR enrichment. The strength of the correlation is represented by the size of the circle and intensity of the color. Blue circles indicate positive correlations. Red circles indicate negative correlations. p values are shown for non-significant correlations ($p > 0.05$).

Significant correlations ($p < 0.05$) (Figure 24) suggest that ASV 002, a close relative of *Clostridium autoethanogenum* (and consequently of its relatives: *Cl. ragsdalei*, *Cl. coskatii*, and *Cl. ljungdahlii*), represents the primary carboxydrotroph converting syngas into acetate and ethanol. Two members of *Clostridium luticellarii* (ASV 005 and 010) and other ASVs assigned to the genera *Caproiciproducens* (ASV 028) and *Clostridium sensu stricto* 12 (ASV 012 and 023) likely contributed to butyrate production. Abundance of *Clostridium autoethanogenum* ASV 002 was negatively correlated to cresol removal, whereas members of *Firmicutes* DTU014 (ASV 003), *Caldicoprobacter* (ASV 017) and an unclassified *Limnochordia* sp. (ASV 019) showed significant correlations to cresol removal ($p < 0.05$).

5.3.2 Thermophilic co-fermentation of Syngas and PAC

During the thermophilic co-fermentation, CO consumption was detected within the first five days after inoculation. The conversion of syngas followed the stoichiometry of the water-gas shift reaction and of hydrogenotrophic methanogenesis. CO was primarily converted to CO₂, H₂ and CH₄ (Figure 25a). The carbon equivalents in CO₂ and CH₄ accounted on average for 84% of the total carbon equivalents from syngas. Similarly, the electron equivalents in H₂ and CH₄ accounted for about 86% of the total electron equivalents from syngas. CO was metabolized at an average rate of 3.1 ± 0.5 mM/h until day 140. Between days 145 and 186, the CO uptake rates increased by 20% to 3.8 ± 0.3 mM/h. H₂ conversion rates alternated between production and consumption depending on the extent of inhibition of methanogenesis. The CO partial pressures mostly fluctuated around 10 kPa to decrease to about 5 kPa between days 145 and 186. H₂ partial pressures ranged from 0.4 to 11.9 kPa (Additional file 4, Figure S3b). The redox potential oscillated between -480 mV and -350 mV (Additional file 4, Figure S3a). Acetate was the primary SCC produced (with selectivity on average higher than 80% during the whole fermentation period) followed by small concentrations of butyrate, propionate and ethanol (all never exceeding 20 mM throughout the fermentation period). For the first 40 days, acetate concentration remained constant at about 50 mM but later increased up to 118 mM after 70 days. Profiles of the concentrations of the undissociated acids are available in the Additional file 4 (Figure S2c). Around day 73, the pH was temporarily increased from 5.5 to 6.7 to test the effect on methanogenesis (Additional file 4, Figure S2a). CH₄ production rates spiked up to 3.6 mM/h for few days until the acetate was completely consumed and the pH was adjusted back to 5.5. From day 77 onwards, acetate concentration steadily increased up to about 130 mM on day 119. Afterwards, it oscillated between 125.1 mM and 68.2 mM until the end of the fermentation period. Phenol, furfural and guaiacol were removed with high efficacies (Figure 3d). The cumulative removal of the cresols, after being produced during the first 26 days of fermentation, increased to on average 22.5% for the rest of the fermentation period. The removal efficacy of each cresol isomer is reported in the Additional file 4 (Figure S2d). The e-mol recovery reached 100% during the first ten fermentation days but later decreased to about 50%, regardless of the increasing e-mol loading from PAC. From day 145 on, the e-mol recovery increased due to the higher CO uptake rates (Figure 1c). Methane was the primary e-mol acceptor for the e-mol from syngas and PAC fed into the system.

After the daily feeding events on days 43, 72 and 101 (corresponding to PAC loadings of 3% and 4% v/v), the CO consumption exhibited a sharp decline. CO uptake rates decreased below 0.5 mM/h, within few hours from feeding (zoomed-in profiles of CO, H₂ and CH₄ production rates around days 43, 72, 101 are available in the Additional file 4, Figure S4). Simultaneously, the redox potential increased to values higher than -100 mV while the VSS were estimated to have fallen below 1 g/L

(Additional file 4, Figure S2e). No air contamination was detected. Similarly, an erroneous addition of about 6 mL of PAC on day 10 caused the CO consumption rate to fall. From about day 40, the removal of phenol, furfural and guaiacol decreased for a few days from 90% to about 54%, 64% and 47%, respectively. Decreasing removal of PAC components was not detected again. Decreasing CH₄ production rates and increasing H₂ partial pressures forwent the decrease of CO uptake rates. On the days following the decrease of CO consumption rate, the bioreactor was inoculated (indicated by red arrows in Figure 25a), resulting in a quick recovery of CO consumption rate. Given the success of the re-inoculation, from day 101 onwards, the fermenter was re-inoculated weekly, to maintain high biomass concentrations (the VSS ranged between 6.5 g/L to 1.5 g/L averaging at 3.3 ± 1.0 g/L). The weekly re-inoculation strategy stabilized the reactor performance as no major disturbances of syngas conversion were observed for the following 90 days.

The microbial community analysis showed that *Limnochordia* MBA03, *Firmicutes* DTU014, a *Lentimicrobium* sp. and an unclassified *Limnochordia* species abounded after each inoculation but were progressively washed out after 43, 72 and 101 days (Figure 25e). On the contrary, bacteria identified as members of *Symbiobacteriales*, *Acinetobacter*, *Thermoanaerobacterium*, *Rummeliibacillus*, *Corynebacterium*, *Syntrophaceticus* and unclassified *Veillonellales-Selenmonadales* were enriched during stable operations. Amplicon sequencing of *mcrA* genes indicated that thermophilic conditions favoured the enrichment of *Methanothermobacter*. *Methanosarcina* spp. and *Methanoculleus* were methanogens abundant in the inoculum but did not perform well in the reactor (Additional file 4, Figure S2f). Weekly re-inoculation of the bioreactor helped also maintain a highly diverse microbiome. From day 101 onwards, the most abundant taxa were *Limnochordia* MBA03, *Symbiobacteriales*, *Acinetobacter*, *Thermoanaerobacterium*, *Corynebacterium* and *Firmicutes* DTU014. Between days 145 and 186, a close relative to *Moorella thermoacetica* was enriched up to 50% abundance, coinciding with higher CO uptake rates. *Methanothermobacter* was consistently enriched also during the re-inoculation phase but its abundance progressively lowered from about 75% after 115 days to about 25% after 213 days in favour of *Methanosarcina* (Additional file 4, Figure S2f).

Upscaling the two-stage process and evaluation of reactors' microbiota

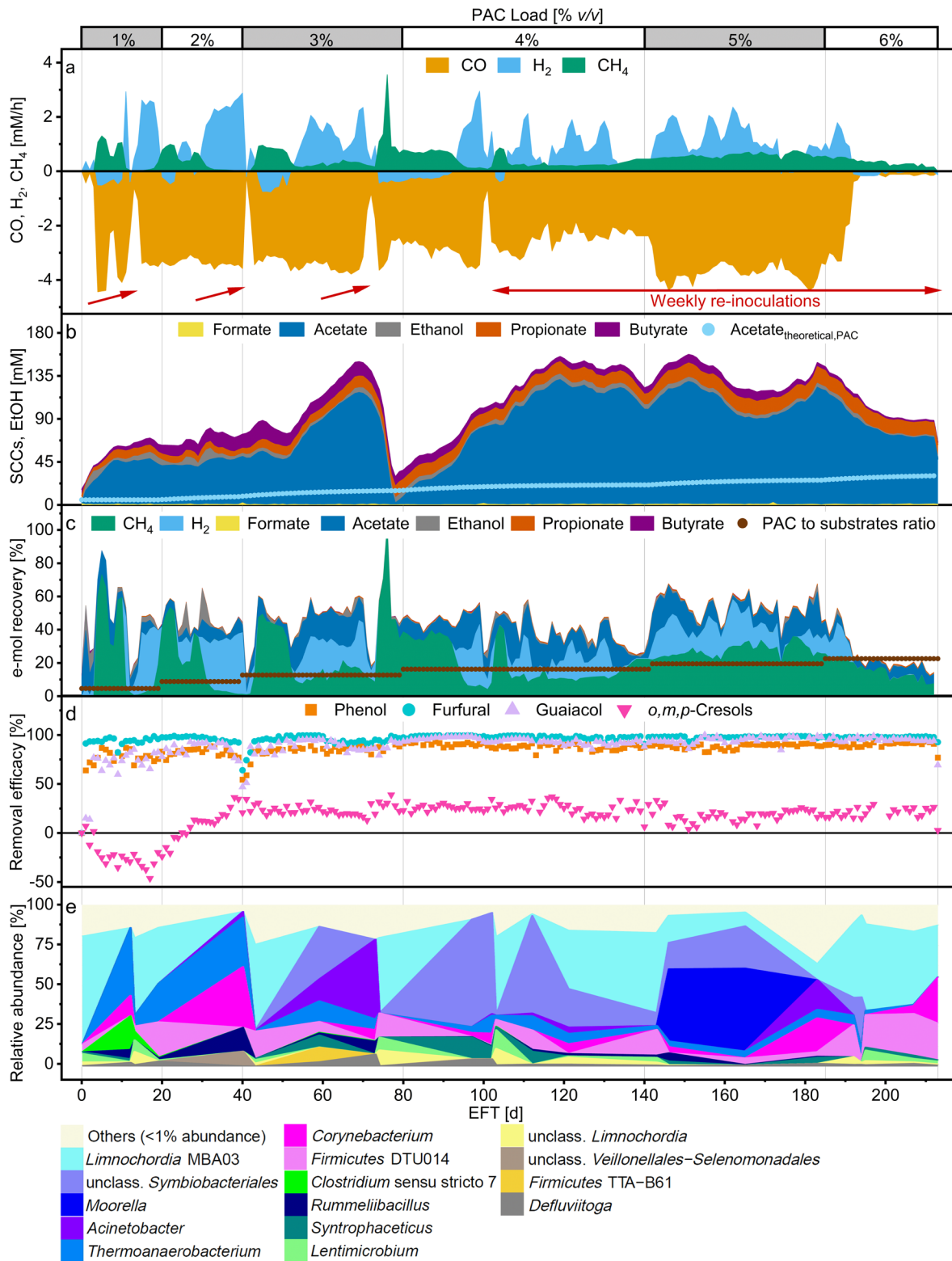


Figure 25. Fermentation profile of the thermophilic process. Top x-axis marks the PAC loading, bottom x-axis shows the elapsed fermentation time (EFT). Red arrows point to re-inoculation events, the red bar indicate the period of weekly re-inoculations. (a) Consumption and production rates of gaseous compounds. Negative values indicate consumption. (b) Formate, acetate, propionate and butyrate (SCCs) and ethanol concentrations in the fermentation broth. Acetatetheoretical,PAC is the theoretical acetate concentration from PAC. (c) Daily e-mol recovery into SCCs from syngas and PAC fed (green); daily ratio of e-mol of PAC in the feed to total e-mol of syngas and PAC fed (gray). (d) Removal efficacies of selected PAC components. Negative efficacy values indicate production. (e) Relative abundance of the enriched microbial genera (based on 16S rRNA amplicon sequencing variants).

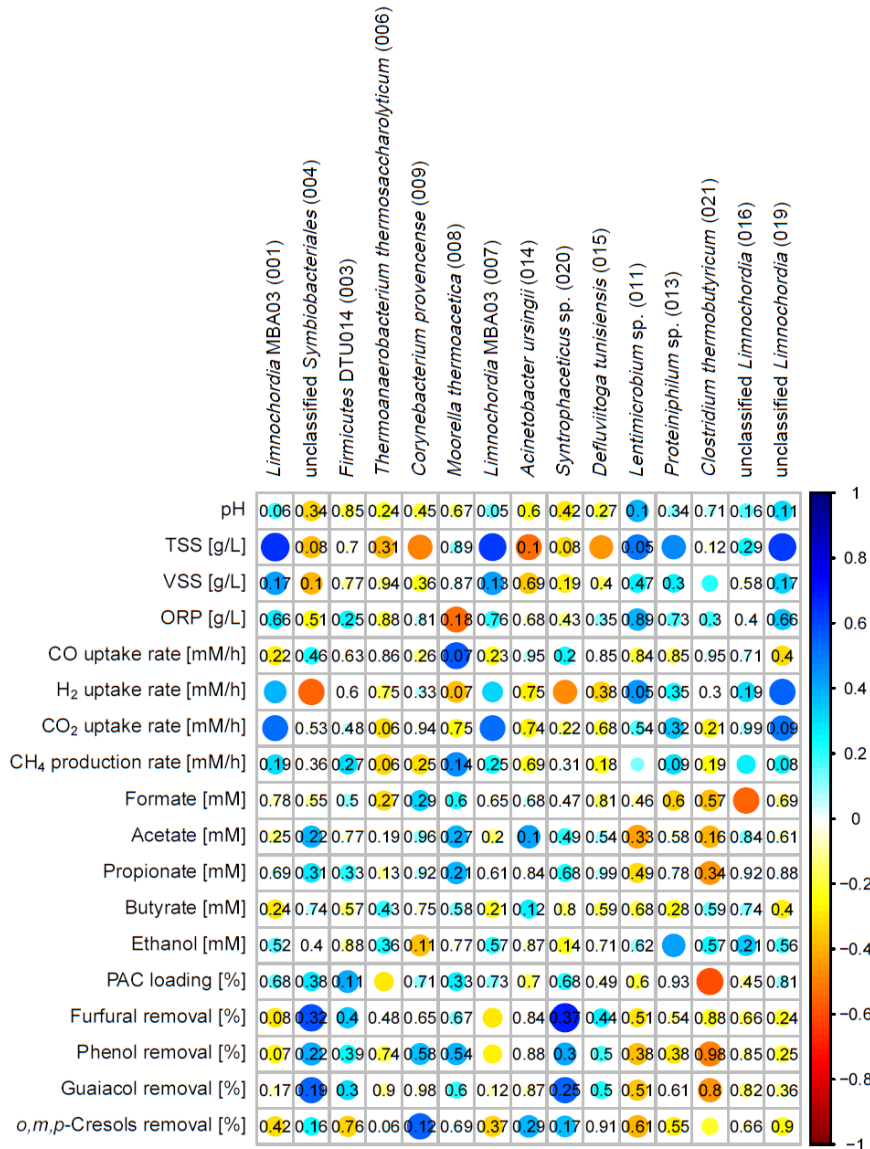


Figure 26. Spearman's rank correlations between relative abundance of amplicon sequencing variants (ASVs) and process parameters for the thermophilic semi-continuous STR enrichment. The strength of the correlation is represented by the size and intensity of the color. Blue circles indicate positive correlations. Red circles indicate negative correlations. p values are shown for non-significant correlations ($p > 0.05$).

Moorella thermoacetica ASV 008 was the only ASV that showed a strong correlation to CO uptake (albeit with high p-value of 0.07). *Symbiobacteriales* ASV 004 and *Syntrophaceticus* ASV 020 showed significant correlations to hydrogen production (Figure 26). Two *Methanothermobacter* species (ASVs 001 and 002) showed significant correlation to H₂ production ($p < 0.05$) while *Methanosarcina thermophila* ASV 003 showed significant correlation to H₂ consumption ($p < 0.05$) (Additional file 4, Figure S3).

5.3.3 L-malate production from SCCs with *A. oryzae*

To assess the overall detoxification process of PAC and explore the potential for carboxylate valorization, the effluent originating from both mesophilic and thermophilic fermentations was used as fermentation medium in subsequent aerobic fermentations. Specifically, 50 mL of reactor broth were collected prior to each increment in PAC loading and underwent centrifugation as described in Materials and Methods. Subsequently, the resulting supernatant was inoculated with *A. oryzae* conidia. The *A. oryzae* fermentations were categorized based on the origin of the reactor effluent (whether from the mesophilic or thermophilic process) and the specific PAC loading within the reactor at the time of sampling (Figure 27).

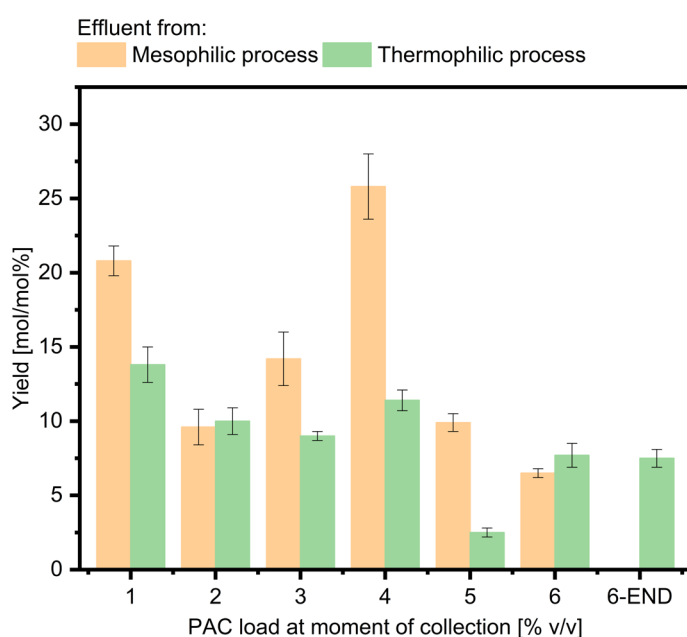


Figure 27. L-malate yields calculated for the highest L-malate concentrations per SCCs consumed. Bars represent mean values with standard deviations (n=3).

Growth of *A. oryzae* was observed in all batch fermentations but one. *A. oryzae* effectively consumed all the SCCs generated during mesophilic and thermophilic syngas and PAC co-fermentations. An exception was detected with the final sample collected from the mesophilic fermenter where no *A. oryzae* growth nor L-malate production were recorded (Additional file 4, Figure S5). The highest L-malate titer observed was 33.0 ± 0.8 mM, produced by *A. oryzae* from the acetate, propionate and butyrate present in the effluent collected from the mesophilic bioreactor after 80 days (Additional file 4, Table S4 and Figure S6). In contrast, the thermophilic reactor produced a maximum of 13.9 ± 1.7 mM of L-malate from sample collected at 120 days, with a 4% PAC loading (Additional file 4, Table S5 and Figure S7). The highest L-malate yield of all *A. oryzae* fermentations, amounting to 25.8 ± 2.2 mol/mol%, was achieved with the medium collected from the mesophilic bioreactor

at 116 days. Overall, the L-malate yields exhibited a decreasing trend as the PAC loading increased in the medium from both reactors.

5.4 Discussion

5.4.1 Reactor microbiomes and performances of the mesophilic and the thermophilic process

The high abundance of *Clostridium sensu stricto* 12 in the mesophilic process suggests the central role they played during the mesophilic syngas and PAC co-fermentation. The dominant ASV 002 was assigned to *Cl. autoethanogenum*, a well-studied carboxydotrophic acetogen known for its application in companies specializing in syngas fermentation [335]. This specie is known to consume CO and H₂/CO₂, yielding acetate and ethanol. The enrichment *Cl. autoethanogenum* was possibly influenced by the reactor design and feed composition. Syngas accounted for over 90% of the total e-mol for the first 40 days of the fermentation.

Although no significant correlation was identified between *Clostridium sensu stricto* 12 and aromatics removal in this work, prior research indicated that *Clostridium sensu stricto* participated in the anaerobic digestion of aromatics-rich wastewaters [336]–[339]. Examples include also the enrichment of *Clostridium sensu stricto* (up to 17.5%) during the degradation of tars from rice husk gasification, where biochar facilitated syntrophic relations with *Methanosaeta* [95]. Another study documented the enrichment of *Clostridium sensu stricto* 1 and 12 up to 5% abundance during the co-fermentation of syngas and PAC in a packed biochar reactor [100]. Similarly, during the anaerobic digestion of phenol-rich coal gasification wastewater with addition of graphene, about 10% of the reactor microbiota was composed of *Clostridium sensu stricto* 5 and *Clostridium sensu stricto* 1 [340].

Here, *Clostridium sensu stricto* 12 may have also been involved in the production of cresol. Even though, some studies reported anaerobic cresol removal, not all cresols exhibit similar removal efficiency [84], [295]. Some other studies described cresol production during the anaerobic digestion of corn straw and within the human intestinal tract [341]–[343]. A screening of 153 human intestinal bacterial species grown on tyrosine showed that 36 species were able to produce phenol while 55 produced *p*-cresol. Four strains belonging to *Clostridium sensu stricto* 11 and 14a produced 100 mM of *p*-cresol while one strain of *Anaerococcus* produced up to 100 mM *p*-cresol [342]. Although *Firmicutes* DTU014 and *Limnochordia* MBA03 were correlated with cresol removal in this study, there is no evidence supporting it. Their persistence in the system was not stable, as they were gradually washed out of the reactor. *Firmicutes* DTU014, *Limnochordia* MBA03 are slow-growing syntrophic electroactive bacteria commonly found in industrial anaerobic digesters [115],

[344]. They have been observed during the thermophilic anaerobic digestion of phenyl acids [345] and during the anaerobic digestion of the aqueous phase of hydrothermal liquefaction [99], but their function still remains unclear.

Other clostridial ASVs affiliated to *Cl. luticellarii*, *Caproiciproducens* and *Clostridium* sensu stricto 12 may have contributed to butyrate production. *Cl. luticellarii* is an acetogenic bacterium that can also produce *n*-butyrate and *iso*-butyrate. Mildly acidic pH (5.5) and 50 mM acetate stimulated *n*-butyrate and *iso*-butyrate production to a selectivity of about 42% [346]. *Cl. luticellarii* was also considered the main candidate for methanol and propionate conversion into valerate in an anaerobic chain elongation open-culture reactor [224]. Similarly, *Caproiciproducens*, a genus commonly found in chain-elongating microbial communities, produces butyrate and caproate [114], [347], [348]. The production of longer-chain carboxylic acids, such as valerate and caproate, has been previously documented in the co-fermentation of syngas and PAC at 30°C [100]. *Anaerococcus*, enriched concurrently with *Caproiciproducens*, can ferment a wide range of carbohydrates, peptone or amino acids to produce carboxylic acids [349] and it has been previously correlated with *iso*-butyrate production in syngas reactors [199]. Only few works have reported the enrichment of *Anaerococcus* during the anaerobic digestion of food waste and swine manure and their function within anaerobic mixed cultures is not clear [341], [350]–[352]. The conversion of SCCs and electron donors into non-monitored longer-chain carboxylates, may have contributed to the reduction in e-mol recoveries. Alternatively, or possibly in conjunction, the diminishing e-mol recovery may be linked to a concurrent decrease in the degradation rates of PAC components. A decrease in degradation could lead to lower SCCs production rates and increasing toxicant concentrations, which could ultimately cause also a cessation of CO uptake.

The elevated concentrations of undissociated acids, reaching about 30 mM (about 1.9 g/L) of acetic acid (within the first 20 days) together with the slow establishment of carboxydrotrophic activity (over 10 days of CO partial pressures of 20 kPa) and the toxicity of PAC compounds may have hindered methanogens causing their gradual washout in favor of acetogenic Clostridia. Acetic acid (*i.e.*, the undissociated form of acetate) concentrations of 0.3 and 2.4 g/L inhibited specific methanogenic activity by 50% and 90%, respectively, during mesophilic mixed culture fermentations of H₂/CO₂ [139]. Similarly, a previous work showed how an increase in CO partial pressure from 0.1 to 0.2 atm at 35°C induced a four-fold decrease in CO methanation yield, while simultaneously elevating specific CO uptake rates and favoring hydrogenogenesis [116]. Other studies reported methanogenesis inhibition during the co-fermentation of PAC and syngas. At 30°C and pH 6, methanogenesis was severely inhibited, and acetate, butyrate, and other carboxylic acids up to caproate accumulated in the fermentation broth [100]. Although that system was not optimized for gas fermentation, 46% of the CO fed into the system was metabolized

throughout the whole experimental period [100]. In another work, syngas and PAC were co-fermented in shaking flasks under mesophilic and thermophilic conditions. There, lower initial PAC loadings completely inhibited methanogenesis before carboxydrotrophic activity and PAC degradation, leading to the accumulation of acetate and other SCCs [295].

Conversely, despite starting under similar conditions to the mesophilic process (in terms of PAC, pH, HRT and gas partial pressures), the thermophilic process produced methane concomitantly with the start of carboxydrotrophic activity. The higher favorability of hydrogenogenic reactions at higher temperatures [128], the quick decrease of CO below 10 kPa, and the low undissociated carboxylates concentrations, all contributed to the enrichment of *Methanosarcina* and *Methanothermobacter*. *Methanosarcina* is a versatile methanogen able to perform acetoclastic, methylotrophic and hydrogenotrophic methanogenesis [353] and may have been responsible for methanogenesis up to the very end of the fermentation. *Methanothermobacter* species such as *Methanothermobacter thermoautotrophicus* or *Methanothermobacter marburgensis* are carboxydrotrophic methanogens able to oxidize CO to produce H₂ and CO₂ and later convert them to CH₄ [354]. For instance, *Mb. marburgensis* is able to grow under up to 50 kPa CO and to produce methane and even traces of acetate [355]. Here, *Mb. marburgensis* may have been the major carboxydrotrophic microorganism in the thermophilic system up to the enrichment of *Mo. thermoacetica*. *Mo. thermoacetica* is a well-known thermophilic acetogenic microorganism with a versatile metabolism, capable of utilizing various substrates such as sugars [356] as well as CO or H₂/CO₂ [357][358]. Previous studies have indicated its ability to degrade lignin-derived products, including furfural, guaiacol, vanillin, and syringol, ultimately producing acetate [359]. Furthermore, *Mo. thermoacetica* has been reported to possess an inducible CO-dependent O-demethylating capability for the degradation of methylated aromatics, which facilitates the integration of O-methyl groups into the acetyl-CoA pathway [360]. However, no evidence suggests that here *Mo. thermoacetica* participated to PAC components removal. *Thermoanaerobacterium thermosaccharolyticum* is an anaerobic thermophilic bacterium that can ferment cellulose and hemicellulose and other cellulosic sugars into H₂, acetate, lactate, ethanol, butyrate and butanol. Thermophilic synthetic co-cultures of *T. thermosaccharolyticum* and *Clostridium thermocellum* converted untreated lignocellulose waste into bioethanol [361]. Solventogenic cells of *T. thermosaccharolyticum* were even reported to degrade paraffin oil, a mixture of saturated hydrocarbons, to produce ethanol and butanol [362]. *Thermoanaerobacterium* and *Syntrophaceticus* were the main genera enriched during several thermophilic anaerobic processes at high loads of different intermediates of lignin degradation [363]. Similarly, *Syntrophaceticus* was enriched during the thermophilic degradation of phenyl acids and was considered a primary acetate oxidizer in association with hydrogenotrophic methanogens [364]. Syntrophic acetate oxidizer like

Syntrophaceticus can convert acetate into H₂ and CO₂ via the oxidative Wood-Ljungdahl pathway [126] only at low H₂ partial pressures, thus forcing syntrophic acetate oxidizers to grow dependently on hydrogenotrophic methanogens [40].

Here, it is possible that *Symbiobacteriales*, *Thermoanaerobacterium* and other acidogenic microorganisms degraded some PAC components into primarily acetate while *Syntrophaceticus* oxidized the acetate into CO₂ and H₂. Then *Methanothermobacter*, *Methanosarcina* and *Methanoculleus* converted acetate and H₂/CO₂ into CH₄. Another work reported similar associations during the thermophilic conversion of phenol into CH₄ in an anaerobic membrane bioreactor [68]. There, *Clostridium sensu stricto* degraded phenol to acetate via benzoate, while syntrophic acetate oxidizers and *Methanothermobacter* associations were essential to maintain a thermodynamically favorable process. *Syntrophaceticus* and other syntrophic bacteria oxidized the acetate from phenol into CO₂ and H₂ whilst *Methanothermobacter* produced CH₄ via hydrogenotrophic methanation. An impaired methanogenic population lead to increasing H₂ partial pressure inhibiting syntrophic acetate oxidizing bacteria and reducing the thermodynamic feasibility of phenol conversion [68]. Here, the accumulation of untreated PAC components or metabolic intermediates of PAC components degradation could have resulted in the inhibition and subsequent wash-out of hydrogenotrophic methanogens such as *Methanosarcina* and *Methanoculleus*, leading to increasing H₂ partial pressure. Higher H₂ partial pressure inhibited syntrophic acetate oxidation [40], altering the overall community dynamics and the bioenergetics involved in the degradation of some PAC components. An already weakened *Methanothermobacter* population, compounded by slow CO growth kinetics [354] and increasing toxicant concentrations in the fermentation broth, might have resulted in the abrupt decrease of carboxidotrophic activity.

The enrichment of *Corynebacterium* and *Acinetobacter* may suggest for some occasional air intrusions. Even though, *Corynebacteria* and *Acinetobacter* have been reported to be mainly active in aerobic environments, they can grow also in anaerobic ones [220], [347], [365]–[369]. In another work, low air contamination below detection limit (but quantified to a daily contamination rate of 220 ± 33 mL_{O₂}/L/d) provided competitive advantage to Actinobacteria and Coriobacteriia over the anaerobic community members but did not completely inhibit methanogenesis during lactate and H₂/CO₂ elongation to medium-chain carboxylates [370]. Similarly, minimal air exposure (5-8% in the reactor headspace) did not affect methanogenesis during the thermophilic anaerobic digestion of switch grass [371]. Facultative anaerobic and aerobic microorganisms can consume the O₂ in the air contamination limiting the strictly anaerobic members of the community to O₂ exposure [372]. The efficacy of this protective mechanism is affected on the composition of the microbial community and the extent of oxygen contamination [373]. Here,

Corynebacterium and *Acinetobacter* may have consumed the oxygen available and possibly mitigated the effects on the bioreactor performances. Despite their enrichment, no significant correlation emerged between low CO uptake rates and the presence of *Corynebacterium* and *Acinetobacter*. Occasional air contamination may have contributed to further weaken the anaerobic microorganisms (already inhibited by PAC components) but there is no evidence that it was the primary cause of lower CO conversion rates. On the other hand, the ability of *Corynebacterium* and *Acinetobacter* to degrade aromatic compounds [86], [374]–[380] may have improved overall reactor performances. Some *Acinetobacter* spp. possess genes encoding a CO dehydrogenase and can grow on CO, although aerobically, as sole carbon and energy source [381], [382], but there is no experimental evidence in this work.

There are numerous documented instances of PAC component degradation during anaerobic digestion of PAC, albeit with varying removal rates and COD recoveries [67]–[70]. These differences can be attributed to the composition of PAC since the degradation of specific PAC components can be significantly influenced by the presence of other toxic compounds [79]–[82]. Nevertheless, some works have attempted to elucidate the degradation pathways of PAC components such as phenol, furfural guaiacol and cresol reporting for the production of short chain carboxylates or methane. For instance, benzoyl-CoA was reported to be a central intermediate during the anaerobic degradation of phenol via 4-hydroxybenzoate. Benzoyl-CoA is subsequently converted via β -oxidation ring opening into three molecules of acetyl-CoA, which are further transformed into acetate [76], [83]. Furfural was reported to be converted into furoic acid via furfuryl alcohol, ultimately leading to the production of acetate [76]. Similarly, the anaerobic degradation of guaiacol generates acetate via demethylation of guaiacol to catechol [359]. The anaerobic degradability of cresols, on the other hand, depends on the position of the hydroxyl group. For example, *m*-cresol, is generally considered the most recalcitrant to anaerobic degradation [84]. Nonetheless, during *m*-cresol degradation, fumarate is added to the methyl group of *m*-cresol to form 3-hydroxybenzyl succinate. Activation and β -oxidation lead to succinyl-CoA and 3-hydroxybenzoyl-CoA [80].

5.4.2 Process stability and re-inoculations

The carboxydrotrophic activity in thermophilic system, as for the mesophilic one, was influenced by the interplay of factors such as PAC loading, biomass concentration and microbial diversity. Temperature likely played a critical role determining the stability of syngas and PAC co-fermentation. Some works assessing the effects of temperature on the anaerobic digestion of phenolic compounds or of the aqueous phase generated from hydrothermal liquefaction of cornstalk reported higher removal of aromatic compounds at mesophilic conditions and accumulation of untreated compounds at thermophilic conditions [67], [383]. Other factors such as inoculum origin and diversity, process operations and reactor design play critical

roles in the successful establishment of functional microbial cultures for wastewater detoxification [384]. Here, PAC loading potentially led to diminished functionality and diversity within both reactor microbiomes, increasing the toxicant level and resulting ultimately in the decline of CO conversion rates. Anaerobic carboxydrotrophic microorganisms rely on carbon monoxide dehydrogenase to catalyze CO conversion into H₂ and CO₂ [385]. This may render CO uptake a rather fragile process when exposed to toxic and very complex wastewaters such as PAC.

The selective pressure exerted by toxic components or other process parameters could enhance tolerance, reducing adaptation time and improving the biodegradation capabilities of the enriched culture [380]. However, a diminishing community richness poses a risk of losing critical functionality vital for the success of the process [340]. Even a minor alteration in a crucial parameter may inhibit a highly specialized microbial consortium [47]. Similarly to bioaugmentation, a strategy commonly employed to recover inhibited anaerobic digestion and other bioprocesses [41], [312], [386]–[389], re-inoculating the reactors resulted in high removal efficacies of PAC components and in sustained carboxydrotrophic activity even under higher PAC loads. Re-inoculations bolstered both biomass concentration and microbial diversity, allowing for quick recovery (consistently within one day) and extending significantly the process time. Another work proved how co-digesting PAC and manure (as source of organics and active cells) improved both methane yields and the maximum PAC loading by diluting toxic compounds [85]. Here, higher multifunctional activity persisted for over 50 and 90 days for the mesophilic and the thermophilic process, respectively, up to 6% v/v (0.8 g_{CO_D}/L/d). Here, this PAC loading level was the maximum achievable, maintaining an average VSS concentration of approximately 3 g/L. Cell retention systems or immobilization technologies may offer alternative approaches for retaining microorganisms within the system. Cell retention, for instance, is a technology employed to improve cell concentrations by preventing cell washout, especially during continuous bioprocesses characterized by low cell densities, such as anaerobic syngas fermentation [143], [390]. Alternatively, packed reactors have been also employed for mixed cultures syngas fermentation processes [391], [392]. Numerous studies have highlighted the advantageous effects of biochar as amendment and packing material during the anaerobic digestion of PAC. There, biochar provided structural support for microbial growth and facilitated interactions among microorganisms, thereby enhancing process performance [20], [24], [93]–[99], [72], [73], [84], [85], [89]–[92].

5.4.3 *L-malate production*

Both mesophilic and thermophilic mixed cultures degraded PAC components to a level that allowed *A. oryzae* to grow (up to PAC loading of 6 v/v %) and to convert SCCs into fungal biomass and L-malate. Among the compounds contained in the bio-oil generated from the pyrolysis of wheat straw, phenol, furfural, guaiacol,

2-cyclopentenone and cresol were severely inhibiting the growth and L-malate production of *A. oryzae* [166]. In a previous work, 2.5 v/v % of the same PAC as used in this study proved to be inhibitory and impeded the growth of *A. oryzae* [295]. Here, the growth of *A. oryzae* was minimal and none in two flasks only with the effluent from the mesophilic process collected on day 116 (4% v/v) and day 213, respectively. These results were likely linked to the accumulation of untreated PAC components, or accumulation of by-products from the degradation of PAC components, as the decreasing e-mol recovery indicated.

Even though process optimization was not the scope of this work, the highest yields achieved in this study are similar to what was described in other works. When grown in shaking flasks on acetate, *A. oryzae* yielded up to 21 % $\text{g}_{\text{L-malate}}/\text{g}_{\text{acetate}}$ but the production was highly dependent upon the initial acetate concentration [161]. In bioreactor experiments optimized for L-malate production from acetate, *A. oryzae* produced about 29 g/L L-malate corresponding to a 29 % $\text{g}_{\text{L-malate}}/\text{g}_{\text{acetate}}$ L-malate yield [156]. During the cultivation of *A. oryzae* with acetate and acetol from a detoxified PAC, L-malate was produced up to 7.3 ± 0.3 g/L (corresponding to a yield of 20 ± 0.01 $\text{g}_{\text{L-malate}}/\text{g}_{\text{substrates}}$) [167]. In a sequential syngas to L-malate fermentation process (with *Cl. ljungdahlii* and *A. oryzae* as microbial catalysts), the fermentation medium rich in acetate from stage one was fed directly to *A. oryzae*. L-malate production with acetate from the syngas fermentation as sole carbon source reached yields of 28 w/w %. The presence of macro- and micronutrients in the fermentation broth from the first stage syngas fermentation was highlighted to have major positive effects on *A. oryzae* growth and improved L-malate yields [148]. Similar synergies may have occurred here.

5.5 Conclusions

This study demonstrates the ability of mesophilic and thermophilic mixed cultures to recover carbon and energy simultaneously from syngas sequestration and PAC components degradation into CH_4 , acetate and other short-chain carboxylates. The carboxylates generated during syngas and PAC co-fermentation were subsequently converted to L-malate by *Aspergillus oryzae* in a second-stage fermentation, increasing the overall process selectivity. The findings highlight the diversity of process regimes that can be achieved by simply changing the operating temperature. The mesophilic process was stable, non-methanogenic and short-chain carboxylates accumulated in the medium. The enrichment of *Caproiciproducens* suggests the potential of the mesophilic process for the production of medium-chain carboxylates. Conversely, the thermophilic process converted syngas and PAC into primarily methane but suffered from unstable CO conversion, potentially due to unfavorable process conditions. The instability was addressed through the regular injection

of fresh inoculum. Integrating animal manure as a substrate during thermophilic conversion of syngas and PAC may resolve possible instability.

This work represents a successful effort in demonstrating the potential of a two-stage process for producing platform chemicals from gaseous and toxic substrates. It identifies critical parameters essential for the co-fermentation of syngas and PAC, thereby laying the groundwork for further advancements in this field. Key areas requiring attention include the optimization of operational parameters, bioreactor design, and the implementation of a two-stage continuous fermentation with particular focus on syngas and PAC flows based on a real pyrolysis process. Addressing these aspects will be crucial in advancing the readiness of this technology for practical applications.

Acknowledgments

The authors acknowledge Institute of Catalysis Research & Technology, Karlsruhe Institute of Technology, for providing the PAC. We thank Ute Lohse for technical assistance in DNA extraction and library preparation for MiSeq amplicon sequencing; Habibu Aliyu for mentoring and Delfine Muller, Magda Ardila and Kevin Schulz for assistance.

Supplementary information

Additional file 4: Table S1. GC-MS characterization of the aqueous condensate deriving from the fast pyrolysis of Miscanthus was performed by the Thünen Institute of Wood Research, (Hamburg, Germany). Table S2. Composition in gCOD/Ld and electron moles (e-mM/d) of the feed (for both syngas and PAC) for both the mesophilic and the thermophilic semi-continuous fermentations. Table S3. Conversion factors for electron balances. Figure S1. Fermentation profile of the mesophilic process. Top x-axis shows increases in PAC loading, bottom x-axis shows the elapsed fermentation time. The red bar indicate the period of weekly re-inoculations. (a) pH and redox potential. (b) Partial pressures of CO and H₂. (c) Concentration of undissociated carboxylates. (d) Removal efficacy of each cresol isomer. Negative values indicate production. (e) Concentrations of total (TSS) and volatile suspended solids (VSS). Figure S2. Fermentation profile of the thermophilic process. Top x-axis shows increases in PAC loading, bottom x-axis shows the elapsed fermentation time. Red arrows point to re-inoculation events, the red bar indicate the period of weekly re-inoculations. (a) pH and redox potential. (b) Partial pressures of CO and H₂. (c) Concentration of undissociated carboxylates. (d) Removal efficacy of each cresol isomer. Negative values indicate production. (e) Concentrations of total and volatile suspended solids. (f) Relative abundance of the enriched archaeal genera (based on mcrA gene amplicon sequencing variants). Others include all microbial genera with

abundance lower than 1%. Figure S3. Spearman's rank correlations between relative abundance of methanogens (based on *mcrA* gene amplicon sequencing variants) and process parameters for the thermophilic semi-continuous STR enrichment. The strength of the correlation is represented by the size of the circle and intensity of the color. Blue circles indicate positive correlations. Red circles indicate negative correlations. *p* values are shown for non-significant correlations ($p < 0.05$). Figure S4. CO, H₂, CH₄ production rates during the decrease in CO uptake rates for the thermophilic syngas and PAC co-fermentation. Table S4. L-malate and SCCs concentrations over time and L-malate highest yields per SCCs consumed. Numbers are mean values with standard deviations calculated from three replicates. The medium was the supernatant of the fermentation broth collected from the mesophilic reactor. Table S5. L-malate and SCCs concentrations over time and L-malate highest yields per SCCs consumed. Numbers are mean values with standard deviations calculated from three replicates. The medium was the supernatant of the fermentation broth collected from the thermophilic reactor. Figure S5. Photos depicting *A. oryzae* growth for all aerobic flask fermentations after 72 hours. The pictures labelled with 6% PAC were recorded from cultivations with the supernatant collected after 207 days of fermentation for both mesophilic and thermophilic process. Pictures labelled with 6% PAC END were recorded from cultivations with the supernatant collected after 213 days of fermentation for both mesophilic and thermophilic process.

6. Final conclusions and outlook

In this work, the potential of hybrid thermochemical and biological processes in waste management has emerged as viable technology to maximise energy recovery and minimize environmental impacts by reducing greenhouse gas emissions and detoxifying pyrolysis wastewater. The biological component relies on the capability of mixotrophic anaerobic communities to simultaneously ferment syngas and PAC, converting them into biofuels or carboxylates. Additionally, the biological part was further extended by coupling it with a secondary aerobic fermentative stage, forming a two-stage process where the carboxylates product of syngas and PAC co-fermentation were converted into high-value platform chemicals such as L-malate to enhance process selectivity.

The research began by evaluating the effects of acetate, a model compound of PAC on syngas fermentation. Experiments were conducted in serum bottles under varying pH levels (6.7 and 5.5), temperatures (37°C and 55°C) and increasing acetate loads (from 0 to 64 g/L). Mixed cultures proved to be able to undertake syngas fermentation even at high acetate concentrations and acidic pH levels, conditions not previously reported. Secondly, the microbial diversity of mixed cultures allowed for a highly flexible and resilient metabolism capable of adapting to changing environmental conditions. Manipulating process conditions and acetate loads allowed for steering the metabolism of the mixed culture, promoting favourable reactions while inhibiting others. Specifically, a pH of 6.7 promoted methanogenic reactions, while lowering the pH to 5.5 intensified the toxicity of undissociated acetic acid, thereby inhibiting methanogenesis at lower acetate loads. Under non-methanogenic conditions, acetate stimulated hydrogenogenesis and the production of various carboxylates, including *n*-valerate, depending on temperature. Acetic acid, the undissociated form of acetate, emerged as the primary inhibitor of methanogenesis, yet unexpectedly, high acetate concentrations promoted CO consumption rates by providing additional carbon and energy to carboxydrotrophic and chain-elongating microorganisms. While species belonging to *Methanobacterium*, *Methanosarcina* and *Methanothermobacter* may have been involved in CO biomethanation, the bacterial species responsible for CO conversion in non-methanogenic experiments remain unclear. One possible candidate for carboxydrotrophic bacteria is *Thermoanaerobacterium*, while a possible candidate for *n*-valerate production was identified in *Oscillibacter*. Acetate contained in PAC proved to be an ideal candidate for process control and an additional substrate.

Three types of PAC derived from the pyrolysis of different feedstock such as lignocellulose, sewage sludge and mixed polyethylene plastics were tested as co-substrate in serum bottles under varying temperatures (37°C and 55°C). Once again, mixed cultures demonstrated their versatility as biocatalysts. They proved to be capable of

simultaneously sequestering syngas and degrading PAC components, thereby detoxifying and recovering energy from both substrates. The products of syngas fermentation and PAC degradation included CH₄, H₂ or carboxylates, with products pool and selectivity depending on the temperature. However, microbial kinetics and energy recovery potential were significantly influenced by the origin and composition of the PAC, leading also to varying levels of toxicity and inhibition. While even small concentrations of lignocellulose and polyethylene PACs were severely toxic and inhibited carboxydrotrophic reactions and PAC components removal, sewage sludge PAC showed both the least toxicity and relative energy recovery when compared to the other PACs. It appears that PAC's toxicity is not result of the presence of individual toxic compounds but rather of the synergistic effect of the mix of several compounds, although some of which indeed toxic.

Moreover, PAC composition significantly affected both PAC components degradation and energy recovery. Some PAC components showed greater bioconversion potential than others. The resistance of N-heterocycles to biodegradation, for instance, likely hindered energy recovery of sewage sludge PAC. Conversely, despite the higher toxicity of lignocellulose and polyethylene PAC, some of their components exhibited great bioconversion potential, enabling high energy recoveries. Furthermore, while compounds like phenol are present in all PAC samples, their removal efficiency varies among different PACs. This differences can be attributed to how the diverse mixtures affect the degradation potential of each compound. Extending incubation time likely enhances energy recovery by allowing for extended reaction periods, increasing degradation and energy recovery, as observed in lignocellulose PAC.

Both carboxydrotrophic and PAC components degradation reactions showed higher resilience to PAC toxicity compared to other reactions, particularly methanogenic ones. These findings are pivotal and lay the necessary groundwork for advancing the development of the two-stage process. Methanogenesis represents a competing pathway for the accumulation of carboxylates in the fermentation medium, and diverting carbon and electron equivalents towards CH₄ instead of carboxylates would contradict the objectives of the two-stage system. Similarly, PAC detoxification is indispensable for the valorization of carboxylates in the effluents from stage one. Like many microorganisms, *A. oryzae* is highly sensitive to PAC's toxicity, with lignocellulose PAC concentrations of 2.5% proving inhibitory to its growth. *A. oryzae* thrived in effluents containing originally 7.5% lignocellulose PAC, confirming that lignocellulose PAC degradation occurred below inhibitory levels, further demonstrating the feasibility of the two-stage process. The carboxylates in the effluent of stage one allowed to achieve L-malate yields comparable to those found in literature, further confirming the potential of the two-stage process.

What learned from the bottles experiments was used to design and operate long-term cultivations with syngas and lignocellulose PAC as substrates. Conducting experiments with two identical stirred tank reactors, each operated at pH 5.5 under mesophilic and thermophilic conditions with syngas and increasing concentrations of lignocellulose PAC, provided valuable insights into how process parameters affect microbial community structure and process stability.

Operating at acidic pH emerged as a successful strategy for inhibiting methanogenic pathways, particularly evident in the mesophilic reactor, where the accumulation of undissociated acetic acid within the fermentation medium acted as the primary inhibitor of methanogenesis. Conversely, under thermophilic conditions, where concentrations of undissociated acetic acid were notably lower, syngas and PAC were predominantly converted into methane. These results corroborate our prior findings indicating that undissociated acetic acid concentrations exceeding 2.7 g/L are sufficient to inhibit methanogenesis. Since acetate was generated from syngas and PAC components metabolism, this strategy may presents an economically viable alternative to the use of costly and non-recoverable chemical methanogenic inhibitors like 2-BES.

Different operating temperatures, however, resulted in the selection of distinct reactors' microbiota, affecting the stability of carboxydrotrophic activity within each reactor. The mesophilic process exhibited remarkable stability over a duration exceeding 150 days up to lignocellulose PAC loads of 5%. *Clostridium sensu stricto* 12, a cluster comprising known carboxydrotrophic microorganisms, dominated the mesophilic microbiota and was significantly correlated to CO consumption, highlighting their relevance in the mesophilic process. However, while certain PAC components were consistently removed from the fermentation broth, the precise contribution of *Clostridium sensu stricto* 12 to this removal remains ambiguous. It is plausible that these microorganisms are resilient to PAC components or intermediate degradation products, potentially mitigating the toxicity. Additionally, the enrichment of *Caproiciproducens* within the mesophilic process hints at its potential for the production of medium-chain carboxylates.

Conversely, the thermophilic process suffered from unstable CO conversion, potentially due to unfavourable process conditions. Noteworthy microbial players in this process included *Symbiobacteriales*, *Syntrophaceticus*, *Thermoanaerobacterium*, *Methanothermobacter* and *Methanosarcina* contributing to aromatics degradation and methanogenesis, respectively. *Moorella thermoacetica* and *Methanothermobacter marburgensis* were the predominant carboxydrotrophs. Unstable CO conversion likely resulted from a chain of interconnected events originating from the wash-out of functional microorganisms from the system. As found in our previous works, methanogens are more susceptible to PAC toxicity and were likely inhibited first. However, methanogenesis inhibition may have altered the overall bioenergetics of

PAC components degradation, increasing toxicants concentrations and culminating in the inhibition of carboxydrotrophic rates. Given that anaerobic carboxydrotrophic microorganisms employ one specific enzyme, the carbon monoxide dehydrogenase, to catalyse CO conversion into H₂ and CO₂, some PAC components or their accumulation above a certain threshold may have hindered carbon monoxide dehydrogenase activity, thereby reducing CO uptake rates.

Since the purpose of this work was to develop multifunctional processes, regular injection of fresh inoculum was identified as optimal strategy to address process recovery and instability. Re-inoculations significantly enhanced biomass concentration and microbial diversity, facilitating rapid recovery (typically within one day) and substantially prolonging the process duration. However, the necessity for re-inoculations underscores the potential benefits of implementing cell retention or immobilization technologies, or integrating the process with other organic waste streams, such as manure, to enhance process stability and efficiency.

The findings from these long-term cultivations may outline the potential for two distinct hybrid thermochemical-biological processes. Mesophilic conditions appear optimal for carboxylates production and the further development of a two-stage process for treating syngas and PAC. In contrast, thermophilic conditions, given the lower carboxylates production rates, may be more suitable for methane production. Syngas, PAC and biochar (as immobilization matrix) could be integrated into thermophilic anaerobic digesters for biogas production.

The foundational knowledge gained in this work lays the groundwork for the future development of biotechnologies centered on the co-fermentation of syngas and toxic wastewaters, such as PAC, into economically viable and sustainable bioprocesses. Such technologies offer the potential to maximize carbon and energy recovery from waste streams, thereby reducing greenhouse gas emissions and wastewater production. However, substantial work remains to be done, particularly in optimizing operational parameters, reactor design and implementing the first stage continuous fermentation system tailored to syngas and PAC flows derived from real pyrolysis processes.

Bibliography

- [1] F. Cherubini and S. Ulgiati, 'Crop residues as raw materials for biorefinery systems - A LCA case study', *Appl. Energy*, vol. 87, no. 1, pp. 47–57, 2010, doi: 10.1016/j.apenergy.2009.08.024.
- [2] B. M. Cieslik, J. Namiesnik, and P. Konieczka, 'Review of sewage sludge management: Standards, regulations and analytical methods', *J. Clean. Prod.*, vol. 90, pp. 1–15, 2015, doi: 10.1016/j.jclepro.2014.11.031.
- [3] N. Evode, S. A. Qamar, M. Bilal, D. Barceló, and H. M. N. Iqbal, 'Plastic waste and its management strategies for environmental sustainability', *Case Stud. Chem. Environ. Eng.*, vol. 4, no. August, 2021, doi: 10.1016/j.cscee.2021.100142.
- [4] I. Fonts, G. Gea, M. Azuara, J. Ábrego, and J. Arauzo, 'Sewage sludge pyrolysis for liquid production: A review', *Renew. Sustain. Energy Rev.*, vol. 16, no. 5, pp. 2781–2805, 2012, doi: 10.1016/j.rser.2012.02.070.
- [5] M. T. Agler, B. A. Wrenn, S. H. Zinder, and L. T. Angenent, 'Waste to bioproduct conversion with undefined mixed cultures: The carboxylate platform', *Trends Biotechnol.*, vol. 29, no. 2, pp. 70–78, 2011, doi: 10.1016/j.tibtech.2010.11.006.
- [6] J. Rajesh Banu *et al.*, 'Lignocellulosic biomass based biorefinery: A successful platform towards circular bioeconomy', *Fuel*, vol. 302, no. May, p. 121086, 2021, doi: 10.1016/j.fuel.2021.121086.
- [7] J. Popp, Z. Lakner, M. Harangi-Rákos, and M. Fári, 'The effect of bioenergy expansion: Food, energy, and environment', *Renew. Sustain. Energy Rev.*, vol. 32, pp. 559–578, 2014, doi: 10.1016/j.rser.2014.01.056.
- [8] R. Rathmann, A. Szklo, and R. Schaeffer, 'Land use competition for production of food and liquid biofuels: An analysis of the arguments in the current debate', *Renew. Energy*, vol. 35, no. 1, pp. 14–22, 2010, doi: 10.1016/j.renene.2009.02.025.
- [9] G. Velvizhi, C. Goswami, N. P. Shetti, E. Ahmad, K. Kishore Pant, and T. M. Aminabhavi, 'Valorisation of lignocellulosic biomass to value-added products: Paving the pathway towards low-carbon footprint', *Fuel*, vol. 313, no. October 2021, p. 122678, 2022, doi: 10.1016/j.fuel.2021.122678.
- [10] F. X. Collard and J. Blin, 'A review on pyrolysis of biomass constituents: Mechanisms and composition of the products obtained from the conversion of cellulose, hemicelluloses and lignin', *Renew. Sustain. Energy Rev.*, vol. 38, pp. 594–608, 2014, doi: 10.1016/j.rser.2014.06.013.
- [11] V. Dhyani and T. Bhaskar, 'A comprehensive review on the pyrolysis of lignocellulosic biomass', *Renew. Energy*, vol. 129, pp. 695–716, 2018, doi: 10.1016/j.renene.2017.04.035.
- [12] K. Q. Tan, M. A. Ahmad, W. Da Oh, and S. C. Low, 'Valorization of hazardous plastic wastes into value-added resources by catalytic pyrolysis-gasification: A review of techno-economic analysis', *Renew. Sustain. Energy Rev.*, vol. 182, no. April, p. 113346, 2023, doi: 10.1016/j.rser.2023.113346.

- [13] H. Shahbeig and M. Nosrati, 'Pyrolysis of municipal sewage sludge for bioenergy production: Thermo-kinetic studies, evolved gas analysis, and techno-socio-economic assessment', *Renew. Sustain. Energy Rev.*, vol. 119, no. July 2019, p. 109567, 2020, doi: 10.1016/j.rser.2019.109567.
- [14] T. Kan, V. Strezov, and T. J. Evans, 'Lignocellulosic biomass pyrolysis: A review of product properties and effects of pyrolysis parameters', *Renew. Sustain. Energy Rev.*, vol. 57, pp. 1126–1140, 2016, doi: 10.1016/j.rser.2015.12.185.
- [15] A. Funke, M. Tomasi Morgano, N. Dahmen, and H. Leibold, 'Experimental comparison of two bench scale units for fast and intermediate pyrolysis', *J. Anal. Appl. Pyrolysis*, vol. 124, pp. 504–514, 2017, doi: 10.1016/j.jaap.2016.12.033.
- [16] A. Niebel *et al.*, 'Fast Pyrolysis of Wheat Straw - Improvements of Operational Stability in 10 Years of Bioliq Pilot Plant Operation', *Energy and Fuels*, vol. 35, no. 14, pp. 11333–11345, 2021, doi: 10.1021/acs.energyfuels.1c00851.
- [17] M. Tomasi Morgano, H. Leibold, F. Richter, D. Stapf, and H. Seifert, 'Screw pyrolysis technology for sewage sludge treatment', *Waste Manag.*, vol. 73, pp. 487–495, 2018, doi: 10.1016/j.wasman.2017.05.049.
- [18] A. Korkmaz, J. Yanik, M. Brebu, and C. Vasile, 'Pyrolysis of the tetra pak', *Waste Manag.*, vol. 29, no. 11, pp. 2836–2841, 2009, doi: 10.1016/j.wasman.2009.07.008.
- [19] G. K. Parku, A. Krutof, A. Funke, D. Richter, and N. Dahmen, 'Using Fractional Condensation to Optimize Aqueous Pyrolysis Condensates for Downstream Microbial Conversion', *Ind. Eng. Chem. Res.*, vol. 62, no. 6, pp. 2792–2803, 2023, doi: 10.1021/acs.iecr.2c03598.
- [20] R. Posmanik, R. A. Labatut, A. H. Kim, J. G. Usack, J. W. Tester, and L. T. Angenent, 'Coupling hydrothermal liquefaction and anaerobic digestion for energy valorization from model biomass feedstocks', *Bioresour. Technol.*, vol. 233, pp. 134–143, 2017, doi: 10.1016/j.biortech.2017.02.095.
- [21] Y. K N *et al.*, 'Lignocellulosic biomass-based pyrolysis: A comprehensive review', *Chemosphere*, vol. 286, no. P2, p. 131824, 2022, doi: 10.1016/j.chemosphere.2021.131824.
- [22] L. Leng *et al.*, 'Valorization of the aqueous phase produced from wet and dry thermochemical processing biomass: A review', *J. Clean. Prod.*, vol. 294, p. 126238, 2021, doi: 10.1016/j.jclepro.2021.126238.
- [23] S. Xin, H. Yang, Y. Chen, X. Wang, and H. Chen, 'Assessment of pyrolysis polygeneration of biomass based on major components: Product characterization and elucidation of degradation pathways', *Fuel*, vol. 113, pp. 266–273, 2013, doi: 10.1016/j.fuel.2013.05.061.
- [24] S. Seyedi, K. Venkiteshwaran, and D. Zitomer, 'Toxicity of various pyrolysis liquids from biosolids on methane production yield', *Front. Energy Res.*, vol. 7, no. FEB, pp. 1–12, 2019, doi: 10.3389/fenrg.2019.00005.
- [25] J. Alvarez *et al.*, 'Characterization of the bio-oil obtained by fast pyrolysis of sewage sludge in a conical spouted bed reactor', *Fuel Process. Technol.*, vol. 149, pp. 169–175, 2016, doi: 10.1016/j.fuproc.2016.04.015.
- [26] B. Wirth and M. T. Reza, 'Continuous Anaerobic Degradation of Liquid

- Condensate from Steam-Derived Hydrothermal Carbonization of Sewage Sludge', *ACS Sustain. Chem. Eng.*, vol. 4, no. 3, pp. 1673–1678, 2016, doi: 10.1021/acssuschemeng.5b01607.
- [27] A. Jaramillo-Arango, I. Fonts, F. Chejne, and J. Arauzo, 'Product compositions from sewage sludge pyrolysis in a fluidized bed and correlations with temperature', *J. Anal. Appl. Pyrolysis*, vol. 121, pp. 287–296, 2016, doi: 10.1016/j.jaap.2016.08.008.
- [28] Z. X. Xu *et al.*, 'Hydrothermal carbonization of sewage sludge: Effect of aqueous phase recycling', *Chem. Eng. J.*, vol. 387, no. June 2019, p. 123410, 2020, doi: 10.1016/j.cej.2019.123410.
- [29] B. A. Black *et al.*, 'Aqueous Stream Characterization from Biomass Fast Pyrolysis and Catalytic Fast Pyrolysis', *ACS Sustain. Chem. Eng.*, vol. 4, no. 12, pp. 6815–6827, 2016, doi: 10.1021/acssuschemeng.6b01766.
- [30] H. Chen *et al.*, 'Hydrothermal conversion of sewage sludge: Focusing on the characterization of liquid products and their methane yields', *Chem. Eng. J.*, vol. 357, no. July 2018, pp. 367–375, 2019, doi: 10.1016/j.cej.2018.09.180.
- [31] T. Sarchami, N. Batta, and F. Berruti, 'Production and separation of acetic acid from pyrolysis oil of lignocellulosic biomass: a review', *Biofuels, Bioprod. Biorefining*, vol. 15, no. 6, pp. 1912–1937, 2021, doi: 10.1002/bbb.2273.
- [32] C. Wang, C. Wu, U. Hornung, W. Zhu, and N. Dahmen, 'Suppression of tar and char formation in supercritical water gasification of sewage sludge by additive addition', *Chemosphere*, vol. 262, p. 128412, 2021, doi: 10.1016/j.chemosphere.2020.128412.
- [33] W. D. Chanaka Udayanga, A. Veksha, A. Giannis, G. Lisak, and T. T. Lim, 'Effects of sewage sludge organic and inorganic constituents on the properties of pyrolysis products', *Energy Convers. Manag.*, vol. 196, no. June, pp. 1410–1419, 2019, doi: 10.1016/j.enconman.2019.06.025.
- [34] A. M. Cunliffe, N. Jones, and P. T. Williams, 'Pyrolysis of composite plastic waste pyrolysis of composite plastic waste', vol. 3330, no. June, pp. 37–41, 2016.
- [35] M. Zeller, N. Netsch, F. Richter, H. Leibold, and D. Stapf, 'Chemical Recycling of Mixed Plastic Wastes by Pyrolysis – Pilot Scale Investigations', *Chemie-Ingenieur-Technik*, vol. 93, no. 11, pp. 1763–1770, 2021, doi: 10.1002/cite.202100102.
- [36] A. López, I. de Marco, B. M. Caballero, M. F. Laresgoiti, A. Adrados, and A. Torres, 'Pyrolysis of municipal plastic wastes II: Influence of raw material composition under catalytic conditions', *Waste Manag.*, vol. 31, no. 9–10, pp. 1973–1983, 2011, doi: 10.1016/j.wasman.2011.05.021.
- [37] M. Usman *et al.*, 'Characterization and utilization of aqueous products from hydrothermal conversion of biomass for bio-oil and hydro-char production: A review', *Green Chem.*, vol. 21, no. 7, pp. 1553–1572, 2019, doi: 10.1039/c8gc03957g.
- [38] A. Anukam, A. Mohammadi, M. Naqvi, and K. Granström, 'A Review of the Chemistry of Anaerobic Digestion: Methods of accelerating and optimizing process efficiency', *Processes*, vol. 7, no. 8, pp. 1–19, 2019.
- [39] A. Basile *et al.*, 'Revealing metabolic mechanisms of interaction in the

- anaerobic digestion microbiome by flux balance analysis', *Metab. Eng.*, vol. 62, no. September, pp. 138–149, 2020, doi: 10.1016/j.ymben.2020.08.013.
- [40] S. Hattori, 'Syntrophic Acetate-Oxidizing Microbes in Methanogenic Environments', *Microbes Environ.*, vol. 23, no. 2, pp. 118–127, 2008, doi: doi:10.1264/jsme2.23.118.
- [41] I. A. Fotidis, D. Karakashev, and I. Angelidaki, 'Bioaugmentation with an acetate-oxidising consortium as a tool to tackle ammonia inhibition of anaerobic digestion', *Bioresour. Technol.*, vol. 146, pp. 57–62, 2013, doi: 10.1016/j.biortech.2013.07.041.
- [42] T. Ito, K. Yoshiguchi, H. D. Ariesyady, and S. Okabe, 'Identification of a novel acetate-utilizing bacterium belonging to Synergistes group 4 in anaerobic digester sludge', *ISME J.*, vol. 5, no. 12, pp. 1844–1856, 2011, doi: 10.1038/ismej.2011.59.
- [43] B. Liu, S. Kleinstaubler, F. Centler, H. Harms, and H. Sträuber, 'Competition Between Butyrate Fermenters and Chain-Elongating Bacteria Limits the Efficiency of Medium-Chain Carboxylate Production', *Front. Microbiol.*, vol. 11, no. March, pp. 1–13, 2020, doi: 10.3389/fmicb.2020.00336.
- [44] J. Weijma *et al.*, 'Competition for H₂ between sulfate reducers, methanogens and homoacetogens in a gas-lift reactor.', *Water Sci. Technol.*, vol. 45, no. 10, pp. 75–80, 2002, doi: 10.2166/wst.2002.0294.
- [45] O. R. Kotsyurbenko, M. V. Glagolev, A. N. Nozhevnikova, and R. Conrad, 'Competition between homoacetogenic bacteria and methanogenic archaea for hydrogen at low temperature', *FEMS Microbiol. Ecol.*, vol. 38, no. 2–3, pp. 153–159, 2001, doi: 10.1016/S0168-6496(01)00179-9.
- [46] S. A. Hashsham *et al.*, 'Parallel processing of substrate correlates with greater functional stability in methanogenic bioreactor communities perturbed by glucose', *Appl. Environ. Microbiol.*, vol. 66, no. 9, pp. 4050–4057, 2000, doi: 10.1128/AEM.66.9.4050-4057.2000.
- [47] J. J. Werner *et al.*, 'Bacterial community structures are unique and resilient in full-scale bioenergy systems', *Proc. Natl. Acad. Sci. U. S. A.*, vol. 108, no. 10, pp. 4158–4163, 2011, doi: 10.1073/pnas.1015676108.
- [48] A. Mutungwazi, G. N. Ijoma, and T. S. Matambo, 'The significance of microbial community functions and symbiosis in enhancing methane production during anaerobic digestion: a review', *Symbiosis*, vol. 83, no. 1, pp. 1–24, 2021, doi: 10.1007/s13199-020-00734-4.
- [49] A. Grimalt-Alemany, I. V. Skiadas, and H. N. Gavala, 'Syngas biomethanation: state-of-the-art review and perspectives', *Biofuels, Bioprod. Biorefining*, vol. 12, no. 1, pp. 139–158, 2018, doi: 10.1002/bbb.1826.
- [50] M. Zheng *et al.*, 'Anaerobic digestion of wastewater generated from the hydrothermal liquefaction of Spirulina: Toxicity assessment and minimization', *Energy Convers. Manag.*, vol. 141, pp. 420–428, 2017, doi: 10.1016/j.enconman.2016.10.034.
- [51] Y. Chen, J. J. Cheng, and K. S. Creamer, 'Inhibition of anaerobic digestion process: A review', *Bioresour. Technol.*, vol. 99, no. 10, pp. 4044–4064, 2008, doi: 10.1016/j.biortech.2007.01.057.
- [52] M. Vítězová, A. Kohoutová, T. Vítěz, N. Hanišáková, and I. Kushkevych,

- 'Methanogenic microorganisms in industrial wastewater anaerobic treatment', *Processes*, vol. 8, no. 12, pp. 1–27, 2020, doi: 10.3390/pr8121546.
- [53] G. Lourinho, L. F. T. G. Rodrigues, and P. S. D. Brito, 'Recent advances on anaerobic digestion of swine wastewater', *Int. J. Environ. Sci. Technol.*, vol. 17, no. 12, pp. 4917–4938, 2020, doi: 10.1007/s13762-020-02793-y.
- [54] P. Xu, H. Han, B. Hou, S. Jia, and Q. Zhao, 'Treatment of coal gasification wastewater by a two-phase anaerobic digestion', *Desalin. Water Treat.*, vol. 54, no. 3, pp. 598–608, 2015, doi: 10.1080/19443994.2014.884474.
- [55] R. Moletta, 'Winery and distillery wastewater treatment by anaerobic digestion', *Water Sci. Technol.*, vol. 51, no. 1, pp. 137–144, 2005, doi: 10.2166/wst.2005.0017.
- [56] K. Kujawa-Roeleveld and G. Zeeman, 'Anaerobic treatment in decentralised and source-separation-based sanitation concepts', *Rev. Environ. Sci. Biotechnol.*, vol. 5, no. 1, pp. 115–139, 2006, doi: 10.1007/s11157-005-5789-9.
- [57] M. Basaglia, L. Favaro, C. Torri, and S. Casella, 'Is pyrolysis bio-oil prone to microbial conversion into added-value products?', *Renew. Energy*, vol. 163, pp. 783–791, 2021, doi: 10.1016/j.renene.2020.08.010.
- [58] Y. Liang *et al.*, 'Utilization of acetic acid-rich pyrolytic bio-oil by microalga *Chlamydomonas reinhardtii*: Reducing bio-oil toxicity and enhancing algal toxicity tolerance', *Bioresour. Technol.*, vol. 133, pp. 500–506, 2013, doi: 10.1016/j.biortech.2013.01.134.
- [59] J. Lange, F. Müller, K. Bernecker, N. Dahmen, R. Takors, and B. Blombach, 'Valorization of pyrolysis water: A biorefinery side stream, for 1,2-propanediol production with engineered *Corynebacterium glutamicum*', *Biotechnol. Biofuels*, vol. 10, no. 1, pp. 1–13, 2017, doi: 10.1186/s13068-017-0969-8.
- [60] S. Arnold, K. Moss, N. Dahmen, M. Henkel, and R. Hausmann, 'Pretreatment strategies for microbial valorization of bio-oil fractions produced by fast pyrolysis of ash-rich lignocellulosic biomass', *GCB Bioenergy*, vol. 11, no. 1, pp. 181–190, 2019, doi: 10.1111/gcbb.12544.
- [61] J. Lian, M. Garcia-Perez, R. Coates, H. Wu, and S. Chen, 'Yeast fermentation of carboxylic acids obtained from pyrolytic aqueous phases for lipid production', *Bioresour. Technol.*, vol. 118, pp. 177–186, 2012, doi: 10.1016/j.biortech.2012.05.010.
- [62] J. Lian *et al.*, 'Separation, hydrolysis and fermentation of pyrolytic sugars to produce ethanol and lipids', *Bioresour. Technol.*, vol. 101, no. 24, pp. 9688–9699, 2010, doi: 10.1016/j.biortech.2010.07.071.
- [63] C. Kubisch and K. Ochsenreither, 'Detoxification of a pyrolytic aqueous condensate from wheat straw for utilization as substrate in *Aspergillus oryzae* DSM 1863 cultivations', *Biotechnol. Biofuels Bioprod.*, vol. 15, no. 1, pp. 1–21, 2022, doi: 10.1186/s13068-022-02115-z.
- [64] S. Arnold, M. Henkel, J. Wanger, A. Wittgens, F. Rosenau, and R. Hausmann, 'Heterologous rhamnolipid biosynthesis by *P. putida* KT2440 on bio-oil derived small organic acids and fractions', *AMB Express*, vol. 9, no. 1, 2019, doi: 10.1186/s13568-019-0804-7.
- [65] S. Arnold, T. Tews, M. Kiefer, M. Henkel, and R. Hausmann, 'Evaluation of small organic acids present in fast pyrolysis bio-oil from lignocellulose as

- feedstocks for bacterial bioconversion', *GCB Bioenergy*, vol. 11, no. 10, pp. 1159–1172, 2019, doi: 10.1111/gcbb.12623.
- [66] B. C. Si *et al.*, 'Continuous production of biohythane from hydrothermal liquefied cornstalk biomass via two-stage high-rate anaerobic reactors', *Biotechnol. Biofuels*, vol. 9, no. 1, pp. 1–15, 2016, doi: 10.1186/s13068-016-0666-z.
- [67] H. Chen *et al.*, 'Mesophilic and thermophilic anaerobic digestion of aqueous phase generated from hydrothermal liquefaction of cornstalk: Molecular and metabolic insights', *Water Res.*, vol. 168, p. 115199, 2020, doi: 10.1016/j.watres.2019.115199.
- [68] V. S. García Rea *et al.*, 'Syntrophic acetate oxidation having a key role in thermophilic phenol conversion in anaerobic membrane bioreactor under saline conditions', *Chem. Eng. J.*, vol. 455, no. August 2022, 2023, doi: 10.1016/j.cej.2022.140305.
- [69] N. S. Battersby and V. Wilson, 'Survey of the anaerobic biodegradation potential of organic chemicals in digesting sludge', *Appl. Environ. Microbiol.*, vol. 55, no. 2, pp. 433–439, 1989, doi: 10.1128/aem.55.2.433-439.1989.
- [70] Y. Li, G. Gu, J. Zhao, and H. Yu, 'Anoxic degradation of nitrogenous heterocyclic compounds by acclimated activated sludge', *Process Biochem.*, vol. 37, no. 1, pp. 81–86, 2001, doi: 10.1016/S0032-9592(01)00176-5.
- [71] L. Yang *et al.*, 'Improve the biodegradability of post-hydrothermal liquefaction wastewater with ozone: Conversion of phenols and N-heterocyclic compounds', *Water Sci. Technol.*, vol. 2017, no. 1, pp. 248–255, 2018, doi: 10.2166/wst.2018.108.
- [72] S. Seyedi, K. Venkiteshwaran, and D. Zitomer, 'Current status of biomethane production using aqueous liquid from pyrolysis and hydrothermal liquefaction of sewage sludge and similar biomass', *Rev. Environ. Sci. Biotechnol.*, vol. 20, no. 1, pp. 237–255, 2021, doi: 10.1007/s11157-020-09560-y.
- [73] H. Zhou, R. C. Brown, and Z. Wen, 'Anaerobic digestion of aqueous phase from pyrolysis of biomass: Reducing toxicity and improving microbial tolerance', *Bioresour. Technol.*, vol. 292, no. August, p. 121976, 2019, doi: 10.1016/j.biortech.2019.121976.
- [74] R. Li *et al.*, 'Enhanced anaerobic digestion of post-hydrothermal liquefaction wastewater: Bio-methane production, carbon distribution and microbial metabolism', *Sci. Total Environ.*, vol. 837, no. May, p. 155659, 2022, doi: 10.1016/j.scitotenv.2022.155659.
- [75] R. Li *et al.*, 'Improved methane production and energy recovery of post-hydrothermal liquefaction waste water via integration of zeolite adsorption and anaerobic digestion', *Sci. Total Environ.*, vol. 651, pp. 61–69, 2019, doi: 10.1016/j.scitotenv.2018.09.175.
- [76] B. Si *et al.*, 'Inhibitors degradation and microbial response during continuous anaerobic conversion of hydrothermal liquefaction wastewater', *Sci. Total Environ.*, vol. 630, pp. 1124–1132, 2018, doi: 10.1016/j.scitotenv.2018.02.310.
- [77] G. Tommaso, W. T. Chen, P. Li, L. Schideman, and Y. Zhang, 'Chemical characterization and anaerobic biodegradability of hydrothermal liquefaction

- aqueous products from mixed-culture wastewater algae', *Bioresour. Technol.*, vol. 178, pp. 139–146, 2014, doi: 10.1016/j.biortech.2014.10.011.
- [78] M. Pham, L. Schideman, J. Scott, N. Rajagopalan, and M. J. Plewa, 'Chemical and biological characterization of wastewater generated from hydrothermal liquefaction of Spirulina', *Environ. Sci. Technol.*, vol. 47, no. 4, pp. 2131–2138, 2013, doi: 10.1021/es304532c.
- [79] G. M. Zhou and H. H. P. Fang, 'Co-degradation of phenol and m-cresol in a UASB reactor', *Bioresour. Technol.*, vol. 61, no. 1, pp. 47–52, 1997, doi: 10.1016/S0960-8524(97)84698-6.
- [80] Y. Chen, J. He, Y. Q. Wang, T. A. Kotsopoulos, P. Kaparaju, and R. J. Zeng, 'Development of an anaerobic co-metabolic model for degradation of phenol, m-cresol and easily degradable substrate', *Biochem. Eng. J.*, vol. 106, pp. 19–25, 2016, doi: 10.1016/j.bej.2015.11.003.
- [81] J. Q. Sun, L. Xu, Y. Q. Tang, F. M. Chen, W. Q. Liu, and X. L. Wu, 'Degradation of pyridine by one Rhodococcus strain in the presence of chromium (VI) or phenol', *J. Hazard. Mater.*, vol. 191, no. 1–3, pp. 62–68, 2011, doi: 10.1016/j.jhazmat.2011.04.034.
- [82] K. T. Hajji, F. Lépine, J. G. Bisailon, and R. Beaudet, 'Simultaneous removal of phenol, ortho- and para-cresol by mixed anaerobic consortia', *Can. J. Microbiol.*, vol. 45, no. 4, pp. 318–325, 1999, doi: 10.1139/cjm-45-4-318.
- [83] O. Franchi, F. Rosenkranz, and R. Chamy, 'Key microbial populations involved in anaerobic degradation of phenol and p-cresol using different inocula', *Electron. J. Biotechnol.*, vol. 35, pp. 33–38, 2018, doi: 10.1016/j.ejbt.2018.08.002.
- [84] T. Hübner and J. Mumme, 'Integration of pyrolysis and anaerobic digestion - Use of aqueous liquor from digestate pyrolysis for biogas production', *Bioresour. Technol.*, vol. 183, pp. 86–92, 2015, doi: 10.1016/j.biortech.2015.02.037.
- [85] S. Fernandez, K. Srinivas, A. J. Schmidt, M. S. Swita, and B. K. Ahring, 'Anaerobic digestion of organic fraction from hydrothermal liquefied algae wastewater byproduct', *Bioresour. Technol.*, vol. 247, no. August 2017, pp. 250–258, 2018, doi: 10.1016/j.biortech.2017.09.030.
- [86] J. Shi, Y. Han, C. Xu, and H. Han, 'Anaerobic bioaugmentation hydrolysis of selected nitrogen heterocyclic compound in coal gasification wastewater', *Bioresour. Technol.*, vol. 278, no. December 2018, pp. 223–230, 2019, doi: 10.1016/j.biortech.2018.12.113.
- [87] J. P. Kaiser, Y. Feng, and J. M. Bollag, 'Microbial metabolism of pyridine, quinoline, acridine, and their derivatives under aerobic and anaerobic conditions', *Microbiol. Rev.*, vol. 60, no. 3, pp. 483–498, 1996, doi: 10.1128/mmbr.60.3.483-498.1996.
- [88] S. Li, X. Zhou, X. Cao, and J. Chen, 'Insights into simultaneous anammox and denitrification system with short-term pyridine exposure: Process capability, inhibition kinetics and metabolic pathways', *Front. Environ. Sci. Eng.*, vol. 15, no. 6, pp. 1–14, 2021, doi: 10.1007/s11783-021-1433-3.
- [89] B. Wirth and J. Mumme, 'Anaerobic Digestion of Waste Water from Hydrothermal Carbonization of Corn Silage', *Appl. Bioenergy*, vol. 1, no. 1, pp.

- 1–10, 2013, doi: 10.2478/apbi-2013-0001.
- [90] K. Zhu, Q. Liu, C. Dang, A. Li, and L. Zhang, ‘Valorization of hydrothermal carbonization products by anaerobic digestion: Inhibitor identification, biomethanization potential and process intensification’, *Bioresour. Technol.*, vol. 341, no. August, p. 125752, 2021, doi: 10.1016/j.biortech.2021.125752.
- [91] S. R. Shanmugam, S. Adhikari, Z. Wang, and R. Shakya, ‘Treatment of aqueous phase of bio-oil by granular activated carbon and evaluation of biogas production’, *Bioresour. Technol.*, vol. 223, pp. 115–120, 2017, doi: 10.1016/j.biortech.2016.10.008.
- [92] D. Fabbri and C. Torri, ‘Linking pyrolysis and anaerobic digestion (Py-AD) for the conversion of lignocellulosic biomass’, *Curr. Opin. Biotechnol.*, vol. 38, no. March, pp. 167–173, 2016, doi: 10.1016/j.copbio.2016.02.004.
- [93] R. Moita and P. C. Lemos, ‘Biopolymers production from mixed cultures and pyrolysis by-products’, *J. Biotechnol.*, vol. 157, no. 4, pp. 578–583, 2012, doi: 10.1016/j.jbiotec.2011.09.021.
- [94] S. Seyedi, K. Venkiteshwaran, N. Benn, and D. Zitomer, ‘Inhibition during anaerobic co-digestion of aqueous pyrolysis liquid from wastewater solids and synthetic primary sludge’, *Sustain.*, vol. 12, no. 8, pp. 8–11, 2020, doi: 10.3390/SU12083441.
- [95] H. Ma, Y. Hu, J. Wu, T. Kobayashi, K.-Q. Xu, and H. Kuramochi, ‘Enhanced anaerobic digestion of tar solution from rice husk thermal gasification with hybrid upflow anaerobic sludge-biochar bed reactor’, *Bioresour. Technol.*, vol. 347, no. January, p. 126688, 2022, doi: 10.1016/j.biortech.2022.126688.
- [96] C. Wen, C. M. Moreira, L. Rehmann, and F. Berruti, ‘Feasibility of anaerobic digestion as a treatment for the aqueous pyrolysis condensate (APC) of birch bark’, *Bioresour. Technol.*, vol. 307, no. December 2019, p. 123199, 2020, doi: 10.1016/j.biortech.2020.123199.
- [97] C. Torri and D. Fabbri, ‘Biochar enables anaerobic digestion of aqueous phase from intermediate pyrolysis of biomass’, *Bioresour. Technol.*, vol. 172, pp. 335–341, 2014, doi: 10.1016/j.biortech.2014.09.021.
- [98] B. Egerland *et al.*, ‘Bioresource Technology Anaerobic digestion of aqueous phase from hydrothermal liquefaction of *Spirulina* using biostimulated sludge’, *Bioresour. Technol.*, vol. 312, no. May, p. 123552, 2020, doi: 10.1016/j.biortech.2020.123552.
- [99] B. Si *et al.*, ‘Anaerobic conversion of the hydrothermal liquefaction aqueous phase: fate of organics and intensification with granule activated carbon/ozone pretreatment’, *Green Chem.*, no. 19, pp. 1305–1318, 2019, doi: 10.1039/c8gc02907e.
- [100] Y. Küçükağa *et al.*, ‘Conversion of Pyrolysis Products into Volatile Fatty Acids with a Biochar-Packed Anaerobic Bioreactor’, *Ind. Eng. Chem. Res.*, vol. 61, no. 45, pp. 16624–16634, 2022, doi: 10.1021/acs.iecr.2c02810.
- [101] J. De Vrieze *et al.*, ‘Ammonia and temperature determine potential clustering in the anaerobic digestion microbiome’, *Water Res.*, vol. 75, no. 0, pp. 312–323, 2015, doi: 10.1016/j.watres.2015.02.025.
- [102] H. Chen, C. Zhang, Y. Rao, Y. Jing, G. Luo, and S. Zhang, ‘Biotechnology for Biofuels Methane potentials of wastewater generated from hydrothermal

- liquefaction of rice straw: focusing on the wastewater characteristics and microbial community compositions’, *Biotechnol. Biofuels*, pp. 1–16, 2017, doi: 10.1186/s13068-017-0830-0.
- [103] B. Omokoko, U. K. Jüntges, M. Zimmermann, M. Reiss, and W. Hartmeier, ‘Isolation of the phe-operon from *G. stearothermophilus* comprising the phenol degradative meta-pathway genes and a novel transcriptional regulator’, *BMC Microbiol.*, vol. 8, pp. 1–10, 2008, doi: 10.1186/1471-2180-8-197.
- [104] Y. L. Qiu, S. Hanada, A. Ohashi, H. Harada, Y. Kamagata, and Y. Sekiguchi, ‘Syntrophorhabdus aromaticivorans gen. nov., sp. nov., the first cultured anaerobe capable of degrading phenol to acetate in obligate syntrophic associations with a hydrogenotrophic methanogen’, *Appl. Environ. Microbiol.*, vol. 74, no. 7, pp. 2051–2058, 2008, doi: 10.1128/AEM.02378-07.
- [105] V. S. Garcia Rea, B. Egerland Bueno, D. Cerqueda-García, J. D. Muñoz Sierra, H. Spanjers, and J. B. van Lier, ‘Degradation of p-cresol, resorcinol, and phenol in anaerobic membrane bioreactors under saline conditions’, *Chem. Eng. J.*, vol. 430, 2022, doi: 10.1016/j.cej.2021.132672.
- [106] J. Watson, T. Wang, B. Si, W. T. Chen, A. Aierzhati, and Y. Zhang, ‘Valorization of hydrothermal liquefaction aqueous phase: pathways towards commercial viability’, *Prog. Energy Combust. Sci.*, vol. 77, p. 100819, 2020, doi: 10.1016/j.pecs.2019.100819.
- [107] H. Khalid *et al.*, ‘Syngas conversion to biofuels and biochemicals: a review of process engineering and mechanisms’, *Sustain. Energy Fuels*, vol. 8, no. 1, pp. 9–28, 2023, doi: 10.1039/d3se00916e.
- [108] L. Perret, B. Lacerda de Oliveira Campos, K. Herrera Delgado, T. A. Zevaco, A. Neumann, and J. Sauer, ‘CO_x Fixation to Elementary Building Blocks: Anaerobic Syngas Fermentation vs. Chemical Catalysis’, *Chemie-Ingenieur-Technik*, vol. 94, no. 11, pp. 1667–1687, 2022, doi: 10.1002/cite.202200153.
- [109] S. W. Ragsdale, ‘Enzymology of the Wood-Ljungdahl pathway of acetogenesis’, *Ann. N. Y. Acad. Sci.*, vol. 1125, pp. 129–136, 2008, doi: 10.1196/annals.1419.015.
- [110] A. M. Henstra, J. Sipma, A. Rinzema, and A. J. M. Stams, ‘Microbiology of synthesis gas fermentation for biofuel production’, *Curr. Opin. Biotechnol.*, vol. 18, no. 3, pp. 200–206, 2007, doi: 10.1016/j.copbio.2007.03.008.
- [111] G. Borrel, P. S. Adam, and S. Gribaldo, ‘Methanogenesis and the wood–ljungdahl pathway: An ancient, versatile, and fragile association’, *Genome Biol. Evol.*, vol. 8, no. 6, pp. 1706–1711, 2016, doi: 10.1093/gbe/evw114.
- [112] H. Lee, J. Bae, S. Jin, S. Kang, and B. K. Cho, ‘Engineering Acetogenic Bacteria for Efficient One-Carbon Utilization’, *Front. Microbiol.*, vol. 13, no. May, 2022, doi: 10.3389/fmicb.2022.865168.
- [113] H. Richter, B. Molitor, M. Diender, and D. Z. Sousa, ‘A Narrow pH Range Supports Butanol, Hexanol, and Octanol Production from Syngas in a Continuous Co-culture of *Clostridium ljungdahlii* and *Clostridium kluyveri* with In-Line Product Extraction’, vol. 7, no. November, 2016, doi: 10.3389/fmicb.2016.01773.
- [114] F. C. F. Baleeiro, S. Kleisteuber, A. Neumann, and S. Heike, ‘Syngas-aided

- anaerobic fermentation for medium-chain carboxylate and alcohol production: the case for microbial communities', *Appl. Microbiol. Biotechnol.*, 2019, doi: 10.1007/s00253-019-10086-9.
- [115] S. Dyksma, L. Jansen, and C. Gallert, 'Syntrophic acetate oxidation replaces acetoclastic methanogenesis during thermophilic digestion of biowaste', *Microbiome*, vol. 8, no. 1, pp. 1–14, 2020, doi: 10.1186/s40168-020-00862-5.
- [116] S. S. Navarro, R. Cimpoaia, G. Bruant, and S. R. Guiot, 'Biomethanation of syngas using anaerobic sludge: Shift in the catabolic routes with the CO partial pressure increase', *Front. Microbiol.*, vol. 7, no. AUG, pp. 1–13, 2016, doi: 10.3389/fmicb.2016.01188.
- [117] J. I. Alves *et al.*, 'Enrichment of anaerobic syngas-converting bacteria from thermophilic bioreactor sludge', *FEMS Microbiol. Ecol.*, vol. 86, no. 3, pp. 590–597, 2013, doi: 10.1111/1574-6941.12185.
- [118] C. Liu, G. Luo, W. Wang, Y. He, R. Zhang, and G. Liu, 'The effects of pH and temperature on the acetate production and microbial community compositions by syngas fermentation', *Fuel*, vol. 224, no. March, pp. 537–544, 2018, doi: 10.1016/j.fuel.2018.03.125.
- [119] L. T. Angenent *et al.*, 'Chain Elongation with Reactor Microbiomes: Open-Culture Biotechnology to Produce Biochemicals', *Environ. Sci. Technol.*, vol. 50, no. 6, pp. 2796–2810, 2016, doi: 10.1021/acs.est.5b04847.
- [120] L. Li, X. Peng, X. Wang, and D. Wu, 'Anaerobic digestion of food waste: A review focusing on process stability', *Bioresour. Technol.*, vol. 248, no. 174, pp. 20–28, 2018, doi: 10.1016/j.biortech.2017.07.012.
- [121] R. Kleerebezem and M. C. van Loosdrecht, 'Mixed culture biotechnology for bioenergy production', *Curr. Opin. Biotechnol.*, vol. 18, no. 3, pp. 207–212, 2007, doi: 10.1016/j.copbio.2007.05.001.
- [122] B. Schink, 'Energetics of Syntrophic Cooperation in Methanogenic Degradation', vol. 61, no. 2, pp. 262–280, 1997.
- [123] J. H. Thiele and J. G. Zeikus, 'Control of Interspecies Electron Flow during Anaerobic Digestion: Significance of Formate Transfer versus Hydrogen Transfer during Syntrophic Methanogenesis in Flocs', vol. 54, no. 1, pp. 20–29, 1988.
- [124] A. Kouzuma, S. Kato, and K. Watanabe, 'Microbial interspecies interactions: Recent findings in syntrophic consortia', *Front. Microbiol.*, vol. 6, no. MAY, pp. 1–8, 2015, doi: 10.3389/fmicb.2015.00477.
- [125] F. C. F. Baleeiro, S. Kleinsteuber, and H. Sträuber, 'Hydrogen as a Co-electron Donor for Chain Elongation With Complex Communities', *Front. Bioeng. Biotechnol.*, vol. 9, no. March, pp. 1–15, 2021, doi: 10.3389/fbioe.2021.650631.
- [126] X. Pan *et al.*, 'Deep insights into the network of acetate metabolism in anaerobic digestion: focusing on syntrophic acetate oxidation and homoacetogenesis', *Water Res.*, vol. 190, p. 116774, 2021, doi: 10.1016/j.watres.2020.116774.
- [127] A. Grimalt-Alemany, M. Łężyk, D. M. Kennes-Veiga, I. V. Skiadas, and H. N. Gavala, 'Enrichment of Mesophilic and Thermophilic Mixed Microbial Consortia for Syngas Biomethanation: The Role of Kinetic and

- Thermodynamic Competition', *Waste and Biomass Valorization*, vol. 11, no. 2, pp. 465–481, 2020, doi: 10.1007/s12649-019-00595-z.
- [128] R. Conrad and B. Wetter, 'Influence of temperature on energetics of hydrogen metabolism in homoacetogenic, methanogenic, and other anaerobic bacteria', *Arch. Microbiol.*, vol. 155, no. 1, pp. 94–98, 1990, doi: 10.1007/BF00291281.
- [129] S. E. Hosseini and M. A. Wahid, 'Hydrogen production from renewable and sustainable energy resources: Promising green energy carrier for clean development', *Renew. Sustain. Energy Rev.*, vol. 57, pp. 850–866, 2016, doi: 10.1016/j.rser.2015.12.112.
- [130] V. De Groof, M. Coma, T. Arnot, D. J. Leak, and A. B. Lanham, 'Medium chain carboxylic acids from complex organic feedstocks by mixed culture fermentation', *Molecules*, vol. 24, no. 3, pp. 1–32, 2019, doi: 10.3390/molecules24030398.
- [131] F. C. F. Baleeiro, L. Varchmin, S. Kleinsteuber, H. Sträuber, and A. Neumann, 'Formate-induced CO tolerance and methanogenesis inhibition in fermentation of syngas and plant biomass for carboxylate production', *Biotechnol. Biofuels Bioprod.*, vol. 16, no. 1, pp. 1–16, 2023, doi: 10.1186/s13068-023-02271-w.
- [132] C. Liu *et al.*, 'CO as electron donor for efficient medium chain carboxylate production by chain elongation: Microbial and thermodynamic insights', *Chem. Eng. J.*, vol. 390, no. December 2019, p. 124577, 2020, doi: 10.1016/j.cej.2020.124577.
- [133] F. Zhang *et al.*, 'Fatty acids production from hydrogen and carbon dioxide by mixed culture in the membrane biofilm reactor', *Water Res.*, vol. 47, no. 16, pp. 6122–6129, 2013, doi: 10.1016/j.watres.2013.07.033.
- [134] F. C. F. Baleeiro, S. Kleinsteuber, and H. Sträuber, 'Recirculation of H₂, CO₂, and Ethylene Improves Carbon Fixation and Carboxylate Yields in Anaerobic Fermentation', *ACS Sustain. Chem. Eng.*, 2022, doi: 10.1021/acssuschemeng.1c05133.
- [135] H. Liu, J. Wang, A. Wang, and J. Chen, 'Chemical inhibitors of methanogenesis and putative applications', *Appl. Microbiol. Biotechnol.*, vol. 89, no. 5, pp. 1333–1340, 2011, doi: 10.1007/s00253-010-3066-5.
- [136] W. Logroño, M. Nikolausz, H. Harms, and S. Kleinsteuber, 'Physiological Effects of 2-Bromoethanesulfonate on Hydrogenotrophic Pure and Mixed Cultures', *Microorganisms*, vol. 10, no. 2, pp. 1–15, 2022, doi: 10.3390/microorganisms10020355.
- [137] W. de A. Cavalcante, R. C. Leitão, T. A. Gehring, L. T. Angenent, and S. T. Santaella, 'Anaerobic fermentation for n-caproic acid production: A review', *Process Biochem.*, vol. 54, pp. 106–119, 2017, doi: 10.1016/j.procbio.2016.12.024.
- [138] S. Esquivel-Elizondo, J. Miceli, C. I. Torres, and R. Krajmalnik-Brown, 'Impact of carbon monoxide partial pressures on methanogenesis and medium chain fatty acids production during ethanol fermentation', *Biotechnol. Bioeng.*, vol. 115, no. 2, pp. 341–350, 2018, doi: 10.1002/bit.26471.
- [139] W. Zhang *et al.*, 'Free acetic acid as the key factor for the inhibition of

- hydrogenotrophic methanogenesis in mesophilic mixed culture fermentation', *Bioresour. Technol.*, vol. 264, no. March, pp. 17–23, 2018, doi: 10.1016/j.biortech.2018.05.049.
- [140] C. M. Spirito, H. Richter, K. Rabaey, A. J. M. M. Stams, and L. T. Angenent, 'Chain elongation in anaerobic reactor microbiomes to recover resources from waste', *Curr. Opin. Biotechnol.*, vol. 27, pp. 115–122, 2014, doi: 10.1016/j.copbio.2014.01.003.
- [141] S. Agnihotri *et al.*, 'A Glimpse of the World of Volatile Fatty Acids Production and Application: A review', *Bioengineered*, vol. 13, no. 1, pp. 1249–1275, 2022, doi: 10.1080/21655979.2021.1996044.
- [142] H. N. Chang, N. J. Kim, J. Kang, and C. M. Jeong, 'Biomass-derived volatile fatty acid platform for fuels and chemicals', *Biotechnol. Bioprocess Eng.*, vol. 15, no. 1, pp. 1–10, 2010, doi: 10.1007/s12257-009-3070-8.
- [143] C. Kantzow, A. Mayer, and D. Weuster-Botz, 'Continuous gas fermentation by *Acetobacterium woodii* in a submerged membrane reactor with full cell retention', *J. Biotechnol.*, vol. 212, pp. 11–18, 2015, doi: 10.1016/j.jbiotec.2015.07.020.
- [144] D. Kiefer, M. Merkel, L. Lilge, M. Henkel, and R. Hausmann, 'From Acetate to Bio-Based Products: Underexploited Potential for Industrial Biotechnology', *Trends Biotechnol.*, vol. 39, no. 4, pp. 397–411, 2021, doi: 10.1016/j.tibtech.2020.09.004.
- [145] A. Mishra, J. N. Ntihuga, B. Molitor, and L. T. Angenent, 'Power-to-Protein: Carbon Fixation with Renewable Electric Power to Feed the World', *Joule*, vol. 4, no. 6, pp. 1142–1147, 2020, doi: 10.1016/j.joule.2020.04.008.
- [146] E. Marcellin, L. T. Angenent, L. K. Nielsen, and B. Molitor, 'Recycling carbon for sustainable protein production using gas fermentation', *Curr. Opin. Biotechnol.*, vol. 76, p. 102723, 2022, doi: 10.1016/j.copbio.2022.102723.
- [147] S. Gildemyn, B. Molitor, J. G. Usack, M. Nguyen, K. Rabaey, and L. T. Angenent, 'Upgrading syngas fermentation effluent using *Clostridium kluyveri* in a continuous fermentation', *Biotechnol. Biofuels*, vol. 10, no. 1, pp. 1–15, 2017, doi: 10.1186/s13068-017-0764-6.
- [148] F. Oswald *et al.*, 'Sequential mixed cultures: From syngas to malic acid', *Front. Microbiol.*, vol. 7, no. JUN, pp. 1–12, 2016, doi: 10.3389/fmicb.2016.00891.
- [149] I. S. Al Rowaihi *et al.*, 'A two-stage biological gas to liquid transfer process to convert carbon dioxide into bioplastic', *Bioresour. Technol. Reports*, vol. 1, pp. 61–68, 2018, doi: 10.1016/j.biteb.2018.02.007.
- [150] B. Lagoa-Costa, H. N. Abubackar, M. Fernández-Romasanta, C. Kennes, and M. C. Veiga, 'Integrated bioconversion of syngas into bioethanol and biopolymers', *Bioresour. Technol.*, vol. 239, pp. 244–249, 2017, doi: 10.1016/j.biortech.2017.05.019.
- [151] G. Strazzera, F. Battista, N. H. Garcia, N. Frison, and D. Bolzonella, 'Volatile fatty acids production from food wastes for biorefinery platforms: A review', *J. Environ. Manage.*, vol. 226, no. August, pp. 278–288, 2018, doi: 10.1016/j.jenvman.2018.08.039.
- [152] I. Kolouchová, O. Schreiberová, K. Sigler, J. Masák, and T. Řezanka, 'Biotransformation of volatile fatty acids by oleaginous and non-oleaginous

- yeast species', *FEMS Yeast Res.*, vol. 15, no. 7, pp. 1–8, 2015, doi: 10.1093/femsyr/fovo76.
- [153] M. Llamas, J. A. Magdalena, C. González-Fernández, and E. Tomás-Pejó, 'Volatile fatty acids as novel building blocks for oil-based chemistry via oleaginous yeast fermentation', *Biotechnol. Bioeng.*, vol. 117, no. 1, pp. 238–250, 2020, doi: 10.1002/bit.27180.
- [154] Z. Gong *et al.*, 'Co-fermentation of acetate and sugars facilitating microbial lipid production on acetate-rich biomass hydrolysates', *Bioresour. Technol.*, vol. 207, pp. 102–108, 2016, doi: 10.1016/j.biortech.2016.01.122.
- [155] A. Chalima, L. Oliver, L. F. De Castro, A. Karnaouri, T. Dietrich, and E. Topakas, 'Utilization of volatile fatty acids from microalgae for the production of high added value compounds', *Fermentation*, vol. 3, no. 4, pp. 1–17, 2017, doi: 10.3390/fermentation3040054.
- [156] A. Kövilein, V. Aschmann, L. Zadavec, and K. Ochsenreither, 'Optimization of l-malic acid production from acetate with *Aspergillus oryzae* DSM 1863 using a pH-coupled feeding strategy', *Microb. Cell Fact.*, vol. 21, no. 1, pp. 1–17, 2022, doi: 10.1186/s12934-022-01961-8.
- [157] P. A. Gibbs, R. J. Seviour, and F. Schmid, 'Growth of filamentous fungi in submerged culture: Problems and possible solutions', *Crit. Rev. Biotechnol.*, vol. 20, no. 1, pp. 17–48, 2000, doi: 10.1080/07388550091144177.
- [158] J. A. Ferreira, A. Mahboubi, P. R. Lennartsson, and M. J. Taherzadeh, 'Waste biorefineries using filamentous ascomycetes fungi: Present status and future prospects', *Bioresour. Technol.*, vol. 215, pp. 334–345, 2016, doi: 10.1016/j.biortech.2016.03.018.
- [159] C. Uwineza, T. Sar, A. Mahboubi, and M. J. Taherzadeh, 'Evaluation of the cultivation of *aspergillus oryzae* on organic waste-derived vfa effluents and its potential application as alternative sustainable nutrient source for animal feed', *Sustain.*, vol. 13, no. 22, 2021, doi: 10.3390/su132212489.
- [160] A. Mahboubi, J. A. Ferreira, M. J. Taherzadeh, and P. R. Lennartsson, 'Value-added products from dairy waste using edible fungi', *Waste Manag.*, vol. 59, pp. 518–525, 2017, doi: 10.1016/j.wasman.2016.11.017.
- [161] A. Kövilein, J. Umpfenbach, and K. Ochsenreither, 'Acetate as substrate for l-malic acid production with *Aspergillus oryzae* DSM 1863', *Biotechnol. Biofuels*, vol. 14, no. 1, pp. 1–15, 2021, doi: 10.1186/s13068-021-01901-5.
- [162] A. Kövilein, C. Kubisch, L. Cai, and K. Ochsenreither, 'Malic acid production from renewables: a review', *J. Chem. Technol. Biotechnol.*, vol. 95, no. 3, pp. 513–526, 2020, doi: 10.1002/jctb.6269.
- [163] T. Werpy and G. Petersen, 'Top Value Added Chemicals from Biomass Volume I-Results of Screening for Potential Candidates from Sugars and Synthesis Gas', *Energy Effic. Renew. Energy*, 2004, doi: 10.2172/15008859.
- [164] Y. Jiang *et al.*, 'Microbial production of L-malate from renewable non-food feedstocks', *Chinese J. Chem. Eng.*, vol. 30, pp. 105–111, 2021, doi: 10.1016/j.cjche.2020.10.017.
- [165] C. Uwineza *et al.*, 'Cultivation of edible filamentous fungus *Aspergillus oryzae* on volatile fatty acids derived from anaerobic digestion of food waste and cow manure', *Bioresour. Technol.*, vol. 337, no. May, p. 125410, 2021, doi:

- 10.1016/j.biortech.2021.125410.
- [166] S. Dörsam, J. Kirchhoff, M. Bigalke, N. Dahmen, C. Syldatk, and K. Ochsenreither, 'Evaluation of pyrolysis oil as carbon source for fungal fermentation', *Front. Microbiol.*, vol. 7, no. DEC, pp. 1–11, 2016, doi: 10.3389/fmicb.2016.02059.
- [167] C. Kubisch and K. Ochsenreither, 'Valorization of a Pyrolytic Aqueous Condensate and Its Main Components for L-Malic Acid Production with *Aspergillus oryzae* DSM 1863', *Fermentation*, vol. 8, no. 3, 2022, doi: 10.3390/fermentation8030107.
- [168] M. Bachmann, S. Völker, J. Kleinekorte, and A. Bardow, 'Syngas from What? Comparative Life-Cycle Assessment for Syngas Production from Biomass, CO₂, and Steel Mill Off-Gases', *ACS Sustain. Chem. Eng.*, vol. 11, no. 14, pp. 5356–5366, 2023, doi: 10.1021/acssuschemeng.2c05390.
- [169] M. Arens, E. Worrell, W. Eichhammer, A. Hasanbeigi, and Q. Zhang, 'Pathways to a low-carbon iron and steel industry in the medium-term – the case of Germany', *J. Clean. Prod.*, vol. 163, pp. 84–98, 2017, doi: 10.1016/j.jclepro.2015.12.097.
- [170] A. Gil, 'Current insights into lignocellulose related waste valorization', *Chem. Eng. J. Adv.*, vol. 8, p. 100186, 2021, doi: 10.1016/j.ceja.2021.100186.
- [171] N. Ghimire, R. Bakke, and W. H. Bergland, 'Liquefaction of lignocellulosic biomass for methane production: A review', *Bioresour. Technol.*, vol. 332, no. April, p. 125068, 2021, doi: 10.1016/j.biortech.2021.125068.
- [172] A. S. Giwa *et al.*, 'Pyrolysis of difficult biodegradable fractions and the real syngas bio-methanation performance', *J. Clean. Prod.*, vol. 233, pp. 711–719, 2019, doi: 10.1016/j.jclepro.2019.06.145.
- [173] C. Torri, G. Pambieri, C. Gualandi, M. Piraccini, A. G. Rombolà, and D. Fabbri, 'Evaluation of the potential performance of hyphenated pyrolysis-anaerobic digestion (Py-AD) process for carbon negative fuels from woody biomass', *Renew. Energy*, vol. 148, pp. 1190–1199, 2020, doi: 10.1016/j.renene.2019.10.025.
- [174] N. Kassem, J. Hockey, C. Lopez, L. Lardon, L. T. Angenent, and J. W. Tester, 'Integrating anaerobic digestion, hydrothermal liquefaction, and biomethanation within a power-to-gas framework for dairy waste management and grid decarbonization: A techno-economic assessment', *Sustain. Energy Fuels*, vol. 4, no. 9, pp. 4644–4661, 2020, doi: 10.1039/d0se00608d.
- [175] L. Gerber, V. Doren, R. Posmanik, F. A. Bicalho, J. W. Tester, and D. L. Sills, 'Prospects for energy recovery during hydrothermal and biological processing of waste biomass', *Bioresour. Technol.*, vol. 225, pp. 67–74, 2017, doi: 10.1016/j.biortech.2016.11.030.
- [176] C. A. Salman, S. Schwede, E. Thorin, and J. Yan, 'Enhancing biomethane production by integrating pyrolysis and anaerobic digestion processes', *Appl. Energy*, vol. 204, pp. 1074–1083, 2017, doi: 10.1016/j.apenergy.2017.05.006.
- [177] S. Righi, V. Bandini, D. Marazza, F. Baioli, C. Torri, and A. Contin, 'Life Cycle Assessment of high ligno-cellulosic biomass pyrolysis coupled with anaerobic digestion', *Bioresour. Technol.*, vol. 212, no. April, pp. 245–253, 2016, doi:

- 10.1016/j.biortech.2016.04.052.
- [178] A. Funke, J. Mumme, M. Koon, and M. Diakité, ‘Cascaded production of biogas and hydrochar from wheat straw: Energetic potential and recovery of carbon and plant nutrients’, *Biomass and Bioenergy*, vol. 58, pp. 229–237, 2013, doi: 10.1016/j.biombioe.2013.08.018.
- [179] C. A. Salman, S. Schwede, E. Thorin, and J. Yan, ‘Predictive Modelling and Simulation of Integrated Pyrolysis and Anaerobic Digestion Process’, *Energy Procedia*, vol. 105, pp. 850–857, 2017, doi: 10.1016/j.egypro.2017.03.400.
- [180] N. Antoniou, F. Monlau, C. Sambusiti, E. Ficara, A. Barakat, and A. Zabaniotou, ‘Contribution to Circular Economy options of mixed agricultural wastes management: Coupling anaerobic digestion with gasification for enhanced energy and material recovery’, *J. Clean. Prod.*, vol. 209, pp. 505–514, 2019, doi: 10.1016/j.jclepro.2018.10.055.
- [181] A. S. Giwa *et al.*, ‘Pyrolysis coupled anaerobic digestion process for food waste and recalcitrant residues: Fundamentals, challenges, and considerations’, *Energy Sci. Eng.*, vol. 7, no. 6, pp. 2250–2264, 2019, doi: 10.1002/ese3.503.
- [182] Y. G. Lee, Y. Ju, L. Sun, S. Park, Y. S. Jin, and S. R. Kim, ‘Acetate-rich Cellulosic Hydrolysates and Their Bioconversion Using Yeasts’, *Biotechnol. Bioprocess Eng.*, vol. 27, no. 6, pp. 890–899, 2022, doi: 10.1007/s12257-022-0217-3.
- [183] K. Zhang, Z. Pei, and D. Wang, ‘Organic solvent pretreatment of lignocellulosic biomass for biofuels and biochemicals: A review’, *Bioresour. Technol.*, vol. 199, pp. 21–33, 2016, doi: 10.1016/j.biortech.2015.08.102.
- [184] A. F. Ferreira and C. A. M. Silva, *Biorefineries*. 2017.
- [185] R. R. Gonzales, P. Sivagurunathan, A. Parthiban, and S. H. Kim, ‘Optimization of substrate concentration of dilute acid hydrolyzate of lignocellulosic biomass in batch hydrogen production’, *Int. Biodeterior. Biodegrad.*, vol. 113, pp. 22–27, 2016, doi: 10.1016/j.ibiod.2016.04.016.
- [186] Z. Ruan, W. Hollinshead, C. Isaguirre, Y. J. Tang, W. Liao, and Y. Liu, ‘Effects of inhibitory compounds in lignocellulosic hydrolysates on *Mortierella isabellina* growth and carbon utilization’, *Bioresour. Technol.*, vol. 183, pp. 18–24, 2015, doi: 10.1016/j.biortech.2015.02.026.
- [187] E. Palmqvist and B. Hahn-Hägerdal, ‘Fermentation of lignocellulosic hydrolysates. I: Inhibition and detoxification’, *Bioresour. Technol.*, vol. 74, no. 1, pp. 17–24, 2000, doi: 10.1016/S0960-8524(99)00160-1.
- [188] P. T. Pienkos and M. Zhang, ‘Role of pretreatment and conditioning processes on toxicity of lignocellulosic biomass hydrolysates’, *Cellulose*, vol. 16, no. 4, pp. 743–762, 2009, doi: 10.1007/s10570-009-9309-x.
- [189] A. K. Chandel, S. S. da Silva, and O. V. Singh, ‘Detoxification of Lignocellulose Hydrolysates: Biochemical and Metabolic Engineering Toward White Biotechnology’, *Bioenergy Res.*, vol. 6, no. 1, pp. 388–401, 2013, doi: 10.1007/s12155-012-9241-z.
- [190] R. Lin, J. Cheng, L. Ding, W. Song, J. Zhou, and K. Cen, ‘Inhibitory effects of furan derivatives and phenolic compounds on dark hydrogen fermentation’, *Bioresour. Technol.*, vol. 196, pp. 250–255, 2015, doi: 10.1016/j.biortech.2015.07.097.

- [191] Q. Feng and Y. Lin, 'Integrated processes of anaerobic digestion and pyrolysis for higher bioenergy recovery from lignocellulosic biomass: A brief review', *Renew. Sustain. Energy Rev.*, vol. 77, no. May 2016, pp. 1272–1287, 2017, doi: 10.1016/j.rser.2017.03.022.
- [192] B. E. L. Baêta, D. R. S. Lima, J. G. B. Filho, O. F. H. Adarme, L. V. A. Gurgel, and S. F. de Aquino, 'Evaluation of hydrogen and methane production from sugarcane bagasse hemicellulose hydrolysates by two-stage anaerobic digestion process', *Bioresour. Technol.*, vol. 218, pp. 436–446, 2016, doi: 10.1016/j.biortech.2016.06.113.
- [193] D. J. Batstone and B. Viridis, 'The role of anaerobic digestion in the emerging energy economy', *Curr. Opin. Biotechnol.*, vol. 27, pp. 142–149, 2014, doi: 10.1016/j.copbio.2014.01.013.
- [194] Z. Zhang *et al.*, 'CO Biomethanation with Different Anaerobic Granular Sludges', *Waste and Biomass Valorization*, vol. 12, no. 7, pp. 3913–3925, 2021, doi: 10.1007/s12649-020-01285-x.
- [195] P. Postacchini, L. Menin, S. Piazzini, A. Grimalt-Alemany, F. Patuzzi, and M. Baratieri, 'Syngas biomethanation by co-digestion with brewery spent yeast in a lab-scale reactor', *Biochem. Eng. J.*, vol. 193, no. January, p. 108863, 2023, doi: 10.1016/j.bej.2023.108863.
- [196] G. Luo, W. Wang, and I. Angelidaki, 'Anaerobic digestion for simultaneous sewage sludge treatment and CO biomethanation: Process performance and microbial ecology', *Environ. Sci. Technol.*, vol. 47, no. 18, pp. 10685–10693, 2013, doi: 10.1021/es401018d.
- [197] D. Arslan, K. J. J. Steinbusch, L. Diels, H. De Wever, C. J. N. Buisman, and H. V. M. Hamelers, 'Effect of hydrogen and carbon dioxide on carboxylic acids patterns in mixed culture fermentation', *Bioresour. Technol.*, vol. 118, pp. 227–234, 2012, doi: 10.1016/j.biortech.2012.05.003.
- [198] D. González-Tenorio, K. M. Muñoz-Páez, G. Buitrón, and I. Valdez-Vazquez, 'Fermentation of organic wastes and CO₂+ H₂ off-gas by microbiotas provides short-chain fatty acids and ethanol for n-caproate production', *J. CO₂ Util.*, vol. 42, no. August, 2020, doi: 10.1016/j.jcou.2020.101314.
- [199] F. C. F. Baleeiro, J. Raab, S. Kleinstaub, A. Neumann, and H. Sträuber, 'Mixotrophic chain elongation with syngas and lactate as electron donors', *Microb. Biotechnol.*, vol. 16, no. 2, pp. 322–336, 2023, doi: 10.1111/1751-7915.14163.
- [200] W. Fuchs, L. Rachbauer, S. K. M. R. Rittmann, G. Bochmann, D. Ribitsch, and F. Steger, 'Eight Up-Coming Biotech Tools to Combat Climate Crisis', *Microorganisms*, vol. 11, no. 6, pp. 1–25, 2023, doi: 10.3390/microorganisms11061514.
- [201] W. A. Telliard, 'Method 1684 Total, Fixed, and Volatile Solids in Water, Solids, and Biosolids Draft January 2001 U.S. Environmental Protection Agency Office of Water Office of Science and Technology Engineering and Analysis Division (4303) U.S. EPA', no. January, pp. 1–13, 2001.
- [202] H. S. Harned and R. W. Ehlers, 'The Dissociation Constant of Acetic Acid from 0 to 60° Centigrade', *Am. Chem. Soc.*, vol. 55, no. 1, pp. 652–656, 1932, doi: <https://doi.org/10.1021/ja01329a027>.

- [203] A. Grimalt-Alemany, K. Asimakopoulos, I. V. Skiadas, and H. N. Gavala, 'Modeling of syngas biomethanation and catabolic route control in mesophilic and thermophilic mixed microbial consortia', *Appl. Energy*, vol. 262, no. December 2019, p. 114502, 2020, doi: 10.1016/j.apenergy.2020.114502.
- [204] M. Diender, A. J. M. Stams, D. Z. Sousa, F. T. Robb, and S. R. Guiot, 'Pathways and Bioenergetics of Anaerobic Carbon Monoxide Fermentation', vol. 6, no. November, pp. 1–18, 2015, doi: 10.3389/fmicb.2015.01275.
- [205] M. C. Schoelmerich and V. Müller, 'Energy - converting hydrogenases : the link between - H₂ metabolism and energy conservation', *Cell. Mol. Life Sci.*, vol. 77, no. 8, pp. 1461–1481, 2020, doi: 10.1007/s00018-019-03329-5.
- [206] M. El-Gammal *et al.*, 'High efficient ethanol and VFA production from gas fermentation: Effect of acetate, gas and inoculum microbial composition', *Biomass and Bioenergy*, vol. 105, pp. 32–40, 2017, doi: 10.1016/j.biombioe.2017.06.020.
- [207] S. Hattori, H. Luo, H. Shoun, and Y. Kamagata, 'Involvement of formate as an interspecies electron carrier in a syntrophic acetate-oxidizing anaerobic microorganism in coculture with methanogens', *J. Biosci. Bioeng.*, vol. 91, no. 3, pp. 294–298, 2001, doi: 10.1016/S1389-1723(01)80137-7.
- [208] A. Schnürer, B. H. Svensson, and B. Schink, 'Enzyme activities in and energetics of acetate metabolism by the mesophilic syntrophically acetate-oxidizing anaerobe', *FEMS Microbiol. Lett.*, vol. 154, no. 2, pp. 331–336, 1997, doi: 10.1016/S0378-1097(97)00350-9.
- [209] M. Westerholm, J. Dolfing, and A. Schnürer, 'Growth Characteristics and Thermodynamics of Syntrophic Acetate Oxidizers', *Environ. Sci. Technol.*, vol. 53, no. 9, pp. 5512–5520, 2019, doi: 10.1021/acs.est.9b00288.
- [210] C. M. Plugge, M. Balk, E. G. Zoetendal, and A. J. M. Stams, 'Gelria glutamica gen. nov., sp. nov., a thermophilic, obligately syntrophic, glutamate-degrading anaerobe', *Int. J. Syst. Evol. Microbiol.*, vol. 52, no. 2, pp. 401–407, 2002, doi: 10.1099/00207713-52-2-401.
- [211] D. Zheng *et al.*, 'Identification of novel potential acetate-oxidizing bacteria in thermophilic methanogenic chemostats by DNA stable isotope probing', *Appl. Microbiol. Biotechnol.*, vol. 103, no. 20, pp. 8631–8645, 2019, doi: 10.1007/s00253-019-10078-9.
- [212] F. Liu and R. Conrad, 'Chemolithotrophic acetogenic H₂/CO₂ utilization in Italian rice field soil', *ISME J.*, vol. 5, no. 9, pp. 1526–1539, 2011, doi: 10.1038/ismej.2011.17.
- [213] E. Perman, A. Schnürer, A. Björn, and J. Moestedt, 'Serial anaerobic digestion improves protein degradation and biogas production from mixed food waste', *Biomass and Bioenergy*, vol. 161, no. April, 2022, doi: 10.1016/j.biombioe.2022.106478.
- [214] J. De Vrieze, T. Hennebel, N. Boon, and W. Verstraete, 'Methanosarcina: The rediscovered methanogen for heavy duty biomethanation', *Bioresour. Technol.*, vol. 112, pp. 1–9, 2012, doi: 10.1016/j.biortech.2012.02.079.
- [215] J. J. Moran, C. H. House, J. M. Vrentas, and K. H. Freeman, 'Methyl sulfide production by a novel carbon monoxide metabolism in Methanosarcina acetivorans', *Appl. Environ. Microbiol.*, vol. 74, no. 2, pp. 540–542, 2008,

doi: 10.1128/AEM.01750-07.

- [216] J. M. O'Brien, R. H. Wolkin, T. T. Moench, J. B. Morgan, and J. G. Zeikus, 'Association of hydrogen metabolism with unitrophic or mixotrophic growth of *Methanosarcina barkeri* on carbon monoxide', *J. Bacteriol.*, vol. 158, no. 1, pp. 373–375, 1984, doi: 10.1128/jb.158.1.373-375.1984.
- [217] Y. Wang, Q. B. Zhao, Y. Mu, H. Q. Yu, H. Harada, and Y. Y. Li, 'Biohydrogen production with mixed anaerobic cultures in the presence of high-concentration acetate', *Int. J. Hydrogen Energy*, vol. 33, no. 4, pp. 1164–1171, 2008, doi: 10.1016/j.ijhydene.2007.12.018.
- [218] R. M. Worden, A. J. Grethlein, J. G. Zeikus, and R. Datta, 'Butyrate production from carbon monoxide by *Butyribacterium methylotrophicum*', *Appl. Biochem. Biotechnol.*, vol. 20–21, no. 1, pp. 687–698, 1989, doi: 10.1007/BF02936517.
- [219] J. Jeong *et al.*, 'Energy conservation model based on genomic and experimental analyses of a carbon monoxide-utilizing, butyrate-forming acetogen, *Eubacterium limosum* KIST612', *Appl. Environ. Microbiol.*, vol. 81, no. 14, pp. 4782–4790, 2015, doi: 10.1128/AEM.00675-15.
- [220] P. He, W. Han, L. Shao, and F. Lü, 'One-step production of C6–C8 carboxylates by mixed culture solely grown on CO', *Biotechnol. Biofuels*, vol. 11, no. 1, pp. 1–13, 2018, doi: 10.1186/s13068-017-1005-8.
- [221] J. P. C. Moreira *et al.*, 'Propionate Production from Carbon Monoxide by Synthetic', *Appl. Environ. Microbiol.*, vol. 87, no. 14, pp. e02839-20, 2021, [Online]. Available: <https://doi.org/10.1128/AEM.02839-20>.
- [222] K. Liu, H. K. Atiyeh, B. S. Stevenson, R. S. Tanner, M. R. Wilkins, and R. L. Huhnke, 'Mixed culture syngas fermentation and conversion of carboxylic acids into alcohols', *Bioresour. Technol.*, vol. 152, pp. 337–346, 2014, doi: 10.1016/j.biortech.2013.11.015.
- [223] Y. Liu, F. Lü, L. Shao, and P. He, 'Alcohol-to-acid ratio and substrate concentration affect product structure in chain elongation reactions initiated by unacclimatized inoculum', *Bioresour. Technol.*, vol. 218, pp. 1140–1150, 2016, doi: 10.1016/j.biortech.2016.07.067.
- [224] S. M. De Smit, K. D. De Leeuw, C. J. N. Buisman, and D. P. B. T. B. Strik, 'Continuous n-valerate formation from propionate and methanol in an anaerobic chain elongation open-culture bioreactor', *Biotechnol. Biofuels*, vol. 12, no. 1, pp. 1–16, 2019, doi: 10.1186/s13068-019-1468-x.
- [225] S. Joshi, A. Robles, S. Aguiar, and A. G. Delgado, 'The occurrence and ecology of microbial chain elongation of carboxylates in soils', *ISME J.*, vol. 15, no. 7, pp. 1907–1918, 2021, doi: 10.1038/s41396-021-00893-2.
- [226] K. Asimakopoulos *et al.*, 'Temperature effects on syngas biomethanation performed in a trickle bed reactor', *Chem. Eng. J.*, vol. 393, no. December 2019, 2020, doi: 10.1016/j.cej.2020.124739.
- [227] K. Ueda *et al.*, 'Genome sequence of *Symbiobacterium thermophilum*, an uncultivable bacterium that depends on microbial commensalism', *Nucleic Acids Res.*, vol. 32, no. 16, pp. 4937–4944, 2004, doi: 10.1093/nar/gkh830.
- [228] T. O. Watsuji, T. Kato, K. Ueda, and T. Beppu, 'CO₂ supply induces the growth of *Symbiobacterium thermophilum*, a syntrophic bacterium', *Biosci.*

- Biotechnol. Biochem.*, vol. 70, no. 3, pp. 753–756, 2006, doi: 10.1271/bbb.70.753.
- [229] K. Ueda and T. Beppu, ‘Lessons from studies of *Symbiobacterium thermophilum*, a unique syntrophic bacterium’, *Biosci. Biotechnol. Biochem.*, vol. 71, no. 5, pp. 1115–1121, 2007, doi: 10.1271/bbb.60727.
- [230] H. Shiratori-Takano *et al.*, ‘Description of *Symbiobacterium ostreiconchae* sp. nov., *Symbiobacterium turbinis* sp. nov. and *Symbiobacterium terraclitae* sp. nov., isolated from shellfish, emended description of the genus *Symbiobacterium* and proposal of *Symbiobacteriaceae* fam. nov’, *Int. J. Syst. Evol. Microbiol.*, vol. 64, pp. 3375–3383, 2014, doi: 10.1099/ijs.0.063750-0.
- [231] F. Liu and R. Conrad, ‘Thermoanaerobacteriaceae oxidize acetate in methanogenic rice field soil at 50°C’, *Environ. Microbiol.*, vol. 12, no. 8, pp. 2341–2354, 2010, doi: 10.1111/j.1462-2920.2010.02289.x.
- [232] N. Shen, K. Dai, X. Y. Xia, R. J. Zeng, and F. Zhang, ‘Conversion of syngas (CO and H₂) to biochemicals by mixed culture fermentation in mesophilic and thermophilic hollow-fiber membrane biofilm reactors’, *J. Clean. Prod.*, vol. 202, pp. 536–542, 2018, doi: 10.1016/j.jclepro.2018.08.162.
- [233] L. Rovira-Alsina, M. D. Balaguer, and S. Puig, ‘Thermophilic bio-electro carbon dioxide recycling harnessing renewable energy surplus’, *Bioresour. Technol.*, vol. 321, 2021, doi: 10.1016/j.biortech.2020.124423.
- [234] Q. He, P. M. Lokken, S. Chen, and J. Zhou, ‘Characterization of the impact of acetate and lactate on ethanolic fermentation by *Thermoanaerobacter ethanolicus*’, *Bioresour. Technol.*, vol. 100, no. 23, pp. 5955–5965, 2009, doi: 10.1016/j.biortech.2009.06.084.
- [235] D. R. Abbanat and J. G. Ferry, ‘Synthesis of acetyl coenzyme A by carbon monoxide dehydrogenase complex from acetate-grown *Methanosarcina thermophila*’, *J. Bacteriol.*, vol. 172, no. 12, pp. 7145–7150, 1990, doi: 10.1128/jb.172.12.7145-7150.1990.
- [236] L. Daniels, G. Fuchs, R. K. Thauer, and J. G. Zeikus, ‘Carbon monoxide oxidation by methanogenic bacteria’, *J. Bacteriol.*, vol. 132, no. 1, pp. 118–126, 1977, doi: 10.1128/jb.132.1.118-126.1977.
- [237] N. Shen, K. Dai, X. Y. Xia, R. J. Zeng, and F. Zhang, ‘Conversion of syngas (CO and H₂) to biochemicals by mixed culture fermentation in mesophilic and thermophilic hollow-fiber membrane biofilm reactors’, *J. Clean. Prod.*, vol. 202, pp. 536–542, 2018, doi: 10.1016/j.jclepro.2018.08.162.
- [238] Y. Q. Wang, S. J. Yu, F. Zhang, X. Y. Xia, and R. J. Zeng, ‘Enhancement of acetate productivity in a thermophilic (55 °C) hollow-fiber membrane biofilm reactor with mixed culture syngas (H₂/CO₂) fermentation’, *Appl. Microbiol. Biotechnol.*, vol. 101, no. 6, pp. 2619–2627, 2017, doi: 10.1007/s00253-017-8124-9.
- [239] S. Godwin *et al.*, ‘Investigation of the microbial metabolism of carbon dioxide and hydrogen in the kangaroo foregut by stable isotope probing’, *ISME J.*, vol. 8, no. 9, pp. 1855–1865, 2014, doi: 10.1038/ismej.2014.25.
- [240] M. Demler and D. Weuster-Botz, ‘Reaction engineering analysis of hydrogenotrophic production of acetic acid by *Acetobacterium woodii*’, *Biotechnol. Bioeng.*, vol. 108, no. 2, pp. 470–474, 2011, doi:

- 10.1002/bit.22935.
- [241] M. Straub, M. Demler, D. Weuster-Botz, and P. Dürre, 'Selective enhancement of autotrophic acetate production with genetically modified *Acetobacterium woodii*', *J. Biotechnol.*, vol. 178, no. 1, pp. 67–72, 2014, doi: 10.1016/j.jbiotec.2014.03.005.
- [242] S. J. Kwon, J. Lee, and H. S. Lee, 'Acetate-assisted carbon monoxide fermentation of *Clostridium* sp. AWRP', *Process Biochem.*, vol. 113, pp. 47–54, 2022, doi: 10.1016/j.procbio.2021.12.015.
- [243] S. Park, M. Yasin, J. Jeong, M. Cha, and H. Kang, 'Acetate-assisted increase of butyrate production by *Eubacterium limosum* KIST612 during carbon monoxide fermentation', *Bioresour. Technol.*, vol. 245, no. June, pp. 560–566, 2017, doi: 10.1016/j.biortech.2017.08.132.
- [244] V. Hess, K. Schuchmann, and V. Müller, 'The ferredoxin: NAD⁺ Oxidoreductase (Rnf) from the acetogen *acetobacterium woodii* requires na⁺ and is reversibly coupled to the membrane potential', *J. Biol. Chem.*, vol. 288, no. 44, pp. 31496–31502, 2013, doi: 10.1074/jbc.M113.510255.
- [245] A. K. Kaster, J. Moll, K. Parey, and R. K. Thauer, 'Coupling of ferredoxin and heterodisulfide reduction via electron bifurcation in hydrogenotrophic methanogenic archaea', *Proc. Natl. Acad. Sci. U. S. A.*, vol. 108, no. 7, pp. 2981–2986, 2011, doi: 10.1073/pnas.1016761108.
- [246] A. Katsyv and V. Müller, 'Overcoming Energetic Barriers in Acetogenic C₁ Conversion', *Front. Bioeng. Biotechnol.*, vol. 8, no. December, pp. 1–23, 2020, doi: 10.3389/fbioe.2020.621166.
- [247] W. Buckel and R. K. Thauer, 'Energy conservation via electron bifurcating ferredoxin reduction and proton/Na⁺ translocating ferredoxin oxidation', *Biochim. Biophys. Acta - Bioenerg.*, vol. 1827, no. 2, pp. 94–113, 2013, doi: 10.1016/j.bbabi.2012.07.002.
- [248] S. Schmidt, E. Biegel, and V. Müller, 'The ins and outs of Na⁺ bioenergetics in *Acetobacterium woodii*', *Biochim. Biophys. Acta - Bioenerg.*, vol. 1787, no. 6, pp. 691–696, 2009, doi: 10.1016/j.bbabi.2008.12.015.
- [249] M. J. Lee and S. H. Zinder, 'Isolation and Characterization of a Thermophilic Bacterium Which Oxidizes Acetate in Syntrophic Association with a Methanogen and Which Grows Acetogenically on H₂-CO₂', *Appl. Environ. Microbiol.*, vol. 54, no. 1, pp. 124–129, 1988, doi: 10.1128/aem.54.1.124-129.1988.
- [250] R. González-Cabaleiro, J. M. Lema, J. Rodríguez, and R. Kleerebezem, 'Linking thermodynamics and kinetics to assess pathway reversibility in anaerobic bioprocesses', *Energy Environ. Sci.*, vol. 6, no. 12, pp. 3780–3789, 2013, doi: 10.1039/c3ee42754d.
- [251] V. Mahamkali *et al.*, 'Redox controls metabolic robustness in the gas-fermenting acetogen *Clostridium autoethanogenum*', *Proc. Natl. Acad. Sci. U. S. A.*, vol. 117, no. 23, pp. 13168–13175, 2020, doi: 10.1073/pnas.1919531117.
- [252] S. Schulz, B. Molitor, and L. T. Angenent, 'Acetate augmentation boosts the ethanol production rate and specificity by *Clostridium ljungdahlii* during gas fermentation with pure carbon monoxide', *Bioresour. Technol.*, vol. 369, no. October 2022, p. 128387, 2023, doi: 10.1016/j.biortech.2022.128387.

- [253] D. Andreides, M. A. Lopez Marin, and J. Zabranska, 'Selective syngas fermentation to acetate under acidic and psychrophilic conditions using mixed anaerobic culture', *Bioresour. Technol.*, vol. 394, no. December 2023, p. 130235, 2024, doi: 10.1016/j.biortech.2023.130235.
- [254] F. Oswald *et al.*, 'Formic acid formation by *Clostridium ljungdahlii* at elevated pressures of carbon dioxide and hydrogen', *Front. Bioeng. Biotechnol.*, vol. 6, no. FEB, 2018, doi: 10.3389/fbioe.2018.00006.
- [255] F. R. Bengelsdorf *et al.*, 'Bacterial Anaerobic Synthesis Gas (Syngas) and CO₂+H₂ Fermentation', in *Advances in Applied Microbiology*, vol. 103, S. Sariaslani and G. M. B. T.-A. in A. M. Gadd, Eds. Academic Press, 2018, pp. 143–221.
- [256] K. Valgepea *et al.*, 'H₂ drives metabolic rearrangements in gas-fermenting *Clostridium autoethanogenum*', *Biotechnol. Biofuels*, vol. 11, no. 1, pp. 1–15, 2018, doi: 10.1186/s13068-018-1052-9.
- [257] J. Bertsch and V. Müller, 'CO metabolism in the acetogen *Acetobacterium woodii*', *Appl. Environ. Microbiol.*, vol. 81, no. 17, pp. 5949–5956, 2015, doi: 10.1128/AEM.01772-15.
- [258] S. W. Ragsdale and E. Pierce, 'Acetogenesis and the Wood-Ljungdahl pathway of CO₂ fixation', *Biochim. Biophys. Acta - Proteins Proteomics*, vol. 1784, no. 12, pp. 1873–1898, 2008, doi: 10.1016/j.bbapap.2008.08.012.
- [259] A. Oren, 'Thermodynamic limits to microbial life at high salt concentrations', *Environ. Microbiol.*, vol. 13, no. 8, pp. 1908–1923, 2011, doi: 10.1111/j.1462-2920.2010.02365.x.
- [260] G. Feijoo, M. Soto, R. Méndez, and J. M. Lema, 'Sodium inhibition in the anaerobic digestion process: Antagonism and adaptation phenomena', *Enzyme Microb. Technol.*, vol. 17, no. 2, pp. 180–188, 1995, doi: 10.1016/0141-0229(94)00011-F.
- [261] Á. Fernández-Naveira, M. C. Veiga, and C. Kennes, 'Effect of salinity on C₁-gas fermentation by *Clostridium carboxidivorans* producing acids and alcohols', *AMB Express*, vol. 9, no. 1, 2019, doi: 10.1186/s13568-019-0837-y.
- [262] P. Dessì *et al.*, 'Microbial electrosynthesis of acetate from CO₂ in three-chamber cells with gas diffusion biocathode under moderate saline conditions', *Environ. Sci. Ecotechnology*, vol. 16, 2023, doi: 10.1016/j.ese.2023.100261.
- [263] M. J. Lee, T. H. Kim, B. Min, and S. J. Hwang, 'Sodium (Na⁺) concentration effects on metabolic pathway and estimation of ATP use in dark fermentation hydrogen production through stoichiometric analysis', *J. Environ. Manage.*, vol. 108, pp. 22–26, 2012, doi: 10.1016/j.jenvman.2012.04.027.
- [264] A. Hierholtzer and J. C. Akunna, 'Modelling sodium inhibition on the anaerobic digestion process', *Water Sci. Technol.*, vol. 66, no. 7, pp. 1565–1573, 2012, doi: 10.2166/wst.2012.345.
- [265] V. Muller, M. Blaut, R. Heise, C. Winner, and G. Gottschalk, 'Sodium bioenergetics in methanogens and acetogens', *FEMS Microbiol. Lett.*, vol. 87, no. 3–4, pp. 373–376, 1990, doi: 10.1016/0378-1097(90)90481-5.
- [266] H. Reno, M. Volker, and G. Gerhard, 'Sodium Dependence of Acetate Formation by the Acetogenic Bacterium *Acetobacterium woodii*', *J. Bacteriol.*,

- vol. 171, no. 10, pp. 5473–5478, 1989.
- [267] H. L. Drake, A. S. Göbner, and S. L. Daniel, ‘Old acetogens, new light’, *Ann. N. Y. Acad. Sci.*, vol. 1125, pp. 100–128, 2008, doi: 10.1196/annals.1419.016.
- [268] A. Oren, ‘Bioenergetic Aspects of Halophilism’, *Microbiol. Mol. Biol. Rev.*, vol. 63, no. 2, pp. 334–348, 1999, [Online]. Available: <http://www.ncbi.nlm.nih.gov/pubmed/10357854>.
- [269] J. Philips, K. Rabaey, D. R. Lovley, and M. Vargas, ‘Biofilm formation by *Clostridium ljungdahlii* is induced by sodium chloride stress: Experimental evaluation and transcriptome analysis’, *PLoS One*, vol. 12, no. 1, pp. 1–25, 2017, doi: 10.1371/journal.pone.0170406.
- [270] L. A. Philipp, K. Bühler, R. Ulber, and J. Gescher, ‘Beneficial applications of biofilms’, *Nat. Rev. Microbiol.*, 2023, doi: 10.1038/s41579-023-00985-0.
- [271] C. Pfitzer *et al.*, ‘Fast Pyrolysis of Wheat Straw in the Bioliq Pilot Plant’, *Energy and Fuels*, vol. 30, no. 10, pp. 8047–8054, 2016, doi: 10.1021/acs.energyfuels.6b01412.
- [272] A. Grimalt-Alemany, M. Łęzyk, L. Lange, I. V. Skiadas, and H. N. Gavala, ‘Enrichment of syngas-converting mixed microbial consortia for ethanol production and thermodynamics-based design of enrichment strategies’, *Biotechnol. Biofuels*, vol. 11, no. 1, pp. 1–22, 2018, doi: 10.1186/s13068-018-1189-6.
- [273] S. Wang, H. Huang, H. H. Kahnt, A. P. Mueller, M. Köpke, and R. K. Thauer, ‘NADP-Specific electron-bifurcating [FeFe]-hydrogenase in a functional complex with formate dehydrogenase in *Clostridium autoethanogenum* grown on CO’, *J. Bacteriol.*, vol. 195, no. 19, pp. 4373–4386, 2013, doi: 10.1128/JB.00678-13.
- [274] Y. Liu, J. Wan, S. Han, S. Zhang, and G. Luo, ‘Selective conversion of carbon monoxide to hydrogen by anaerobic mixed culture’, *Bioresour. Technol.*, vol. 202, pp. 1–7, 2016, doi: 10.1016/j.biortech.2015.11.071.
- [275] M. Rother and W. W. Metcalf, ‘Anaerobic growth of *Methanosarcina acetivorans* C2A on carbon monoxide: An unusual way of life for a methanogenic archaeon’, *Proc. Natl. Acad. Sci. U. S. A.*, vol. 101, no. 48, pp. 16929–16934, 2004, doi: 10.1073/pnas.0407486101.
- [276] J. Sipma, P. N. L. Lens, A. J. M. Stams, and G. Lettinga, ‘Carbon monoxide conversion by anaerobic bioreactor sludges’, *FEMS Microbiol. Ecol.*, vol. 44, no. 2, pp. 271–277, 2003, doi: 10.1016/S0168-6496(03)00033-3.
- [277] T. V. Slepova, I. I. Rusanov, T. G. Sokolova, E. A. Bonch-Osmolovskaya, and N. V. Pimenov, ‘Radioisotopic tracing of carbon monoxide conversion by anaerobic thermophilic prokaryotes’, *Microbiology*, vol. 76, no. 5, pp. 523–529, 2007, doi: 10.1134/S0026261707050025.
- [278] M. A. Thompson, A. Mohajeri, and A. Mirkouei, ‘Comparison of pyrolysis and hydrolysis processes for furfural production from sugar beet pulp: A case study in southern Idaho, USA’, *J. Clean. Prod.*, vol. 311, no. May, p. 127695, 2021, doi: 10.1016/j.jclepro.2021.127695.
- [279] L. J. Jönsson, B. Alriksson, and N.-O. Nilvebrant, ‘Bioconversion of lignocellulose: inhibitors and detoxification’, *Biotechnol. Biofuels*, vol. 6, no. 16, 2013.

- [280] L. G. Ljungdahl, 'Acetate Synthesis in Acetogenic Bacteria', *Annu. Rev. Microbiol.*, vol. 40, no. 89, pp. 415–450, 1986.
- [281] R. Bache and N. Pfennig, 'Selective isolation of *Acetobacterium woodii* on methoxylated aromatic acids and determination of growth yields', *Arch. Microbiol.*, vol. 130, no. 3, pp. 255–261, 1981, doi: 10.1007/BF00459530.
- [282] B. Schink and N. Pfennig, 'Fermentation of trihydroxybenzenes by *Pelobacter acidigallici* gen. nov. sp. nov., a new strictly anaerobic, non-sporeforming bacterium', *Arch. Microbiol.*, vol. 133, no. 3, pp. 195–201, 1982, doi: 10.1007/BF00415000.
- [283] S. Kato, K. Chino, N. Kamimura, E. Masai, I. Yumoto, and Y. Kamagata, 'Methanogenic degradation of lignin-derived monoaromatic compounds by microbial enrichments from rice paddy field soil', *Sci. Rep.*, vol. 5, no. June, pp. 4–6, 2015, doi: 10.1038/srep14295.
- [284] P. M. Fedorak and S. E. Hrudey, 'The effects of phenol and some alkyl phenolics on batch anaerobic methanogenesis', *Water Res.*, vol. 18, no. 3, pp. 361–367, 1984, doi: 10.1016/0043-1354(84)90113-1.
- [285] B. Y. Schink, B. Philipp, and J. Müller, 'Anaerobic Degradation of Phenolic Compounds', vol. 23, no. 2000, pp. 12–23, 2000.
- [286] J. J. Milledge, B. V. Nielsen, and P. J. Harvey, 'The inhibition of anaerobic digestion by model phenolic compounds representative of those from *Sargassum muticum*', *J. Appl. Phycol.*, vol. 31, no. 1, pp. 779–786, 2019, doi: 10.1007/s10811-018-1512-4.
- [287] K. Kato, S. Kozaki, and M. Sakuranaga, 'Degradation of ligning compounds by bacteria from termite guts', *Biotechnol. Lett.*, vol. 20, no. 5, pp. 459–462, 1998, doi: 10.1023/A:1005432027603.
- [288] X. F. Huang *et al.*, 'Isolation and characterization of lignin-degrading bacteria from rainforest soils', *Biotechnol. Bioeng.*, vol. 110, no. 6, pp. 1616–1626, 2013, doi: 10.1002/bit.24833.
- [289] E. G. Ozbayram, S. Kleinstaub, M. Nikolausz, B. Ince, and O. Ince, 'Bioaugmentation of anaerobic digesters treating lignocellulosic feedstock by enriched microbial consortia', *Eng. Life Sci.*, vol. 18, no. 7, pp. 440–446, 2018, doi: 10.1002/elsc.201700199.
- [290] S. Tuesorn *et al.*, 'Enhancement of biogas production from swine manure by a lignocellulolytic microbial consortium', *Bioresour. Technol.*, vol. 144, pp. 579–586, 2013, doi: 10.1016/j.biortech.2013.07.013.
- [291] P. M. Fedorak and S. E. Hrudey, 'Inhibition of anaerobic degradation of phenolics and methanogenesis by coal coking wastewater', *Water Sci. Technol.*, vol. 19, no. 1–2, pp. 219–228, 1987, doi: 10.2166/wst.1987.0203.
- [292] M. Machida *et al.*, 'Genome sequencing and analysis of *Aspergillus oryzae*', *Nature*, vol. 438, no. 7071, pp. 1157–1161, 2005, doi: 10.1038/nature04300.
- [293] A. Kövilein, V. Aschmann, S. Hohmann, and K. Ochsenreither, 'Immobilization of *Aspergillus oryzae* DSM 1863 for l-Malic Acid Production', *Fermentation*, vol. 8, no. 1, p. 26, 2022, doi: 10.3390/fermentation8010026.
- [294] V. Schmitt, L. Derenbach, and K. Ochsenreither, 'Enhanced l-Malic Acid Production by *Aspergillus oryzae* DSM 1863 Using Repeated-Batch

- Cultivation', *Front. Bioeng. Biotechnol.*, vol. 9, no. January, pp. 1–15, 2022, doi: 10.3389/fbioe.2021.760500.
- [295] A. Robazza, C. Welter, C. Kubisch, F. C. F. Baleeiro, K. Ochsenreither, and A. Neumann, 'Co-Fermenting Pyrolysis Aqueous Condensate and Pyrolysis Syngas with Anaerobic Microbial Communities Enables L-Malate Production in a Secondary Fermentative Stage', *Fermentation*, vol. 8, no. 10, 2022, doi: 10.3390/fermentation8100512.
- [296] Z. Wang *et al.*, 'Distinguishing responses of acetoclastic and hydrogenotrophic methanogens to ammonia stress in mesophilic mixed cultures', *Water Res.*, vol. 224, no. May, 2022, doi: 10.1016/j.watres.2022.119029.
- [297] D. J. W. Blum and R. E. Speece, 'A database of chemical toxicity to environmental bacteria and its use in interspecies comparisons and correlations', *Res. J. Water Pollut. Control Fed.*, vol. 63, no. 3, pp. 198–207, 1991, doi: 10.2307/25043983.
- [298] S. Astals, M. Peces, D. J. Batstone, P. D. Jensen, and S. Tait, 'Characterising and modelling free ammonia and ammonium inhibition in anaerobic systems', *Water Res.*, vol. 143, pp. 127–135, 2018, doi: 10.1016/j.watres.2018.06.021.
- [299] O. Yenigün and B. Demirel, 'Ammonia inhibition in anaerobic digestion: A review', *Process Biochem.*, vol. 48, no. 5–6, pp. 901–911, 2013, doi: 10.1016/j.procbio.2013.04.012.
- [300] I. W. Koster and G. Lettinga, 'Anaerobic digestion at extreme ammonia concentrations', *Biol. Wastes*, vol. 25, no. 1, pp. 51–59, 1988, doi: 10.1016/0269-7483(88)90127-9.
- [301] H. Wang, Y. Zhang, and I. Angelidaki, 'Ammonia inhibition on hydrogen enriched anaerobic digestion of manure under mesophilic and thermophilic conditions', *Water Res.*, vol. 105, pp. 314–319, 2016, doi: 10.1016/j.watres.2016.09.006.
- [302] I. A. Fotidis, D. Karakashev, T. A. Kotsopoulos, G. G. Martzopoulos, and I. Angelidaki, 'Effect of ammonium and acetate on methanogenic pathway and methanogenic community composition', *FEMS Microbiol. Ecol.*, vol. 83, no. 1, pp. 38–48, 2013, doi: 10.1111/j.1574-6941.2012.01456.x.
- [303] J. Zhao *et al.*, 'Clarifying the Role of Free Ammonia in the Production of Short-Chain Fatty Acids from Waste Activated Sludge Anaerobic Fermentation', *ACS Sustain. Chem. Eng.*, vol. 6, no. 11, pp. 14104–14113, 2018, doi: 10.1021/acssuschemeng.8b02670.
- [304] H. Zhang, Y. Peng, P. Yang, X. Wang, X. Peng, and L. Li, 'Response of process performance and microbial community to ammonia stress in series batch experiments', *Bioresour. Technol.*, vol. 314, no. 174, p. 123768, 2020, doi: 10.1016/j.biortech.2020.123768.
- [305] X. Peng, S. Y. Zhang, L. Li, X. Zhao, Y. Ma, and D. Shi, 'Long-term high-solids anaerobic digestion of food waste: Effects of ammonia on process performance and microbial community', *Bioresour. Technol.*, vol. 262, no. 174, pp. 148–158, 2018, doi: 10.1016/j.biortech.2018.04.076.
- [306] F. Liu *et al.*, 'Thermodynamic restrictions determine ammonia tolerance of functional floras during anaerobic digestion', *Bioresour. Technol.*, vol. 391,

- no. October 2023, 2024, doi: 10.1016/j.biortech.2023.129919.
- [307] D. Xu and R. S. Lewis, 'Syngas fermentation to biofuels: Effects of ammonia impurity in raw syngas on hydrogenase activity', *Biomass and Bioenergy*, vol. 45, pp. 303–310, 2012, doi: 10.1016/j.biombioe.2012.06.022.
- [308] L. Oliveira, A. Rückel, L. Nordgauer, P. Schlumprecht, E. Hutter, and D. Weuster-Botz, 'Comparison of Syngas-Fermenting Clostridia in Stirred-Tank Bioreactors and the Effects of Varying Syngas Impurities', *Microorganisms*, vol. 10, no. 4, p. 681, 2022, doi: 10.3390/microorganisms10040681.
- [309] A. Rückel, J. Hannemann, C. Maierhofer, A. Fuchs, and D. Weuster-Botz, 'Studies on Syngas Fermentation With *Clostridium carboxidivorans* in Stirred-Tank Reactors With Defined Gas Impurities', *Front. Microbiol.*, vol. 12, no. April, pp. 1–16, 2021, doi: 10.3389/fmicb.2021.655390.
- [310] X. Shi, J. Lin, J. Zuo, P. Li, X. Li, and X. Guo, 'Effects of free ammonia on volatile fatty acid accumulation and process performance in the anaerobic digestion of two typical bio-wastes', *J. Environ. Sci. (China)*, vol. 55, pp. 49–57, 2017, doi: 10.1016/j.jes.2016.07.006.
- [311] J. A. Frank *et al.*, 'Novel Syntrophic Populations Dominate an Ammonia-Tolerant Methanogenic Microbiome', *mSystems*, vol. 1, no. 5, pp. 1–13, 2016, doi: 10.1128/msystems.00092-16.
- [312] H. Tian, M. Yan, L. Treu, I. Angelidaki, and I. A. Fotidis, 'Hydrogenotrophic methanogens are the key for a successful bioaugmentation to alleviate ammonia inhibition in thermophilic anaerobic digesters', *Bioresour. Technol.*, vol. 293, no. May, p. 122070, 2019, doi: 10.1016/j.biortech.2019.122070.
- [313] M. Westerholm, L. Levén, and A. Schnürer, 'Bioaugmentation of syntrophic acetate-oxidizing culture in biogas reactors exposed to increasing levels of ammonia', *Appl. Environ. Microbiol.*, vol. 78, no. 21, pp. 7619–7625, 2012, doi: 10.1128/AEM.01637-12.
- [314] S. Poirier, A. Bize, C. Bureau, T. Bouchez, and O. Chapleur, 'Community shifts within anaerobic digestion microbiota facing phenol inhibition: Towards early warning microbial indicators?', *Water Res.*, vol. 100, pp. 296–305, 2016, doi: 10.1016/j.watres.2016.05.041.
- [315] L. Xu *et al.*, 'New attempts on acidic anaerobic digestion of poly (butylene adipate-co-terephthalate) wastewater in upflow anaerobic sludge blanket reactor', *J. Hazard. Mater.*, vol. 461, no. September 2023, p. 132586, 2024, doi: 10.1016/j.jhazmat.2023.132586.
- [316] S. Ismail *et al.*, 'Response of anammox bacteria to short-term exposure of 1,4-dioxane: Bacterial activity and community dynamics', *Sep. Purif. Technol.*, vol. 266, no. August 2020, p. 118539, 2021, doi: 10.1016/j.seppur.2021.118539.
- [317] Y. Shen, L. Jarboe, R. Brown, and Z. Wen, 'A thermochemical-biochemical hybrid processing of lignocellulosic biomass for producing fuels and chemicals', *Biotechnol. Adv.*, vol. 33, no. 8, pp. 1799–1813, 2015, doi: 10.1016/j.biotechadv.2015.10.006.
- [318] H. H. P. Fang, D. W. Liang, T. Zhang, and Y. Liu, 'Anaerobic treatment of phenol in wastewater under thermophilic condition', *Water Res.*, vol. 40, no.

- 3, pp. 427–434, 2006, doi: 10.1016/j.watres.2005.11.025.
- [319] J. A. Dijk, A. J. M. Stams, G. Schraa, H. Ballerstedt, J. A. M. De Bont, and J. Gerritse, ‘Anaerobic oxidation of 2-chloroethanol under denitrifying conditions by *Pseudomonas stutzeri* strain JJ’, *Appl. Microbiol. Biotechnol.*, vol. 63, no. 1, pp. 68–74, 2003, doi: 10.1007/s00253-003-1346-z.
- [320] C. Vogt, S. Kleinsteuber, and H. H. Richnow, ‘Anaerobic benzene degradation by bacteria’, *Microb. Biotechnol.*, vol. 4, no. 6, pp. 710–724, 2011, doi: 10.1111/j.1751-7915.2011.00260.x.
- [321] L. Review and A. Data, ‘Toxicology and Biodegradability of Tier Three Gasoline Blendstocks Literature Review of Available Data’, no. September, 2019.
- [322] B. Wu, C. He, S. Yuan, Z. Hu, and W. Wang, ‘Hydrogen enrichment as a bioaugmentation tool to alleviate ammonia inhibition on anaerobic digestion of phenol-containing wastewater’, *Bioresour. Technol.*, vol. 276, no. December 2018, pp. 97–102, 2019, doi: 10.1016/j.biortech.2018.12.099.
- [323] M. Djebbar, F. Djafri, M. Boucekara, and A. Djafri, ‘Adsorption of phenol on natural clay’, *Appl. Water Sci.*, vol. 2, no. 2, pp. 77–86, 2012, doi: 10.1007/s13201-012-0031-8.
- [324] M. E. K. M. Hassouna, M. S. Abdel-Tawab, and A. A. M. Abdel-Aleem, ‘Use of biokaolinite clay for the microbial removal of phenol from real industrial wastewater samples by *Dermacoccus nishinomiyaensis* and *Kocuria rosea*’, *Environ. Qual. Manag.*, no. December 2023, pp. 1–17, 2024, doi: 10.1002/tqem.22181.
- [325] B. Biswas, B. Sarkar, R. Rusmin, and R. Naidu, ‘Bioremediation of PAHs and VOCs: Advances in clay mineral-microbial interaction’, *Environ. Int.*, vol. 85, pp. 168–181, 2015, doi: 10.1016/j.envint.2015.09.017.
- [326] X. Sun, H. K. Atiyeh, R. L. Huhnke, and R. S. Tanner, ‘Syngas fermentation process development for production of biofuels and chemicals: A review’, *Bioresour. Technol. Reports*, vol. 7, p. 100279, 2019, doi: 10.1016/j.biteb.2019.100279.
- [327] M. Erkelens, A. S. Ball, and D. M. Lewis, ‘The application of activated carbon for the treatment and reuse of the aqueous phase derived from the hydrothermal liquefaction of a halophytic *Tetraselmis* sp.’, *Bioresour. Technol.*, vol. 182, pp. 378–382, 2015, doi: 10.1016/j.biortech.2015.01.129.
- [328] S. Ashoor *et al.*, ‘Bioupgrading of the aqueous phase of pyrolysis oil from lignocellulosic biomass: a platform for renewable chemicals and fuels from the whole fraction of biomass’, *Bioresour. Bioprocess.*, vol. 10, no. 1, 2023, doi: 10.1186/s40643-023-00654-3.
- [329] C. Stark, S. Münbinger, F. Rosenau, B. J. Eikmanns, and A. Schwentner, ‘The Potential of Sequential Fermentations in Converting C1 Substrates to Higher-Value Products’, *Front. Microbiol.*, vol. 13, no. June, 2022, doi: 10.3389/fmicb.2022.907577.
- [330] H. G. Lim, J. H. Lee, M. H. Noh, and G. Y. Jung, ‘Rediscovering Acetate Metabolism: Its Potential Sources and Utilization for Biobased Transformation into Value-Added Chemicals’, *J. Agric. Food Chem.*, vol. 66, no. 16, pp. 3998–4006, 2018, doi: 10.1021/acs.jafc.8b00458.

- [331] M. J. Scarborough, C. E. Lawson, J. J. Hamilton, T. J. Donohue, and D. R. Noguera, 'Metatranscriptomic and Thermodynamic Insights into Medium-Chain Fatty Acid Production Using an Anaerobic Microbiome', *mSystems*, vol. 3, no. 6, 2018, doi: 10.1128/msystems.00221-18.
- [332] D. Kiefer, M. Merkel, L. Lilge, R. Hausmann, and M. Henkel, 'High cell density cultivation of *Corynebacterium glutamicum* on bio-based lignocellulosic acetate using pH-coupled online feeding control', *Bioresour. Technol.*, vol. 340, no. June, p. 125666, 2021, doi: 10.1016/j.biortech.2021.125666.
- [333] M. Llamas, E. Tomás-Pejó, and C. González-Fernández, 'Volatile fatty acids from organic wastes as novel low-cost carbon source for *Yarrowia lipolytica*', *N. Biotechnol.*, vol. 56, pp. 123–129, 2020, doi: 10.1016/j.nbt.2020.01.002.
- [334] A. Mahboubi, J. A. Ferreira, M. J. Taherzadeh, and P. R. Lennartsson, 'Production of fungal biomass for feed, fatty acids, and glycerol by *Aspergillus oryzae* from fat-rich dairy substrates', *Fermentation*, vol. 3, no. 4, 2017, doi: 10.3390/fermentation3040048.
- [335] J. Daniell, M. Köpke, and S. D. Simpson, 'Commercial Biomass Syngas Fermentation', *Energies*, vol. 5, pp. 5372–5417, 2012, doi: 10.3390/en5125372.
- [336] J. Tai, S. S. Adav, A. Su, and D. J. Lee, 'Biological hydrogen production from phenol-containing wastewater using *Clostridium butyricum*', *Int. J. Hydrogen Energy*, vol. 35, no. 24, pp. 13345–13349, 2010, doi: 10.1016/j.ijhydene.2009.11.111.
- [337] K. L. Ho, Y. Y. Chen, and D. J. Lee, 'Biohydrogen production from cellobiose in phenol and cresol-containing medium using *Clostridium* sp. R1', *Int. J. Hydrogen Energy*, vol. 35, no. 19, pp. 10239–10244, 2010, doi: 10.1016/j.ijhydene.2010.07.155.
- [338] X. J. Guo *et al.*, 'Diversity and degradation mechanism of an anaerobic bacterial community treating phenolic wastewater with sulfate as an electron acceptor', *Environ. Sci. Pollut. Res.*, vol. 22, no. 20, pp. 16121–16132, 2015, doi: 10.1007/s11356-015-4833-8.
- [339] H. Luo *et al.*, 'Co-production of solvents and organic acids in butanol fermentation by: *Clostridium acetobutylicum* in the presence of lignin-derived phenolics', *RSC Adv.*, vol. 9, no. 12, pp. 6919–6927, 2019, doi: 10.1039/c9ra00325h.
- [340] Y. Li, Q. Wang, L. Liu, S. Tabassum, J. Sun, and Y. Hong, 'Enhanced phenols removal and methane production with the assistance of graphene under anaerobic co-digestion conditions', *Sci. Total Environ.*, vol. 759, p. 143523, 2021, doi: 10.1016/j.scitotenv.2020.143523.
- [341] J. T. Qiao, Y. L. Qiu, X. Z. Yuan, X. S. Shi, X. H. Xu, and R. B. Guo, 'Molecular characterization of bacterial and archaeal communities in a full-scale anaerobic reactor treating corn straw', *Bioresour. Technol.*, vol. 143, pp. 512–518, 2013, doi: 10.1016/j.biortech.2013.06.014.
- [342] Y. Saito, T. Sato, K. Nomoto, and H. Tsuji, 'Identification of phenol- and p-cresol-producing intestinal bacteria by using media supplemented with tyrosine and its metabolites', no. June, pp. 1–11, 2018, doi: 10.1093/femsec/fiy125.

- [343] I. J. Passmore *et al.*, ‘Para-cresol production by *Clostridium difficile* affects microbial diversity and membrane integrity of Gram-negative bacteria’, *PLoS Pathog.*, vol. 14, no. 9, 2018, doi: 10.1371/journal.ppat.1007191.
- [344] K. Heitkamp *et al.*, ‘Monitoring of seven industrial anaerobic digesters supplied with biochar’, *Biotechnol. Biofuels*, vol. 14, no. 1, pp. 1–14, 2021, doi: 10.1186/s13068-021-02034-5.
- [345] E. M. Prem, A. Schwarzenberger, R. Markt, and A. O. Wagner, ‘Effects of phenyl acids on different degradation phases during thermophilic anaerobic digestion’, *Front. Microbiol.*, vol. 14, no. April, pp. 1–16, 2023, doi: 10.3389/fmicb.2023.1087043.
- [346] Q. Mariën, A. Regueira, and R. Ganigué, ‘Steerable isobutyric and butyric acid production from CO₂ and H₂ by *Clostridium luticellarii*’, *Microb. Biotechnol.*, no. July, pp. 1–16, 2023, doi: 10.1111/1751-7915.14321.
- [347] S. Crognale *et al.*, ‘Ecology of food waste chain-elongating microbiome’, *Front. Bioeng. Biotechnol.*, vol. 11, no. April, pp. 1–12, 2023, doi: 10.3389/fbioe.2023.1157243.
- [348] J. Tang *et al.*, ‘Caproate production from xylose via the fatty acid biosynthesis pathway by genus *Caproiciproducens* dominated mixed culture fermentation’, *Bioresour. Technol.*, vol. 351, no. February, p. 126978, 2022, doi: 10.1016/j.biortech.2022.126978.
- [349] S. Yang, Z. Chen, and Q. Wen, ‘Impacts of biochar on anaerobic digestion of swine manure: Methanogenesis and antibiotic resistance genes dissemination’, *Bioresour. Technol.*, vol. 324, no. January, p. 124679, 2021, doi: 10.1016/j.biortech.2021.124679.
- [350] A. Li *et al.*, ‘A pyrosequencing-based metagenomic study of methane-producing microbial community in solid-state biogas reactor’, *Biotechnol. Biofuels*, vol. 6, no. 1, pp. 1–17, 2013, doi: 10.1186/1754-6834-6-3.
- [351] L. Solli, O. E. Håvelsrud, S. J. Horn, and A. G. Rike, ‘A metagenomic study of the microbial communities in four parallel biogas reactors’, *Biotechnol. Biofuels*, vol. 7, no. 1, pp. 1–15, 2014, doi: 10.1186/s13068-014-0146-2.
- [352] T. Lu, T. Su, X. Liang, Y. Wei, J. Zhang, and T. He, ‘Dual character of methane production improvement and antibiotic resistance genes reduction by nano-Fe₂O₃ addition during anaerobic digestion of swine manure’, *J. Clean. Prod.*, vol. 376, no. September, p. 134240, 2022, doi: 10.1016/j.jclepro.2022.134240.
- [353] N. Lackner, A. Hintersonleitner, A. O. Wagner, and P. Illmer, ‘Hydrogenotrophic methanogenesis and autotrophic growth of *Methanosarcina thermophila*’, *Archaea*, vol. 2018, 2018, doi: 10.1155/2018/4712608.
- [354] S. M. Tiquia-Arashiro, *Thermophilic Carboxydrotrophs and their Applications in Biotechnology*. Springer Briefs in Microbiology, 2014.
- [355] M. Diender, R. Pereira, H. J. C. T. Wessels, A. J. M. Stams, D. Z. Sousa, and J. F. Holden, ‘Proteomic Analysis of the Hydrogen and Carbon Monoxide Metabolism of *Methanothermobacter marburgensis*’, vol. 7, no. July, pp. 1–10, 2016, doi: 10.3389/fmicb.2016.01049.
- [356] M. Ehsanipour, A. V. Suko, R. Bura, A. Vajzovic, and S. Renata, ‘Fermentation of lignocellulosic sugars to acetic acid by *Moorella thermoacetica*’, *J. Ind.*

- Microbiol. Biotechnol.*, vol. 43, no. 6, pp. 807–816, 2016, doi: 10.1007/s10295-016-1756-4.
- [357] R. Takors *et al.*, ‘Minireview Using gas mixtures of CO , CO 2 and H 2 as microbial substrates : the do ’ s and don ’ ts of successful technology transfer from laboratory to production scale’, vol. 11, pp. 606–625, 2018, doi: 10.1111/1751-7915.13270.
- [358] H. L. Drake and S. L. Daniel, ‘Physiology of the thermophilic acetogen *Moorella thermoacetica*.’, *Res. Microbiol.*, vol. 155, no. 10, pp. 869–883, 2004, doi: 10.1016/j.resmic.2004.10.002.
- [359] Y. Nakamura, H. Miyafuji, H. Kawamoto, and S. Saka, ‘Acetic acid fermentability with *Clostridium thermoaceticum* and *Clostridium thermocellum* of standard compounds found in beech wood as produced in hot-compressed water’, *J. Wood Sci.*, vol. 57, no. 4, pp. 331–337, 2011, doi: 10.1007/s10086-010-1169-3.
- [360] A. El Kasmi, S. Rajasekharan, and S. W. Ragsdale, ‘Anaerobic Pathway for Conversion of the Methyl Group of Aromatic Methyl Ethers to Acetic Acid by *Clostridium thermoaceticum*’, *Biochemistry*, vol. 33, no. 37, pp. 11217–11224, 1994, doi: 10.1021/bi00203a018.
- [361] J. Pang *et al.*, ‘Enhancing the ethanol yield from salix using a *Clostridium thermocellum* and *Thermoanaerobacterium thermosaccharolyticum* co-culture system’, *BioResources*, vol. 13, no. 3, pp. 5377–5393, 2019, doi: 10.15376/biores.13.3.5377-5393.
- [362] S. M. Landuyt, E. J. Hsu, B. T. Wang, and S. S. Tsay, ‘Conversion of paraffin oil to alcohols by *Clostridium thermosaccharolyticum*’, *Appl. Environ. Microbiol.*, vol. 61, no. 3, pp. 1153–1155, 1995, doi: 10.1128/aem.61.3.1153-1155.1995.
- [363] E. M. Prem, M. Mutschlechner, B. Stres, P. Illmer, and A. O. Wagner, ‘Lignin intermediates lead to phenyl acid formation and microbial community shifts in meso- and thermophilic batch reactors’, *Biotechnol. Biofuels*, vol. 14, no. 1, pp. 1–23, 2021, doi: 10.1186/s13068-020-01855-0.
- [364] E. M. Prem, B. Stres, P. Illmer, and A. O. Wagner, ‘Microbial community dynamics in mesophilic and thermophilic batch reactors under methanogenic, phenyl acid-forming conditions’, *Biotechnol. Biofuels*, vol. 13, no. 1, pp. 1–17, 2020, doi: 10.1186/s13068-020-01721-z.
- [365] C. H. Zierdt, C. Webster, and W. S. Rude, ‘Study of the anaerobic corynebacteria’, *Int. J. Syst. Bacteriol.*, vol. 18, no. 1, pp. 33–47, 1968, doi: 10.1099/00207713-18-1-33.
- [366] J. D. Reid and M. A. Joya, ‘A study of the morphologic and biochemical characteristics of certain anaerobic corynebacteria’, *Int. J. Syst. Bacteriol.*, vol. 19, no. 2, pp. 273–280, 1969.
- [367] A. Michel, A. Koch-Koerfges, K. Krumbach, M. Brocker, and M. Bott, ‘Anaerobic growth of *Corynebacterium glutamicum* via mixed-acid fermentation’, *Appl. Environ. Microbiol.*, vol. 81, no. 21, pp. 7496–7508, 2015, doi: 10.1128/AEM.02413-15.
- [368] T. Nishimura, A. A. Vertès, Y. Shinoda, M. Inui, and H. Yukawa, ‘Anaerobic growth of *Corynebacterium glutamicum* using nitrate as a terminal electron

- acceptor', *Appl. Microbiol. Biotechnol.*, vol. 75, no. 4, pp. 889–897, 2007, doi: 10.1007/s00253-007-0879-y.
- [369] S. Dekic, J. Hrenovic, E. van Wilpe, C. Venter, and I. Goic-Barisic, 'Survival of emerging pathogen *Acinetobacter baumannii* in water environment exposed to different oxygen conditions', *Water Sci. Technol.*, vol. 80, no. 8, pp. 1581–1590, 2019, doi: 10.2166/wst.2019.408.
- [370] F. C. F. Baleeiro, M. S. Ardila, S. Kleinstuber, and H. Sträuber, 'Effect of Oxygen Contamination on Propionate and Caproate Formation in Anaerobic Fermentation', *Front. Bioeng. Biotechnol.*, vol. 9, no. September, pp. 1–13, 2021, doi: 10.3389/fbioe.2021.725443.
- [371] J. P. Sheets, X. Ge, and Y. Li, 'Effect of limited air exposure and comparative performance between thermophilic and mesophilic solid-state anaerobic digestion of switchgrass', *Bioresour. Technol.*, vol. 180, pp. 296–303, 2015, doi: 10.1016/j.biortech.2015.01.011.
- [372] D. Nguyen and S. K. Khanal, 'A little breath of fresh air into an anaerobic system: How microaeration facilitates anaerobic digestion process', *Biotechnol. Adv.*, vol. 36, no. 7, pp. 1971–1983, 2018, doi: 10.1016/j.biotechadv.2018.08.007.
- [373] D. Botheju, B. Lie, and R. Bakke, 'Oxygen effects in anaerobic digestion - II', *Open Waste Manag. J.*, vol. 4, no. 2, pp. 1–19, 2011, doi: 10.4173/mic.2010.2.2.
- [374] N. Khoury, W. Dott, and P. Kämpfer, 'Anaerobic degradation of phenol in batch and continuous cultures by a denitrifying bacterial consortium', *Appl. Microbiol. Biotechnol.*, vol. 37, no. 4, pp. 529–531, 1992, doi: 10.1007/BF00180982.
- [375] Q. Gu, Q. Wu, J. Zhang, W. Guo, H. Wu, and M. Sun, 'Community analysis and recovery of phenol-degrading bacteria from drinking water biofilters', *Front. Microbiol.*, vol. 7, no. APR, pp. 1–11, 2016, doi: 10.3389/fmicb.2016.00495.
- [376] X. H. Shen, N. Y. Zhou, and S. J. Liu, 'Degradation and assimilation of aromatic compounds by *Corynebacterium glutamicum*: Another potential for applications for this bacterium?', *Appl. Microbiol. Biotechnol.*, vol. 95, no. 1, pp. 77–89, 2012, doi: 10.1007/s00253-012-4139-4.
- [377] U. Haußmann, S. W. Qi, D. Wolters, M. Röner, S. J. Liu, and A. Poetsch, 'Physiological adaptation of *Corynebacterium glutamicum* to benzoate as alternative carbon source - A membrane proteome-centric view', *Proteomics*, vol. 9, no. 14, pp. 3635–3651, 2009, doi: 10.1002/pmic.200900025.
- [378] K. L. Ho, B. Lin, Y. Y. Chen, and D. J. Lee, 'Biodegradation of phenol using *Corynebacterium* sp. DJ1 aerobic granules', *Bioresour. Technol.*, vol. 100, no. 21, pp. 5051–5055, 2009, doi: 10.1016/j.biortech.2009.05.050.
- [379] K. Brinkrolf, I. Brune, and A. Tauch, 'Transcriptional regulation of catabolic pathways for aromatic compounds in *Corynebacterium glutamicum*.', *Genet. Mol. Res.*, vol. 5, no. 4, pp. 773–789, 2006.
- [380] D. Mosca Angelucci, E. Clagnan, L. Brusetti, and M. C. Tomei, 'Anaerobic phenol biodegradation: kinetic study and microbial community shifts under high-concentration dynamic loading', *Appl. Microbiol. Biotechnol.*, vol. 104,

- no. 15, pp. 6825–6838, 2020, doi: 10.1007/s00253-020-10696-8.
- [381] K. S. Kim, Y. T. Ro, and Y. M. Kim, ‘Purification and some properties of carbon monoxide dehydrogenase from *Acinetobacter* sp. strain JC1 DSM 3803.’, *J. Bacteriol.*, vol. 171, no. 2, pp. 958–964, 1989, doi: 10.1128/jb.171.2.958-964.1989.
- [382] Cho JW, Yim HS, and Kim YM, ‘*Acinetobacter* isolates growing with carbon monoxide.’, *Kor J Microbiol.*, vol. 23, no. 1, pp. 1–8, 1985.
- [383] A. Schnu, ‘Effects of temperature on biological degradation of phenols , benzoates and phthalates under methanogenic conditions’, vol. 55, pp. 153–160, 2005, doi: 10.1016/j.ibiod.2004.09.004.
- [384] M. C. Tomei, D. Mosca Angelucci, E. Clagnan, and L. Brusetti, ‘Anaerobic biodegradation of phenol in wastewater treatment: achievements and limits’, *Appl. Microbiol. Biotechnol.*, vol. 105, no. 6, pp. 2195–2224, 2021, doi: 10.1007/s00253-021-11182-5.
- [385] S. W. Ragsdale, ‘Life with carbon monoxide’, *Crit. Rev. Biochem. Mol. Biol.*, vol. 39, no. 3, pp. 165–195, 2004, doi: 10.1080/10409230490496577.
- [386] R. M. W. Ferguson, R. Villa, and F. Coulon, ‘Bioengineering options and strategies for the optimization of anaerobic digestion processes’, *Environ. Technol. (United Kingdom)*, vol. 3, no. 1, pp. 1–14, 2014, doi: 10.1080/09593330.2014.907362.
- [387] J. R. Town and T. J. Dumonceaux, ‘Laboratory-scale bioaugmentation relieves acetate accumulation and stimulates methane production in stalled anaerobic digesters’, *Appl. Microbiol. Biotechnol.*, vol. 100, no. 2, pp. 1009–1017, 2016, doi: 10.1007/s00253-015-7058-3.
- [388] B. Basak *et al.*, ‘Rapid recovery of methane yield in organic overloaded-failed anaerobic digesters through bioaugmentation with acclimatized microbial consortium’, *Sci. Total Environ.*, vol. 764, p. 144219, 2021, doi: 10.1016/j.scitotenv.2020.144219.
- [389] N. V. Pimenov *et al.*, ‘Bioaugmentation of Anammox Activated Sludge with a Nitrifying Bacterial Community as a Way to Increase the Nitrogen Removal Efficiency’, *Microbiology*, vol. 91, no. 2, pp. 133–142, 2022, doi: 10.1134/S0026261722020102.
- [390] L. Perret, N. Boukis, and J. Sauer, ‘Influence of Increased Cell Densities on Product Ratio and Productivity in Syngas Fermentation’, *Ind. Eng. Chem. Res.*, vol. 62, no. 35, pp. 13799–13810, 2023, doi: 10.1021/acs.iecr.3c01911.
- [391] M. D. Bredwell, P. Srivastava, and R. M. Worden, ‘Reactor design issues for synthesis-gas fermentations’, *Biotechnol. Prog.*, vol. 15, no. 5, pp. 834–844, 1999, doi: 10.1021/bp990108m.
- [392] K. Asimakopoulos, H. N. Gavala, and I. V. Skiadas, ‘Biomethanation of Syngas by Enriched Mixed Anaerobic Consortia in Trickle Bed Reactors’, *Waste and Biomass Valorization*, vol. 11, no. 2, pp. 495–512, 2020, doi: 10.1007/s12649-019-00649-2.

List of figures

Figure 1. Schematic diagram of a pyrolysis process.....	4
Figure 2. Effect of temperature on the product distribution during the pyrolysis of lignocellulose biomass.....	5
Figure 3. Putative anaerobic degradation pathways of some selected PAC components.....	10
Figure 4. Scheme of the Wood–Ljungdahl pathway and energy conservation.....	13
Figure 5. Overview of the general metabolism of anaerobic mixed cultures fed with syngas.....	15
Figure 6. Schematic diagram of the putative metabolic network of mixotrophic anaerobic cultures co-fermenting syngas and PAC.	21
Figure 7. Scheme of the two-stage process developed in this work. In the first stage, syngas and PAC are co-fermented with anaerobic mixed cultures.	22
Figure 8. Electron mole balancing between substrates (CO and H ₂ , acetate if consumed) and products (CH ₄ , formate, ethanol, propionate, butyrate and valerate and H ₂ , acetate if produced) at different process conditions and increasing acetate concentrations.	29
Figure 9. Kinetics of consumption of syngas components (CO, H ₂ and CH ₄) and formation of some short-chain carboxylates (formate, acetate, propionate, n-butyrate and valerate) and ethanol at different process conditions and increasing acetate concentrations.....	30
Figure 10. Average relative abundance of triplicate samples of the enriched microbial genera (based on 16S rRNA amplicon sequencing variants).	32
Figure 11. Relative abundance of the enriched archaeal genera (based on mcrA gene amplicon sequencing variants).	34
Figure 12. Normalized rates compared to control experiments in absence of supplemented acetate.	36
Figure 13. Schematic representation of the experimental design.....	47
Figure 14. C-mol (a) and e-mol (b) balances for experiments M-CTRL, T-CTRL, M-BES and T-BES.	51
Figure 15. Rates of consumption and/or production of CO (a), CH ₄ (b) and H ₂ (c) at increasing PAC loadings at mesophilic (37 °C) and thermophilic (55 °C) temperatures.....	54

Figure 16. (a) M-PAC and T-PAC CO uptake rates normalized to control experiments M-CTRL and T-CTRL, respectively. (b) C-mol balances for M-PAC and T-PAC experiments.	55
Figure 17. Removal efficacies for some selected PAC compounds after syngas mixed culture fermentations per-formed at 37 °C and 55 °C.....	57
Figure 18. Growth of <i>A. oryzae</i> in aerobic flasks containing medium from syngas fermentations and abiotic controls.	59
Figure 19. Acetate and L-malate from <i>A. oryzae</i> fermentations in the medium from meso-philic syngas fermentations (a), (b) and thermophilic syngas fermentations (c), (d).	60
Figure 20. Effects of increasing SS-PAC loading on the metabolism of mesophilic (a, c, e) and thermophilic (b, d, f) mixed cultures.	73
Figure 21. Total ammonium nitrogen (TAN) production rates and nitrate removal rates for mesophilic (a) and thermophilic (b) SS-PAC experiments.....	74
Figure 22. Effects of increasing PE-PAC loading on the metabolism of mesophilic (a, c, e) and thermophilic (b, d, f) mixed cultures.	75
Figure 23. Fermentation profile of the mesophilic process.	92
Figure 24. Spearman’s rank correlations between relative abundance of dominant amplicon sequencing variants (ASVs) and process parameters for the mesophilic semi-continuous STR enrichment.	93
Figure 25. Fermentation profile of the thermophilic process.	96
Figure 26. Spearman’s rank correlations between relative abundance of amplicon sequencing variants (ASVs) and process parameters for the thermophilic semi-continuous STR enrichment.	97
Figure 27. L-malate yields calculated for the highest L-malate concentrations per SCCs consumed.	98

List of tables

Table 1. Most significant reactions in syngas fermentation with anaerobic mixed cultures.	14
Table 2. Summary of the concentrations of acetate, acetic acid (HAc) and Na ⁺ under the different experimental conditions.	26
Table 3. Overview of experiments. MC is mixed culture; AB is abiotic; Asp is <i>Aspergillus oryzae</i>	48

Supplementary information

Additional file 1

Fermentation medium

For each liter of modified BA medium were added: 100 mL of mineral salt solution, 800 mL of phosphate buffer solution, 10 mL of vitamin solution, 10 mL of trace elements solution, 5 mL of resazurin solution and 3 mL of reducing agent solution.

The mineral salt solution was prepared with the following salt concentrations: NH_4Cl , 161.2 g/L; $\text{MgCl}_2 \times 6\text{H}_2\text{O}$, 5.4 g/L; $\text{CaCl}_2 \times 2\text{H}_2\text{O}$ 6.5 g/L, NaCl, 30 g/L.

The phosphate buffer solution was prepared with 136 g/L KH_2PO_4 .

The vitamin solution was composed of: biotin, 0.002 g/L; folic acid, 0.002 g/L; pyridoxin, 0.01 g/L; thiamin, 0.005 g/L; riboflavin, 0.005 g/L; nicotinic acid, 0.005 g/L; Ca-pantothenate, 0.005 g/L; vitamin B12, 0.005 g/L; aminobenzoic acid, 0.005 g/L; liponic acid, 0.005 g/L).

Trace elements solution contained the following compounds: $\text{FeCl}_2 \times 4\text{H}_2\text{O}$, 1.5 g/L; MnCl_2 , 0.1 g/L; $\text{CoCl}_2 \times 6\text{H}_2\text{O}$, 0.19 g/L; ZnCl_2 , 0.07 g/L; $\text{CuCl}_2 \times 2\text{H}_2\text{O}$, 0.002 g/L; $\text{NiCl}_2 \times 6\text{H}_2\text{O}$, 0.024 g/L; $\text{Na}_2\text{MoO}_4 \times 2\text{H}_2\text{O}$, 0.036 g/L; H_3BO_3 , 0.006 g/L; $\text{Na}_2\text{SeO}_3 \times 5\text{H}_2\text{O}$, 0.003 g/L; $\text{Na}_2\text{WO}_4 \times 2\text{H}_2\text{O}$, 0.02 g/L.

The reducing agent solution contained 100 g/L of L-cysteine.

The resazurin solution contained 1 g/L resazurin sodium salt.

E-mol balances

Table S1. Conversion factors for electron balances.

Compound	Chemical Formula	Molecular Weight	mol e ⁻ /mol
Formate	CH_2O_2	46.1	2.0
Acetate	$\text{C}_2\text{H}_4\text{O}_2$	60.0	8.0
Ethanol	$\text{C}_2\text{H}_6\text{O}$	46.0	12.0
Propionate	$\text{C}_3\text{H}_6\text{O}_2$	74.0	14.0
Butyrate	$\text{C}_4\text{H}_8\text{O}_2$	88.1	20.0
Valerate	$\text{C}_5\text{H}_{10}\text{O}_2$	102.1	26
Hydrogen	H_2	2.0	2.0
Carbon Monoxide	CO	28.0	2.0
Carbon Dioxide	CO_2	44.0	0.0
Methane	CH_4	16.0	8.0

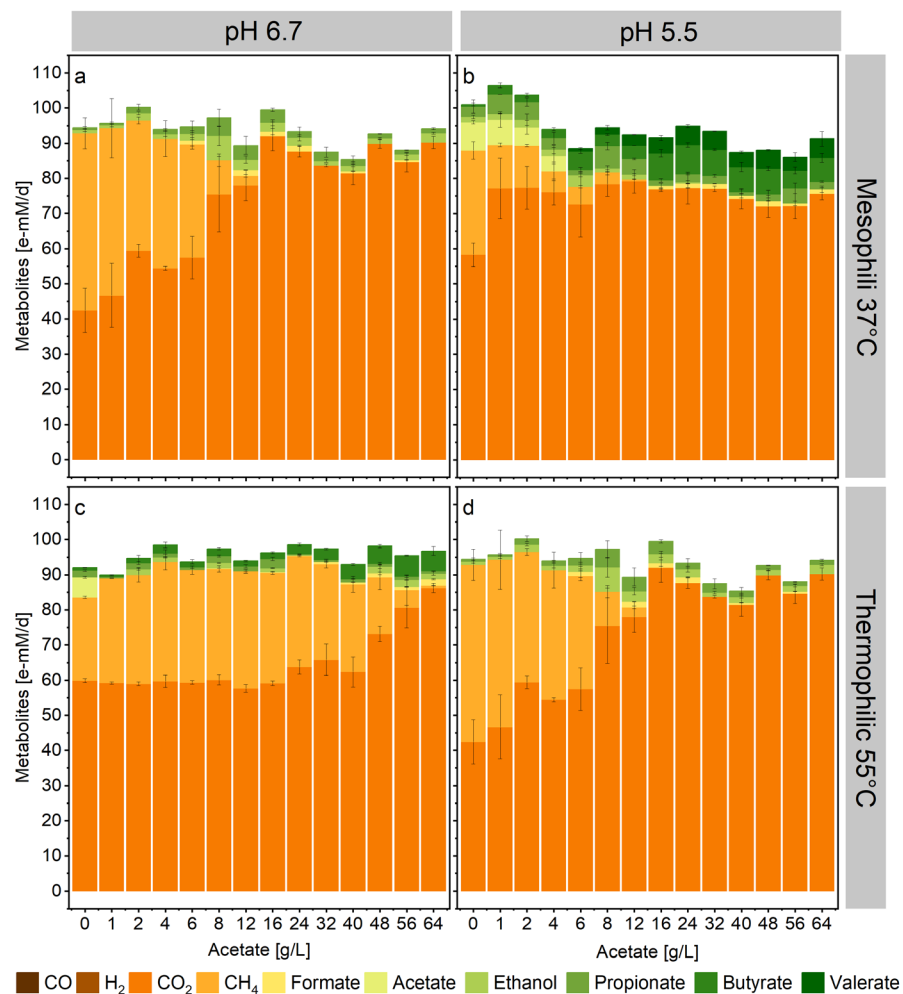


Figure S1. Carbon balancing between substrates (CO and acetate if consumed) and products (CH₄, CO₂, formate, ethanol, propionate, butyrate and valerate and H₂, acetate if produced) at different process conditions and increasing acetate concentrations. Error bars represent standard deviation among replicates ($n=3$).

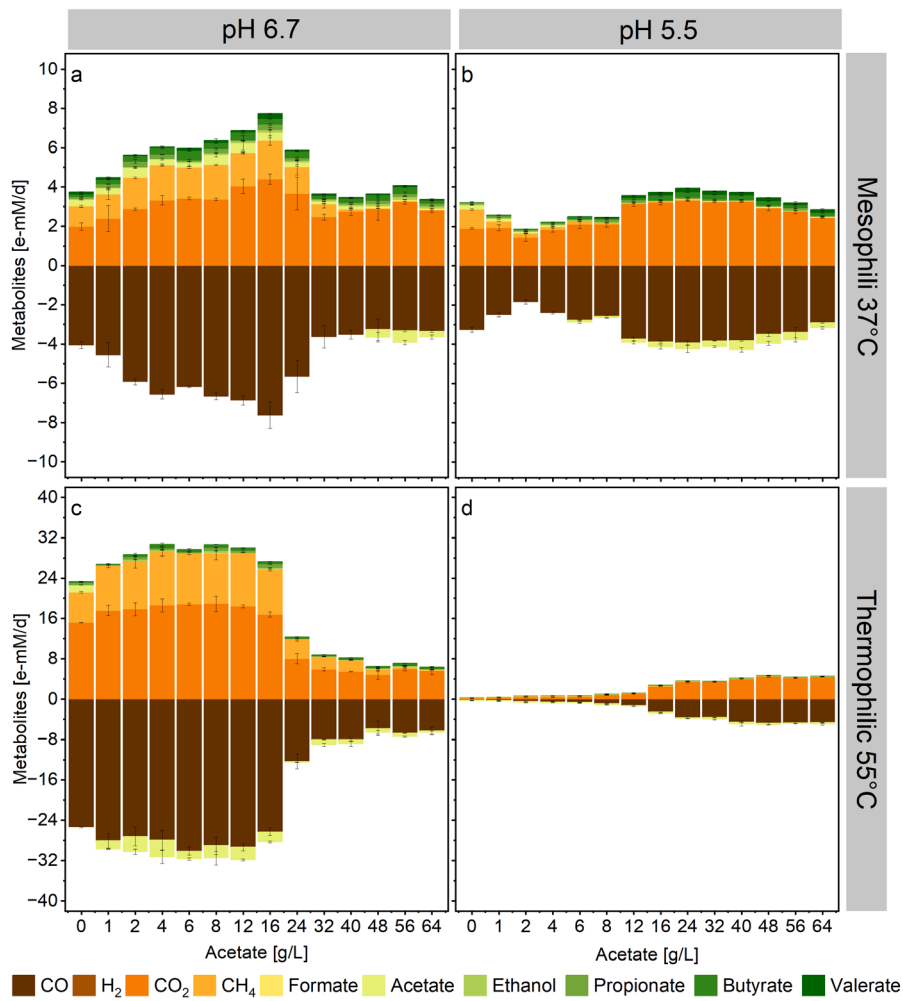


Figure S2. Kinetics of consumption and formation of syngas components (CO, H₂, CO₂ and CH₄) and some short-chain carboxylates (formate, acetate, propionate, butyrate and valerate) and ethanol at different process conditions and increasing acetate concentrations. Negative values indicate consumption. Error bars represent standard deviation among replicates ($n=3$).

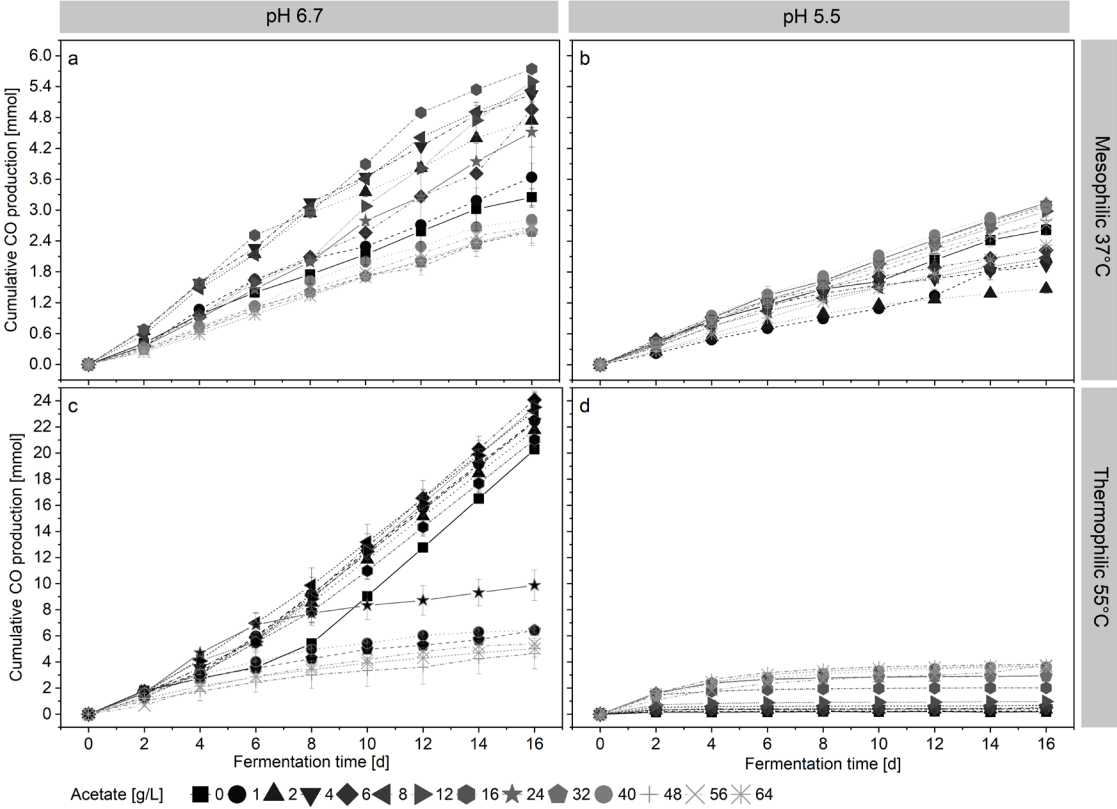


Figure S3. Consumption of CO over time. Error bars represent standard deviation among replicates ($n=3$).

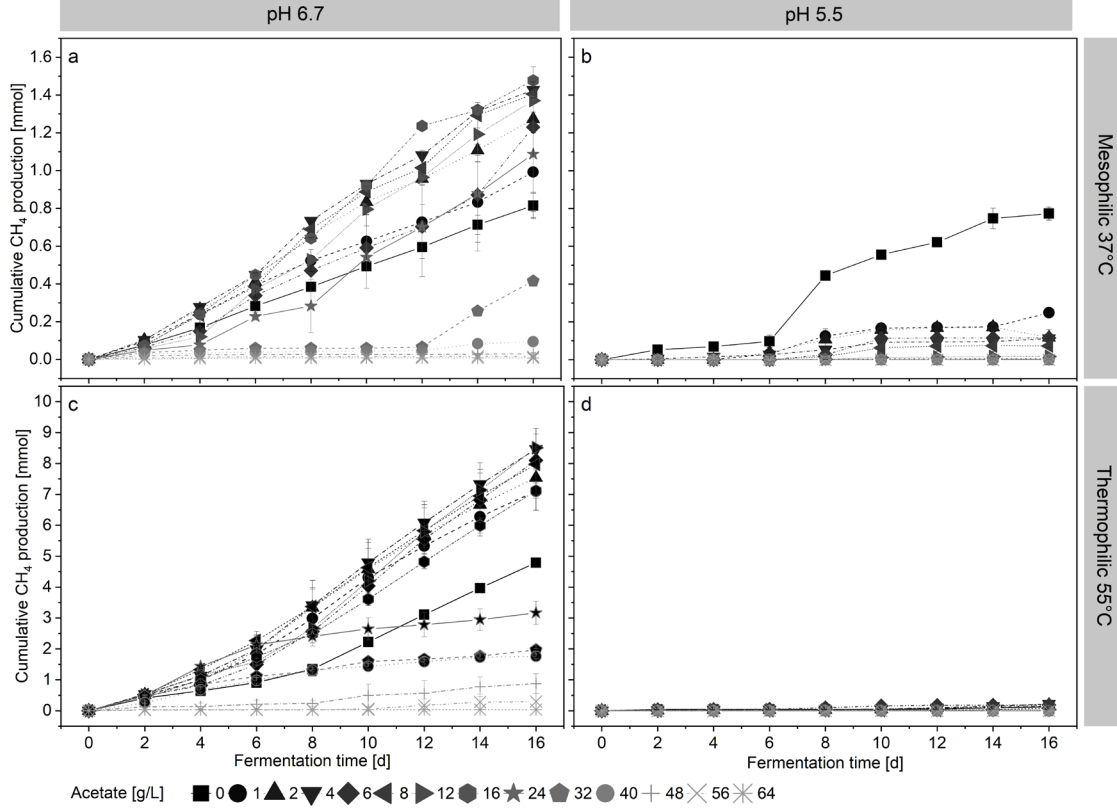


Figure S4. Production of CH₄ over time. Error bars represent standard deviation among replicates (*n*=3).

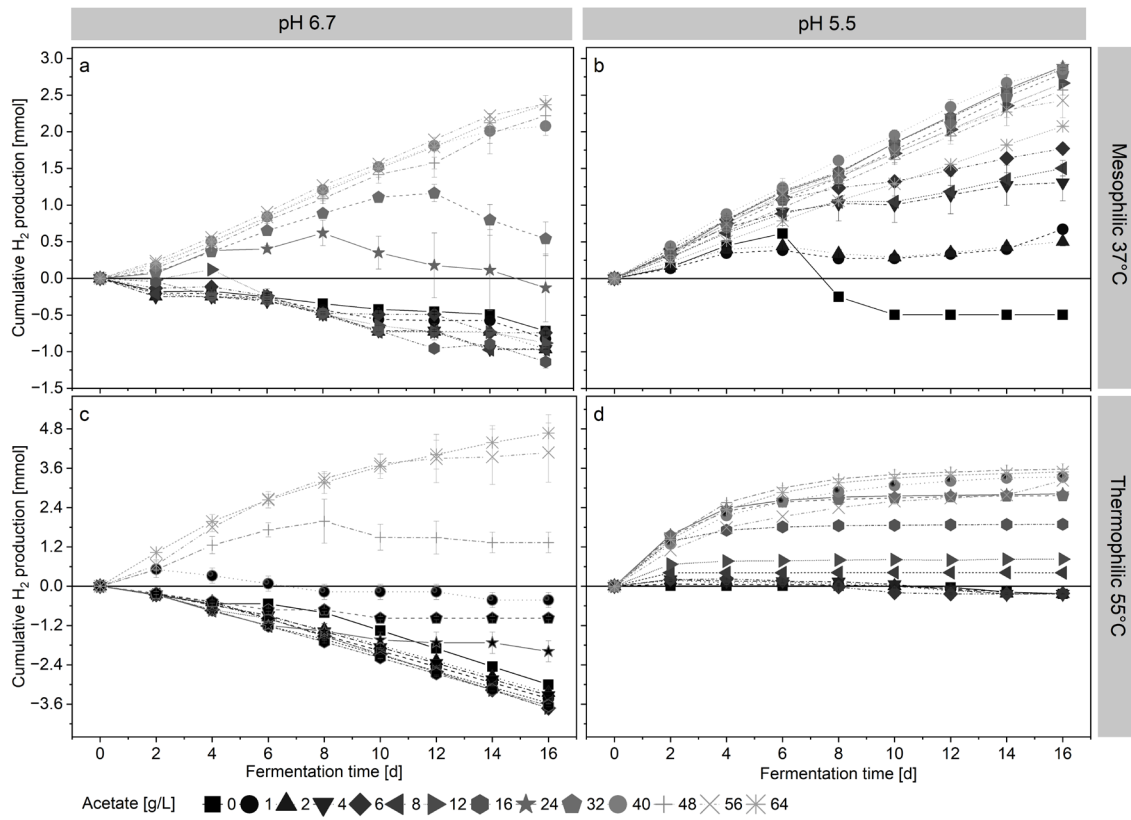


Figure S5. Production of H₂ over time. Negative values indicate consumption. Error bars represent standard deviation among replicates (*n*=3).

Supplementary information

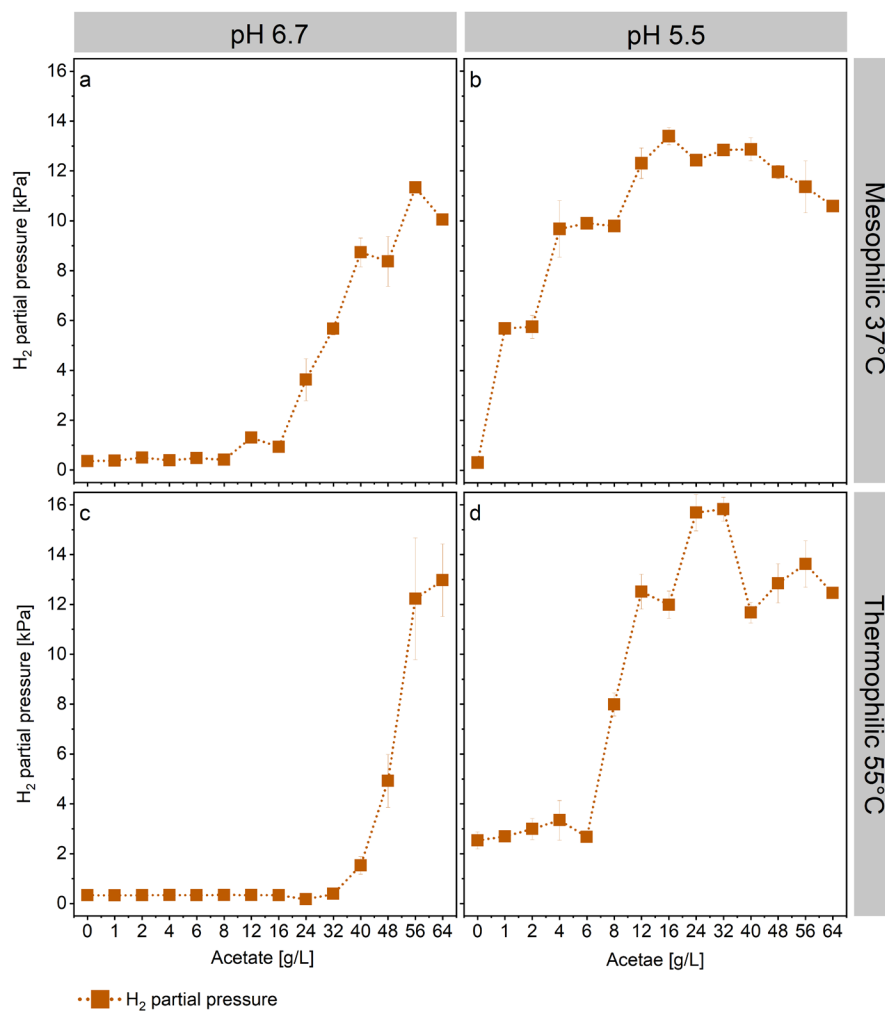


Figure S6. Average H₂ partial pressure throughout the whole fermentation time. Values were determined from H₂ concentrations in the headspace of the bottles at sampling time.

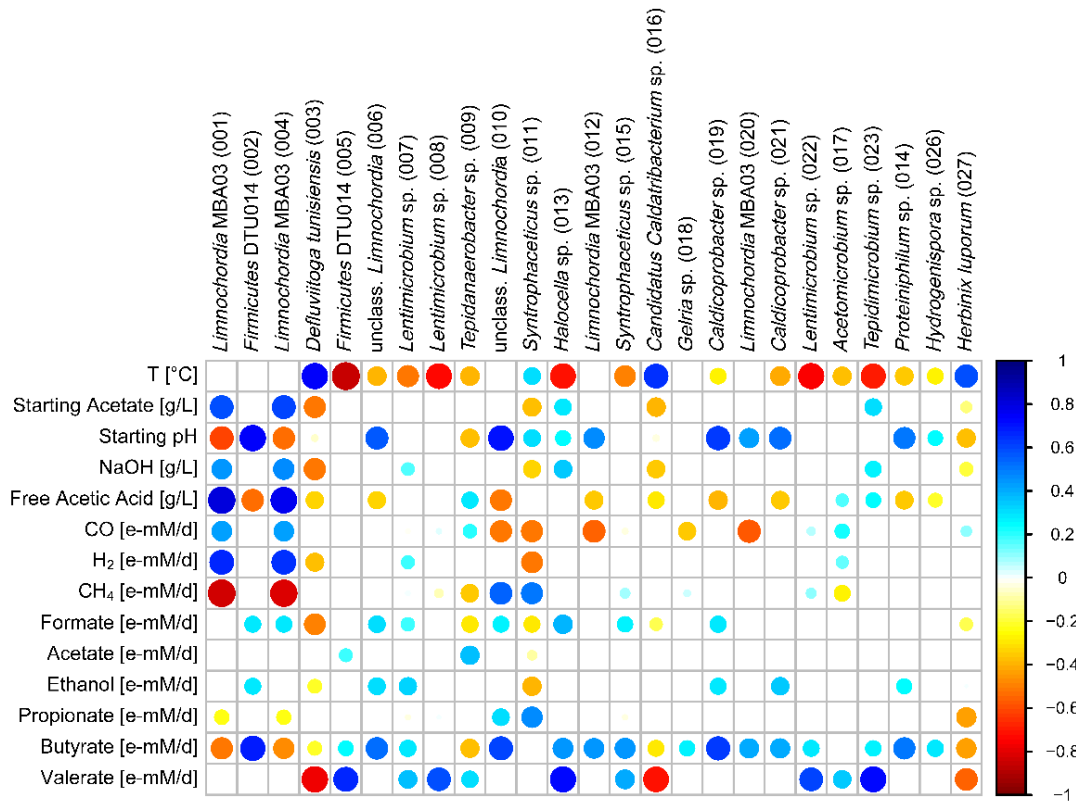


Figure S7. Spearman's rank correlations between relative abundance of dominant amplicon sequencing variants (ASVs) based on 16S rRNA gene and process parameters. The strength of the correlation is represented by the size of the circle and intensity of the color. Blue circles indicate positive correlations. Red circles indicate negative correlations. p values are shown for non-significant correlations ($p > 0.05$).

Supplementary information

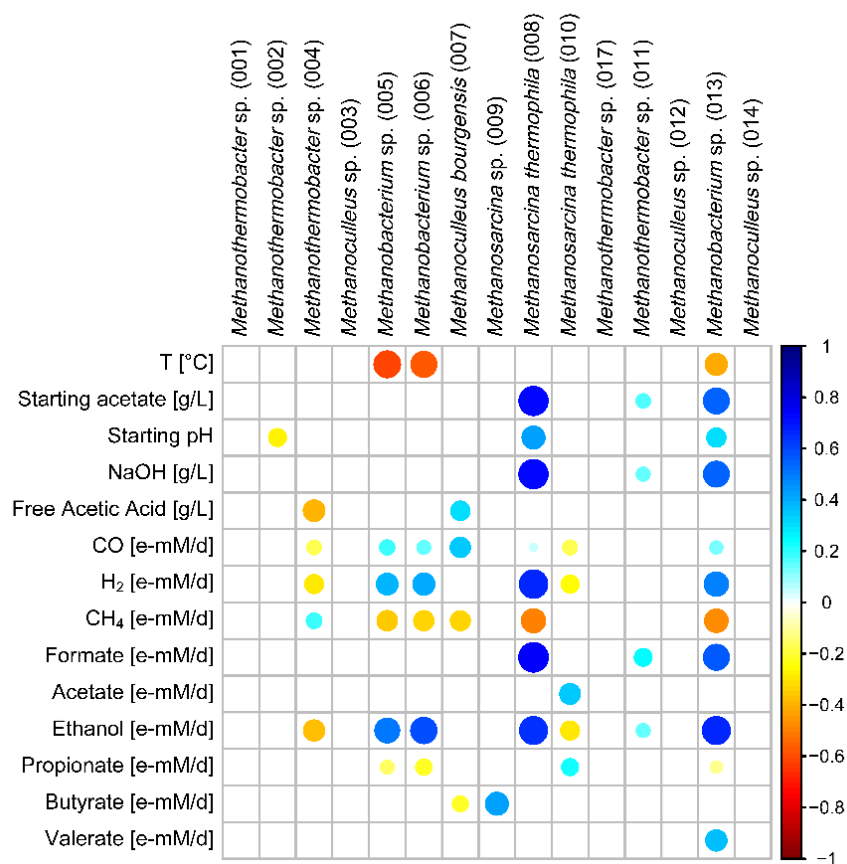


Figure S8. Spearman's rank correlations between relative abundance of dominant amplicon sequencing variants (ASVs) based on *mcrA* gene and process parameters. The strength of the correlation is represented by the size of the circle and intensity of the color. Blue circles indicate positive correlations. Red circles indicate negative correlations. p values are shown for non-significant correlations ($p > 0.05$).

Additional file 2

Table S1. Conversion factors for carbon and electron balances.

Compound	Chemical Formula	(g/mol)	mol C/mol	mol e ⁻ /mol
Acetate	C ₂ H ₄ O ₂	60.0	2.0	8.0
Propionate	C ₃ H ₆ O ₂	74.0	3.0	14.0
Lactate	C ₃ H ₆ O ₃	90.0	3.0	12.0
L-Malate	C ₄ H ₆ O ₅	134.1	4.0	12.0
<i>n</i> -Butyrate	C ₄ H ₈ O ₂	88.0	4.0	20.0
<i>n</i> -Valerate	C ₅ H ₁₀ O ₂	102.1	5.0	26.0
<i>n</i> -Caproate	C ₆ H ₁₂ O ₂	116.1	6.0	32.0
Heptanoate	C ₇ H ₁₄ O ₂	130.2	7.0	38.0
Ethanol	C ₂ H ₆ O	46.0	2.0	12.0
Propanol	C ₃ H ₈ O	60.1	3.0	18.0
Butanol	C ₄ H ₁₀ O	74.0	4.0	24.0
Hydrogen	H ₂	2.0	0.0	2.0
Carbon Monoxide	CO	28.0	1.0	2.0
Carbon Dioxide	CO ₂	44.0	1.0	0.0
Methane	CH ₄	16.0	1.0	8.0

Table S2. Productivities (mM/d) of selected metabolites calculated at 39 days EFT for bottles of the control experiments M-CTRL, T-CTRL, M-BES, T-BES. Gas productivities are the mean value of the productivities calculated between each sampling interval. C2-C6 metabolites productivities were calculated by dividing the net metabolite accumulation (mM) at the end of the fermentation by the total fermentative time. Not detected (nd).

Compound [mM/d]	M-CTRL		T-CTRL		M-BES		T-BES	
	Av.	St.Dev.	Av.	St.Dev.	Av.	St.Dev.	Av.	St.Dev.
CO	-8.17	0.45	-34.30	1.02	-7.68	0.59	-28.70	1.60
CH ₄	4.03	0.18	11.98	0.36	nd	nd	nd	nd
H ₂	-7.10	0.54	-12.77	0.40	-0.76	0.18	29.00	1.59
CO ₂	-1.13	0.06	23.11	0.94	2.16	0.20	27.36	1.38
Lactate	nd	nd	0.01	0.01	0.01	0.00	0.01	0.01
Acetate	0.33	0.05	0.23	0.07	0.95	0.04	0.67	0.09
Propionate	0.03	0.02	0.07	0.03	0.20	0.04	nd	nd
<i>n</i> -Butyrate	0.01	0.01	0.05	0.03	0.18	0.01	0.01	0.01
<i>n</i> -Valerate	nd	nd	nd	nd	0.09	0.03	nd	nd
<i>n</i> -Caproate	nd	nd	nd	nd	0.05	0.01	nd	nd
Ethanol	0.03	0.01	0.04	0.02	0.06	0.02	0.15	0.01
Propanol	nd	nd	nd	nd	0.02	0.016	nd	nd
Butanol	nd	nd	nd	nd	0.02	0.015	nd	nd

Supplementary information

Table S3. Acetate, propionate and *n*-butyrate productivities for all bottles of M-PAC and T-PAC experiments. The productivities were calculated by dividing the net metabolite accumulation (mM) at the end of the fermentations by the total fermentative time (39 d).

PAC [%]	M-PAC			T-PAC		
	Acetate [mM/d]	Propionate [mM/d]	<i>n</i> -Butyrate [mM/d]	Acetate [mM/d]	Propionate [mM/d]	<i>n</i> -Butyrate [mM/d]
0.5	0.93	0.18	0.15	0.17	0.08	0.08
1	0.85	0.23	0.06	0.05	0.12	0.05
1.5	0.87	0.22	0.32	0.63	0.13	0.21
2	0.73	0.47	0.24	1.68	0.04	0.04
2.5	0.85	0.18	0.06	1.67	0.10	0.15
3	0.73	0.23	0.31	1.48	0.04	0.01
3.5	0.89	0.11	0.11	2.33	0.08	0.01
4	0.92	0.07	0.13	1.68	0.09	0.07
5	0.90	0.18	0.13	1.17	0.07	0.03
7.5	0.80	0.14	0.03	0.69	0.11	0.00
10	0.25	0.05	0.02	0.23	0.00	0.03
15	0.06	0.00	0.03	0.06	0.00	0.00
20	0.00	0.00	0.00	0.00	0.00	0.02
30	0.03	0.00	0.00	0.00	0.00	0.00

Table S4. Productivities of CO, CH₄, H₂, CO₂ and VFAs in mM/d at increasing PAC concentrations and different temperatures. Negative productivity indicates consumption. Gas productivities are the mean value of the productivities calculated between each sampling interval. The VFAs productivities were calculated by dividing the net metabolite accumulation (mM) at the end of the fermentations by the total fermentative time.

PAC [%]	0.5	1	1.5	2	2.5	3	3.5	4	5	7.5	10	15	20	30
Mesophilic PAC Fermentations (M-PAC)														
CO [mM/d]	-23.59	-17.77	-15.33	-4.43	-1.87	-1.22	-1.24	-1.56	-0.94	-1.35	-0.39	-0.40	-0.38	-0.34
CH ₄ [mM/d]	5.73	3.97	2.09	0.13	0.05	0.00	0.00	0.00	0.00	0.00	0.00	0.00	0.00	0.00
H ₂ [mM/d]	-8.52	-6.08	-6.12	-0.80	-0.21	-0.11	-0.47	-0.29	-0.14	-0.21	-0.11	-0.11	-0.09	-0.07
CO ₂ [mM/d]	8.81	6.50	3.95	1.65	0.88	0.62	0.65	0.67	0.72	0.76	0.28	0.27	0.22	0.35
VFAs p [mM/d]	1.26	1.15	1.40	1.44	1.10	1.27	1.11	1.12	1.21	0.97	0.32	0.10	0.00	0.033
CO/M-CTRL [%]	231.5	151.3	141.1	50.15	23.91	16.03	15.74	18.95	15.74	8.45	4.37	4.37	4.96	3.79
C-mol balance [%]	76.7	82.5	75.0	131.6	246.1	293.2	246.2	207.7	270.4	265.4	297.1	163.2	146.4	151.4
e-mol balance [%]	94.5	99.5	93.1	173.7	384.6	477.0	290.0	286.8	473.6	292.2	308.6	124.6	-	-
Thermophilic PAC Fermentations (T-PAC)														
CO [mM/d]	-33.57	-34.8	-36.1	-14.74	-12.21	-12.33	-9.10	-9.02	-3.83	-0.59	-0.36	-0.36	-0.38	-0.15
CH ₄ [mM/d]	10.37	12.59	12.33	2.03	0.12	0.02	0.00	0.00	0.00	0.00	0.00	0.00	0.00	0.00
H ₂ [mM/d]	-12.44	-12.66	-12.68	4.99	4.79	13.09	8.22	9.18	3.82	0.44	0.28	0.20	0.13	0.05
CO ₂ [mM/d]	22.18	24.51	25.10	10.01	8.50	12.69	8.31	8.71	3.83	0.94	0.53	0.42	0.38	0.16
VFAs p [mM/d]	0.33	0.22	0.96	1.76	1.91	1.53	2.42	1.84	1.27	0.80	0.26	0.06	0.02	0.00
CO/M-CTRL [%]	97.56	101.3	104.8	36.70	34.80	35.48	26.00	27.15	15.03	1.56	1.02	0.81	1.22	0.41
C-mol balance [%]	100.0	108.3	109.9	109.7	102.2	122.5	140.3	134.5	142.4	436.0	279.4	147.8	111.6	113.5
e-mol balance [%]	96.1	109.7	115.3	121.3	89.5	126.8	141.4	138.3	189.1	618.5	365.2	122.8	-	-

Supplementary information

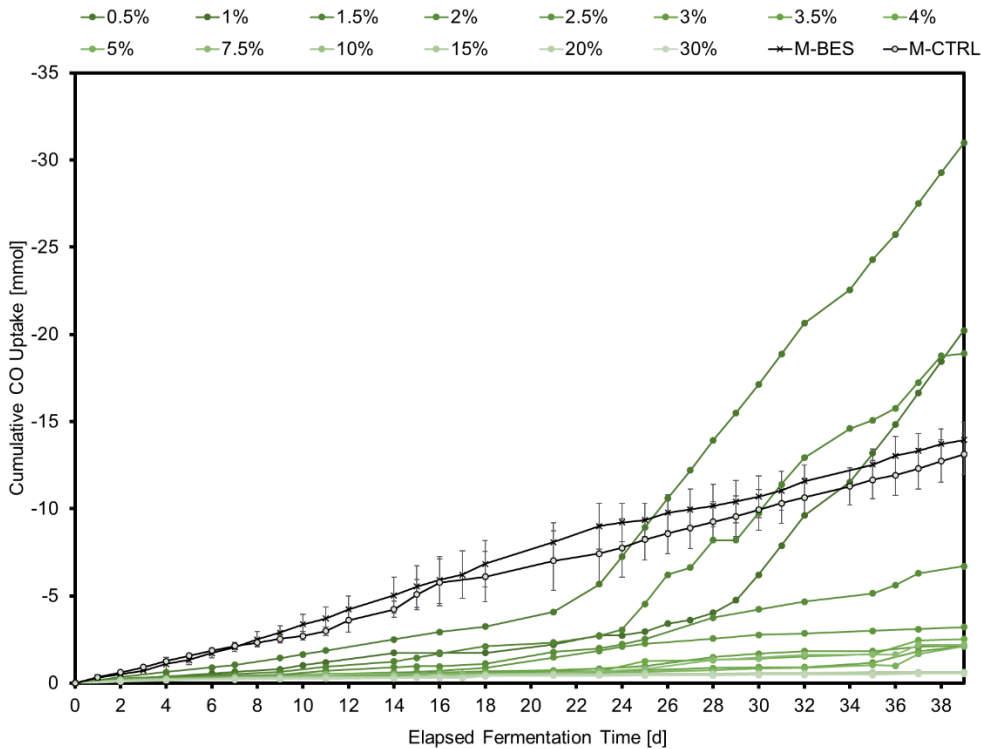


Figure S1. Cumulative CO uptake in mmol for experiments M-BES, M-CTRL and M-PAC.

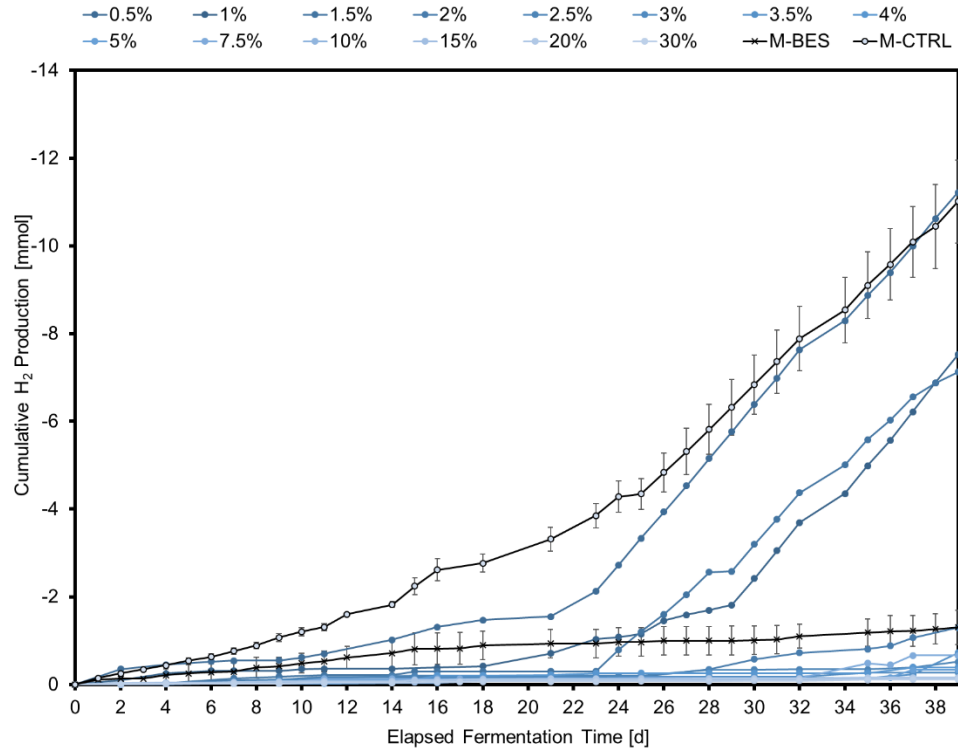


Figure S2. Cumulative H₂ uptake in mmol for experiments M-BES, M-CTRL and M-PAC.

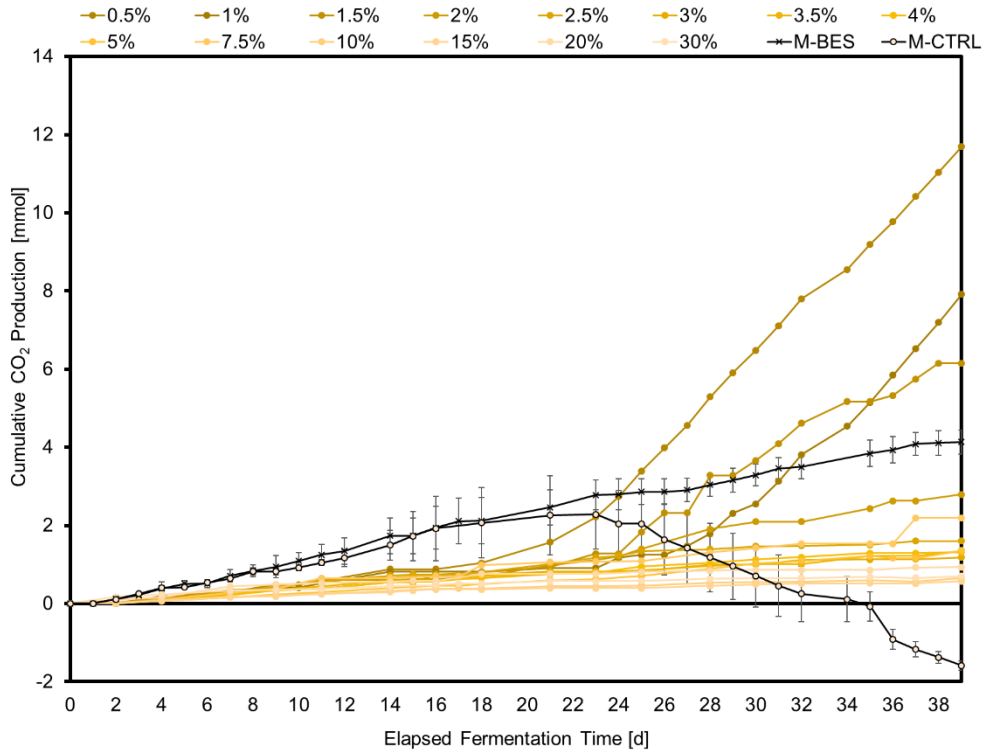


Figure S3. Cumulative CO₂ production in mmol for experiments M-BES, M-CTRL and M-PAC. Negative values mean consumption.

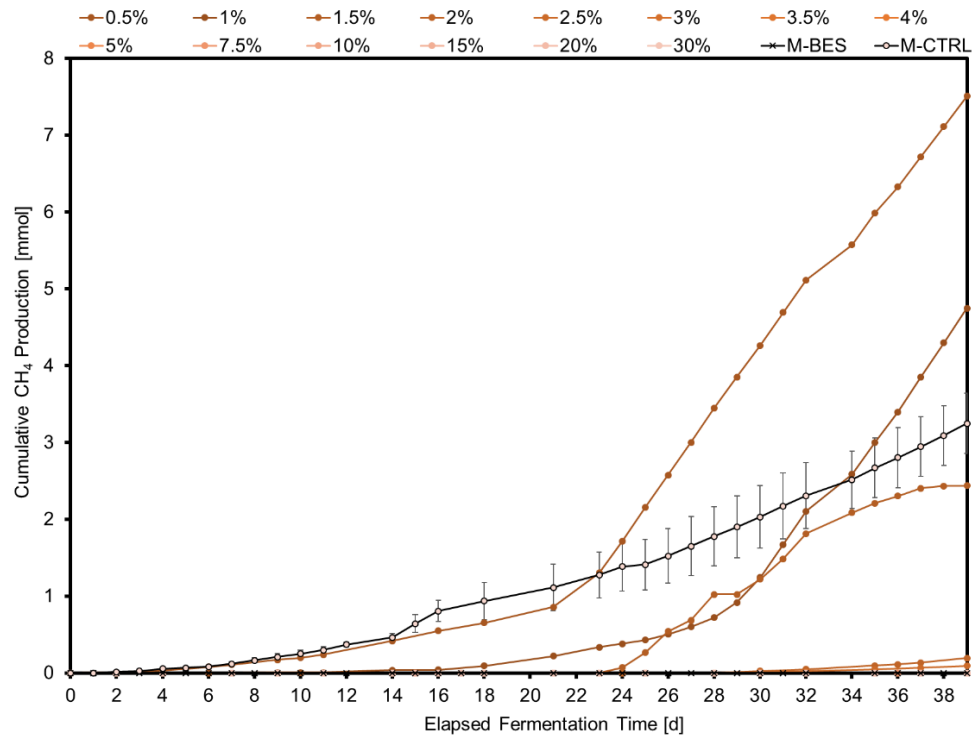


Figure S4. Cumulative CH₄ production in mmol for experiments M-BES, M-CTRL and M-PAC.

Supplementary information

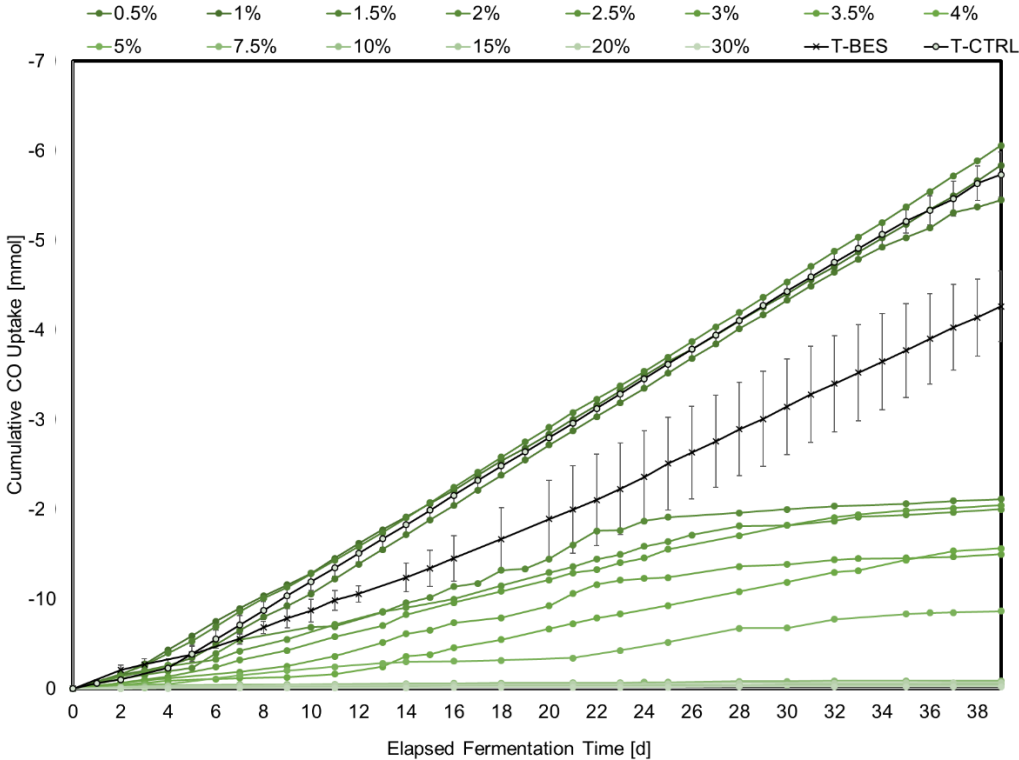


Figure S5. Cumulative CO uptake in mmol for experiments T-BES, T-CTRL and T-PAC.

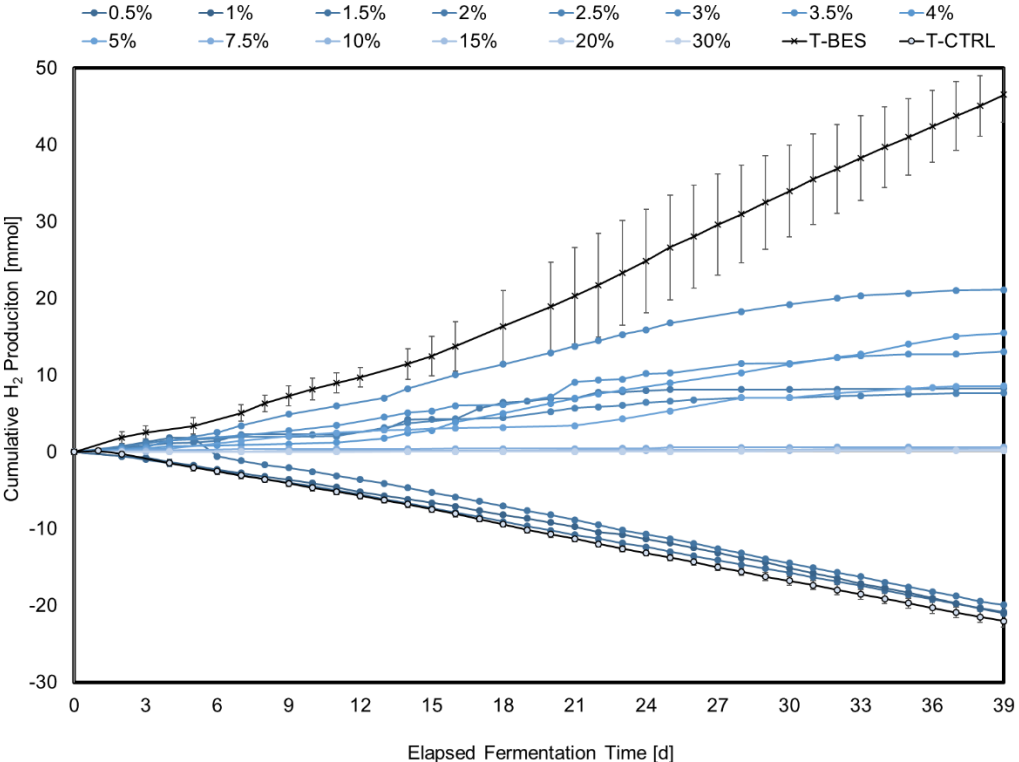


Figure S6. Cumulative H₂ uptake in mmol for experiments T-BES, T-CTRL and T-PAC. Negative values mean consumption.

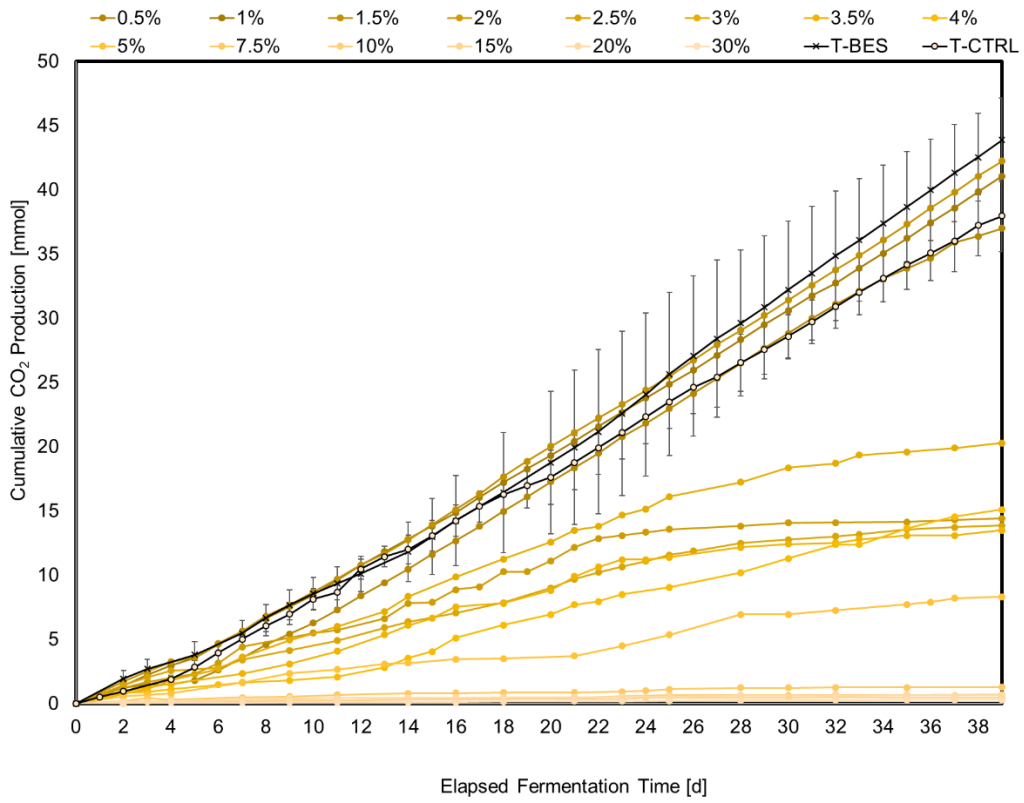


Figure S7. Cumulative CO₂ production in mmol for experiments T-BES, T-CTRL and T-PAC.

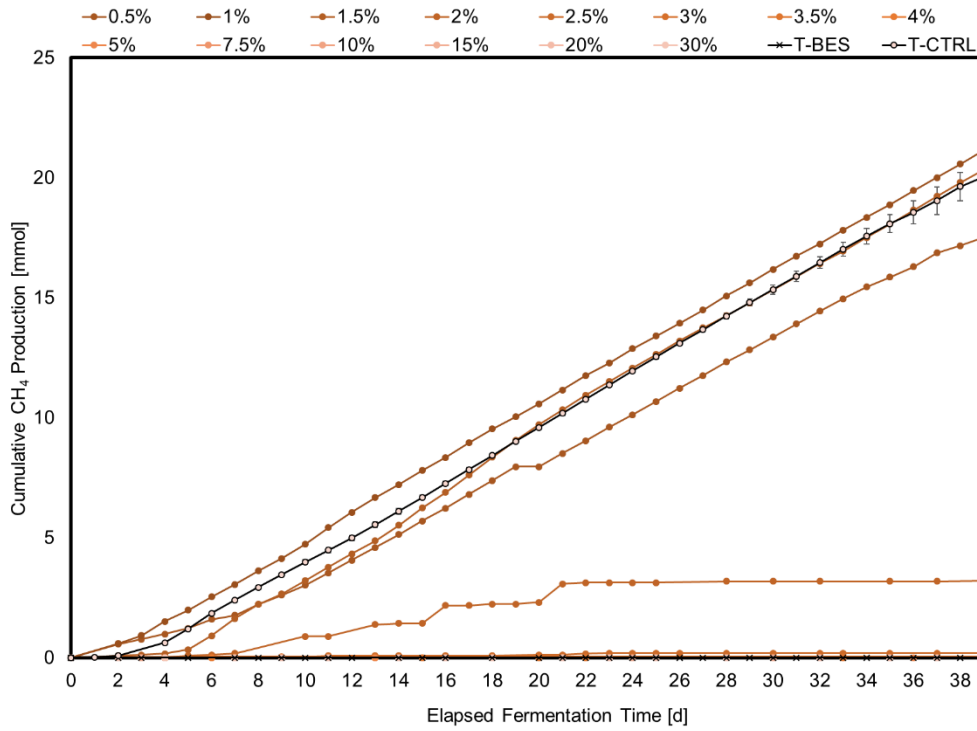


Figure S8. Cumulative CH₄ production in mmol for experiments T-BES, T-CTRL and T-PAC.

Additional file 3*Mass balance of the pyrolysis of sewage sludge and mixed PE plastics*

Table S1. Mass balances of the pyrolysis of sewage sludge and HDPE, LDPE plastics.

Sample		Dry SS	SS	SS Av.	HDPE	LDPE	Av. PE
Waste Flow	g/h	1200	1200	1200	1000	1000	1000
PAC	g/h	155.8	371.8	263.8	66.8	55.2	61
Syngas	g/h	236.2	241	238.6	266.4	250.2	258.3
Yield _{PAC+Syngas}	%	32.7	51.1	41.9	33.3	30.5	31.9

Characterization of the sewage sludge PAC and the mixed PE plastics PAC

Table S2. Anions and cations concentration for sewage sludge PAC and the mixed PE plastics PAC.

Parameter	Concentration	Sewage Sludge PAC	PE Plastics PAC
Fluoride	mg/l	n.b.	n.b.
Chloride	mg/l	< 100	1720
Nitrite	mg/l	< 5.0	n.b.
Bromide	mg/l	n.b.	< 5.0
Nitrate	mg/l	448	5.87
Phosphate	mg/l	< 10	< 10
Sulfate	mg/l	1940	168
Aluminium	mg/l	1.8	1.6
Arsenic	mg/l	3.7	< 0.1
Barium	mg/l	0.11	< 0.1
Calcium	mg/l	15	6.2
Cadmium	mg/l	< 0.1	< 0.1
Cobalt	mg/l	0.22	< 0.1
Chrome	mg/l	5.9	3.7
Copper	mg/l	< 0.1	< 0.1
Iron	mg/l	47	26
Magnesium	mg/l	1.6	0.23
Manganese	mg/l	< 0,1	0.32
Nickel	mg/l	13	3.3
Phosphor	mg/l	4.3	0.12
Lead	mg/l	< 0.1	< 0.1
Antimony	mg/l	3.7	< 0.2
Silicium	mg/l	128	29
Tin	mg/l	0.67	0.63
Thallium	mg/l	< 0.1	< 0.1
Zinc	mg/l	0.11	1.2

Table S3. HPLC and GC-MS characterization of the raw aqueous condensate deriving from the fast pyrolysis of sewage sludge. The GC-MS characterization was performed by the Thünen Institute of Wood Research, (Hamburg, Germany). The total GC-MS chromatogram area: 1.06E+08. Area of 12 identified peaks =

9.30E+07 (88%). Area of unknown peaks = 1.27E+07 (12%). Error bars represent standard deviation among replicates ($n=2$).

Compound		Concentration g/L	
		Average	St.Dev.
Acetate	HPLC	9.9	0.02
Propionate	HPLC	3.73	0.05
Butyrate	HPLC	1.85	0.01
Phenol	HPLC	0.53	0.02
Guaiacol	HPLC	0.62	0.01
<i>p</i> -Cresol	HPLC	0.49	0.02
<i>m</i> -Cresol	HPLC	3.46	0.24
Pyridine	HPLC	3.1	0.02
4-Penten-2-one, 4-methyl- (NIST MQ 92)	GC-MS	2.46	0.12
3-Penten-2-one, 4-methyl- (NIST MQ 92)	GC-MS	5.69	0.22
2-Pentanone, 4-amino-4-methyl- (NIST MQ 86)	GC-MS	27.69	0.42
Acetamide (NIST MQ 94)	GC-MS	1.18	0.1
unknown N-Compound (no NIST spectrum found)	GC-MS	41.11	0.93
unknown N-Compound (no NIST spectrum found)	GC-MS	1.06	0.03
unknown N-Compound (no NIST spectrum found)	GC-MS	1.38	0.02
Triacetoneamine (NIST MQ 87)	GC-MS	32.55	0.01
2-Pyrrolidinone (NIST MQ 94)	GC-MS	1.59	0.03
unknown N-Compound (no NIST spectrum found)	GC-MS	0.60	0.02

Table S4. HPLC and GC-MS characterization of the raw aqueous condensate deriving from the fast pyrolysis of mixed PE plastics. The GC-MS characterization was performed by the Thunen Institute of Wood Research, (Hamburg, Germany). The total GC-MS chromatogram area: 2.89E+07. Area of 11 identified peaks = 2.22E+07 (76.8%). Area of unknown peaks = 6.70E+06 (23.2%). Error bars represent standard deviation among replicates ($n=2$).

Compound		Concentration g/L	
		Average	St.Dev.
Acetate	HPLC	14.26	0.26
Propionate	HPLC	2.73	0.01
Butyrate	HPLC	0.62	0.07
<i>p</i> -Cresol	HPLC	0.37	0.02
Benzene	HPLC	0.58	0.03
Butanol, 1-	GC-MS	0.39	0.01
Acetol (Hydroxyacetone)	GC-MS	8.93	0.21
Cyclopentanone	GC-MS	1.21	0.24
Phenol	GC-MS	9.62	0.08
<i>m</i> -Cresol	GC-MS	1.24	0.12
Benzonitrile (NIST MQ 84)	GC-MS	1.14	0.01
1,3-Dioxolane, 2,2-dimethyl-	GC-MS	0.20	0.02
1,4-Dioxane (NIST MQ 83)	GC-MS	0.16	0.01
2-Chloroethanol (NIST MQ 86)	GC-MS	0.55	0.004

Table S5. Conversion factors for electron balances.

Compound	Chemical Formula	Molecular Weight	mol e ⁻ /mol
Formate	CH ₂ O ₂	46.1	2.0
Acetate	C ₂ H ₄ O ₂	60.0	8.0
Propionate	C ₃ H ₆ O ₂	74.0	14.0
Butyrate	C ₄ H ₈ O ₂	88.1	20
Hydrogen	H ₂	2.0	2.0
Carbon Monoxide	CO	28.0	2.0
Carbon Dioxide	CO ₂	44.0	0.0
Methane	CH ₄	16.0	8.0

Syngas and Sewage Sludge PAC co-fermentation

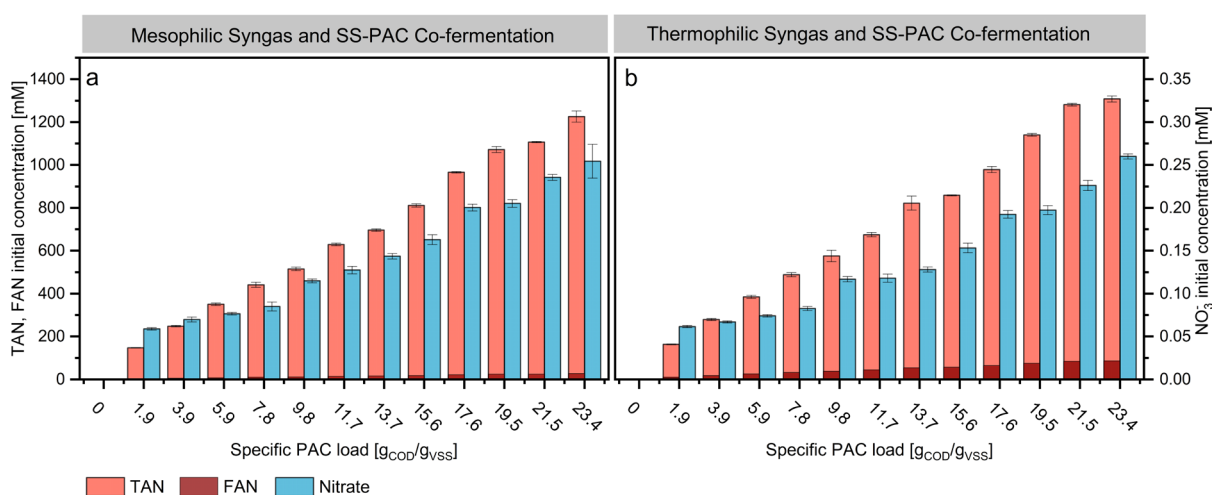


Figure S1. Total ammonium nitrogen (TAN), free ammonia nitrogen (FAN), and nitrate concentrations [mM] at inoculation conditions for M-SS-PAC and T-SS-PAC experiments. Error bars represent standard deviation among replicates ($n=3$).

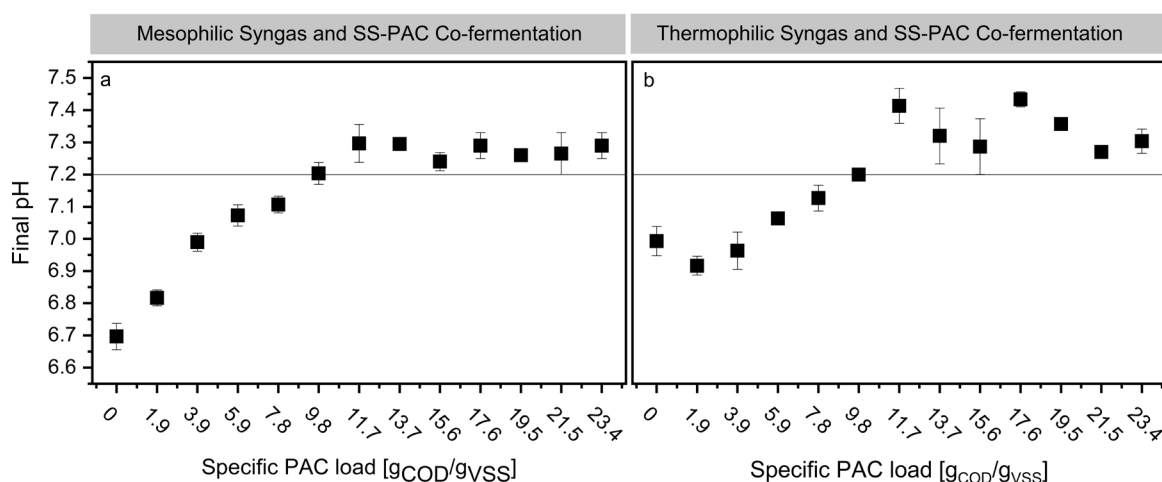


Figure S2. Final average pH from fermentation at increasing sewage sludge PAC loadings. Error bars represent standard deviation among replicates ($n=3$).

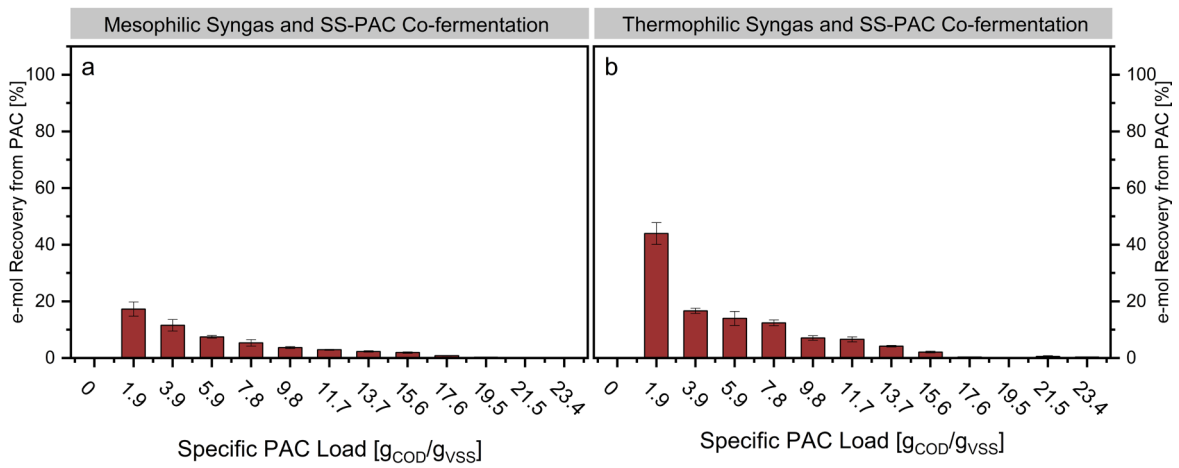


Figure S3. e-mol recoveries from SS-PAC calculated as described in Eq.2 for M-SS-PAC and T-SS-PAC experiments. Error bars represent standard deviation among replicates ($n=3$).

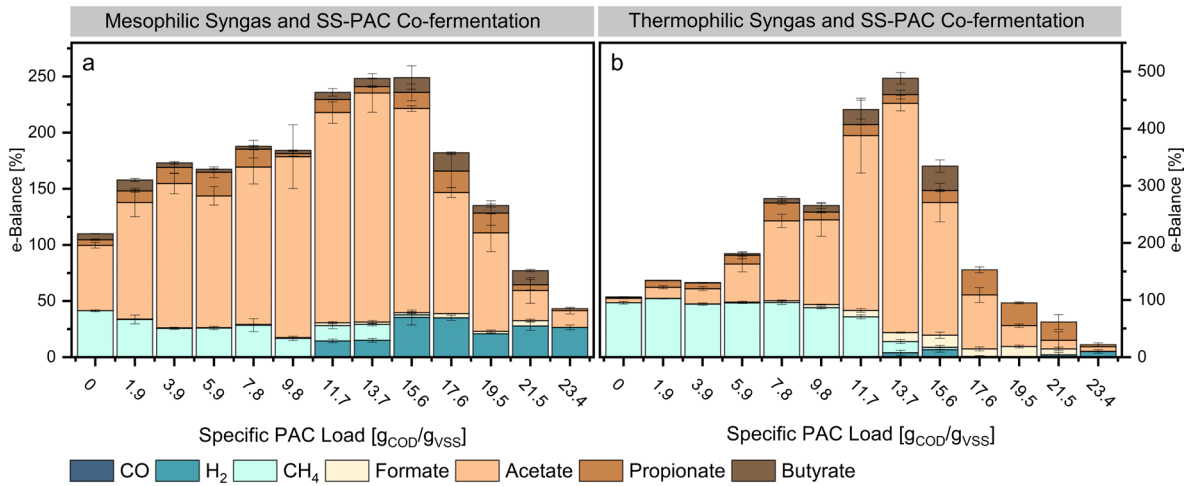


Figure S4. The graphs a and b show the e-equivalents balance [$e\text{-mol}_{\text{products}}/e\text{-mol}_{\text{syngas, fixed}}$] for each load of SS-PAC. Values above 100% indicate that the sum of the e-mol in the products is higher than the e-mol consumed from syngas. Error bars represent standard deviation among replicates ($n=3$).

Syngas and HDPE/LDPE PAC co-fermentation

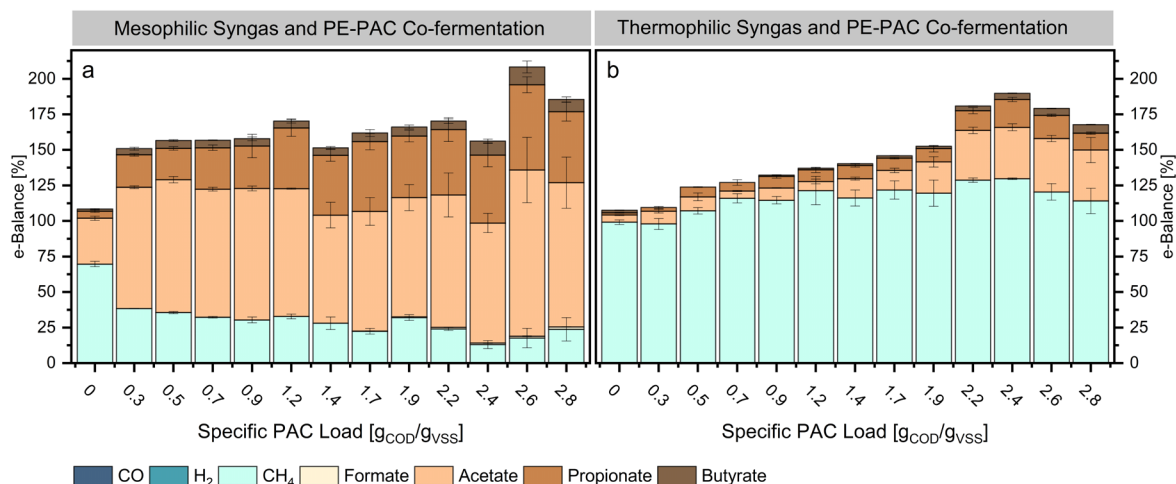


Figure S5. The graphs a and b show the e-equivalents balance $[e\text{-mol}]_{\text{products}}/e\text{-mol}]_{\text{syngas, fixed}}$ for each load of PE-PAC. Values above one indicate that the sum of the e-mol in the products is higher than the e-mol consumed from syngas. Error bars represent standard deviation among replicates ($n=3$).

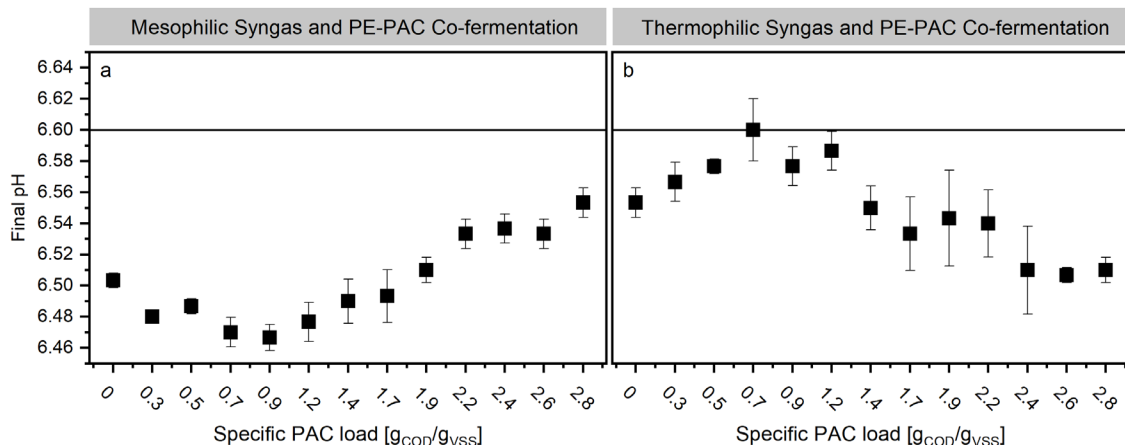


Figure S6. Final average pH from fermentation at increasing mixed PE plastics PAC loadings. Error bars represent standard deviation among replicates ($n=3$).

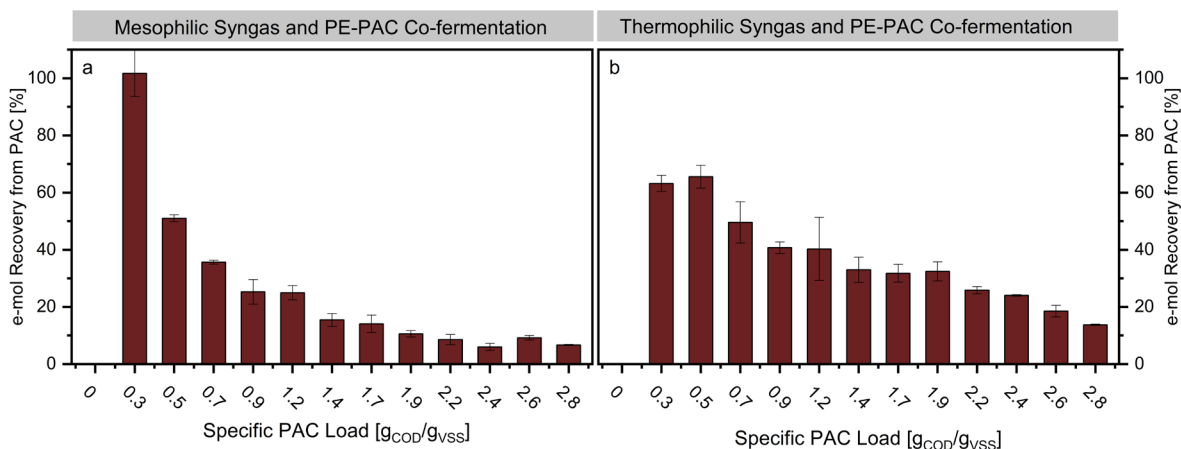


Figure S7. e-mol recoveries from SS-PAC calculated as described in Eq.2 for M-SS-PAC and T-SS-PAC experiments. Error bars represent standard deviation among replicates ($n=3$).

Additional file 4*Characterization of the Miscanthus Pyrolysis Aqueous Condensate*

Table S1. GC-MS characterization of the aqueous condensate deriving from the fast pyrolysis of Miscanthus was performed by the Thünen Institute of Wood Research, (Hamburg, Germany).

Compound	wt.% wet	
	Average	St.Dev.
Water Content	81.700	1.744
Acetic acid	3.406	0.790
Propionic acid	0.508	0.080
Butyric acid	0.050	0.000
Acetic acid 2-hydroxyethyl ester	0.040	0.004
Propanoic acid methyl ester	0.013	0.007
Ethylene glycol	1.541	0.861
2-Propen-1-ol (NIST MQ 84)	0.050	0.010
Acetaldehyde, hydroxy-	0.496	0.079
Propionaldehyde, 3-hydroxy	0.087	0.007
Butyraldehyde	0.018	0.002
Crotonaldehyde, cis	0.156	0.004
Crotonaldehyde, trans	0.043	0.004
2-Butenal, 2-methyl- (NIST MQ 92)	0.011	0.002
poss: 2-Pentenal, (E)- (NIST MQ 89)	0.012	0.002
Butanedial or Propanal (NIST MQ 88)	0.037	0.015
Acetol (Hydroxypropanone)	2.704	0.616
Acetylacetone (Hexandione, 2,5-)	0.006	
Butanone, 2-	0.128	0.006
Butanone, 1-hydroxy-2-	0.288	0.042
Butandione, 2,3- (Diacetyl)	0.364	0.012
Acetoin (Hydroxy-2-butanone, 3-)	0.041	0.009
Propan-2-one, 1-acetyloxy-	0.062	0.020
Cyclopentanone	0.083	0.003
Cyclopenten-1-one, 2-	0.145	0.029
Cyclopenten-1-one, 2,3-dimethyl-2-	0.009	0.003
Cyclopenten-1-one, 2-methyl-2-	0.051	0.009
Cyclopenten-1-one, 3-methyl-2-	0.022	0.004
Cyclopenten-1-one, 2-hydroxy-2-	0.010	0.002
Cyclopenten-3-one, 2-hydroxy-1-methyl-1-	0.062	0.007
Cyclohexen-1-one, 2-	0.004	0.001
Methyl vinyl ketone = 2-Butenone (NIST MQ 90)	0.013	0.004
poss: 2-Butanone, 3-methyl- (NIST MQ 88)	0.031	0.006
3-Buten-2-one, 3-methyl- (NIST MQ 88)	0.031	0.002
2,3-Pentanedione	0.068	0.007
3-Penten-2-one (NIST MQ 84)	0.036	0.004

Supplementary information

2-Butanone, 4-hydroxy- (NIST MQ 84)	0.021	0.003
poss: 2-Pentanone, 4-hydroxy- (NIST MQ 82)	0.017	0.004
Isomere of 2-Cyclopenten-1-one, 3-methyl-	0.011	0.002
2-Butanone, 1-hydroxy-3-methyl- (NIST MQ 78)	0.009	0.002
2-Cyclopenten-1-one, 3,4-dimethyl-	0.013	0.002
4-Cyclopentene-1,3-dione (NIST MQ 86)	0.009	
2-Cyclopenten-1-one, 2,3,4-trimethyl- (NIST MQ 88)	0.005	0.002
Isomere of Cyclopenten-1-one, 2,3-dimethyl-2-	0.020	
Furanone, 2(5H)-	0.073	0.020
Furaldehyde, 2-	0.399	0.067
Furaldehyde, 3-	0.026	0.006
Furaldehyde, 5-methyl-2-	0.018	0.005
Ethanone, 1-(2-furanyl)-	0.021	0.003
Furan-2-one, 5-methyl-, (5H)-	0.018	0.001
Furan-2-one, 3-methyl-, (5H)-	0.016	0.008
Furan-2-one, 2,5-dihydro-3,5-dimethyl-	0.023	0.007
Butyrolactone, γ -	0.030	0.008
Furan, tetrahydro-2-methoxy- (NIST MQ (/))	0.005	
Furan-2-one, 4-methyl-(5H)- (NIST MQ 88)	0.008	0.004
Benzene, 1-methoxy-3-methyl-	0.003	
Benzene, 1-methoxy-4-methyl-	0.006	
Benzaldehyde	0.005	0.001
poss: Benzaldehyde, 2-hydroxy-	0.008	0.002
Phenol	0.056	0.010
Cresol, o-	0.028	0.005
Cresol, p-	0.027	0.005
Cresol, m-	0.016	0.002
Phenol, 2,5-dimethyl-	0.007	0.000
Phenol, 2,4-dimethyl-	0.005	0.002
Phenol, 2,6-dimethyl-	0.004	0.001
Phenol, 4-ethyl-	0.036	0.013
Phenol, ethyl-methyl-	0.004	0.001
Guaiacol	0.072	0.016
Guaiacol, 4-methyl-	0.033	0.009
Guaiacol, 4-ethyl-	0.015	0.004
Guaiacol, 4-allyl- (Eugenol)	0.007	0.002
Guaiacol, 4-propyl-	0.002	0.001
Guaiacol, 4-propenyl- cis (Isoeugenol)	0.007	0.003
Vanillin	0.019	
Syringol	0.010	0.003
Syringol, 4-methyl-	0.003	0.001
2-Acetyl-5-norbornene (NIST MQ 92)	0.005	0.001
1,3-Dioxolane, 2-methyl- (NIST MQ 62)	0.019	0.007
1,3-Dioxolane, 2-ethyl-	0.003	0.001
poss: 1,4-Dioxin, 2,3-dihydro-	0.012	0.003

2,2'-Bi-1,3-dioxolane (NIST MQ 87)	0.018	0.003
------------------------------------	-------	-------

Fermentation medium

The modified BA medium was composed as follows. For each liter of medium added: 100 mL of mineral salt solution, 800 mL of phosphate buffer solution, 10 mL of vitamin solution, 10 mL of trace elements solution, 5 mL of resazurin solution and 3 mL of reducing agent solution. The mineral salt solution was prepared with the following salt concentrations: NH_4Cl , 161.2 g/L; $\text{MgCl}_2 \times 6\text{H}_2\text{O}$, 5.4 g/L; $\text{CaCl}_2 \times 2\text{H}_2\text{O}$ 6.5 g/L, NaCl , 30 g/L. The phosphate buffer solution was prepared with 136 g/L KH_2PO_4 . The vitamin solution was composed of: biotin, 0.002 g/L; folic acid, 0.002 g/L; pyridoxin, 0.01 g/L; thiamin, 0.005 g/L; riboflavin, 0.005 g/L; nicotinic acid, 0.005 g/L; Ca-pantothenate, 0.005 g/L; vitamin B12, 0.005 g/L; aminobenzoic acid, 0.005 g/L; liponic acid, 0.005 g/L). The trace elements solution contained the following compounds: $\text{FeCl}_2 \times 4\text{H}_2\text{O}$, 1.5 g/L; MnCl_2 , 0.1 g/L; $\text{CoCl}_2 \times 6\text{H}_2\text{O}$, 0.19 g/L; ZnCl_2 , 0.07 g/L; $\text{CuCl}_2 \times 2\text{H}_2\text{O}$, 0.002 g/L; $\text{NiCl}_2 \times 6\text{H}_2\text{O}$, 0.024 g/L; $\text{Na}_2\text{MoO}_4 \times 2\text{H}_2\text{O}$, 0.036 g/L; H_3BO_3 , 0.006 g/L; $\text{Na}_2\text{SeO}_3 \times 5\text{H}_2\text{O}$, 0.003 g/L; $\text{Na}_2\text{WO}_4 \times 2\text{H}_2\text{O}$, 0.02 g/L. The reducing agent solution contained 100 g/L of L-cysteine. The resazurin solution contained 1 g/L resazurin sodium salt. All reagent-grade chemicals were purchased from Sigma-Aldrich (Schnelldorf, Germany) or Carl Roth (Karlsruhe, Germany).

Syngas and PAC load composition

Table S2. Composition in gCOD/Ld and electron moles (e-mM/d) of the feed (for both syngas and PAC) for both the mesophilic and the thermophilic semi-continuous fermentations.

PAC load	1 % v/v	2 % v/v	3 % v/v	4 % v/v	5 % v/v	6 % v/v
gCOD _{PAC} /Ld	0.13	0.25	0.38	0.51	0.63	0.76
gCOD _{Syngas} /Ld	2.6	2.6	2.6	2.6	2.6	2.6
gCOD _{Total} /Ld	2.73	2.85	3.0	3.1	3.2	3.3
e-mol _{PAC} /Ld	15.8	31.7	47.5	63.3	79.1	95.0
e-mol _{Syngas} /Ld	326.3	326.3	326.3	326.3	326.3	326.3
e-mol _{Substrates} /Ld	342.1	358.0	373.8	389.6	405.5	421.3

Equations

Estimation of VSS concentration

Between each re-inoculation event, the concentration of volatile suspended solids (VSS) at time $t=j$ was determined as described by Eq. S1.

$$\text{VSS}_{\text{Est},j} = \text{TSS}_j - \text{TFS}_{\text{Res},j} \text{ [g/L]} \quad \text{Eq.S1}$$

Where TSS_j was determined experimentally at time $t=j$. As mentioned in the materials and methods section, the weight of the dried pellet was measured and assumed

to be representative of the suspended fraction (TSS) of the total solids (TS). The residual amount of the total fixed solids ($TFS_{Res,j}$) was calculated using the following equation:

$$TFS_{Res,j} = TFS_{Res,j-1} - TFS_{Res,j-1} * \frac{1}{HRT} [g/L] \quad Eq.S2$$

$TFS_{Res,j-1}$ is the residual amount of the total fixed solids determined at time $t=j-1$. HRT is the hydraulic retention time and was $HRT = 20$ d in this study. The initial TFS was determined by multiplying the TFS of the inoculum by the dilution factor of the inoculation.

PAC components removal

The concentration of each selected PAC component in the fermentation medium was determined via HPLC analysis of a solution composed of BA medium with PAC concentrations similar to those reported in Table S2. The removal efficacy of a selected PAC component i at time $t=j$ was calculated with the following equation:

$$Removal\ Efficacy_{m,j} = \frac{C_{m,j}}{C_{Th.Broth,m,j}} * 100 [\%] \quad Eq.S3$$

Where $C_{m,j}$ is the concentration of compound i at time $t=j$ determined experimentally via HPLC and $C_{Th.Broth,m,j}$ is the theoretical concentration of the compound i at time $t=j$ in the fermentation broth considering an accumulation in an abiotic system, as shown in equation Eq.S4.

$$C_{Th.Broth,i,j} = C_{Th.Broth,i,j-1} + d * (C_{Feed,i} - C_{Th.Broth,i,j-1}) [g/L] \quad Eq.S4$$

Where $C_{Th.Broth,m,j}$ is the theoretical concentration of the compound i at time $t=j-1$; $C_{Feed,m}$ is the determined concentration of the compound i in the feed and d is the dilution rate of the system. The volume of the broth is considered constant and equal to 1.5 L and constant are considered to be also the daily feed and removal (0.075 L/d) of the fermentation broth.

E-mol balances

The daily e-mol recovery was calculated as described by Eq. 5 to determine the daily load of e-mol from PAC.

$$e\text{-mol Recovery}_j = \frac{\sum e\text{-mol}_{Products}}{\sum e\text{-mol}_{Substrates}} * 100 [\%] \quad Eq.S5$$

The $\sum e\text{-mol}_{Substrates}$ is the sum of the daily e-mol from syngas and from PAC per broth volume fed into the bioreactors. The volume of the broth is considered constant and equal to 1.5 L. Hydrogen is considered a substrate only when it was consumed, otherwise a product and was accounted as such.

$$e\text{-mol}_{Syngas} = \dot{n}_{CO} * ee_{qCO} + \dot{n}_{H_2} * ee_{qH_2} [e\text{-M/d}] \quad Eq.S6$$

$$e\text{-mol}_{PAC} = \frac{\dot{m}_{COD,PAC}}{ee_{qPAC}} [e\text{-M/d}] \quad Eq.S7$$

Where \dot{n} of CO and H₂ are the daily uptake rates determined as described in another work [148]. $\dot{m}_{\text{COD,PAC}}$ is the daily flow rate of gCOD of PAC in the feed. We assumed that 1 mol of electron equivalents is equal to 8 gCOD. Considering that the COD (Chemical oxygen demand) is the oxygen required to completely oxidize the carbonaceous fraction of organic compounds and that 1 eeq. is released upon complete oxidation of carbonaceous compounds, then from the half reaction R.S1, it can be assumed that 1/4 mol of O₂ (8 g) would be consumed in accepting the 1 e-mol.



The $\text{e-mol}_{\text{Products}}$ is the sum of the daily production rate in e-mol of methane, H₂ (when produced), formate, acetate, ethanol, propionate and butyrate. It was calculated as described in equation Eq.S8. Negative productivities were not accounted.

$$\text{e-mol}_{i,j} = \text{e-M}_{i,j-1} * d + \text{e-M}_{i,j} - \text{e-M}_{i,j-1} \quad \text{Eq.S8}$$

For compounds like acetate and propionate, which have a significant concentration in the PAC, the daily acetate e-mol feed was subtracted to the value calculated with Eq.S8.

Table S3. Conversion factors for electron balances.

Compound	Chemical Formula	Molecular Weight	mol e ⁻ /mol
Formate	CH ₂ O ₂	46.1	2.0
Acetate	C ₂ H ₄ O ₂	60.0	8.0
Propionate	C ₃ H ₆ O ₂	74.0	14.0
Butyrate	C ₄ H ₈ O ₂	88.1	20.0
Ethanol	C ₂ H ₆ O	46.0	12.0
Hydrogen	H ₂	2.0	2.0
Carbon monoxide	CO	28.0	2.0
Carbon dioxide	CO ₂	44.0	0.0
Methane	CH ₄	16.0	8.0

Mesophilic process

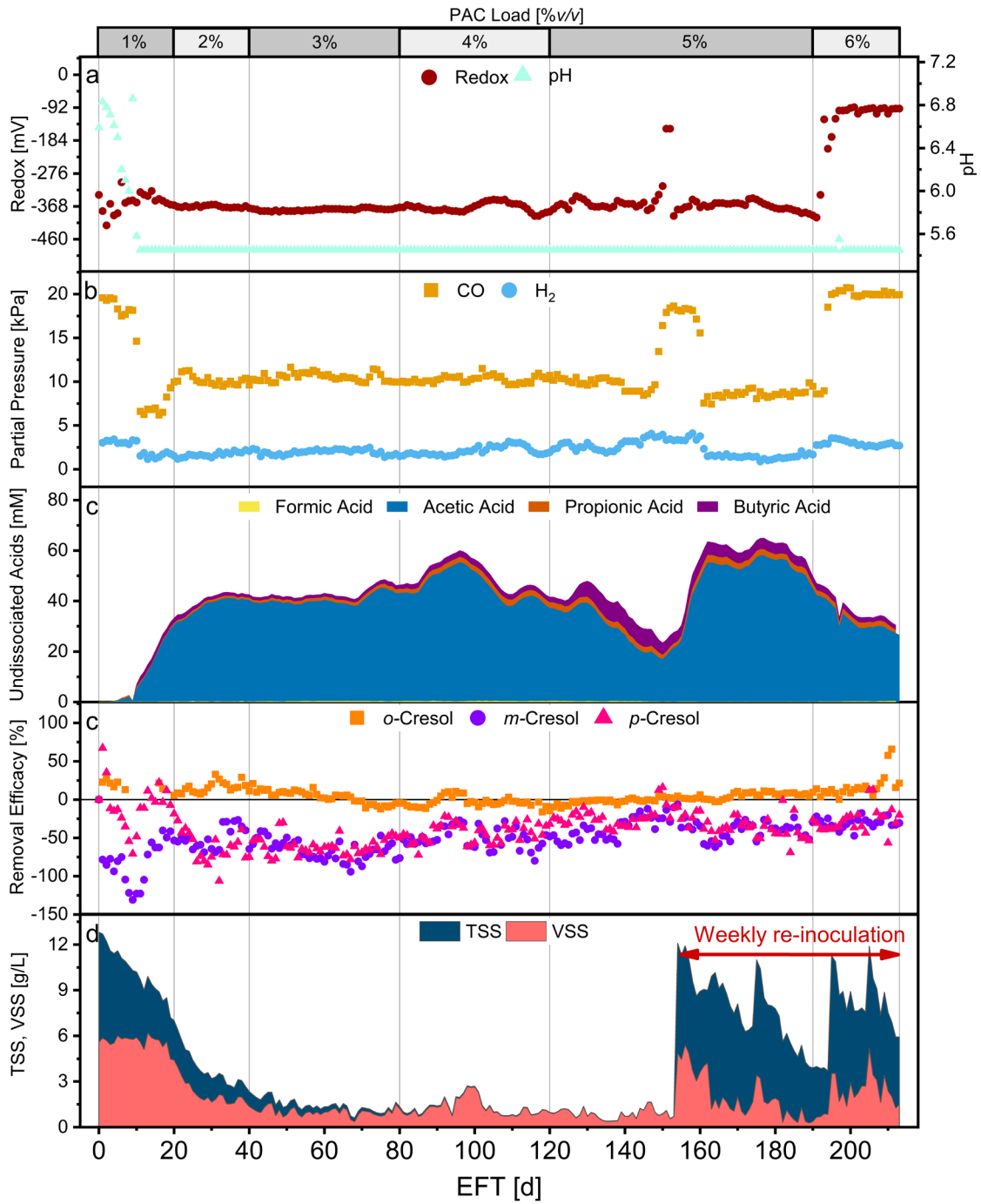


Figure S1. Fermentation profile of the mesophilic process. Top x-axis shows increases in PAC loading, bottom x-axis shows the elapsed fermentation time. The red bar indicate the period of weekly re-inoculations. (a) pH and redox potential. (b) Partial pressures of CO and H₂. (c) Concentration of undissociated carboxylates. (d) Removal efficacy of each cresol isomer. Negative values indicate production. (e) Concentrations of total (TSS) and volatile suspended solids (VSS).

Thermophilic process

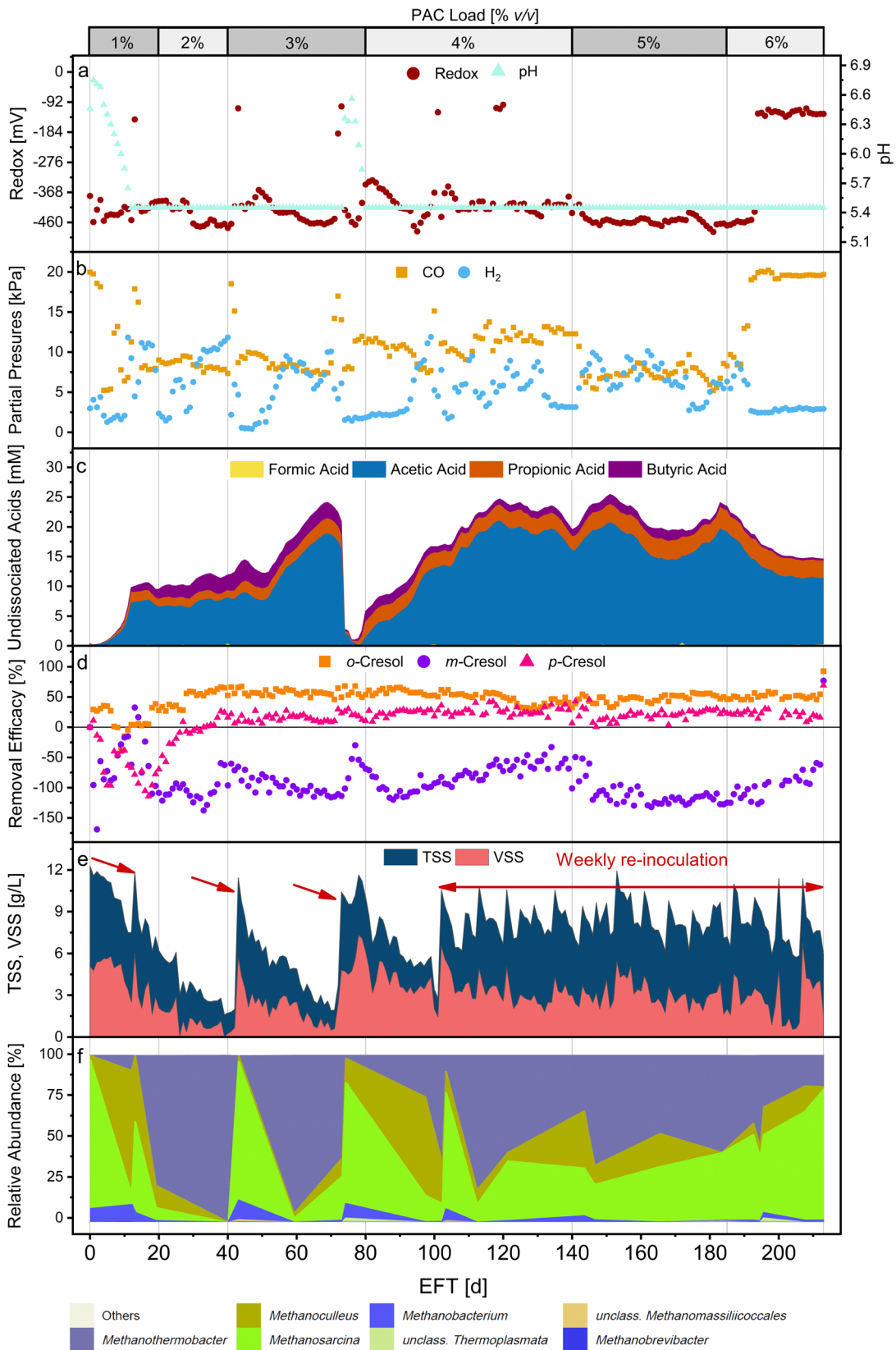


Figure S2. Fermentation profile of the thermophilic process. Top x-axis shows increases in PAC loading, bottom x-axis shows the elapsed fermentation time. Red arrows point to re-inoculation events, the red bar indicate the period of weekly re-inoculations. (a) pH and redox potential. (b)

Supplementary information

Partial pressures of CO and H₂. (c) Concentration of undissociated carboxylates. (d) Removal efficacy of each cresol isomer. Negative values indicate production. (e) Concentrations of total and volatile suspended solids. (f) Relative abundance of the enriched archaeal genera (based on mcrA gene amplicon sequencing variants). Others include all microbial genera with abundance lower than 1%.

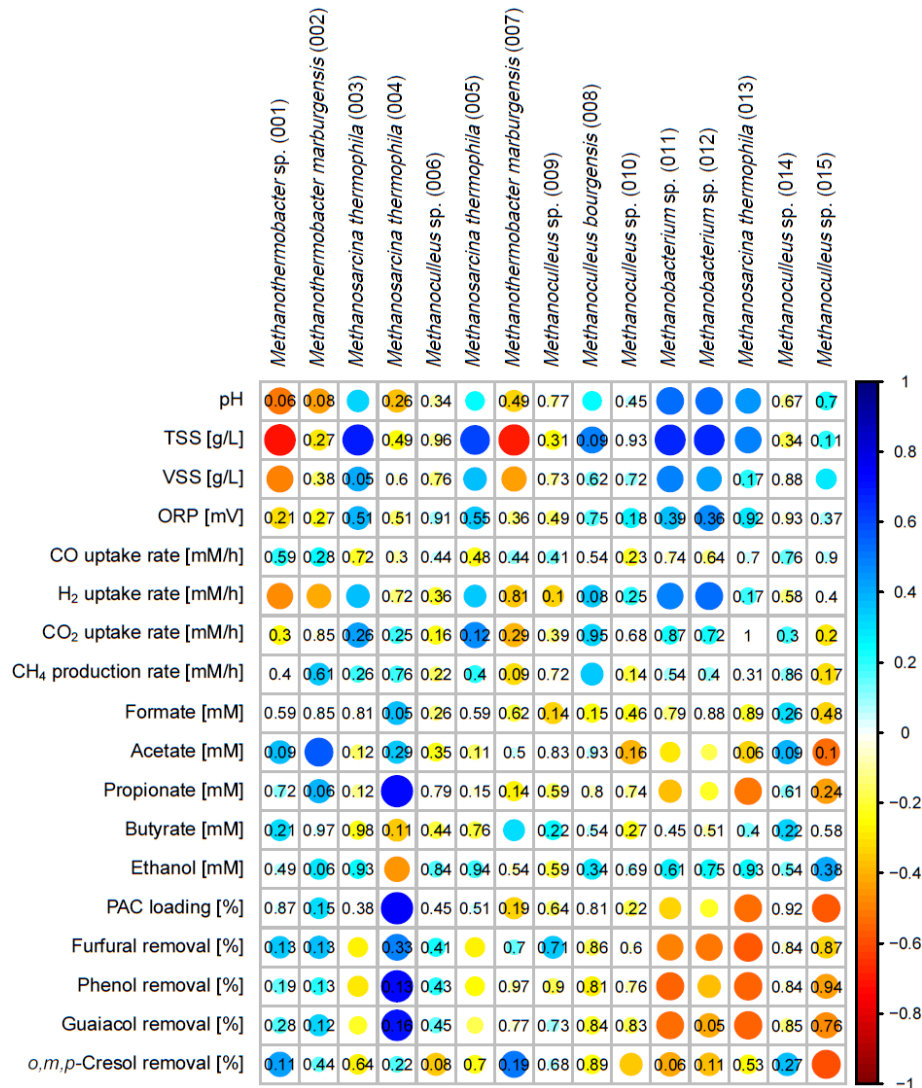


Figure S3. Spearman's rank correlations between relative abundance of methanogens (based on mcrA gene amplicon sequencing variants) and process parameters for the thermophilic semi-continuous STR enrichment. The strength of the correlation is represented by the size of the circle and intensity of the color. Blue circles indicate positive correlations. Red circles indicate negative correlations. p values are shown for non-significant correlations ($p < 0.05$).

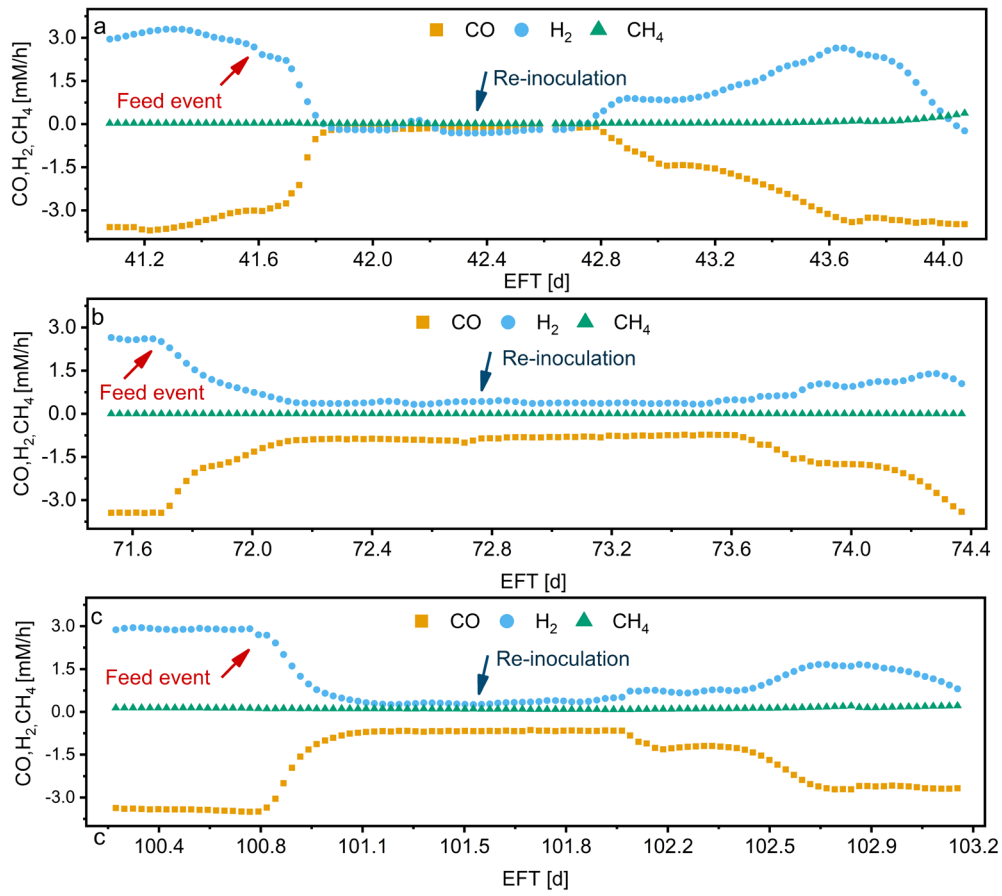


Figure S4. CO, H₂, CH₄ production rates during the decrease in CO uptake rates for the thermophilic syngas and PAC co-fermentation.

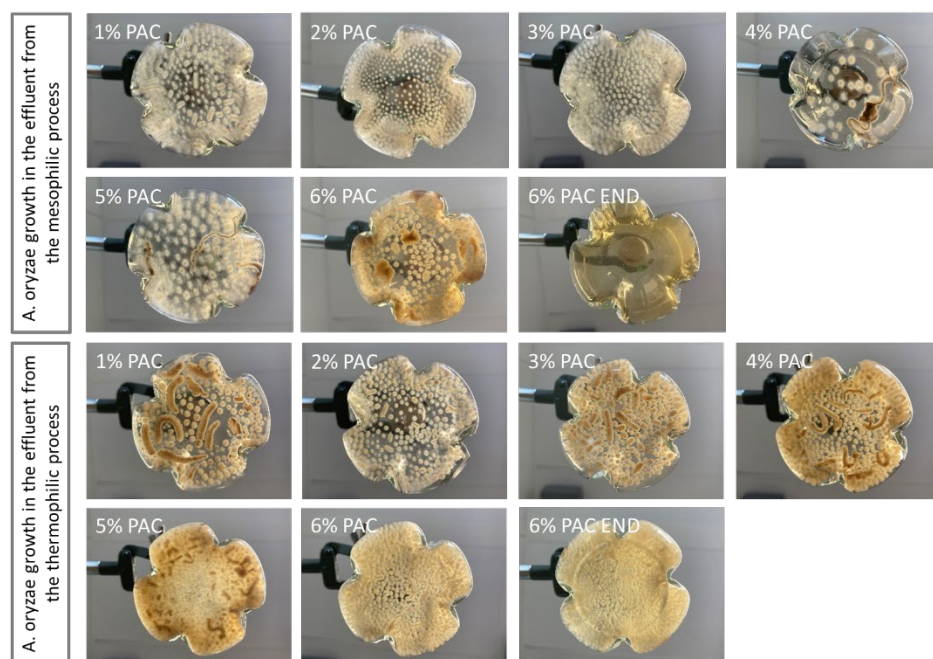
Growth of Aspergillus oryzae in reactor effluent

Figure S5. Photos depicting *A. oryzae*'s growth for all aerobic flask fermentations after 72 hours. The pictures labelled with 6% PAC were recorded from cultivations with the supernatant collected after 207 days of fermentation for both mesophilic and thermophilic process. Pictures labelled with 6% PAC END were recorded from cultivations with the supernatant collected after 213 days of fermentation for both mesophilic and thermophilic process.

Table S4. L-malate and SCCs concentrations over time and L-malate highest yields per SCCs consumed. Numbers are mean values with standard deviations calculated from three replicates. The medium was the supernatant of the fermentation broth collected from the mesophilic reactor.

	PAC load	Time [h]	0	24	48	72	96
20 days	1%	L-malate [mM]	0.0	0.0	2.1 ± 0.7	18.4 ± 0.5	11.9 ± 1.8
		SCCs [mM]	209 ± 5.5	180 ± 2.4	162 ± 3.7	121 ± 3.5	0.0
40 days	2%	L-malate [mM]	0.0	0.0	3.7 ± 2.1	16.7 ± 1.2	20.5 ± 2.1
		SCCs [mM]	218 ± 0.8	236 ± 4.2	212 ± 7.3	168 ± 3.2	0.0
80 days	3%	L-malate [mM]	0.0	0.0	5.8 ± 0.4	28 ± 3.7	33 ± 0.8
		SCCs [mM]	234 ± 2.7	224 ± 3.1	207 ± 1.7	165 ± 4.5	2.7 ± 0.1
116 days	4%	L-malate [mM]	0.0	0.0	0.6 ± 0.1	4.3 ± 0.8	14.4 ± 1.9
		SCCs [mM]	252 ± 4.6	242 ± 5.1	248 ± 0.7	257 ± 2.2	196 ± 2.2
190 days	5%	L-malate [mM]	0.0	0.0	0.4 ± 0.1	8.2 ± 3.9	28.8 ± 1.7
		SCCs [mM]	303 ± 0.8	307 ± 3.6	306 ± 3.4	311 ± 2.6	13 ± 2.0
207 days	6%	L-malate [mM]	0.0	0.0	3 ± 0.5	11 ± 1.7	15 ± 0.6
		SCCs [mM]	240 ± 2.1	239 ± 1.7	219 ± 3.7	155 ± 4.4	10.8 ± 1.8
213 days	6%	L-malate [mM]	0.0	0.0	0.0	0.0	0.0
		SCCs [mM]	162.2 ± 4.8	156.5 ± 3.3	170.8 ± 3.6	174.6 ± 1.8	171.8 ± 3.9

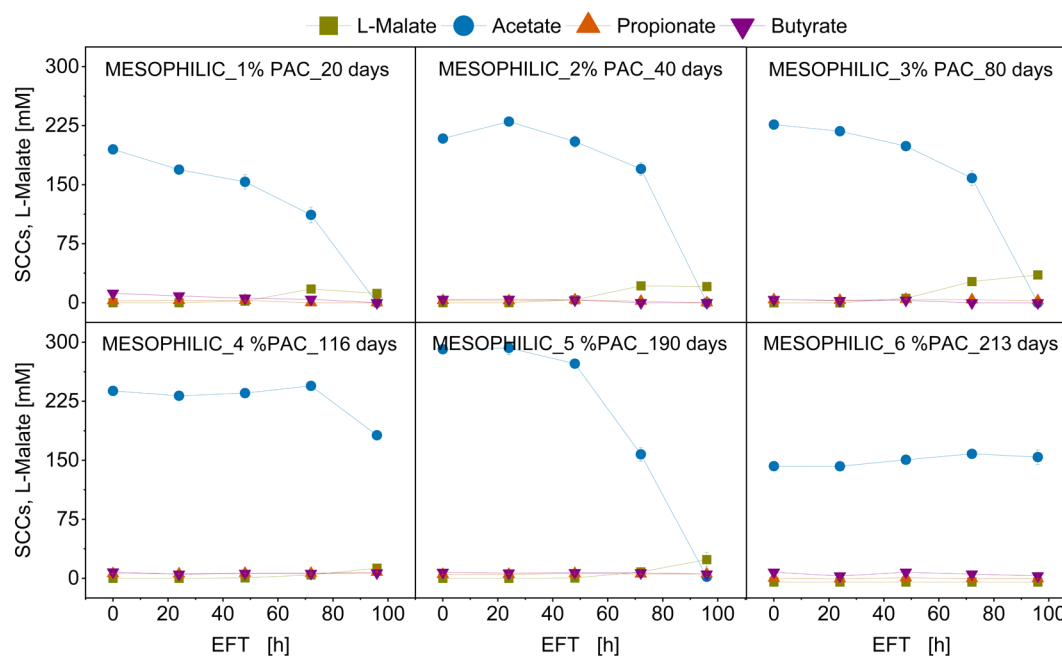


Figure S6. L-malate, acetate, propionate and butyrate concentrations over time. Numbers are mean values with standard deviations calculated from three replicates. The medium was the supernatant of the fermentation broth collected from the mesophilic reactor.

Table S5. L-malate and SCCs concentrations over time and L-malate highest yields per SCCs consumed. Numbers are mean values with standard deviations calculated from three replicates. The medium was the supernatant of the fermentation broth collected from the thermophilic reactor.

	PAC load	Time [h]	0	24	48	72	96
20 days	1%	L-malate [mM]	0.0	0.0	4.2 ± 0.4	0.3 ± 0.2	0.0
		SCCs [mM]	52.3 ± 1.7	42 ± 3.9	22.6 ± 1.7	12.1 ± 0.7	0.0
40 days	2%	L-malate [mM]	0.0	0.0	1.1 ± 0.8	4.6 ± 0.4	0.0
		SCCs [mM]	59 ± 0.6	57.2 ± 1.6	44.5 ± 0.7	13.7 ± 0.3	4.4 ± 1.2
80 days	3%	L-malate [mM]	0.0	0.0	1.6 ± 0.6	7.4 ± 0.7	0.0
		SCCs [mM]	94.3 ± 1.6	87 ± 0.8	68 ± 2.3	12.2 ± 2.0	4.7 ± 0.6
120 days	4%	L-malate [mM]	0.0	0.0	7.3 ± 0.3	13.9 ± 1.7	0.0
		SCCs [mM]	122 ± 1.5	105 ± 3.1	43 ± 2.8	0.0	0.0
185 days	5%	L-malate [mM]	0.0	0.0	2.7 ± 0.7	2.8 ± 0.2	0.0
		SCCs [mM]	114 ± 5.2	104 ± 5.2	50.1 ± 2.0	0.0	0.0
207 days	6%	L-malate [mM]	0.0	0.0	5.6 ± 0.5	4.4 ± 1.1	0.0
		SCCs [mM]	79.5 ± 1.5	66 ± 5.4	7.0 ± 0.1	0.0	0.0
213 days	6%	L-malate [mM]	0.0	0.0	5.0 ± 0.3	3.1 ± 1.1	0.0
		SCCs [mM]	74 ± 0.8	66.6 ± 1.6	8.8 ± 1.2	0.0	0.0

Supplementary information

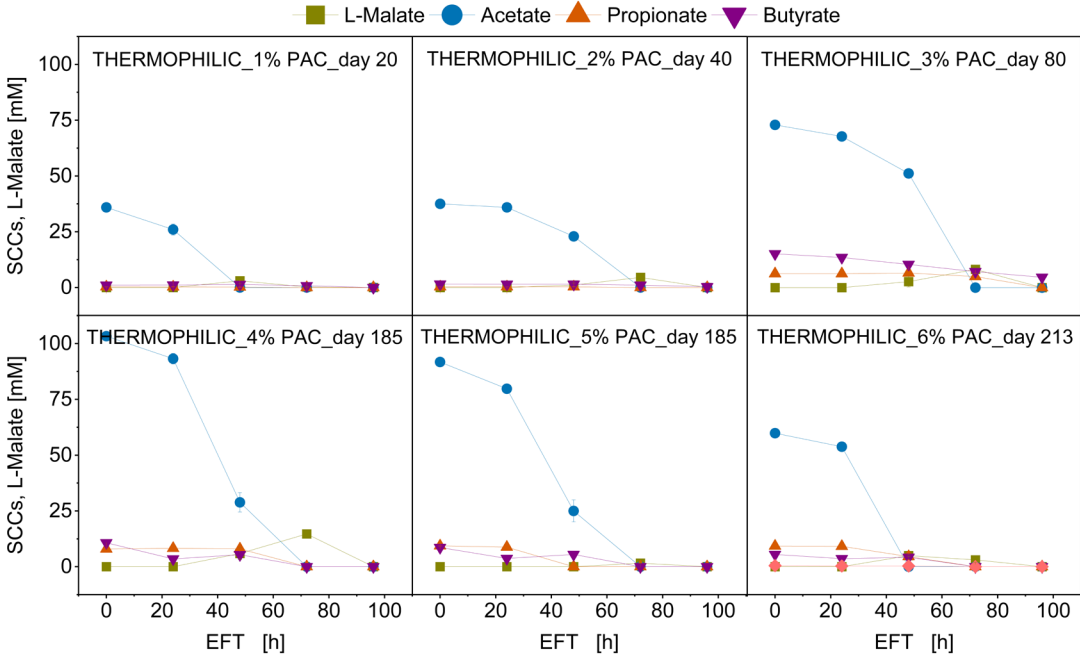


Figure S7. L-malate, acetate, propionate and butyrate concentrations over time. Numbers are mean values with standard deviations calculated from three replicates. The medium was the supernatant of the fermentation broth collected from the thermophilic reactor.

